THE UNIVERSITY
of EDINBURGH

Acanthamoeba Programmed Cell Death

Zisis Koutsogiannis

THE UNIVERSITY *of* EDINBURGH

Doctor of Philosophy

The University of Edinburgh

2018

Abstract

Acanthamoeba is a free-living amoeba, ubiquitously distributed in the natural environment including soil and a plethora of water habitats. It is characterised as an opportunistic parasite that is able to cause several diseases, including life threating granulomatous *Acanthamoeba* encephalitis and a painful vision-threating keratitis. There is a clear and emerging need to understand how to treat infections caused by this dangerous pathogen, since pharmaceutical approaches have been considered insufficient. The presence and the importance of cell death pathways in unicellular organisms including *Acanthamoeba* is not yet fully understood and its existence is still debated. This research study presents a set of key characteristics and findings, comprising morphological, biochemical and molecular evidence of *Acanthamoeba* programmed cell death. Distinctive apoptotic features comprising cell shrinkage, membrane vesiculation and granules appearance which could be easily described as apoptotic like 'bodies' formation and nuclear shrinkage, accompanied by large scale chromatin condensation in dense clusters, have been primarily observed. Additionally, mitochondrial dysfunction, characterized by extended mitochondrial outer membrane permeabilization and release of apoptotic factors including cytochrome c, was also noted, indicating a mitochondrially mediated cell death pathway. During the expansion of the aforementioned apoptotic characteristics *Acanthamoeba* trophozoites were found to maintain their membrane integrity and homeostasis, at least at the early stages of the process. In-depth transcriptomic analysis based on RNA-sequence analysis revealed a plethora of differentially expressed genes between *Acanthamoeba* undergoing cell death and control trophozoites, indicating the correlation of a more defined and conserved signalling self-destruct program. These discoveries suggest that *Acanthamoeba* could undergo programmed cell death, which morphologically resembles apoptosis-like cell death, under specific stress conditions. Furthermore, similar characteristics are also found in cell death processes in higher eukaryotes and other unicellular organisms, indicating that biological principles behind this behaviour are widespread and well conserved among species. Identification of *Acanthamoeba's* cell death signalling pathways might provide alternatives not only to microorganism's refractory infection treatment, but also a more extended manipulation might become feasible across other species and systems.

Lay summary

The concept of regulated cell death mechanisms in multicellular organisms is not new as amongst other things, they confer the ability of development, differentiation, maintenance of homeostasis and also a means by which old, non-functional and malignant cells are discarded. Intriguingly though, forms of regulated cell death are not exclusive to multicellular life forms but are also found among unicellular eukaryotes including bacteria, fungi and protists. Since the cell death field continues to grow constantly and novel mechanisms that orchestrate multiple cell death pathways are revealed, a question that arises is whether *Acanthamoeba,* which is a unicellular potentially pathogenic protozoan, possesses such mechanisms, which could mediate its own cell death, why such mechanisms might have been conserved and what kind advantages this may offer to *Acanthamoeba* populations.

The main objectives of the study were to identify apoptotic or any other kind of regulated cell death features including firstly morphological, secondly biochemical and thirdly molecular characteristics, which might indicate a more complex death signalling pathway. Accordingly, the presence of a variety of characteristics associated to regulated cell death were evaluated and a potential cell death signalling pathway was described and proposed. Methodically, it was shown that a significant number of apoptotic characteristics which were used previously to describe apoptosis and programmed cell death phenomena in other systems, cells or organisms were also notable in *Acanthamoeba* cell death after treatment with G-418 aminoglycoside.

Furthermore, RNA-sequence analysis revealed a great variety of differentially expressed genes (DEGs) in *Acanthamoeba* trophozoites undergoing cell death compared with control amoebae, rendering feasible the detection of genes and proteins that participate in the phenomenon. The great number of DEGs as well as the nature of those genes, contributed positively to the conclusion that *Acanthamoeba* cell death, under some circumstances, may be a finely regulated biological procedure.

Own work declaration

I declare that the thesis has been composed completely by myself and that the work has not be submitted for any other degree or professional qualification. I confirm that the work submitted is my own, except where explicitly stated otherwise or where work which has formed part of jointly-authored publications has been included. I confirm that appropriate credit has been given within this thesis where reference has been made to the work of others.

Zisis Koutsogiannis,

July 2018

Acknowledgements

I would like to express my gratitude to my supervisor Dr. Sutherland K. Maciver for all the support, encouragement and advices provided throughout this project and simultaneously for making my time working there such a productive and positive part of my life. I would also like to thank my PhD committee, Dr. Sari Pennings and Dr. Ewan McLeod.

I would like to thank Phasefocus company that gave me the opportunity to use their new high contrast microscope and simutaneously for the additional guidance provided on the results analysis. Special thanks also to Dr. Anisha Kubasik-Thayil for the seminars on confocal microscopy.

Table of Contents

Abbreviations **15**

Chapter 1 Introduction 17
1.1 Amoebae 17
1.2 Free Living Amoeba 20
1.3 *Acanthamoeba* 20
1.3.1 Taxonomy of *Acanthamoeba* 22
1.3.2 *Acanthamoeba* life cycle 25
1.3.3 *Acanthamoeba* morphology and cell biology 30
1.3.4 *Acanthamoeba* Distribution and Ecology 32
1.3.4.1 *Acanthamoeba* bacteria interactions 33
1.3.4.2 *Acanthamoeba* viruses interactions 36
1.3.4.3 *Acanthamoeba* Fungi interactions 38
1.3.5 Diseases and pathogenicity 38
1.3.4.1 *Acanthamoeba* Keratitis 39
1.3.4.1 *Acanthamoeba* Granulomatous Encephalitis 41
1.3.4.1 *Acanthamoeba* Rhinosinusitis 43
1.3.4.1 Cutaneous Acanthamebiasis 44

Chapter 2 Cell Death **45**
2.1 Cell death 45
2.2 Apoptosis 46
2.2.1 Intrinsic or mitochondria mediated apoptosis 48
2.2.2 Extrinsic apoptosis 50
2.3 Necrosis 50
2.4 Autophagy dependent cell death 52
2.5 Calcium and cell death 53
2.5.1 Mitochondrial role in Calcium mediated cell death signalling 55
2.6 Ras signaling in cell death 58
2.7 Regulated cell death in protozoan parasites 60
2.8 Amoebicide drug 63
2.8.1 G-418 aminoglycoside 63

2.8.2 Polymyxin B 64
2.9 Aims of study.....65

Chapter 3 Materials and Methods **67**
3.1 Culture media.....67
3.1.1 AX2 Media.....67
3.1.1 Neff's saline buffer.....67
3.1.1 Lysogeny broth 67
3.2 Bacterial cultures.....67
3.2.1 Escherichia coli 67
3.2.2 bacterial cryopreservation 67
3.3 *Acanthamoeba* cultures.....68
3.3.1 *Acanthamoeba* isolation 68
3.3.2 Axenic *Acanthamoeba* Cultures.....69
3.3.2 *Acanthamoeba* cryopreservation 69
3.4 *Acanthamoeba* viability curves by Trypan blue exclusion assay 71
3.5 Microscopy.....71
3.5.1 Optical microscopy 71
3.5.2 Time-lapse video microscopy.....72
3.5.3 High contrast quantitative imaging and microscopy 72
3.5.4 Confocal Microscopy 73
3.6 Fluorescent techniques 73
3.6.1 Intracellular $[Ca^{++}]_c$ concentration.....73
3.6.2 Intracellular pH measurement (pHi) 74
3.6.3 Hoechst staining protocol and Hoechst fluorescence intensity.....75
3.6.4 CTC - Formazan accumulation and fluorescence intensity 77
3.6.5 Plasma membrane permeability.....78
3.6.6 Mitochondrial membrane potential ΔΨm 79
3.7 Molecular techniques.....81
3.7.1 DNA extraction from *Acanthamoeba* 81
3.7.2 PCR for 18S rDNA amplification 81
3.7.3 PCR purification.....83
3.7.4 DNA and RNA electrophoresis.....83

3.7.5 18S rDNA Sequencing 83
3.7.6 Acanthamoeba RNA extraction 84
3.7.7 *Acanthamoeba* RNA quantification and qualification 84
3.7.8 Illumina RNA sequencing workflow 85
3.7.8.1 *Acanthamoeba* cDNA libraries and sample preparation 85
3.7.8.2 Clustering 85
3.7.8.3 Sequencing 88
3.7.8.4 Data analysis 88
3.8 Cytochrome c detection by western blotting 89
3.8.1 SDS PAGE 90
3.8.2 Protein transfer 92
3.8.3 Cytochrome c immune-detection 93
3.8.4 Visualization 93
3.9 Bioinformatics 93
3.9.1 Basic local alignment search tool (BLAST) 93
3.9.2 Sequence alignments and phylogeny tree 94
3.9.3 mRNA seq bioinformatics tools and workflow 95
3.9.3.1 Quality control of RNA seq raw reads 95
3.9.3.2 Mapping reads to genome 96
3.9.3.1 Differential Expression analysis 97

Chapter 4 Molecular phylogeny of *Acanthamoeba* **99**
4.1 Introduction 99
4.2 Results- Phylogeny 100
4.3 Discussion 105

Chapter 5 *Acanthamoeba* cell death 107
5.1 Introduction 107
5.2 Results 108
5.2.1 Polymyxin b induced cell death 108
5.2.2 G-418 aminoglycoside induced cell death 112
5.2.2.1 G-418 aminoglycoside induced cell death inhibition or delay 115

5.3 Discussion....118

Chapter 6 Apoptotic morphological features of *Acanthamoeba* programmed cell death....123

6.1 Introduction Morphologic hallmarks of apoptosis....123

6.2 Results....124

6.2.1 Cell shrinkage....124

6.2.2 Chromatin alternations....129

6.2.3 DNA Fragmentation....135

6.2.4 Membrane permeability....136

6.3 Discussion....138

Chapter 7 Apoptotic biochemical features of *Acanthamoeba* programmed cell death....141

7.1 Introduction- Biochemical hallmarks of apoptosis....141

7.2 Results....142

7.2.1 Intracellular calcium concertation....142

7.2.2 Mitochondrial dysfunction....143

7.2.3 Cytochrome c detection....149

7.3 Discussion....151

Chapter 8: RNA seq analysis of Acanthamoeba programmed cell death....154

8.1 Introduction....154

8.2 Results....156

8.2.1 Isolated RNA quality....156

8.2.2 Quality control of the obtained sequences....157

8.3 Differential expression analysis....158

8.3.1 Exploring differences between libraries....158

8.3.2 Dispersion estimation....161

8.3.2.1 Biological coefficient variation....161

8.3.2.2 Moderated tagwise dispersion....163

8.4 Differentially Expressed Genes analysis....163

8.5 Discussion....180

Chapter 9 Gene profile analysis of *Acanthamoeba* programmed cell death..187

9.1 Introduction....187

9.2 Results 188
9.2.1 *Acanthamoeba* metacaspase expression 188
9.2.2 Protein kinases gene expression 189
9.2.2.1 Ser/Thr kinases gene expression 190
9.2.3 Protein phosphatases expression 195
9.2.4 *Acanthamoeba* calmodulin genes expression 199
9.2.5 *Acanthamoeba* endonucleases expression 200
9.2.6 *Acanthamoeba* deoxy-ribonucleases expression 203
9.2.7 *Acanthamoeba* cysteine proteases 204
9.2.8 *Acanthamoeba* serine proteases 204
9.2.9 *Acanthamoeba* Ras family genes expression 208
9.2.10 *Acanthamoeba* autophagy regulator genes expression 208
9.2.11 *Acanthamoeba* ubiquitin related genes expression 212
9.2.12 *Acanthamoeba* glutathione S-transferase gene expression 215
9.2.13 *Acanthamoeba* cyst-specific genes 216
9.3 Discussion 218
Chapter 10 Discussion 231
Appendix 1 - R transcript 240
Appendix 2 - Supplementary Figures 247
Appendix 3 - Publications 251
References 252

List of Figures

Chapter 1 Introduction

Figure 1.1: Simplified life cycle of *Acanthamoeba* 27
Figure 1.2: *Acanthamoeba's* growth diagram in axenic conditions, over time 27
Figure 1.3: Characteristic morphological shapes of *Acanthamoeba* trophozoites and cysts. 30
Table 1.1: Major groups and genera of amoeboid super-groups 19
Table 1.2: Differential taxonomic classification of *Acanthamoeba* 22
Table 1.3: Different genotypes of *Acanthamoeba* strains 25
Table 1.4: Summary of *Acanthamoeba* bacteria interactions 34
Table 1.5: Integrated *Acanthamoeba*-virus interactions 37

Chapter 2 Cell death

Figure 2.1: Representaive calcium-dependent signaling pathways 55
Figure 2.2: Representation of mitochondrial cell death pathway 58

Chapter 3 Materials and Methods

Figure 3.1: *Acanthamoeba* isolation 70
Figure 3.2: CTC reduction to red CTF 78
Figure 3.3: Mitochondrial membrane potential depolarization based on JC-1 fluorescence signal.....80
Figure 3.4: cDNA library preparation and illumina adapters ligation.....87
Figure 3.5: Simplified clustering procedure.....87
Figure 3.6: Illumina sequencing and data processing workflow 89
Figure 3.7: Protein transfer sandwich and scaffolds for western blot 92
Figure 3.8: RNA seq data workflow 94

Table 3.1: 18S rDNA primers information 82
Table 3.2: PCR components final volume and concentration.....82
Table 3.3: Running (a) and stacking (b) gel composition 91
Table 3.4: List of *Acanthamoeba* genotypes and GenBank accession numbers..94

Chapter 4 Molecular Phylogeny of *Acanthamoeba*

Figure 4.1: Phylogenetic tree of isolated the *Acanthamoeba* strain based on the full 18S rDNA gene.....102
Figure 4.2: Phylogenetic tree of isolated *Acanthamoeba* strain based on ASA.S1 fragment 103
Figure 4.3: Trophozoite and cyst morphology of isolated *Acanthamoeba*.....104

Chapter 5 *Acanthamoeba* cell death

Figure 5.1a: Effect of PMB on *Acanthamoeba* viability in NSB 109
Figure 5.1b: Effect of PMB on *Acanthamoeba* viability in AX2.....110
Figure 5.2: Characteristic effect of PMB on *Acanthamoeba* trophozoites 110
Figure 5.3: Effect of PMB on *Acanthamoeba* Calcium intracellular levels.....111
Figure 5.4: Effect of PMB in intracellular pH of *Acanthamoeba* 112
Figure 5.5: Effect of G-418 aminoglycoside on *Acanthamoeba* in NSB 113

Figure 5.6: Effect of G-418 aminoglycoside on *Acanthamoeba* in different media at room temperature....113

Figure 5.7 a, b: Effect of G-418 aminoglycoside on *Acanthamoeba* trophozoites in different media at 37℃....114

Figure 5.8: Effect of G-418 aminoglycoside on *Acanthamoeba* trophozoites after washing....115

Figure 5.9: Effect of Cysteine proteases inhibitors on *Acanthamoeba* viability G-418 treated....117

Figure 5.10: Effect of DMSO, Lovastatin and Caffeine on *Acanthamoeba* viability G-418 treated....117

Figure 5.11: *Acanthamoeba* viability after treatment with G-418 in combination to RR....118

Chapter 6 Apoptotic morphological features of *Acanthamoeba* programmed cell death

Figure 6.1 a, b: Confluency and dry mass....125

Figure 6.2 a, b: Dry mass density during incubation....126

Figure 6.3 a, b: Cell coverage area....127

Figure 6.4: Velocity diagram....128

Figure 6.5: Morphology of G-418 treated and untreated *Acanthamoeba* trophozoites....130

Figure 6.6: Representative Hoechst 33345 staining time series of apoptotic chromatin condensation....131

Figure 6.7: Characteristic sign of chromatin ring formation....131

Figure 6.8: 3D representation of apoptotic chromatin morphology....132

Figure 6.9: Hoechst signal intensity diagrams....132

Figure 6.10: Chromatin condensation after caffeine treatment....133

Figure 6.11: Nuclear morphology after 2.5% DMSO treatment....134

Figure 6.12: Representative 1.8% agarose DNA gel electrophoresis....135

Figure 6.13: Sytox green signal intensity of *Acanthamoeba* trophozoites....136

Figure 6.14: Sytox green fluorescence intensity of *Acanthamoeba*....137

Chapter 7 Apoptotic biochemical features of *Acanthamoeba* programmed cell death

Figure 7.1: Effect of G-418 on *Acanthamoeba* intracellular calcium levels....143

Figure 7.2: Respiration activity of G-418 treated and untreated *Acanthamoeba* 144

Figure 7.3: Illustration of formazan reduction during treatment with G-418 146

Figure 7.4: Mitochondrial ΔΨm variations of treated and untreated *Acanthamoeba* during time 147

Figure 7.5: JC-1 emission intensities during time of incubation 147

Figure 7.6: Fluorescent microscopy of G-418 treated and untreated *Acanthamoeba* trophozoites loaded with JC-1.....148

Figure 7.7: Ponceau S staining after transfer.....149

Figure 7.8: Western blot image of cyt c *Acanthamoeba* cytosolic fraction.....150

Figure 7.9: Western blot image of cyt c *Acanthamoeba* mitochondrial fraction ..150

Chapter 8: RNA seq analysis of Acanthamoeba programmed cell death

Figure 8.1: Representative RNA electrophoresis quality of isolated *Acanthamoeba* RNA 156

Figure 8.2: Summary of FastQC report.....157

Figure 8.3: MDS plot 160

Figure 8.4: Scatterplot of biological coefficient.....162

Figure 8.5: Moderated tagwise dispersion 164

Figure 8.6: Scatter plots of DEGs 165

Figure 8.7: Volcano plots of DEGs during incubation FDR 0.001.....166

Figure 8.8: Volcano plots of DEGS during incubation FDR 0.05.....167

Figure 8.9: DEGs between G-418 treated and untreated Acanthamoeba.....169

Figure 8.11: Profile expression of the 20 most DEGs after 3 hours of treatment 171-172

Figure 8.11: Profile expression of the 20 most DEGs after 3 hours of treatment .....174 -175

Figure 8.12: Profile expression of the 20 most DEGs after 6 hours of treatment 177-178

Figure 8.13: Heatmap of the DEGs 179

Table 8.1: List of the most DEGs after 1 hour of treatment.....170

Table 8.2: List of the most DEGs after 3 hours of treatment 173

Table 8.3: List of the most DEGs after 6 hours of treatment 176

Chapter 9 Gene profile analysis of *Acanthamoeba* programmed cell death

Figure 9.1: *Acanthamoeba* metacaspase profile expression.....189
Figure 9.2: Acanthamoeba ser/thr protein kinases profile expression.....191
Figure 9.3: *Acanthamoeba* Ca^{2+} calmodulin dependent kinases profile expression 192
Figure 9.4: *Acanthamoeba* MAPKs profile expression.....193
Figure 9.5: *Acanthamoeba* tyrosine kinases profile expression 194
Figure 9.6: *Acanthamoeba* ser/thr protein phosphatases profile expression.....197
Figure 9.7: *Acanthamoeba* tyrosine protein phosphatases 198
Figure 9.8: *Acanthamoeba* calmodulin profile expression.....199
Figure 9.9 a, b: *Acanthamoeba* endonucleases profile expression.....201-202
Figure 9.10: *Acanthamoeba* deoxyribonucleases profile expression 203
Figure 9.11: *Acanthamoeba* cysteine proteases profile expression 205
Figure 9.12: *Acanthamoeba* serine proteases profile expression.....206
Figure 9.13: A*canthamoeba* ubiquitin proteases profile expression 207
Figure 9.14: *Acanthamoeba* Ras family genes profile expression.....209-210
Figure 9.15: *Acanthamoeba* autophagy related genes profile expression.....211
Figure 9.16: *Acanthamoeba* ubiquitination related genes profile expression.....213
Figure 9.17: *Acanthamoeba* ubiquitination proteasome related genes.....214
Figure 9.18: *Acanthamoeba* glutathione S-transferase profile expression 215
Figure 9.19: *Acanthamoeba* cyst specific proteins profile expression 217
Figure 9.20: *Acanthamoeba* potential MAPK pathway 221

Chapter 10 Discussion

Figure 10.1: *Acanthamoeba* intrinsic or mitochondria mediated death pathway.234
Figure 10.2: *Acanthamoeba* apoptosis-like cell death timeline 235

Abbreviations

Acmcp: *Acanthamoeba* metacaspase

ACD: Accidental cell death

AGE/GAE: *Acanthamoeba* or Amoebic granulomatous encephalitis

AK: *Acanthamoeba* Keratitis,

AIF: Apoptosis inducing factor

APS: Ammonium persulfate

ATG: Autophagy related genes

ATP: Adenosine triphosphate

AX2: Axenic amoeba culture

BCECF Acid: 2', 7'-Bis-(2-Carboxyethyl)-5-(and-6)-Carboxy-fluorescein

Bp: Base pairs

$[Ca^{2+}]_m$: mitochondrial calcium concentration

$[Ca^{2+}]_c$: cytosolic calcium concentration

CM: Confocal microscopy

CNS: Central nervous system

CPM: Counts per million

CTC: 5-cyano-2, 3-ditolyl tetrazolium chloride

Cyt c: Cytochrome c

DDT: Dichlorodiphenyltrichloroethane

ddH_2O: double distilled water

DAPI: 4′,6-diamidino-2-phenylindole

DE: Differentially expressed

DMSO: Dimethyl sulfoxide

EDTA: Ethylene-diamine-tetra-acetic acid

EGTA Ethylene glycol-bis (β-aminoethyl ether)-N,N,N′,N′-tetraacetic acid

EndoG: Endonuclease G

ER: Endoplasmic reticulum

Fc: Fold change

FDR: False discovery rate

FLA: Free living amoeba

HEPES: 4-(2-hydroxyethyl)-1-piperazineethanesulfonic acid

JC-1: Tetra-ethyl-benzimidazolyl-carbo-cyanine iodide

JNK: c-Jun N-terminal kinases

kDa: kilodaltons

LB: Luria broth

MAPK: Mitogen activated kinases

MOM: Mitochondrial outer membrane

NCCD: Nomenclature Committee on Cell Death

NSB: Neff's saline buffer

PAGE: Polyacrylamide gel electrophoresis

PBS: Phosphate buffer saline

PCD: Programmed cell death

PCR: Polymerase chain reaction

PFA: Paraformaldehyde

SDS: Sodium dodecyl sulphate

SE: Standard error

SSU: Small subunit

TAE: Tris-acetate-EDTA buffer

TBS: Tris-buffered saline

TB: Trypan blue

TBST: Tris-buffered saline-1% tween 20

TE: Tris-EDTA

TGM: Tris-Glycine Buffer

Z-VAD-FMK: carbobenzoxy-valyl-alanyl-aspartyl-[O-methyl]- fluoromethylketone

ΔΨm: Mitochondrial membrane potential

Chapter 1

Introduction

1.1 Amoebae

August Johann Rösel von Rosenhof in 1755 was the first to describe an organism resembling Amoeba. The first naturalists referred to amoeboid as “Proteus animalcule”, after the name of Proteus, a sea god of Greek mythology who was capable of assuming many forms. The final etymology derives from Bory de Saint-Vincent (1822) and C. G. Ehrenberg (1830) who named the genus, Amiba/Amoeba (after the Greek “ἀμοιβή” amoibè), which means change.

Principally, the term “amoeba” is used to describe a simple eukaryotic organism that is capable of altering its shape and simultaneously moves in a crawling fashion. Amoebae are also characterized by the lack of a stable cellular form. Cytoplasmic extensions, known as pseudopodia, differ in shape and morphology from genus to genus, but mainly serve the main purposes of all amoebae including locomotion and food-prey capture by phagocytosis (Harvey et al., 2013). This is generally achieved by the synchronized action of actin microfilaments.

Amoebae are one the most well adapted and widely distributed microorganisms in our planet, (Bradley and Marciano-Cabral, 1996) as numerous and various genus have been isolated, on all continents including Antarctica (Brown et al., 1982), from poorly accessible areas and extreme environments to more mild climates. They also essentially contribute to ecosystem stability by providing valuable nutrients to plants, as a result of their consumption of bacteria (Clarholm, 2002).

Amoeboid organisms are found in every major ancestry of eukaryotes and do not constitute a distinctive genetically determined taxonomic group. Some of them are more genetically related to algae, fungi or animals than to other amoeboid groups. Although having such a wide and diverse phylogenetic provenance, amoebae share

numerous morphological and behavioural features. The classification of these organisms has historically relied upon morphological characteristics and locomotion, however modern molecular techniques have provided extensive and reliable alternatives for a more profound and thorough amoeboid organism classification.

The numerous amoeboid genera are classified in seven super-groups comprising Amoebozoa (Lobosa, Conosa), Rhizaria (Cercozoa, Foraminifera, Radiolaria), Excavata (Heterolobosea, Parabasalidea), Heterokonta (Chrysophyceae, Xanthophyceae, Labyrinthulomycetes), Alveolata (Dinoflagellata) and Nuclearids (Micronuclearia, Nuclearia, Fonticula), (Table 1). Amoebozoa, Excavata and Rhizaria compose the most amoebae-rich groups. More precisely, the Amoebozoa group, in which is categorized the majority of the amoeboid population, are mainly characterized by lobose pseudopods including free-living amoebae like *Acanthamoeba* and *Balamuthia mandrillaris*, some amoeboflagellates, like *Phalansterium* (Cavalier et al., 2004), *Multicilia* (Nikolaev et al., 2006) and finally slime moulds like dictyostelids (Bapteste et al., 2002; Adl et al., 2005).

Rhizaria is another large entity of generally unicellular eukaryotes, but the greater portion consists of amoebae with filose (Cercozoa; Radiolaria), reticulose (Foraminifera), or microtubule-supported pseudopods (McFadden et al., 1994; Nikolaev et al., 2004). The Excatvata group includes Vahlkampfiidae, Gruberellidae and Parabasalidae, some of which possess the ability to transform between amoeboid and flagellate forms and are simultaneously considered by some as the oldest members of the family of flagellated organisms. Parasitic amoeboid species comprising Rhizocloris, Synchroma, Labyrinthulomycetes and Chrysamoeba are found in the group of Heterkonta which is mainly composed of and characterized by algae species, ranging from giant multicellular kelp to unicellular diatoms (Hibberd 1971; Patil et al., 2009). Finally, Nucleariids refer to a group of phagotrophic filose amoebae that phenotypically resemble to their distant holozoan relatives more than their holomycotan phylogenetic relatives (López-Escardó et al., 2017).

Like their diversity, amoeboid cell size is quite variable. Some species are of comparable sizes to bacteria (2.3 to 3 μm diameter) and others can attain up to 20 cm in diameter (Gooday, et al., 2004; Mylnikov et al., 2015). The majority of amoeboid species are microscopic, but in some cases, observation with the naked eye is also feasible.

Supergroups	Major Groups and Genera
Amoebozoa	• **Lobosa:** *Acanthamoeba, Amoeba, Balamuthia, Chaos, Clydonella, Discamoeba, Echinamoeba, Filamoeba, Flabellula, Gephyramoeba, Glaeseria, Hartmannella, Hydramoeba, Leptomyxa, Lingulamoeba, Mastigina, Mayorella, Metachaos, Neoparamoeba, Paramoeba, Polychaos, Platyamoeba, Protoacanthamoeba, Rhizamoeba, Saccamoeba, Sappinia, Stereomyxa, Thecamoeba, Trichamoeba, Trichosphaerium, Vannella, Unda, Vexillifera* • **Conosa:** *Endamoeba, Entamoeba, Hyperamoeba, Mastigamoeba, Mastigella, Pelomyxa, Dictyostelium, Physarum*
Rhizaria	• Cercozoa: • Filosa: • Monadofilosa: *Gyromitus, Paulinella* • Chlorarachniophyceae • Endomyxa: • Foraminifera • Radiolaria
Excavata	• Heterolobosea: • *Vahlkampfiidae: Monopylocystis, Naegleria, Neovahlkampfia, Paratetramitus, Paravahlkampfia, Psalteriomonas, Sawyeria, Tetramitus, Vahlkampfia, Willaertia* • Gruberellidae: *Gruberella, Stachyamoeba* • Parabasalidea: *Dientamoeba, Histomonas*
Heterokonta	Chrysophyceae: Chrysamoeba, Rhizochrysis Xanthophyceae: Rhizochloris Labyrinthulomycetes
Alveolata	Dinoflagellata: *Dinamoeba, Pfiesteria*
Nucleariid	*Micronuclearia, Nuclearia*

Table 1.1: Major groups and genera of amoeboid super-groups

1.2 Free-living Amoeba

Free-Living Amoeboid (FLA) are quite widely distributed in the natural environment due to food source availability and can be found in soil, water habitats, both fresh or marine and man-made aquatic environments respectively, where they interact with other micro-organisms including viruses, fungi and bacteria.

They are characterized as potentially pathogenic protozoa as they can cause several diseases to humans and animals (Culbertson et al., 1958), while being simultaneously capable of surviving and proliferating without the presence of a valid host. These amphizoic amoebae can harbor endosymbionts and other pathogenic agents, offering them protection against hostile conditions and immune systems. The most frequently studied FLA, due to their potential for developing pathogenic activity, comprise *Naegleria fowlerii,* which causes Primary Amoebic Meningoencephalitis, (Gautam et al., 2012) species belonging to the genus of *Acanthamoeba* that are able to cause Amoebic Keratitis (AK) and Amoebic Granulomatous Encephalitis (AGE)*, Balamuthia mandrillaris,* which is also considered a causative agent of AGE (Tavares et al., 2006) and *Sappinia,* which also has been reported to cause encephalitis (Gelman et al., 2001; Abdul Majid MA *et.al.* 2017).

In addition to their pathogenicity, FLA usually serve as environmental reservoirs (King et al., 1988; Molmeret, 2005) for pathogenic micro-organisms such as *Legionella pneumophila* (Cirillo et al., 1994), *Mycobacterium avium (*Miltner *and* Bermudez *2000;* Wheat et al., 2014*), Burkholderia spp.* (Inglis et al., 2000) *and Vibrio cholerae* (Van der Henst et al., 2016), which are capable of surviving and multiplying inside FLA. Intracellular growth of those pathogens within an amoeba has revealed a significantly increased bacterial resistance to antibiotic substances and simultaneously increased bacterial virulence (Cirillo et al., 1997; Cabral et al., 2003).

1.3 Acanthamoeba

Acanthamoeba was firstly described in 1930 by Castellani, who observed the presence of an amoeba in fungi *Cryptococcus pararoseus* cultures (Castellani, 1930). The amoeboid organisms were later recognized as a new species and named *Hartmannella castellanii* (Douglas, 1930). Volkonsky divided the genus *Hartmannella* into the three independent genera (*Hartmannella, Acanthamoeba, Glaeseria*) and re-categorized *Hartmannella castellanii* as *Acanthamoeba castellanii* (Volkonsky, 1931). The name "Acanthamoeba" was derived from the characteristic spike-like projections that it bears called "Acanthopodia", from the Greek word Acanthus, which means spine-like forms.

Members of the genus of *Acanthamoeba* are widely distributed in almost all natural and man-made environments, including soil and water. Furthermore, the micro-organism has been also isolated from AK infected individuals (Zhao et al., 2010; Behera and Satpathy, 2016), from contact-lens wearers (Gomez et al., 2016), pharyngeal swabs (Brindley et al., 2009), brain and corneal necro-biopsies (Lalitha et al., 1985; Zamora et al., 2014).

Notwithstanding the fact that *Acanthamoeba* was classified among infectious microorganisms from the seventies, only in the later years has there been an increased interest in microorganism function and characteristics. This is undoubtedly due to infections associated to *Acanthamoeba,* which have been increased considerably during latest years and simultaneously, upon to identification of *Acanthamoeba* genus pathogenicity, as members of the microorganism are responsible of causing numerous opportunistic diseases to humans (Cabral et al., 2003; Thomas et al., 2010; Cardas et al., 2012). Moreover, its diverse role and its ability to host other pathogenic agents, including viruses, bacteria and fungi, has also lead in that direction.

1.3.1 Taxonomy of *Acanthamoeba*

As a result of uncanonical and unspecified amoeboid cell shape and due to polyphyletic origin, taxonomic classification of *Acanthamoeba* genus presents some challenges and varies slightly from author to author (Table 2). Initially, *Acanthamoeba* genus was categorized into 3 different groups I, II and III (Pussard and Pons, 1977) based on morphological characteristics, which by the way have been proven to be of a very low phylogenetic significance. Anaphorically, mitotic spindle, trophozoites, cyst's endo- and ecto-structures were the main factors used for *Acanthamoeba* cataloguing (Pussard and Pons, 1977).

	NCBI	ITIS	Corsaro 2015
Super-Kingdom	Eukariota	Eukariota	Eukariota
Kingdom		Protozoa	Protozoa
Sub-kingdom			Sacromastigota
Phyllum	Amoebozoa		Amoebozoa
Sub-Phyllum		Sacrodina	Lobosa
Super-Class		Rhizopoda	
Class	Discosea	Lobosa	Discosea
Sub-Class			Longamebia
Order	Longamoeba	Amoebida	Centralmoebida
Sub-Order	Centramoebida		
Family	Acanthamoebidae	Acanthamoebidae	Acanthamoebidae
Genus	*Acanthamoeba*	*Acanthamoeba*	*Acanthamoeba*

Table 1.2: Differential taxonomic classification of *Acanthamoeba* based on National Centre for Biotechnology Information NCBI, Integrated Taxonomic Information System (ITIS) and Corsaro et al., 2015.

More precisely, group I mainly includes large amoebae with a stellate endocyst shape and distinct demarcation between endocyst and ectocyst. *A. astronyxis, A. comandoni, A. echinulata and A. tubiash* are categorized in group I. In the second group (Group II) are included amoebae with usually smaller size cysts (mean diameter less than 18μm) which show dissimilar structures of endocyst, such as polygonal, triangular, round, oval and stellate and a crumpled ectocyst. This group comprises a plethora of *Acanthamoeba* genus including *A. castellanii, A. mauritaniensis, A. polyphaga, A. lugdunensis, A. divionensis, A. paradivionensis, A. griffin, A. triangularis and A. hatchetti*. Finally, in the third and last group (Group III) are included amoebae with rounded endo- and ecto-cyst like *A. palestinensis, A. culbertsoni, A. lenticulata, A. jacobsi and A. healyi* (Pussard and Pons, 1977).

Iso-enzyme profile comparisons had been also proposed as an additional method for *Acanthamoeba* phylogeny clarification. Proteolytic profile analysis of esterases and acid-phosphatases along with other enzymes (Jonckheere, 1983; Costas and Griffiths, 1980, 1985) could have been used in that way, however this procedure was abandoned, as it had relatively low phylogenetic value. Later and in the same way De Jonckheere used iso-enzymes as a classification method. Acid-phosphatases, glucose phosphatase isomerases, phosphogluco-mutases, leucine amino peptidases, alcohol dehydrogenases and malate dehydrogenases were analysed in order to indicate a potential physiological protein pattern, which in turn could lead in a form of phylogenic clarification (De Jonckheere, 1983). Later, Kong suggested that a combination of an iso-enzyme profile comparison and a simultaneous mtDNA fingerprint (restriction fragment length polymorphism) analysis, could have proven important in *Acanthamoeba's* strain identification, characterization and differentiation (Kong et al., 1995).

Nowadays, the most favoured method for classification of *Acanthamoeba* genotypes has been the examination and the assiduous comparison of the small-subunit (SSU) 18S ribosomal DNA (rDNA) gene through DNA sequencing. The 18S gene is more than 2kb and differs from genus to genus, providing an ideal alternative in species categorization. Based on 18S discrepancy, Schroeder recommended the analysis of a smaller diagnostic fragment of the 18S gene (ASA.S1 113bp) as a highly trustworthy way of *Acanthamoeba* classification (Shroeder et al., 2001). Notwithstanding the fact that analysis of ASA.S1

fragment presented an interesting and quick classification of various strains, the length of the full 18S gene is considered essential for precise identification. Smaller gene region analysis, such as of ASA.S1 fragments, could be indicative of a lineage but it is not particularly decisive as it could be characterized by lack of information, which is only obtainable from the full gene sequence (Corsaro, 2015).

Currently, *Acanthamoeba* ıs classified into 20 different genotypes (Table 3) T1-T20, based on 18S rRNA gene sequence analysis, while the taxonomy is continuously variable (Booton et al et., 2002; Hewett et al., 2003; Marciano-Cabral et al., 2003; Hyun Hee Kong 2009; Corsaro, 2010; Navarro et al., 2015; Siddiqui and Khan, 2012; Corsaro et al., 2015). Each genotype presents approximately 5% genetic sequence dissimilarity among different genotypes and simultaneously, at least 5% difference in the 18S rDNA comparisons is required for a new genotype to be defined and identified (Fuerst, 2015). The T4 genotype has been described as the most encountered (up to 88%) and is associated with many amoebic human infections (Stothard et al., 1998; Walochnik et al., 2000; Booton et al., 2005). Moreover, it is the genus of *Acanthamoeba* most frequently found in the natural environment (Maciver et al., 2013; Nuprasert et al., 2010).

While numerous molecular features have been applied for the classification of *Acanthamoeba* species, the identification system could be still upgraded. A partial combination of the aforementioned methods could provide the best taxonomy result with the most closely related species. For example, sequence analysis of the 18S rDNA with simultaneous analysis of the 16S mtDNA sequence could provide additional data to subcategorize the strains of the genotype T4, in which the most clinical and environmental isolates belong (Kong and Chung, 1996; Kong, 2009).

Genotypes	Species	AK	GAE	Morphological Group
T1	*A. castellanii*	-	+	II
T2	*A. palestiniensis; A. polyphaga*	-	+	III
T3	*A. griffini; A. pearcei*	+	-	II
T4	*A. castellanii; A. ludgunensis; A. polyphaga; A. triangularis*	+	+	II
T5	*A. lenticulata*	+	+	III
T6	*A. hatchetii; A. palestiniensis*	+	-	III
T7	*A. astronyxis*	-	-	I
T8	*A. tubiashi*	-	-	I
T9	*A. comandoni*	-	-	I
T10	*A. culbertsoni*	-	+	III
T11	*A. stevensoni*	+	-	II
T12	*A. healyi*	-	+	III
T13		-	-	II
T14		-	-	III
T15	*A. jacobsi*	+	-	III
T16		-	-	II
T17		-	-	I
T18	*A. byersi*	-	+	I
T19	*A. micheli*	-	-	II
T20		-	+	II

Table 1.3: Different genotypes of *Acanthamoeba* strains. *Acanthamoeba* Keratitis (AK) and Granulomatous *Acanthamoeba* Encephalitis (GAE) columns display the strain's reported ability to cause the diseases. Morphological group refers to the morphogroup of each strain.

1.3.2 *Acanthamoeba* life cycle

The life-cycle of *Acanthamoeba* is quite flexible and is separated into two different major stages or forms: an active, feeding, vegetative and dividing trophozoite unicellular form, ranging from 20 to 40 μm and a dormant resistant double-wall cyst form, ranging from 5 to 25 μm (Neff, 1957; Visvesvara et al., 2009), (Figure 1). The decrease in cell surface area is approximately 65% and simultaneously the cell volume is lowered around 80%. This massive transformation is mainly due to dehydration (Lorenzo-Morales et al., 2013) and excretion of cytoplasmic constituents.

In the stage of trophozoite, *Acanthamoeba* enjoys nutrient adequacy and optimal external conditions (neutral pH, temperature ~30°C, osmotic pressure around 50-80 mOsmol). *Acanthamoeba* trophozoites feed on bacteria, algae and yeast by phagocytosis and other organic particles such as small peptides and amino acids by pinocytosis (Neff, 1957; Cabral and Cabral, 2003). Furthermore, they reproduce mitotically (binary fission and non-sexual) resulting in two genetically identical daughter cells under favourable conditions (Martinez and Visvesvara, 1997; Khan, 2006). Despite the fact that organisms which reproduced asexually accumulate harmful mutations in an irreversible manner, it has been proposed that *Acanthamoeba* avoids Muller's ratchet effect though polyploidy (Maciver, 2016).

It appears that in axenic conditions, a microorganism's growth demonstrates a classic exponential growth phase, after an initial lag phase, followed by a post-log phase showing a reduction in growth rate and finally a stationery stage is observed (Band and Mohrlok, 1973), (Figure 2). A number of factors such as lack of nutrients and increasing waste concentrations could decrease growth and simultaneously increase fractional encystation (Neff et al., 1958).

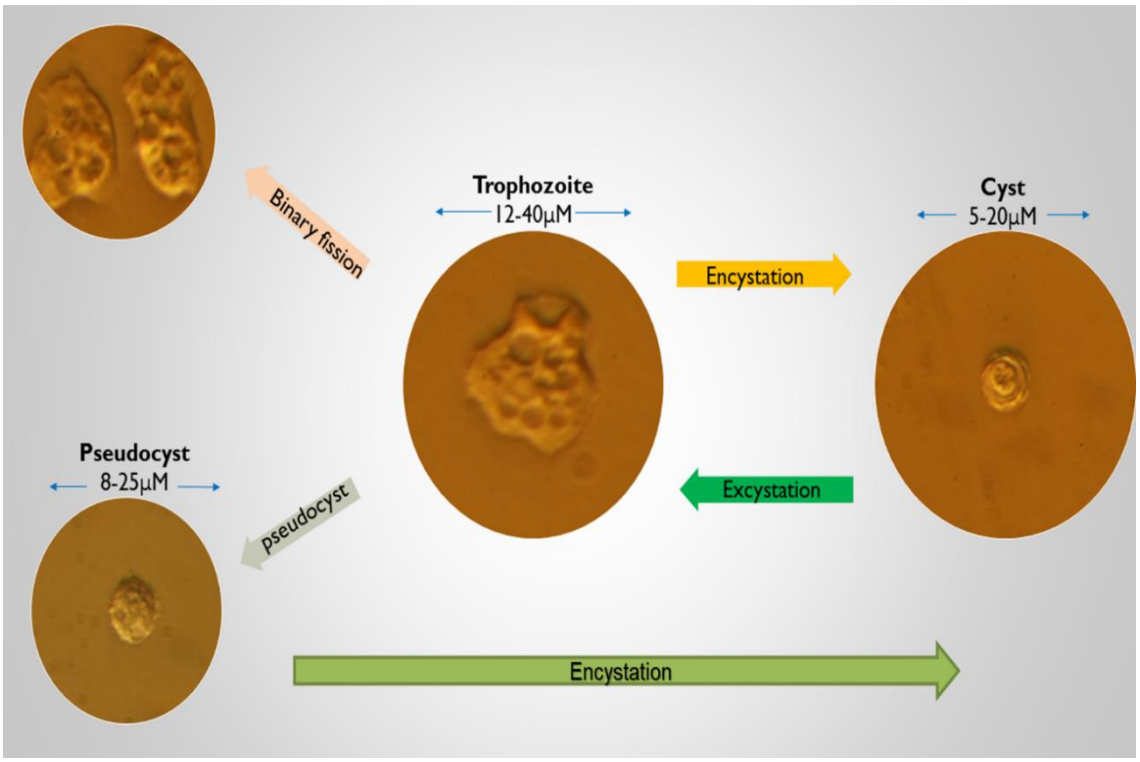

Figure 1.1: Simplified life cycle of *Acanthamoeba*

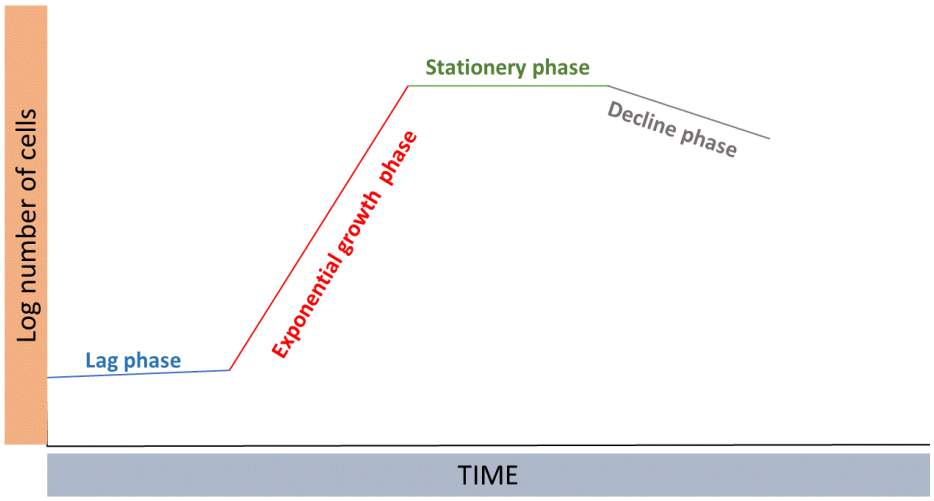

Figure 1.2: *Acanthamoeba's* growth diagram in axenic conditions, over time.

The differentiation into a mature, resistant and dormant double-wall cyst (Figure 1), a process widely known as encystation, is encouraged when adverse and unfavourable conditions prevail, such as lack of food (Neff et al., 1964), by the presence of a variety of chemicals (Kilvington et al., 2008), by wide-ranging fluctuations in environmental temperature, pH variations (Brindley et al., 2009), osmolarity deviations (Cordingley et al., 1996) and even after infection by bacteria species like *Francisella tularensis* (El-Etr et al., 2009).

Biochemical differentiation, cell growth termination and numerous morphological alterations are some of the characteristics that accompany encystation. Cysts present minimal metabolic activity as the cellular levels of proteins, RNA, glycogen and triacyglycerides are reduced considerably. Furthermore, RNA levels are reduced by 50%. It was reported that one hour after translocation of *Acanthamoeba* trophozoites to non-nutrients medium, rRNA reduction reaches 70-80%, compared to *Acanthamoeba* trophozoites that grown in a nutrient media, whereas after 7 hours rRNA synthesis is not detectable. Meanwhile, RNA polymerase I, II, III activities remain stable during encystation (Schulze and Jantzen, 1982; Steven and Pachler, 1973; Detke and Paule, 1778a, 1979). Bio-molecular synthesis is essential during encystment since presence of RNA and protein synthesis inhibitors such as Cycloheximide or Actinomycin, *Acanthamoeba* failed to form fully mature cysts indicating the importance of protein synthesis (Stewart and Weisman, 1972).

Cyst double-wall formation allows *Acanthamoeba's* survival in adverse and unfavourable conditions. They are characterized mainly by their high resistance, secondly by their minimal metabolic activity (low levels of cellular proteins, RNA and glycogen) and finally by maintaining the pathogenicity of pathogenic strains. These airborne formations can be viable for more than 25 years (Sriram et al., 2008) and 'sprout' again under favourable conditions. Moreover, cysts provide protection to amoebae after treatment with anti-microbial substances, pharmaceutical factors (Bowers and Korn, 1969) and simultaneously, are responsible for the high resistance to a host's immune system attack, rendering *Acanthamoeba* treatment and eradication particularly problematic.

Throughout the period of encystation, characteristic structures that are called ostioles are monitoring the exterior conditions. When these become favourable or are at least capable of supporting developmental progression, trophozoites emerge from cysts through ostioles, by a process that is widely known as excystation.

There are two more life stages of *Acanthamoeba* that are actually included in the more general biphasic model. For instance, pre-cysts and immature cysts are two states of the *Acanthamoeba* life cycle that present differences compared to trophozoites and mature double wall cysts. This terminology has been used to clarify and highlight different morphological characteristics and simultaneously specify the intermediate level of encystment, which occurs during the encystation process (Chávez-Munguía et al., 2013). Additionally, another state of *Acanthamoeba* existence is the form of a single-walled pseudocyst (Figure 1), which resists immediate insult but lacks rudimentary characteristics of the cyst wall layers (Kliescikova et al., 2011a; Kliescikova et al., 2011b). DMSO, acetone, methanol and propylene glycol are some solvents that can induce this particular formation, which provides a superior resistance to *Acanthamoeba* against cleaning product solutions. As well as morphological dissimilarities, cysts and pseudocysts also present great dissimilarities and variability in their gene expression profiles (Kliescikova et al*.,* 2011b).

In 2006, Tice et al. showed that *Prostelium pyriformis* was basically a genus of *Acanthamoeba* and renamed the species as *Acanthamoeba pyriformis*. *A. pyriformis* is able of forming a fruiting-like body called sporocarp. The sporocarp is formed by a non-cellular stalk with a walled spore at the top and fails to form in aquatic habitats. *Acanthamoeba pyriformis* is the first species of *Acanthamoeba* identified to include facultative sporocarps in its life cycle while the existence of sporocarpy in other Acanthamoebidae has not yet been reported (Tice et al., 2006).

1.3.3 *Acanthamoeba* morphology and cell biology

Characteristic domains and organelles such as plasma membrane, Golgi apparatus, lysosomes, ribosomes, large numbers of dumbbell-shaped and spherical mitochondria, nucleus and numerous vacuoles are present in Acanthamoebidae cells as in all eukaryotic unicellular organisms (Khan, 2006). More specifically, more than one vacuole are typically distinguished and their role includes water expulsion for osmotic regulation (contractive vacuoles) and digestive purposes (digestive vacuoles) (Siddiqui et al., 2012; Lorenzo-Morales, 2013).

Acanthamoeba trophozoites are fairly large compared to other protozoa and are characterized by the typical formation on their surface of acanthopodia, which are spine-like projections. Acanthopodia are cytoskeletal structures that extend from the main cell body, contributing to the microorganism's representative shape (Figure 1.3).

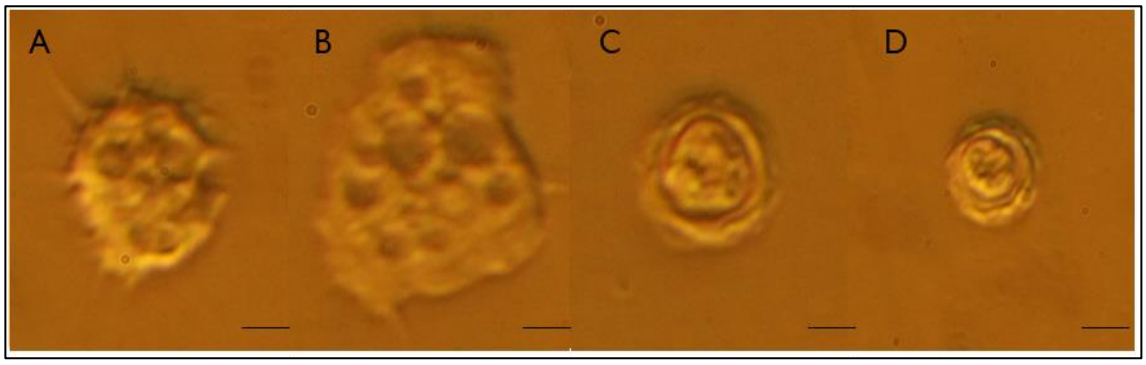

Figure 1.3: Characteristic morphological shapes of *Acanthamoeba* trophozoites and cysts. Acanthopodia (A) and other formations like nucleus, plenty of vacuoles (B) and double wall cyst formations are easily distinguished (C, D), 5μm scale bar.

The biological role of acanthopodia generally comprises locomotion, adhesion to biological surfaces and food engulfment, which are achieved through a combination of actin, myosin and other cytoskeletal proteins (Gordon et al., 1976; Baines et al., 1992). Plasma membrane is composed of approximately 33% protein, 25% phospholipids, 29% lipo-phosphonoglycan and 13% sterols (Khan, 2006). Mannose-binding protein is also expressed in *Acanthamoeba* trophozoites plasma membrane and is crucial to host-cell adhesion (Gordon et al., 1993).

Acanthamoebidae are typically uni-nucleate and polyploid (numerous chromosomes from 2.2 x 10^5 bp to 2 x 10^6 bp) microorganisms, however multinucleate individuals have been also detected. Its genome size is 4.1 Mb (Clarke et al., 2013) and encodes 15,455 compact intron-rich genes, of which an important percentage is predicted to have originated from inter-kingdom lateral gene transfer. It is estimated that there are on average 3 exons per gene in *Acanthamoeba*, while at the same time, *Entamoeba histolytica* contains approximately 1.3 exons per gene and *Dictyostelium discoideum* around 2.3 exons per gene (Aderson et al., 2005).

Acanthamoeba cysts are characterized by a dormant resistant double-walled form that offers an advantage in microorganism survival, in environmental extreme fluctuations and on antimicrobial substances exposure. The size ranges from 15 to 30μm (Martinez et al, 1997). *Acanthamoeba* cysts have a double-layered wall, forming the endo- and the ecto-cyst. The ectocyst (the external wall of the cyst) consists mainly of proteins and polysaccharides while the endocyst is composed of cellulose (Tomlinson and Jones 1962; Blanton and Villemez, 1978; Hirukawa et al., 1998). Cellulose accounts for approximately 10% of the cyst weight and is not detected in trophozoites. Carbohydrates are present in both walls, but ectocyst is reported to have a greater quantity of proteins (Dudley et al., 2009). Despite the fact that the cyst's composition usually differs from one species to another, it was first reported that cyst wall components are practically composed of 33% proteins, 35% cellulose, 8% ash, 6% lipids and 20% unspecified components (Neff and Neff, 1969; Dudley et al., 2009).

Throughout cell differentiation the carbohydrate content of *Acanthamoeba* alters. Trophozoite carbohydrates are composed mainly of glucose (approximately 98%),

whereas *Acanthamoeba* cysts have lower and equal quantities of glucose and galactose (approximately 45% respectively) among carbohydrates (Dudley et al., 2009). Mannose-binding protein is not detected in cyst formations, explaining the incapability of cysts to bind to any host cells, while cellulose and acid-insoluble protein are not detected in trophozoites (Fouque et al., 2012; Neff and Neff, 1969; Tomilson and Jones, 1962). Finally, cysts are also characterized by three or four distinctive formations which is called ostioles and are organs responsible for environmental variation detection and excystation (Bowers and Korn, 1969).

1.3.4 Distribution and Ecology

Acanthamoeba species have been isolated from diverse environments, including fresh water, seawater, beaches (Lorenzo-Morales et al., 2005), lakes, rivers, ocean sediment, chlorinated swimming pools, lakes, tap water (Jeong, 2007; Bagheri et al., 2010), bottled mineral water (Rivera et al., 1981; Maschio et al., 2014), humidifiers (Tyndall et al., 1995), air conditioning system (Astorga et al., 2011), air, sewage (Sawyer et al., 1992), soil, compost (Conza et al., 2013), hospitals, dental treatment units, surgical instruments (Rezaeian, 2008), animal faeces (Rezaeian et al., 2008), dialysis units, nasal cavities, paranasal sinuses (Visversvara, 2013), throats and intestines, as well as from infected tissues, skin lesions, including cerebral tissue, skin wounds and corneas (De Jonckheere, 1987; Khan, 2006).

Given the fact that *Acanthamoeba* is so widely distributed, interaction with humans is inevitable. It was reported that more than 85% of individuals possess anti-*Acanthamoeba* antibodies and specifically secretory IgA, regardless of region, nationality and gender (Cursons et al., 1980; Chappell et al., 2001; Brindley, 2009).

Acanthamoeba plays a significant role in bacterial population regulation as it consumes bacteria in order to fulfil its nutritional requirements and simultaneously contributes to nutrient cycling and to geo-microbial loop conservation. It also preys on fungi, algae and other protists through phagocytosis (Weisman and Korn, 1967; Bowers

and Olszewski, 1972). Cytoplasmic body formations called phago-lysosomes are essential for intracellular digestion of microorganisms and other pathogens. These formations are created when the membranes of both phagosomes and lysosome merge and hydrolytic enzymes are discharged into the phagosomes, digesting particles that have been ingested. Microorganisms are decomposed within phagolysosomes by a combination of acidification, oxidative and non-oxidative procedures (Haas, 2007; Strassmann and Shu, 2017). After this point the useful derivatives are transferred to the microorganism's cytoplasm for further processing, whereas others are exported by exocytosis (Bowers, 1983).

Soil fertilization is based to a large extent on amoeboid metabolic products, which include plant-absorbable nitrogen derivatives (Woods et al., 1982; Bodelier, et al., 1993). It was proven that the soil that contained Acanthamoebae and other bacteria showed considerably higher mineralization of nitrogen, carbon and phosphorus in comparison to soil containing only bacterial populations (Woods et al., 1982; Bodelier, et al., 1993).

1.3.4.1 *Acanthamoeba*-bacteria interactions

Generally, there are 3 different types of interaction, developed among *Acanthamoeba* and bacteria. Some of these relationships are regulated by external factors such as temperature, availability of nutrients and ability to infect different adjacent cell populations. A characteristic example is the established interaction among *Acanthamoeba* and *L. pneumophila* in which, at temperatures around 37°C, *L. pneumophila* acts as a pathogen while at temperatures around 20 °C it is digested by *Acanthamoeba* (Anand et al., 1983).

The first group principally comprises relationships that benefit amoebae over bacteria. Despite the plethora of Gram-positive bacteria, *Acanthamoeba* shows a preference for Gram negatives (Weeker, 1993) such as *Escherichia coli* and *Klebsiella aerogenes,* although it can actively feed on other species like *Agrobacterium tumefaciens, Chromatium vinosum, Anacystis nidulans, Gloeocapsa alpicola, Anabaena flos-aquae,*

Pseudomonas fluorescens, Bacilus subtilis, Serratia marcescens, Bacillus megaterium and Micrococcus luteus (Wright et al., 1981; Weeker, 1993).

The second group includes relationships that benefit bacteria over amoeba such as with *Bacillus anthracis, Ralstonia picketti, Vibrio cholerae, Helicobacter pylori, Listeria monocytogenes, Mycobacterium avium, Parachlamydia acanthamoebae, Chlamydia pneuminiae, Burkholderia cepacia, Coxiella burnetii and Pseudomonas aeruginosa* (Greub and Raoult, 2004; Khan, 2009; Michel and Hauröder, 1997). These bacterial pathogens can survive and reproduce inside *Acanthamoeba,* which acts as bacterial transmission vehicle or "Trojan horse" and a biological reservoir; furthermore it provides increased resistance to the host's immune attacks and enhanced resistance to antibiotics and biocides (Barker et al., 1995; Walochnik et al., 1999). When the conditions are favourable, growing bacterial masses lyse their host amoebae and infect surrounding hosts such as animals and humans, causing diseases (Essig et al., 1997; Amann et al., 1997; Greub and Raoult 2004; Dey et al., 2012).

The third group includes interactions that are beneficial to both amoebae and bacteria. *Acanthamoeba* spp. in the presence of bacteria present a greater virulence than those growing axenically (Larkin et al., 1991), while bacteria including *Legionella pneumophila* and *Mycobacterium avium* can increase their virulence and pathogenicity (Cirillo et al., 1997). Furthermore, bacteria grown inside *Acanthamoeba* can present enhanced resistance to antibiotics, increased thermotolerance and improved invasiveness (Walochnik et al., 1999).

Species	**Human Disease**	**Location**	**Relationship status**
Bacillus anthracis	Anthrax	Vacuoles	Parasitic
Burkholderia cepacian	Pneumonia	Extracellular	Symbiotic/ Parasitic
B. pseudomallei	Melioidosis	Extracellular	Symbiotic

Candidatus Nucleicultrix amoebiphila		Nucleus	Symbiotic/ Parasitic
Chlamydia pneumoniae	Pneumonia	Vacuoles	Symbiotic/ Parasitic
Coxiella burnetti	Q Fever	Vacuoles	Symbiotic
Escherichia coli	Dysentery	Vacuoles	Symbiotic
Francisella tularensis	Tularemia	Vacuoles	Symbiotic
Helicobacter pylori	Asymptomatic	Vacuoles	Symbiotic
Legionella pneumophilla	Legionnaire's disease	Cytoplasm	Symbiotic/ Parasitic
Legionella anisa	Pontiac fever	Cytoplasm	Symbiotic/ Parasitic
Listeria monocytogenes	Listeriosis	Cytoplasm	Symbiotic
Mycobacterium avium	intracellular infection	Cytoplasm	Symbiotic
Mycobacterium leprae	Leprosy	Lysosomes	Symbiotic
M. ulcerans	Buruli ulcer	Cytoplasm	Symbiotic
Parachlamydia acanthamoebae	Respiratory Infections	Vacuoles	Symbiotic/ Parasitic
Pseudomonas auruginosa	Infects human cells	Extracellular	Symbiotic/ Parasitic
Ralstonia pickettii	Several infections	Vacuoles	Parasitic
Sarcobium lyticum	Respiratory infections	Cytoplasm	Parasitic
Salmonella typhimurium	Salmonellosis	Vacuoles	Symbiotic/ Parasitic
Simkania negevensis	Obstructive pulmonary disease	Cytoplasm	Parasitic

Taylorellae equigenitalis	Unknown	Cytoplasm	Symbiotic
Staphyloccocus aureus	Several infections	Cytoplasm	Symbiotic/ Parasitic
Vibrio cholera	Cholera	Cytoplasm	Symbiotic
Vibrio parahaemoliticus	Gastroenteratis	Extracellular	Symbiotic

Table 1.4: Summary of *Acanthamoeba* bacteria interactions

1.3.4.2 *Acanthamoeba*-virus interactions

Viruses are enormously diverse and abundant parasites which can infect organisms from all three major domains of life and likewise other viruses (Konin et al., 2006; Bernard La Scola et al., 2008, Desnues et al., 2012). They are also powerful tools for gene transfer (Miller and Rosman, 1989) and microbial evolution. Evidence suggests that past interactions with viruses and amoebae have left recognizable traces in the DNA of the latter, ranging up to several tens of kb and encoding viral proteins (Maumus and Blanc, 2016). It is not yet known whether these insertions are a product of an active viral activity or have emerged after accidental incorporation of viral DNA floating intracellularly. The best-known viruses that use members of amoebae for hosting purposes are the Mimivirus, Megavirus and Pandovirus. It has been found that 27 % (or 4,156) of *Acanthamoeba* genes are orphan genes (Clarke et al., 2013), while at the same time a large percentage of these genes are not usually shared, even among genetically closely related microorganisms.

Type	Virion type	Reference
Mimivirus	Icosahedral	Abrahão et al., 2014
Moumouvirus	Icosahedral	Yoosuf et al., 2012
Megavirus chilensis	Icosahedral	Legendre et al., 2012
Marseillevirus	Icosahedral	Colson et al., 2013
Melbournevirus	Icosahedral	Doutre et al., 2014
Cannesvirus	Icosahedral	Virus host DB
Tokyovirus	Icosahedral	Takemura, 2016
Lausannevirus	Icosahedral	Thomas et al., 2013
Port-Miou virus	Icosahedral	Doutre et al., 2015
Noumeavirus	Icosahedral	Fabre et al., 2017
Insectomime	Icosahedral	Boughalmi et al., 2013
Tunisvirus	Icosahedral	Aherfi et al., 2014
Brazilian Mvirus	Icosahedral	Dornas et al., 2014
Golden mussels	Icosahedral	Nunez et al., 2016
P. salinus	Amphora	Antwerpen et al., 2015
P. quercus	Amphora	Legendre et al., 2017
P. inopinatum	Amphora	Aherfi et al., 2016
P. dulcis	Amphora	Aherfi et al., 2016
P. neocaledonia	Amphora	Fabre et al., 2017
P. macleodensis	Amphora	Legendre et al., 2017
P. sibericum	Amphora	Legendre et al., 2015
P. massiliensis	Amphora	Pagnier et al., 2015
Cedratvirus A11	Amphora	Andreani et al., 2016
C. lausannensis	Amphora	Bertelli et al., 2015
Pacmanvirus	Icosahedral	Andreani et al., 2017
Mollivirus sibericum	Spherical	Maumus and Blanc 2017

Table 1.5: Integrated *Acanthamoeba*-virus interactions

1.3.4.3 *Acanthamoeba* and fungi interactions

Although identified relationships among fungi and *Acanthamoeba* are very rare, at least one fungal species has been reported to survive and reproduce inside *Acanthamoeba*. *Cryptococcus neoformans* presents features that contribute to increased mammalian virulence while at the same time promoting fungal survival inside *Acanthamoeba* (Steenbergen et al., 2001). These characteristics may have evolved as *Cryptococcus neoformans* defense mechanisms against amoebae.

1.3.5 Diseases and pathogenicity

Acanthamoeba trophozoites are the causative agents of at least four different types of diseases in humans including *Acanthamoeba* Keratitis, fatal Granulomatous Amoebic Encephalitis, *Acanthamoeba* rhinosinusitis and cutaneous Acanthamebiasis or granulomatous dermatitis. Immunocompromised individuals, including AIDS patients and patients who had recently an organ transplant, are particularly vulnerable to *Acanthamoeba* infections (Cabral and Cabral, 2003). Modern therapeutic approaches to *Acanthamoeba* infections have been various and quite challenging due to the microorganism's adaptable life style and resistance to amoebicidal substances.

Acanthamoeba's pathogenicity is principally devided into direct and indirect factors. The first category includes mechanisms which are directly utilized by the amoeba in order to breache host's cell biological barriers. *Acanthamoeba's* adhesion to host's cells, which is achieved by adhesion proteins, such as mannose-binding protein (Garate et al., 2004), or *Acanthamoeba's* proteolytic activity which is accomplished by a plethora of secretory proteases comprising neuroaminidases, elastases and glycosidases are categorized into the direct factors of pathgenicity. Phagocytosis is also categorized into

the same class. However, factors as trophozoite morphology, phenotypic switching (e.g. from trophozoites to cysts or pseudocysts formation), physiological tolerance in temperature, pH, osmolarity, chemotaxis and finally drug resistance are also play an important but indirect role in microorganism pathogenicity and should be taken under serious consideration.

1.3.5.1 *Acanthamoeba* Keratitis

Acanthamoeba Keratitis (AK) is a sight-threatening inflammation of the cornea and is considered an important ocular microbial infection that can cause partial or complete loss of vision. Historically, was firstly described in the United Kingdom in 1974 (Nagington et al., 1974), but was first reported in a 59-year old Texan farmer who had been subjected to perforation of the infected cornea and lens extraction (Jones et al., 1975) after unsuccessful treatment.

In AK, *Acanthamoeba* trophozoites infect the eye, penetrate the epithelial barrier and invade the cornea. The variety of proteases produced leads to corneal epithelial destruction and corneal stromal matrix dialysis (Clarke and Niederkorn, 2006). AK is accompanied by several symptoms, which comprise extreme levels of pain, photophobia, blurry vision, eye redness and extensive tear production (Wang et al., 1997; Verani et al., 2009, Khan, 2006). The most distinguishing clinical feature of AK is the existence of a ring-like stromal infiltrate, or perineural infiltrates (Marciano-Cabral and Cabral, 2003; Carballo et al., 2012). Clinical features like hyperthermia, lack of discharge and eyelid ptosis have been also reported (Niederkorn et al., 1999). *Acanthamoeba* genotypes that have been associated with corneal infections comprise *A. castellanii, A. cubertsoni, A. polyphaga, A. hatchetti, A. rhysodes, A, lugdunesis, A quina* and *A. griffini* (Siddiqui et al., 2012) (Table 3).

Infection commonly affects individuals with a damaged cornea and contact lens wearers (Nagington et al., 1974; Visvesvara, 1975; Moore et al., 1985). This is due to

presence of bacterial biofilms (Simmons et al., 1998) and protein particles in contact lenses, allowing adhesion, infection and growth of *Acanthamoeba*. Disease statistics have risen considerably over the years due to increased usage of contact lenses, cleaning of contact lenses with contaminated water, better diagnostics (Lorenzo-Morales et al., 2013) and simultaneously in some cases, reduced personal hygiene.

Acanthamoeba Keratitis is more prevalent in developed countries due to the increased number of contact-lens wearers (Stehr-Green et al., 1989; Lorenzo-Morales et al., 2013), however numerous cases of the disease have been reported across the globe. AK has also been described in non-contact lenses wearers (Sharma et al., 2000). Globally, the prevalence of the disease is estimated to be 1-33 cases per million. More precisely, in the United Kingdom 17-21 cases of *Acanthamoeba* keratitis per million contact lens wearers occur. The percentage of the AK occurrence is believed to be higher than in other European countries and United States of America due to storage in domestic tap water (Radford et al., 2002; Kilvington et al., 2004). Interestingly, an exceptionally high rate of 1.49 proven AK cases per 10,000 have been reported in West Scotland (Seal et al., 1999).

The pathogenesis of *Acanthamoeba* Keratitis is based primarily on factors such as trophozoite adhesion to the cornea which is considered an crucial primary step in the infectious cascade and is achieved through cornea mannose-specific surface receptors, secretion of extracellular proteases, phagocytosis and direct host's cell death while at the same time, factors such as anti-amoebic drug resistance, cell differentiation from infectious trophozoite to dormant cyst and physiological variations can contribute indirectly to *Acanthamoeba* pathogenesis (Clarke and Niederkorn, 2006; Lorenzo-Morales et al., 2015). For instance, pathogenic *Acanthamoeba* strains have been isolated from biocidal solutions for lens care (Russel et al., 1996), while McClellan et al., reported that *Acanthamoeba* cysts are both immunogenic and antigenic (McClellan et al., 2002).

Acanthamoeba keratitis can be very problematic to diagnose and to treat, since it greatly resembles herpes simplex virus keratitis, *Pseudomonas aeruginosa* keratitis and various fungal infections (Lorenzo-Morales et al., 2015). As a consequence, there is often a significant delay in forming an appropriate treatment strategy. The most frequently used

process for diagnosis is *in vivo* confocal microscopy (IVCM), as it is non-invasive and offers great sensitivity. Furthermore, corneal or tear specimens are routinely used for cell culture, in order to identify *Acanthamoeba* infection. PCR (Ikeda et al., 2012) and immunofluorescence are also greatly used (Marciano-Cabral and Cabral, 2003). The utilization of combined and different assays for quick and successful diagnosis of AK is strongly recommended as molecular techniques alone are reported to be inadequate (Scheid and Balczun, 2017).

There is no standard therapeutic procedure that can guarantee a 100% positive outcome. However, recent approaches involve the usage of combined antimicrobials like biguanides, diamidines, (Oldenburg et al., 2011; Carvalho et al., 2016) and chlorhexidine (Clarke et al., 2012) for treating both trophozoites and cysts with noteworthy outcomes. In many cases, corneal transplant (keratoplasty) is the only possibility to reduce the parasite load on the cornea and increase recovery chances (Hammersmith, 2006), especially in late diagnosis cases. After the completion of the therapy, close observation for long periods is warranted, to rule out disease reoccurrence.

1.3.5.2 Granulomatous Amoebic Encephalitis (GAE)

Granulomatous Amoebic Encephalitis is a high-fatality rate but rare infection of the Central Nervous System (CNS) that is mainly caused by *Acanthamoeba spp*, while *Balamuthia mandrillaris* (Visvesvara et al.,1990), *Sappinia diploidea* (Gelman et al., 2003), *Naegleria fowleri* and *Paravahlkampfia francinae* have been also reported as GAE causative agents (Guarner et al., 2007; Visvesvara et al., 2009). GAE occurs generally but not invariably, in immunocompromised patients, such as HIV patients (Sangruchi et al., 1994; Martinez et al., 2000) or pharmaceutical secondarily immunocompromised individuals who had recently an organ transplant surgery (Anderlini et al., 1994; Steinberg et al., 2002). GAE is lethal subacute cause of meningoencephalitis typically occurring

within 2 months of initial symptoms appearance and is rarely identified in patients before death.

The symptomology of GAE can mimic a brain abscess or bacterial meningitis and includes fever, headache, seizures, nausea, stiff neck, vomiting, somnolence, photophobia, confusion, hemi-paralysis and coma (Visversara, 2007; Crary, 2011). Sometimes GAE displays a chronic course with atypical symptoms including seizures, headaches, encephalopathy abnormalities and low-grade fever (Meersseman et al., 2007). The pathologic morphology of an infected brain presents oedema and numerous necrotic and hemorrhagic nodules located generally in the cerebral hemispheres, in midbrain, in pons, in medulla oblongata and in cerebellum (Pittella, 2013; Yu Yee Ong et al., 2017). GAE is responsible for pro-inflammatory responses and physiological cortical mutilation. Additionally, granuloma development suggests participation of the host immune response composed of $CD4^+$ and $CD8^+$ T cells (Lanocha-Arendarczyk et al., 2018).

Nasal passage to lower respiratory tract and skin trauma are the main ways by which amoebae gain access to the host. Later, *Acanthamoeba* can cross the blood brain barrier (Martinez, 1991) and infect the brain. The incubational period to disease varies from several days to months, however life expectancy drops to days once the infection reaches the CNS (Khan, 2006; Zamora et al., 2014). *Acanthamoeba* genotypes that have been associated to GAE comprise *A. culbertsoni, A. castellanii, A. lenticulata, A. byersi, A. palestiniensis, A. polyphaga, A. healyi and A. triangularis* (Table 3).

The mechanism by which *Acanthamoeba* traverses the blood-brain barrier has been superficially analysed however, experimental data propose the involvement of microorganism-characteristic proteins, including mannose-binding protein and serine proteases (Siddiqui et al., 2011). The proteolytic action of serine proteases may lead to loss of integrity of tight junction proteins ZO-1 and occludin, which in turn could mediate increased passage permeability (Pittella, 2013).

Unfortunately, in most cases identification of GAE is post mortem and includes cultivation, microscopic detection of the amoebae morphological forms and PCR

techniques from biopsy samples (Guarner et al., 2007; Visversara, 2013; Zamora et al., 2014). MRI imaging techniques have also been mobilized without a significant outcome, as several diseases such as brain tumours and brain abscesses present similar characteristics, rendering GAE initially inconspicuous. When the infection passes through the blood brain barrier, it is practically impossible to stop its expansion, as the majority of the anti-amoeboid pharmaceutical substances that have been used, including rifampin, voriconazole, fluconazole gluconate, cotrimoxazole, miltefosine, amikacin, pentamidine, amphotericin B and others, are incapable of passing the blood-brain barrier (Visvesvara, 2010; Webster et al., 2012; Zamora et al., 2014; Duggal et al., 2017). However, if the identification of *Acanthamoeba* as the infectious agent is verified soon enough, there are enhanced possibilities of effective treatment by a combination of four or five amoebicides (Martinez et al., 1991, 2000; Slater et al., 1994; Aichenburg et al., 2008). Also, therapy completion, close observation is warranted, to rule out disease imminent reoccurrence.

1.3.5.3 *Acanthamoeba* Rhinosinusitis

Acanthamoeba Rhinosinusitis is a rare inflammation of the sinuses that mainly affects immunocompromised patients and HIV carriers. It is characterized by nasal obstruction, headaches, fever, crusting, otorrhea and epistaxis (Dickson et al., 2009; Rivera et al., 2002; Commarato, 2015). Furthermore, necrosis of bone and cartilage structures in the nasal cavity has also been reported (Dickson et al., 2009). The disease diagnosis is problematic as it resembles viral and bacterial rhinosinusitis and until now there has been no specific treatment process. In some cases, paranasal sinuses have been removed surgically (Teknos et al., 2001) as in all other *Acanthamoeba* infections, rapid identification and aggressive antibiotic combinations are essential to a successful treatment.

1.3.5.4 Cutaneous Acanthamebiasis

Acanthamoeba is able to cause extraordinarily rare cutaneous lesions which are described as erythematous polymorphic and intradermal nodules, ranging from millimetres to centimetres in diameter (Hunt et al., 1995; Casper et al., 1999). Furthermore, papules, plaques, pustules and intramuscular blisters have been described (Deluol et al., 1996; Dunand et al., 1997; Paltiel et al., 2004). Lesions have been reported to be pruritic (Murakawa et al., 1995) and generally advance through ulceration. In many cases a necrotic scar of dead cells develops around the skin lesion.

Cutaneous lesions tend to be a characteristic feature of immunocompromised patients and particularly in GAE poor prognosis cases. These alterations constitute a late sign of the infection (Paltiel et al., 2004). Interestingly, in cases where CNS is not involved, cutaneous acanthamoebic alterations are acute to subacute and simultaneously more easily treatable with an appropriate therapy strategy.

Chapter 2

Introduction

2.1 Cell Death

For many years, scientists considered cell death to be an imminent consequence of cell life, however evidence suggests a more complex set of genetically encoded mechanisms for precise cell elimination. From a conceptual standpoint, a cell is considered dead when its internal organization collapses or is incapable of maintaining essential cellular functions such as respiration or reproduction. Recently the Nomenclature Committee on Cell Death (NCCD) has set some criteria according to which a cell is considered dead when its membrane integrity has been lost, cell cytoplasm lost and its nucleus has experienced breakdown and fragmentation into distinct bodies (Kroemer et al., 2009).

In 2005, Melino categorized the forms of cell death into eleven different types that were distinguishable in eukaryotes, according to morphological, enzymological, physiological or pathological criteria (Melino et al. 2005). Nowadays, the number of different cell death types has increased to 22, based on updated guidelines which were proposed and introduced by the NCCD for the description and clarification of cell death, based on morphological, biochemical and functional parameters (Galluzzi et al., 2018). However, it should be mentioned that many authors tend not to follow this classification literally.

Generally, cell death is divided into two large categories including accidental cell death (ACD) and regulated cell death (RCD). Regulated cell death (RCD) is an important biological process that promotes the elimination of the undesirable cells (eg. cancerous or pathogen infected) and is considered among the most significant areas of cell biology. It is associated with two diametrically opposed situations, occuring after intra- or

extracellular environment perturbations or in the absence of any exogenous stimulus. On the other hand, as its name suggests, ACD occurs naturally after violent alterations or physical trauma in cell structure and homeostasis (Galluzzi et al., 2018).

Three major morphological types of regulated cell death that have been described as the most frequently occurring types and include apoptosis, necrosis and autophagy-dependent cell death. A stable accumulation of evidence proposes that cell death types are usually controlled by parallel pathways, engage the same sub cellular regulator organelles such as mitochondria and may be also characterized by the same initiator and effector molecules (Roach et al., 2000; Baehrecke, 2002).

2.2 Apoptosis

Apoptosis derives from the Greek “ἀπόπτωσις” which means “falling off” and was used initially by Kerr, Wyllie and Currie in 1972 to describe a specific subtype of regulated cell death, based on morphological and biochemical criteria (Kerr et al., 1972, 2002; Kroemer et al., 2009). It is an active, ATP-dependent internal process (Elmore 2007) that requires activation of bio-molecular signalling pathways to initiate it. Apoptosis is an essential mechanism in organ development and differentiation and also a crucial process by which old, non-functional and malignant cells are discarded. Disorders and mutations of genes that regulate apoptotic pathways could cause several diseases. In almost 50% of all human malignancies, genes involved in apoptosis are suppressed (Ozaki and Nakagawara, 2011; Lowe and Lin, 2000; Fernald and Kurokawa, 2013), whereas premature or incorrect stimulation of cell death pathways is implicated in many neurodegenerative disorders, including Alzheimer’s disease (Laferla et al., 1995) and Parkinson’s disease (Mochizuki et al., 1996).

Apoptosis is initiated by extracellular or intracellular stress signal transduction, originating mainly from microenviromental perturbations including endoplasmic reticulum stress, DNA damage and ROS overload and occurs normally as a programmed sequence of events. It has been broadly studied in metazoans and higher eukaryotes, while it is considered to be the natural regulator of tissue homeostasis, growth, differentiation and

morphogenesis (Vaux and Korsmeyer 1999; Teng et al., 2011; Suzanne and Steller, 2013). Furthermore, apoptosis acts also as a natural defense mechanism when cells' physiological integrity is compromised either by disease development or by noxious agents (Norbury and Hickson, 2001). Numerous stimuli (extracellular in extrinsic apoptosis; intracellular in intrinsic apoptosis) are able to activate the downstream apoptotic signalling processes, however the biological response depends to a large extent on pathophysiological conditions, type and level of stimuli and finally cell type (Elmor, 2007).

Despite the fact that apoptosis has been related to metazoans and higher eukaryotes, forms of apoptosis or apoptosis-like cell death have been identified in several unicellular microorganisms including bacteria, yeasts and parasitic protozoans (Lewis 2000; Madeo et al., 1999; Christensen et al., 1995; Vardi et al., 1999). Morphologically and biochemically, apoptosis is characterized by cell shrinkage and decreased cytoplasmic volume, rounded up cellular formations, retraction of pseudopods, gradual nuclear pyknosis upon to chromatin condensation, karyorrhexis (although in many cases this is not required and is not employed as an exclusive characteristic to define apoptosis), mitochondrial dysfunction, membrane blebbing and apoptotic-body formation. Furthermore, apoptosis as a term and form of regulated cell death is characterized by major functional and biochemical heterogeneity.

The process of apoptosis is genetically controlled and relies on numerous intracellular signalling systems. It is usually caspases (cysteine proteases) dependent and energy-dependent procedure. Caspases have proteolytic action and are able to cleave proteins at aspartic acid residues. Furthermore, different caspases show different specificities concerning amino acid identification (Cohen, 1997; Rai et al., 2005). At least fourteen different caspases have been identified in mammalian cells and have been categorized by their function. Caspases 2, 8, 9 and 10, have long pro-domains, require dimerization in order to function and are characterized as signal initiators responsible for downstream cascade activation. Caspases 3, 6 and 7 are considered effectors and are responsible for cell disassembly by cleavage of cell components. The outcome of their precise and selective cleavage is responsible for apoptosis' special morphological features (Fink and Cookson, 2005). Finally, caspases 1, 4, 5, 13 and 14 act as

inflammatory caspases. Apoptosis is irreversible once caspases are activated and is considered to be a quick process, as all necessary biochemical components, including complex protein cascades and the required molecular machinery for downstream signal transduction, are already existent in cells. Therefore, there is no need for additional protein synthesis (Elmor, 2007).

Two well studied and known mechanisms of apoptosis include the mitochondria-mediated pathway (intrinsic apoptosis) and the transmembrane receptor interaction-mediated pathway (extrinsic apoptosis).

2.2.1 Intrinsic or mitochondria-mediated apoptosis

In the case of intrinsic apoptosis, intracellular signals produced by various stress conditions and in combination with apoptotic factors that are released from mitochondria after outer membrane permeabilization (MOMp), such as cytochrome c (cyt c), smac/DIABLO, Apoptosis Induction Factor (AIF) and endonuclease G (Endo G) lead to cell death (Peixoto et al., 2011; Elmore, 2007). Permeabilization of MOM is considered to be the most critical and irreversible step for intrinsic apoptosis. Cytochrome c and smac/DIABLO are considered to be initiators of the caspase-dependent mitochondrial pathway, whereas EndoG and AIF can induce caspase-independent apoptotic cell death (Cande et al., 2002). More precisely, cytochrome c binds to Apaf-1 (Apoptotic protease activating factor 1), forming an apoptosome which in turn is responsible for initiator Cas 9 activation (Hill et al., 2004). Cas-9 activates caspase effector 3, which has proteolytic action and leads to cell death. Whereas cytochrome c activates APAF1 and caspase 9, smac binds IAPs, such as XIAP and cIAP proteins, leading to inhibition of their caspase-binding activity and allows caspase activation of apoptosis (Bai et al., 2014). However, reports have implied that even after sufficient caspase inhibition, some of the morphological features of apoptosis still remain visible (Chipuk and Green et al., 2005). AIF and Endo-G nuclease, on the other hand, translocate into the nucleus and cause

chromatin condensation and DNA fragmentation in a caspase-independent manner (Joza et al., 2001; Li et al., 2001).

Apoptosis inducing factor (AIF) is a phylogenetically early mitochondrial intermembrane flavoprotein first characterized in mammalian cells, capable of inducing chromatin condensation and DNA fragmentation without any caspase activity (Cande et al., 2002). Under normal conditions, AIF is located between the inner and outer mitochondrial membranes, nevertheless upon apoptosis induction, AIF is released from mitochondria and translocates to the cytosol and the nucleus. AIF has been associated with numerous mammalian and unicellular organisms' apoptosis and programmed cell death processes, including those in *Caenorhabditis elegans* (Wang et al., 2002), *Tetrahymena thermophila* (Akematsu and Endoh, 2010) and the slime mould *Dictyostelium discoideum* (Arnout et al., 2001). Observations like these strengthen the assumption that AIF-mediated cell death is a phylogenetically multi- and unicellular organism conserved form of cell death.

The members of the Bcl-2 family are evolutionarily-conserved proteins that share BH domains (-BH1, -BH2, -BH3, -BH4) and are considered the regulators of mitochondrial pro-apoptotic and anti-apoptotic events. These proteins are localized to the mitochondrial outer membrane and are reported to form voltage-dependent anion channel porins, (Arbel and Shoshan-Barmatz, 2010), which have either an inhibitory effect on cell death induction or instead prevent the protective influence of numerous apoptotic blockers (Cory and Adams, 2002), by inhibiting or promoting the release of pro-apoptotic factors respectively. The pro-apoptotic proteins in the BCL-2 family include Bcl-10, Bax, Bak, Bid, Bad, Bim, Bik and Blk and promote mitochondrial permeabilization while the anti-apoptotic proteins include Bcl-2, Bcl-x, Bcl-XL, Bcl-XS, Bcl-w and BAG and promote cell survival. Anti-apoptotic members of the Bcl-2 family contain a BH1, a BH2 and in some cases a BH4 domain, while at the same time pro-apoptotic members of the family contain a BH3 domain. BH3-only BCL-2 family proteins are effectors of canonical mitochondrial apoptosis (Lomonosova and Chinnadurai, 2009). BH3 only proteins were also shown to induce mitochondrial membrane remodelling through MOM regulation.

Interestingly, other members of the Bcl-2 family such as Noxa, which is a BH3 pro-apoptotic protein, are not restricted only to Bax/Bak-mediated cytochrome c release and standard mitochondrial downstream caspase cascade, but are involved in numerous pathways including mitochondrial dysregulation, endoplasmic stress and activation of apoptosis signal-regulating kinase 1 (ASK1) and its effectors c-Jun N-terminal kinase pathway and p38 (Chen et al., 2005; Hassan et al., 2008). In conclusion, BH3 domain-containing proteins are considered significant regulators of mitochondrial function and apparently cell death controllers.

2.2.2 Extrinsic apoptosis pathway

In the second scenario, the apoptotic machinery is directly activated by extracellular ligands that bind to transmembrane death receptors such as TNFR1, FasR1, DR3, DR4 and DR5 (Peter and Kramer, 1998; Rubio-Moscardo et al., 2005). Tumour necrosis factor (TNF) receptors present similar cysteine-rich extracellular domains and 80-amino acid cytoplasmic domains (Ashkenazi and Dixit, 1998) that are capable of transmitting the death signal from the outer cell membrane to the inner cell signalling machinery. Caspases play also a crucial role in signal transmission (Kischkel et al., 1995).

2.3 Necrosis

Necrosis (from the Greek “νέκρωσις” which means death) is a form of premature cell death caused mainly by autolysis and is defined by the absence of specific morphological characteristics, compared to apoptotic and autophagy-dependent cell death (Galluzzi et al., 2012). Typical features of necrosis include cytoplasmic and endoplasmic reticulum swelling, cell membrane rupture and the spread of intracellular contents (Marcel and Jäättelä, 2001).

For a quite long period, necrosis has been merely thought of as an accidental type of cell death and was used as a counterpoint to apoptosis, since their induction mechanisms and death morphologies significantly differ. However, there is evidence suggesting that necrosis could be a finely regulated process (Festjens et al., 2006; Golstein and Kroemer, 2007) and simultaneously, that there might be an overlap between these two biological processes (Nikoletopoulou et al., 2013). Furthermore, Denecker et al in 2003 proposed that an apoptotic ongoing process could be converted to a necrotic process either if the level of ATP diminishes significantly, or the volume and caspase availability decrease considerably. Death domain receptors in combination with caspases have also been linked to necrosis (Degterev et al., 2005; Kalai et al., 2002) and at the same time, extreme alterations in intracellular homeostasis have been reported to lead to a necrotic phenotype (Van den Berghe et al., 2014).

In general, cell type, nature of the signal, developmental stage of the cell and physiologic milieu are some of the basic factors that could determine and define the way and the dynamics by which a cell dies (Fiers et al., 1999; Zeiss, 2003).

Necrosis is commonly considered to be a fairly diverse, passive and energy-independent form of cell death, not defined by the presence of any apoptotic marker or common biochemical denominator and mainly used to describe non-apoptotic cell death (Elmor, 2007; Kroemer, 2009). In necrotic death, cell membrane integrity is lost in the very early stages and numerous factors are released from the cell and are able to trigger inflammatory responses. Necrosis is characterized by the large number of cells that are usually under that same pathophysiological effect in a small period of time (Galluzzi et al., 2012). Characteristic examples of agents that cause necrotic cell death include viruses and bacterial infections, radiation, heat, plenty of chemical substances and physical trauma caused by external factors (Kroemer, 2007).

2.4 Autophagy-dependent cell death

Autophagy, derived from the Greek 'αὐτόφαγος', meaning "to eat oneself", is an evolutionarily conserved, physiological, programmed, catabolic and destructive self-cell mechanism which degrades useless long-lived proteins, organelles, dysfunctional cell cytoplasmic macromolecules and cell components (Mizushima, 2007; Cuervo 2004; Klionsky, 2007). It has a large diversity of physiological and pathophysiological actions including anti-aging processes, tumour suppression abilities (Hippert et al., 2006), nutrient adjustment (Moriyasu and Ohsumi 1996), protein and organelle lysis (Hara et al. 2006), development, lysis of pathogens (Tallóczy et al., 2002: Nakagawa et al., 2004), regulated cell death (Datan et al., 2012; Yonekawa, 2013) and sometimes even antigen presentation capabilities (Mizushima, 2005).

In many cases, autophagy acts as a pro-survival mechanism, rendering cells able to cope with various stress conditions including injuries, starvation, infections and intracellular homeostatic alterations in order to preserve energy levels and the continuation of bio-anabolic procedures (Lum et al., 2005). Through the plethora of pro-survival roles, under specific conditions, autophagy can also execute a well-defined regulated cell death subtype, known and described as autophagic cell death (Levine et al., 2005). The term 'autophagic cell death' is regularly used to describe a form of regulated cell death that occurs primarily via the activation of the autophagy mechanism and is inhibited largely by the suppression of autophagy. Autophagic cell death differs morphologically from apoptosis and other forms of regulated cell death and is mainly characterized by increased levels of intracellular autophagy, including great vacuole assemblage. Simultaneously absence of chromatin condensation or DNA fragmentation (Levine et al., 2005) is considered a typical morphological feature of autophagic cell death. Furthermore, in case of apoptosis, there is a collapse of the cytoskeletal structure, but preservation of intracellular organelles until late in the death process, however in autophagic cell death, there is early lysis of intracellular components but conservation of the cytoskeletal structure until the late process stages. Numerous pro-apoptotic signals

are able to induce autophagic cell death, such as TNF ligands and the calcium/calmodulin–regulated ser/thr kinases (Inbal et al., 2002).

Autophagy has been proposed to protect cells and act conversely to cell death, however there are many examples where the autophagic mechanism and machinery are required for cell death induction. This phenomenon occurs mainly in developmental and cell differentiation processes (Nelson and Baehrecke, 2014). For instance, in the protist *Acanthamoeba*, autophagy plays a crucial role in trophozoite transformation and differentiation, from an energetic, vegate and infectious trophozoite to a dormant double-wall cyst. Typically, the process of encystment begins with autophagy and cell protein compartment degradation. In addition, numerous autophagy genes have been also associated with *Acanthamoeba* encystation including Atg3 (Moon et al., 2011), Atg8 (Moon et al., 2013), Atg12 (Kim et al., 2015) and Atg16 (Song et al., 2012). However, it is as yet unclear whether the phenomenon of autophagy could efficaciously lead to a regulated autophagic cell death in *Acanthamoeba* parasites. Interactions among autophagy and cell death pathways and how autophagy regulates and is being regulated by cell mechanisms are not entirely distinct and require further investigation. Nevertheless, crosstalk among these procedures would not be uncommon or unexpected.

2.5 Calcium and Cell Death

Calcium (Ca^{2+}) is a universal second messenger, involved in the regulation of an extensive variety of physiological and pathophysiological events. Calcium ion signalling has been shown to critically impact almost every aspect of cellular life such as morphogenesis, cell cycle regulation, gene transcription, cell proliferation, cell survival and cell death initiation. A dysfunction of calcium signalling in these processes could potentially lead to numerous cancer types and many degenerative diseases. Based on this complex signalling ability, Ca^{2+} often orchestrates conflicting interests within the same cell.

Numerous studies have revealed that an increase of intracellular calcium concentration, which is achieved either by ER stress (Pinton et al., 2001; Kruman et al., 1998; Choi., 1995) or by Ca^{2+} activated membrane channels, (Martikainen et al., 1991; Tombal et al., 1999) appears to mediate fatal effects in cells, while the magnitude of the rise is often indicative of the occurring cell death type. Calcium release from endoplasmic reticulum, cell's calcium repository and increased calcium influx through membrane channels have been both considered to be highly apoptogenic (Pinton and Rizzuto, 2006). Furthermore, calcium signalling has been inextricably associated with all major forms and subforms of regulated cell death including apoptosis, autophagic cell death, anoikis, programmed cell death, necroptosis and necrosis.

Contrariwise, cytosolic calcium overload can also lead to many anti-apoptotic, differentiation, proliferation and generally survival signals besides kinases positive modulation (Figure 2.1). Kinases phosphorylate transcription factors such as NF-kB, which are considered to be highly anti-apoptotic agents, or other genes products that might positively or negatively regulate apoptotic activity and death induction (Sun and Carpenter., 1998; Mattson et al., 2000; Bok et al., 2007). However, in most cases, an increased and prolonged intracellular concentration leads to fatal consequences.

Different concentrations of ER calcium indicate that a variable amount of Ca^{2+} can be released into the cytosol. For instance, a decreased amount of Ca^{2+} released from ER also decreases the amount taken up by the mitochondria (Djebbar et al., 2009; Pinton et al., 2001b; Scorrano et al., 2003), which apparently leads to increased survival rates (Nakamura et al., 2000; Xu et al., 2001). Conversely, cell viability is greatly reduced when the amount of Ca^{2+} release from ER is significantly increased (Pinton et al., 2008; Bastianutto et al., 1995). Consequently, the amount of calcium releasable by ER appears to be strongly related to death signal transduction, rather than the $[Ca^{2+}]_{ER}$ itself.

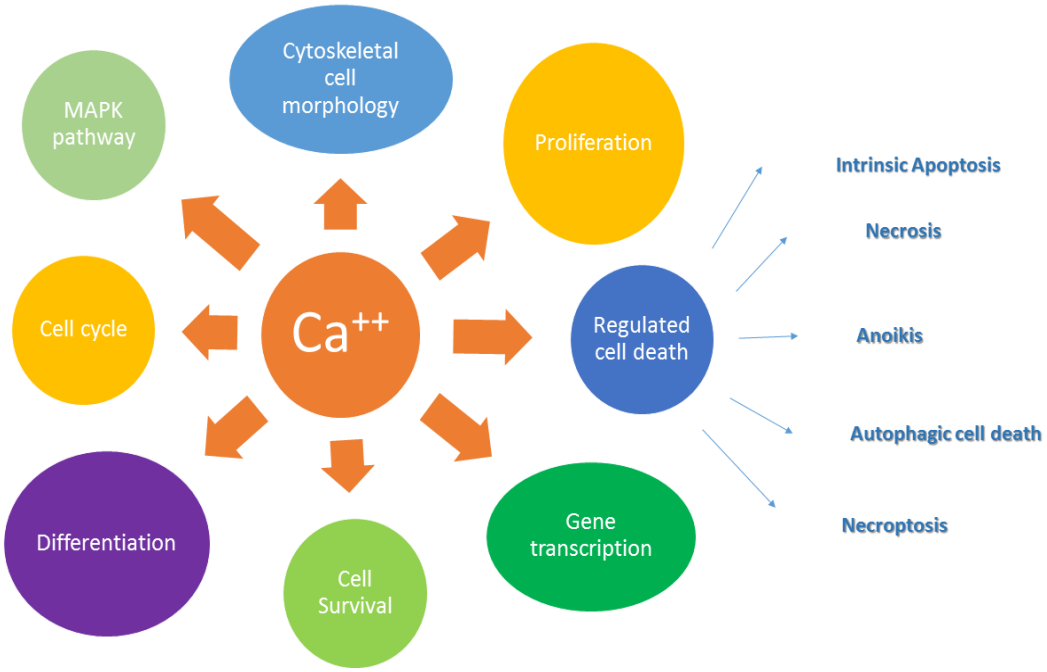

Figure 2.1: Representative calcium signalling pathways

2.5.1 Mitochondrial role in Calcium cell death signalling

It is widely acknowledged that mitochondria constitute the bio-energetic and metabolic centre of all eukaryotic life. Several forms of regulated cell death are characterized by mitochondrial damage, which in turn irreversibly leads to mitochondrial dysfunction.

Under physiological conditions, calcium ions circulate between endoplasmic reticulum and mitochondria. There is experimental evidence that under resting conditions, $[Ca^{2+}]_c$ is parallel to $[Ca^{2+}]_m$ (Murgia et al., 2009). In order to achieve this, Ca^{2+} ATPases transfer calcium into the ER, whereas IP3R channels release it back into the cytosol. In mitochondria, a low-affinity uniporter allows the entry of $[Ca^{2+}]$, while a Na^{+}/Ca^{2+} exchanger is responsible for the $[Ca^{2+}]_m$ discharge (Clapham, 2007). Generally,

Ca^{2+} is a regulator of mitochondrial function and viability while concurrently $[Ca^{2+}]_m$ homeostasis appears to be a key point of cell death signalling.

Endoplasmic reticulum and mitochondria are in some manner physically and biologically bonded. In numerous cases of regulated cell death, ER stress and IP3R have been implicated directly in mitochondrial calcium overload (Scorrano et al., 2003). Furthermore, IP3R gene knockdown or IP3R inhibition have resulted in a decreased $[Ca^{2+}]_m$ and simultaneously in decreased cell mortality (Khan et al., 1996; Blackshaw et al., 2000). In healthy cells, which are capable of maintaining control of their intracellular metabolic activities, fluctuations in $[Ca^{2+}]_c$ pulses, even during cell stimulation signals, are easily manageable through the distinctive ability of mitochondria to accumulate calcium (RaM rapid calcium uptake mode; Gunter et al., 2004). However under pathological and stress conditions, whereas intracellular calcium concentration rises and presents a more prolonged and higher pulse, mitochondria fail to manage extensive accumulation of calcium intra-mitochondrially, which in turn leads to mitochondrial outer membrane permeabilization, mitochondrial swelling and sometimes even mitochondrial collapse (Bianchi et al., 2004; Murgia et al., 2009).

Physiologically, a significant and prolonged $[Ca^{2+}]_m$ escalation has many critical outcomes, ranging from a foreseeable stimulation of the sensitive calcium-dependent dehydrogenases (pyruvate, iso-citrate and α-ketoglutarate), which in turn leads to increased ATP production, to unspecific Ca^{2+} binding to protein scaffolds that are responsible of the mitochondrial Permeability Transition Pore (mPTP) regulation (Rizzuto et al., 2008; Ichas and Mazat 1998). In addition, mPTP is also greatly affected by the dissipation of the transmembrane potential across the inner mitochondrial membrane due to calcium accumulation (Dockzi et al., 2010). So conclusively, increased $[Ca^{2+}]_m$ seems to favour mPTP opening (Hunter et al., 1979; Brustovetsky et al., 2002;), which is one of the basic mechanisms that regulates mitochondrial form and controls the release of apoptogenic factors that reside exclusively within this organelle's membranes. The opening of mPTP causes mitochondrial swelling as a consequence of water influx into inner domains of the organelle, which in turn renders the outer mitochondrial membrane (OMM) permeable, leading to the release of numerous apoptotic factors into the cytosol such as Apoptosis Inducing Factor (AIF), endonuclease G (EndoG), cytochrome c (cyt c)

and smac/DIABLO. More precisely, cytochrome c, along with APAF-1 which already exists in cytosol, form a large quaternary protein structure called the apoptosome, which in turn leads to caspase downstream activation, while AIF and EndoG translocate from cytosol to nucleus, where they mediate chromatin condensation and DNA fragmentation (Cande et al., 2002, 2004; Dougas et al., 2000). It should be mentioned that mitochondrial dysfunction and fragmentation occurs relatively early in apoptotic or mitochondria-mediated cell death.

Mitochondria and MOM integrity play an essential role in regulated cell death and are directly associated with both necrotic and apoptotic cell death procedures (Murgia et al., 2009). After MOM permeabilization ATP biosynthesis is not simply blocked, but ATP hydrolysis is also encouraged, rendering the cell incapable of covering its own energetic requirements, a factor that strengthens even more the progression towards cell death. Moreover, it has been proposed that mitochondria also define the cell's response to $[Ca^{2+}]_c$ and determine which process will be later followed. In principle, a low level of calcium uptake by mitochondria might lead to autophagy, while at the same time, increased mitochondrial Ca^{2+} influx could lead to cell death through apoptotic or necrotic processes (Bootman et al., 2018) based on additional regulators and co-factors.

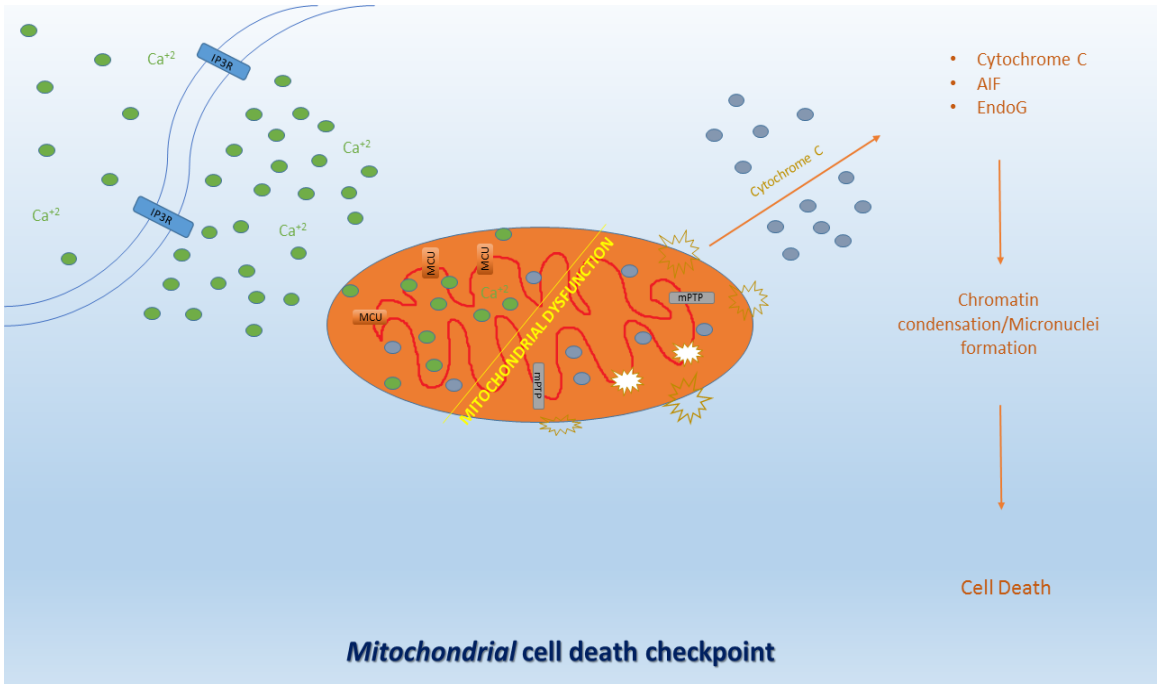

Figure 2.2: Representation of mitochondrial cell death pathway.

2.6 Ras signalling in Cell Death

Ras subfamily proteins are small GTPases that are mainly located in the intracellular membranes of all eukaryotes, where they modulate various aspects of cell behaviour such as proliferation, differentiation, senescence, survival and cell death processes. Ras versatility is facilitated by its capability to bind and trigger a different range of effector molecules. Its activation is based on guanine-nucleotide-exchange, factors which exchange bound GDP for GTP, while its inactivation depends on GTPase activation, when GTP is hydrolysed to GDP.

Experimental findings have also led to the proposal that Ras proteins, instead of being on the cell membrane, could also be located in other endogenous cell membranoid organelles such as endoplasmic reticulum (ER), Golgi apparatus, endosomes and even

mitochondria, where they might be responsible for induction of apoptosis and other forms of regulated cell death (Prior and Hancock, 2012; Howe et al., 2001; Philips et al., 2006). More precisely, Ras located on the endoplasmic reticulum has been shown to mediate MAPK/ERK activation and cell differentiation (Chiu et al., 2002), indicating that the required activation agents are not specifically limited to the cell membranoid area. Additionally, it was observed that Akt and Jnk pathway activation was more effective when activated by ER-restricted Ras than by any other type of GTPase (Chiu et al., 2002). This might depend on variable amounts of regulators and effectors that are localized in each organelle and in turn allow diverse ways of downstream signal transduction. Nowadays it is commonly accepted that Ras signalling shows compartmentalization, which potentially enhances the specificity of signalling cascades. However, the outcomes of signalling pathways that are under the control of distinct intracellular Ras locations might be highly variable among various cell types and patho-physiological conditions as well as signal nature and signal intensity dependent (Chiu et al., 2002).

Reports of Ras-mediated cell death stimulation, rather than potentiation of cell survival, came from experimental procedures in which activated Ras forms were ectopically expressed. Over-expression and hyper activation of Ras proteins has been shown to enhance pro-apoptotic dynamics, overriding cell growth, proliferation and generally survival signals induced by the PI3K effector pathway (Kauffmann et al., 1997). The observation that Ras signalling can encourage both proliferation and cell death has driven the assumption that the signalling pathways that regulate both these functions could be more closely associated than initially assumed. Various representative studies have shown that ectopic expression of activated Ras is capable of inducing cell death under special conditions (Overmeyer and Maltese, 2011). Simultaneously, endogenous Ras activation could be a vital checkpoint in cell death pathway initiation, in response to pharmacological or environmental stress insults.

It is proposed that modest Ras activation tends to promote cell growth and anti-apoptotic signals while excessive and prolonged activation tends to promote cell death and growth arrest (Zhu et al., 1998; Vos et al., 2000). Cangol and Chambar have reported that the RAS/RAF/ERK pathway, characterized by a prolonged ERK activation, could be considered to be a critical cell death promoter, in response to various stress conditions,

in a plethora of different cell types (Cangol and Chambar, 2010). However, the subcellular localization in which ERK receives sustained activation plays a crucial role in cell death induction. Additionally, the ERK signalling pathway could mediate either apoptotic processes by induction of mitochondrial cytochrome c release, or autophagic vacuolization (Cangol and Chambar, 2010).

2.7 Regulated cell death in unicellular protozoan parasites

For higher eukaryotes and metazoans, the possession of genes directly related to cell death is perfectly comprehensible and reasonable, while it is questionable how such genes could possibly benefit unicellular organisms. The molecular pathways that could potentially orchestrate such processes in unicellular parasites including *Acanthamoeba* have not yet been fully understood and described, however there is strong evidence for their existence.

Theoretically, parasitic unicellular organisms could have developed PCD pathways as an altruistic behaviour, in order to preserve their population dynamics (Welburn et al., 1997; Lee et al., 2002), to avoid killing the host and consequently threatening their existence (Zaggler et al., 2002) and finally to avoid any potential infection spread by pathogenic bacteria and viruses that could possibly threaten the entirely colony's survival. Apart from these actions, PCD in protozoa might offer a more sophisticated way of genetic selection to optimize biological fitness in the offspring.

Apoptosis-like programmed cell death has been described in numerous unicellular microorganisms, including the protist parasites *Plasmodium* (Al-Olayan, 2002; Arambage, 2009; Sinden and Billingsley, 2001)*, Leishmania* (Das et al., 2001) and *Trypanosoma* (Ameisen et al., 1995; Duszenko, 2006) and it was observed that cell death in eukaryotic protozoan parasites shared common features with regulated cell death and apoptosis in multicellular organisms. These features included nuclear DNA fragmentation, cell shrinkage, chromosomal condensation, mitochondrial dysfunction,

accumulation of cytochrome c in the cytoplasm, formation of apoptotic bodies and phosphatidylserine externalization (Das et al., 2001; Duszenko, 2006).

Despite the fact that stress signals that lead to apoptotic cell death are the same and comprise a variety of agents such as drugs, radiation, temperature or oxidative stress, it would be unwise to assume that in both situations the same protein machinery and same pathways exist. For example caspases, which are the key players in metazoan apoptotic pathways, are absent from protozoan parasites undergoing regulated cell death, suggesting a different machinery. Notwithstanding the fact that protozoan genomes do not encode caspases, they encode a biochemically relatively close family of orthologuous proteins called metacaspases and are present in protists and plant cells. It has been proved that metacaspases are capable of playing roles similar to their close caspase relatives and they have been also associated with programmed cell death in plants and yeast (Sundström et al., 2009; Reape et al., 2010; Madeo et al., 2002; Gutierez et al., 2010).

The established view of metacaspases in protozoan cell death includes their role as effector rather than executioner molecules. E-64 and Z-VAD-fmk cysteine protease inhibitors have reported to produce a remarkable decrease in DNA fragmentation percentage compared to control populations in induced cell death in *Entamoeba* (Villalba et al., 2007; Ramos et al., 2007). Pre-treatment with metacaspase inhibitors such as antipain or TLCK also resulted in decreased apoptotic events in *Leishmania donovani* cell death and at the same time, *L. donovani* metacaspase anti-sense mRNA produced a negative response, repressing the signalling cascade (Chowdury et al., 2014). Cysteine protease inhibitors and anti-sense mRNA did not increase viability rates, supporting the argument for a secondary role for metacaspases in cell death introduction. Moreover, when other metacaspases like TbMCA4 (*T. brucei* metacaspase 4) were expressed in *S. cerevisiae*, transformed cells showed decreased growth, mitochondrial respiratory dysfunction and cell death (Szallies et al., 2002). Metacaspases of *T. cruzi* TcMCA3 and TcMCA5, suggesting a potential role in the apoptosis-like cell death of the parasite, have been shown to translocate to the nucleus during the induction of cell death and simultaneously their overexpression has been found to increase sensitivity to cell death induction (Kosec et al., 2006).

In general, metacaspases are not certainly involved in protozoan regulated cell death induction. Reports mention their crucial role in cell physiology including variable cell functions, like cell cycle and stress signalling pathway regulation (Saheb et al., 2015; Tsiatsiani et al., 2011; Helms et al., 2006). In *Acanthamoeba* a type-I metacaspase (Acmcp) was identified and was shown to be expressed during encystment. Additionally, Acmcp had a close relationship with contractile vacuole regulation, contractile vacuole localization and mediated membrane trafficking (Saheb et al., 2013). Whether Acmcp is involved in *Acanthamoeba* cell death is not clear yet, however a crucial role should not be ruled out.

Autophagic cell death could be a possible cell death modality for parasitic and non- protozoans, as the subcellular machinery that is essential for autophagy is conserved among protists and simultaneously, evidence of an efficient autophagic pathway has been confirmed in *Leishmania* spp and in trypanosomes (Besteiro et al., 2008; Williams et al., 2006; Li., et al., 2012; Alvarez, 2008). Originally, autophagic pathways are exploited as a cell survival mechanism and and cell remodelling during differentiation, though under sustained pro-survival signals and simultaneous inhibition of anti-survival signals, theoretically autophagy could result in autophagic cell death (Brennanda et al., 2011).

Nevertheless it should be mentioned that null mutation of autophagy genes may inhibit vacuolization but not cell death in an *in vitro* model of autophagic cell death (Costa et al., 2004). That fact renders autophagy as a mechanism neither adequate for nor essential to autophagic cell induction (Levine et al., 2005).

2.8 Amoebicide drugs

In this study, 2 different types of amoebicides were used, in order to induce cell death in *Acanthamoeba* cells. G-418 and Polymyxin b were known to have an impact on *Acanthamoeba* viability as Peng et al. had used concentrations of G-418 for the selection of transfected *Acanthamoeba* trophozoites (Peng et al., 2005), while Polymyxin B had previously been used to treat Acanthamoeboid infenctions (Wright et al., 1985; John et al., 1990).

2.8.1 G-418 aminoglycoside

The aminoglycoside antibiotic G-418 is an analogue of neomycin sulphate and has an action mechanism comparable to that of neomycin. It is produced by *Micromonospora rhodorangea* and is reported to be toxic to prokaryotes (Mingeot et al., 1999), mammalian cells (Bacon et al., 1990) and protists (Gokhale, 2008). It can be used either as an infection treatment agent or for selection of genetically engineered cells after gene transfection in laboratory research. Vectors containing the G-418 resistance gene are usually used for gene transfection in eukaryotes, with selection of transfected cells based upon cultivation in the presence of G-418.

G-418 typically enters the cells by endocytosis, pinocytosis or cationic membrane permeation. It inhibits polypeptide synthesis by blocking the elongation stage in both prokaryotes and eukaryotes after binding to ribosomes, resulting in cell death and is among the most commonly used antibiotics world-wide. Furthermore, in mammals and eukaryotes G-418 has been associated with caspase activation, cytochrome c release, increase in poisonous ROS levels, activation of c-Jun N-terminal kinases (JNKs) and finally, protein cleavage by calpains (Dehne et al., 2002). Additionally, G-418 was shown

to rapidly accumulate in ER, where it might mediate ER stress (Jin et al., 2004), which in turn could result in intracellular calcium rise or release of unfolded pro-apoptotic proteins and subsequent induction of cell death. Furthermore, G-418 has been previously used to induce cell death to *Entamoeba histolytica* (Villalba et al., 2007).

2.8.2 Polymyxin b (PMB)

Polymyxin b (PMB) is a cationic antibiotic commonly used against Gram-negative bacteria. It is produced from *Bacillus polymyxa* bacteria and has a positive action in outer cell membrane structure destabilization. PMB alters the outer membrane permeability as a consequence of its attachment to the negatively charged site in the lipopolysaccharide layer. As a result, water from the extracellular environment enters the cytoplasm, which in turn leads to total cell breakage.

PMB has been used successfully in combination with other antibiotics in *Acanthamoeba* Keratitis patients (John et al., 1990), however its action mechanism has not been described in depth. It is furthermore characterized by high neurotoxicity and nephrotoxicity (Neiva et al., 2013). PMB has been reported to mediate caspase-dependent apoptosis in kidney proximal tubular cells (Azad et al., 2013, 2015).

2.9 Aims of the study

The current antimoebic strategies related to *Acanthamoeba* infections are mainly characterized by multiple and adverse side effects including acute inflammatory responses, increased host cell cytotoxicity and incomplete microorganism elimination. However, the perspective of a controlled and selective RCD induction in *Acanthamoeba* cells could be considered as extremely beneficial to microorganism-persistent treatment, by diminishing undesirable and toxic effects of administered drugs. Simultaneously, manipulation of PCD pathways could be considered as the most efficient and targeted therapeutic approach not only for *Acanthamoeba* infections but also for other microorganism infections that share common charateristics.

Although different types of regulated cell death have been extensively studied in mammalian cells and higher eukaryotes, only in recent years have RCD mechanisms been closely associated and reported in numerous taxa of unicellular organisms, such as protists. It has been shown that apoptosis-like mechanisms in protozoa share numerous biochemical and morphological characteristics with apoptosis in multicellular organisms. Nevertheless, both evolutionary clarification and signaling pathways involved in protozoan RCD are poorly understood and identified.

Manipulation of RCD pathways provides a novel therapy potential that has been evaluated in many unicellular protozoa but never in the genus of *Acanthamoeba*. Taking into consideration that other amoebae in the kingdom of protozoan and eukaryotes quite similar to *Acanthamoeba* can undergo programmed cell death (Nuewga et al., 2004; Al-Olayan et al., 2002) it was easily assumable that amoebae of the genus of *Acanthamoeba* might undergo programmed like cell death procedures likewise.

The main objective of the study was the detection, identification and characterization of any possible evidence that could suggest the existence of a conserved apoptotic, or programmed cell death pathway in *Acanthamoeba*. As was previously reported, protozoan programmed cell death shares common features with PCD and

apoptosis in multicellular organisms. Consequently, observations of specific morphological, biochemical and molecular characteristics such as alterations in the cytoskeleton of the amoebae, nuclear changes in chromatin condensation, DNA fragmentation, fluctuations in the concentration of intracellular ions and cations, mitochondrial dysfunction, release of pro-apoptotic agents into *Acanthamoeba* cytosol and relative overexpression or underexpression of genes associated with programmed cell death could verify the hypothesis.

Identification of apoptotic or any other kind of regulated cell death features, including primarily morphological, secondly biochemical and thirdly molecular characteristics, might be indicative of a more complex, conserved death-signalling pathway. A potential understanding of *Acanthamoeba* cell death triggering mechanisms and pathways will provide the possibility of identifying targets for therapy, not only limited to *Acanthamoeba* infections but also for many other parasitic microorganisms that share common programmed cell death mechanisms and characteristics.

Chapter 3

Materials and Methods

All chemicals used in experimental procedures were purchased from Sigma, except those that are stated differently.

3.1 Culture Media

3.1.1 Neff's saline Buffer (NSB):

NaCl 0.01% (w/v), $MgSO_4 7H_2O$ 0.0004% (w/v), $CaCl_2$ 0.0004% (w/v), Na_2HPO_4 0.014% (w/v), KH_2PO_4 0.013% (w/v).

3.1.2 AX2 media:

Tryptone 14.3% (w/v), Yeast extract 0.715% (w/v), Glucose 1.54% (w/v) Na_2HPO_4 0.051% (w/v), KH_2PO_4, 0.0486% (w/v), pH=6.5

3.1.3 Lysogeny broth (LB):

Prepared as Invitrogen's Lysogeny Broth Base according to the manufacturer's instructions.

3.2 Bacterial culture

3.2.1 *Escherichia coli*

E. coli was grown overnight in LB media, at 37°C in a shaking incubator.

3.2.2 Bacterial cryopreservation

Bacteria were grown to logarithmic phase and centrifuged. Supernatant was discarded and fresh media with 20% glycerol was added to the bacterial pellet, which was transferred to cryogenic tubes. Bacteria were stored at -20°C overnight, before being transferred to -80°C.

3.3 *Acanthamoeba* cultures

3.3.1 *Acanthamoeba* isolation

This technique has been undertaken with special precautions and care, as members of the genus of *Acanthamoeba* are potentially pathogenic to humans.

First, small quantities of approximately 10g soil samples, from highly organic substrates in George Square gardens, University of Edinburgh, Edinburgh, Scotland, were collected and dissolved carefully in Neff's saline buffer, placed on a non-nutrition 2.0% agar plate (2% agar; 98% sterile Neff's saline buffer) and left overnight at room temperature. Pieces of 2-3 cm^3 were removed with the use of a scalpel and placed upside down on a second fresh no-nutrient 2.0% agar plate onto which *E.coli* bacteria had been spread and allowed to dry for a few hours. By this means, bacteria, metazoans, nematodes and other non-crawling protists were excluded, as they were trapped under the pieces of agar while amoebae were free to spread and consume the existing *E.coli.* After a few days of incubation at room temperature, amoebae had grown parametrically of the agar block forming a growth ''ring'' that was visible to naked eye. Continuing their course to the agar plate edges amoebae consumed the available bacterial substrate and gradually formed cysts as a result of desiccation and lack of food.

Later, small blocks of 2-3 cm^3 were excised, after microscopic examination in order to transfer only one kind of cyst and the entire process repeated with a new 2.0% no-nutritient and 50μg/mL carbenicillin agar plate, covered by heat-killed *E.coli* bacteria (incubated for 15 minutes at 65℃). After that step the culture was almost clonal, however the process was repeated once again for further accuracy. Finally, once amoebae formed cysts, they were transferred with the use of an inoculation loop to AX2 media and grown axenically presence of 50 μg/mL carbenicillin and 100 μg/mL ampicillin. After approximately 6 to 7 days of incubation at room temperature amoebae were cultured routinely without any sign of potential contamination.

3.3.2 Axenic *Acanthamoeba* Cultures

Acanthamoeba trophozoites (ATCC 50492; genotype T4; Neff's strain and G.S. isolate) were routinely cultured in a sterile AX2 medium, at room temperature or at 30ºC. T-25, T-75, T- 125 corning flaks, 6, 12, 24 well plates or even sterile Erlenmeyer flasks, were used to *Acanthamoeba* growth. Occasionally, antibiotics were added to *Acanthamoeba* cultures (approx. 50 μg/mL carbenicillin; 100 μg/mL ampicillin).

3.3.3 *Acanthamoeba* cryopreservation

Acanthamoeba were centrifuged at 500 g for 10 minutes and afterwards supernatant was discarded. The pellet was diluted in AX2 media in the presence of 10% DMSO and cultures were transferred immediately to sterile cryogenic vials. Initial 2 hours room temperature incubation was followed by overnight storage at -20°C. Subsequently, *Acanthamoeba* cells were stored at -80°C for long periods.

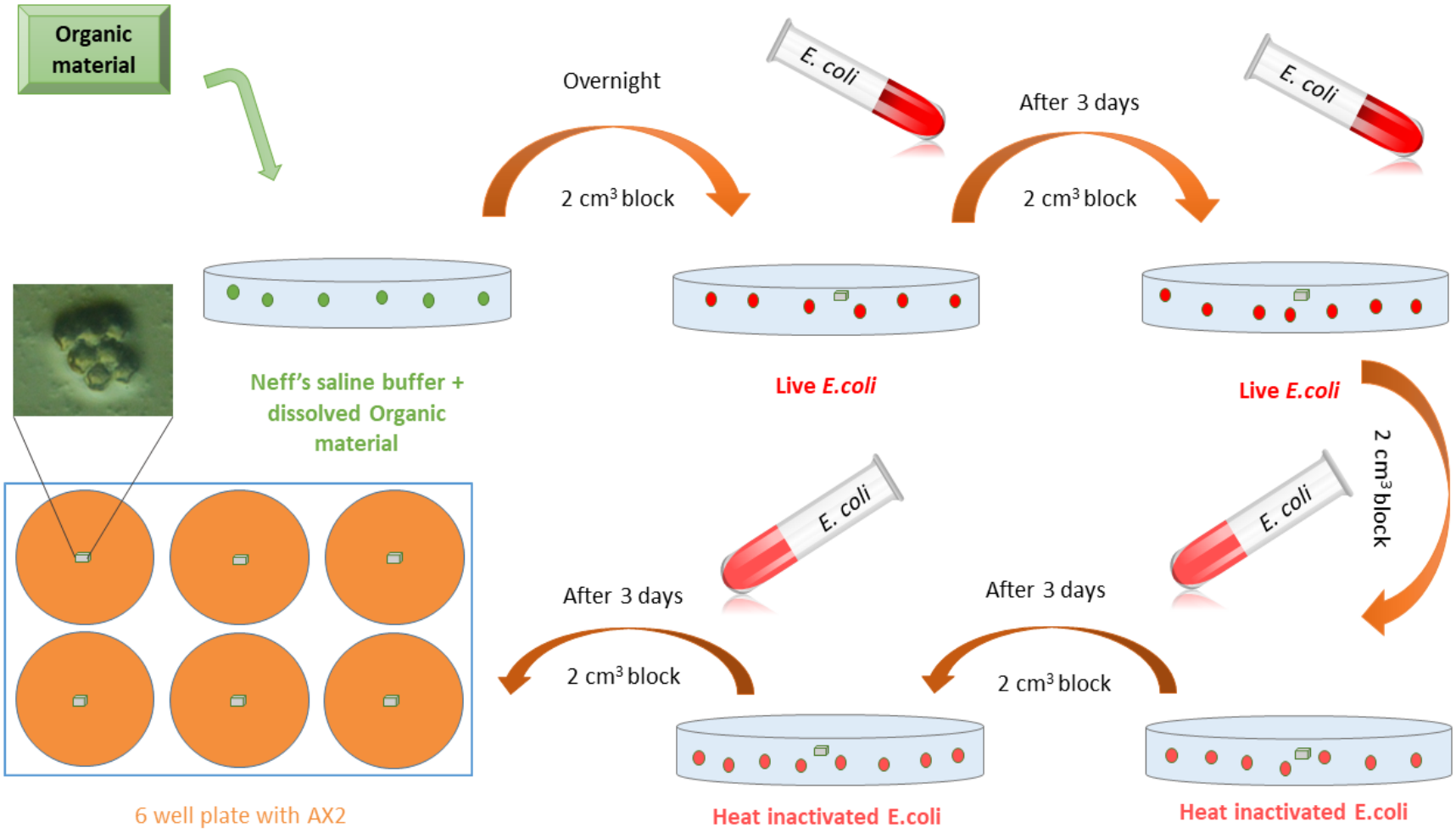

Figure 3.1: Schematic representation of *Acanthamoeba* isolation.

3.4 *Acanthamoeba* viability curves by Trypan blue exclusion assay

Viability curves of trophozoites were determined in the absence (Untreated: UN) or presence of 100, 200 µg/mL G-418 and 10, 100 µg/mL Polymyxin b, by the Trypan blue exclusion assay in various buffers and temperatures (0.4 mL TB 0.4%; 0.6 mL cell suspension). Nonviable cells with permeable membranes selectively absorb the dye, rendering their cytoplasm blue-coloured while at the same time, live cells with intact membranes remain uncoloured. Cell viability (%) was measured as:

$$\frac{\boldsymbol{Total\ Viable\ Cells}}{\boldsymbol{Total\ number\ of cells}} \times 100$$

Cells were counted in a haemocytometer under bright field in a light microscope. Data were expressed as the mean ± SD of three independent experiments. Statistical significance analysis between treated and untreated trophozoites was analysed by Student's paired t-test, one tail distribution, $P<0.05$, (Excel, Microsoft office).

3.5 Microscopy

3.5.1 Optical microscopy

Acanthamoeba cultures and cells were observed and monitored under a Leica DM IRB inverted microscope. A Canon EOS 1100D camera was plugged into the Leica microscope rendering photographs and video feasible. EOS utility software was used to capture, store and analyze the images.

3.5.2 Time-lapse video microscopy

Images were taken at pre-regulated fixed manner and time from treated *Acanthamoeba* cells to observe progression of cell death. EOS utility software was used to capture, store and analyze the images.

3.5.3 High-contrast quantitative imaging and microscopy

High-contrast microscopy was used to analyze morphological features of *Acanthamoeba* PCD. High-contrast microcopy experiments were completed by Livecyte™ which is a system for live cell analysis that enables Kinetic Cytometry. This equipment produces quantitative data without the need for cell labelling with at the same time the analysis of morphological and kinetic behavior of robotically followed individual cells over hours or days. The primary idea behind this function employment is ptychography which generates high-contrast, high-fidelity images without halos or speckling, which after adequate processing enables direct measurement of the physical properties of a cell. Furthermore, the Livecyte system allows a stable regulation of outer conditions such as temperature, humidity and CO_2 levels, as it is mounted in a special incubator.

Livecyte is a combinatorial system that provides the appropriate hardware and software needed for further analysis. Briefly, the system comprises a transmission inverted microscope, 4X to 40X objectives, 6 position turret, LED illumination for bright field/fluorescence imaging, bright field, ptychographic phase and fluorescence modalities, 120mm x75mm travel, sCMOS camera for high sensitivity phase and fluorescence.

Briefly, *Acanthamoeba* were grown on a 12-well plate to confluency. 75 µg/mL (EC_{90}) G-418 was added to half of the wells (treated population) and the other half used as controls (untreated population). Later the plate was placed carefully in the incubator

and the microscope was set up to take pictures every 20 minutes from every well at a predefined region at 10X and 20X magnification.

Experiments were conducted under the supervision and auspices of Phasephocus at the University of York, York, England, U.K. Technical support was also provided.

3.5.4 Confocal Microscopy (CM)

Acanthamoeba cells were fixed on slides in order to examine nuclear pyknosis, chromatin condensation and DNA alterations. Later, slides were examined under an epifluorescence microscope Nikon A1R, standard fluorescence detector wavelength 400-750 nm; pixel size: max. 4096 x 4096 pixels; A1-DU4 4 detections units; Epi-Filter cube DAPI; Excitation/Emission (nm):350/461 by NIS Elements software. Picture analysis was later processed primarily by Image analysis Software Imaris and secondly by ImageJ.

3.6 Fluorescence techniques

3.6.1 Intracellular $[Ca^{2+}]_c$ concentration

Alterations in the intracellular levels of calcium ions $[Ca^{2+}]_c$ after induction of cell death were monitored by the fluorescent probe Fura-2, a ratiometric dye that binds to free Ca^{2+} (Takahashi et al., 1999). Membrane permeant Fura 2/AM (pentaacetoxymethyl ester) which was applied, is Ca^{2+}-insensitive however, when inside the cell, esterases cleave the AM group rendering Fura 2 and Ca^{2+} association possible. Amoebae were initially cultured routinely in a 6-well plate. After 0-30-60-90-120-150 minutes of treatment accordingly with G-418 75 μg/mL and 10μg/mL Polymyxin b, trophozoites were harvested and washed twice in N.S.B. at 500 x g for 5 minutes at room temperature. Later,

trophozoite pellets were resuspended in Fura 2/AM loading buffer containing 6μM Fura 2AM, 116 μM NaCl, 5.4 μM KCl, 0.8 μM MgSO4, 5.5 μM D-glucose, 0.05 M HEPES, pH=7.4 for 30 minutes at 37°C with occasional agitation (Chowdhury et al., 2014, Villalba et al., 2007). Afterwards trophozoites were centrifuged and washed with 1 mL N.S.B. twice to remove extracellular dye. 150 to 180 μL of the final trophozoite suspension were transferred to a cuvette already containing 1.850 mL (approx. 5×10^4 mL^{-1} cells) phosphate saline buffer. Fura 2-loaded trophozoites were excited at 340/380 nm and 510 nm emission measured in a Perkin-Elmer Fluorimeter. The Ca^{2+} was determined at room temperature based on the following equation.

$$[\boldsymbol{Ca^{2+}}] = \boldsymbol{K_d} \times \boldsymbol{\beta} \times \frac{[\boldsymbol{R} - \boldsymbol{Rmin}]}{[\boldsymbol{Rmax} - \boldsymbol{R}]}$$

Where, **R**= sample ratio fluorescence $\mathbf{R_{min}}$= zero calcium conditions (EGTA 10μM), $\mathbf{R_{max}}$= calcium-saturated conditions ($CaCl_2$ 10mM + 10μM Ionomycin), **β**= ratio of R_{min}/R_{max} at 380nm, $\mathbf{K_d}$= 224 nM at 30°C. Data were analysed with Biolight Luminescence system BL studio 1.04.01 and were expressed as the mean ± SE of three independent experiments.

3.6.2 Intracellular pH measurement (pHi)

Variations in the intracellular pHi are significant parameters in physiological cell functions since they affect numerous metabolic processes such as cell growth, differentiation, enzymic activity, receptor-mediated signal transduction, ion transport, endocytosis and other cellular processes. In order to monitor intracellular pH fluctuations, BCECF-AM acetomethyl ester was used (on the same principle as Fura-2AM). BCECF is a fluorescent dye that responds to pH alterations and is the most widely used fluorescent indicator for measuring cytosolic pH. The excitation spectrum of the dye experiences a slight alteration with pH variation, whereas the wavelength of the emission

maximum remains unaffected. Generally, at low pH, BCECF has a low fluorescence intensity and the fluorescence signal rises with rising pH.

Briefly, *Acanthamoeba* were cultured routinely in a 6-well plate. AX2 media was removed and replaced with Neff's saline buffer plus a defined amount of PMB. After treatment for 30-60-90 minutes with 10µg/mL Polymyxin b, trophozoites were harvested and washed twice in Neff's saline buffer and centrifuged at 500 x g for 5 minutes at room temperature. Later, *Acanthamoeba* trophozoites were resuspended in BCECF loading buffer containing: 10µM BCECF, 14 mM KCl, 10µM $CaCl_2$, 0.05 M HEPES, for 30 minutes at 37°C. Trophozoites were washed with Neff's saline buffer twice to remove extracellular dye and resuspended in 1mL of fresh Neff's buffer. Approximately, 5 $x10^4$ mL^{-1} cells in 2mL NSB V_{final} were used to determine the signal ratio of emission intensity at 535 nm when the dye is excited at 490 nm and at 440 nm (Kracke, 1992). More specifically, intracellular pH was determined based on the following equation:

$$[H^+]=K_a\,(R-R_A)/(R_B-R)\times f$$

Where, $\mathbf{f}=f_{acidic440}/f_{basic440}$, **R** = signal ratio of excitation 490 and 440 nm with emission at 535 nm, $\mathbf{R_{min}}$ = basic conditions, $\mathbf{R_{max}}$= acidic conditions, pK_a= 6.97 (Rink et al., 1982; Ozkan and Mutharasa 2002). Data were analyzed with a Biolight Luminescence system, BL studio 1.04.01 were expressed as the mean ± SE of three independent experiments.

3.6.3 Hoechst staining protocol and Hoechst fluorescence intensity

Hoechst 33342 nucleic acid stain is a common cell-permeant nuclear counterstain that emits blue fluorescence when bounds to ds DNA. The fluorescent emits blue-cyan fluorescent light around 461 nm when excited with ultraviolet light at 350 nm. It is primarily used to detect changes in DNA and chromatin structure during the cell cycle, however

lately it has been used to detect and to characterize nuclei in apoptotic and non-apoptotic cells. Hoechst staining is less toxic than DAPI but it is more cell-permeant at the same time.

Hoechst 33258 was first used for this experiment but failed dramatically and constantly to bind to *Acanthamoeba* trophozoite dsDNA despite the numerous concentrations, buffers, incubation periods and fixation techniques that have been applied. Surprisingly Hoechst 33258 showed greater affinity for the *Acanthamoeba* cytoplasm than *Acanthamoeba* nucleus.

Briefly, *Acanthamoeba* trophozoites were cultured in a 6-well plate to confluency. Later they were washed twice with NSB, treated with 75 μg/mL (EC_{90}) G-418 in Neff's saline buffer and incubated at 37ºC for preschedule periods of time (0 to 8 hours). Amoebae were removed from plates and centrifuged at 500 g for 5 minutes. Pellets were washed once with Neff's saline buffer and 4% paraformaldehyde (PFA) for 15 minutes at room temperature was applied in order to fix *Acanthamoeba* trophozoites (PFA 10% was freshly produced on the day of experiments). Cells were washed again with Neff's saline buffer and centrifuged at 500 g for 5 minutes. 10μM Hoechst 33342 (final concentration) was applied and trophozoites incubated at 37°C in dark for 30 minutes. Loaded cells were washed once with 1 mL Neff's saline buffer to remove excess dye. 20-50μL of the final suspension were applied to labelled slides with mounting media. Slides were left overnight in a dark chamber to dry out and were observed by confocal microscopy the next day. The identical Hoechst 33258 staining protocol was followed in order to detect changes in chromatin condentation in caffeine treated *Acanthamoeba* trophozoites with the difference that amoebae were treated with 10 μM caffeine in NSB at room temperature for 24 hours.

Slides were examined under an epifluorescence microscope (Nikon A1R). DAPI filters were applied in order to detect fluorescence. Picture analysis was later made primarily by Image analysis Software Imaris and ImageJ. Emission signal intensity of Hoechst 33342 was monitored and measured by a LS55 ElmerPerkin luminescence spectrometer when excited at 500nm. Fluorescence data were analysed with Biolight Luminescence system BL studio 1.04.01. Experiments were repeated at least 3 times

and data expressed as the mean ± SE, student's paired t-test, one tail distribution, $P<0.05$, (Excel, Microsoft office).

3.6.4 CTC- Formazan accumulation and fluorescence intensity

CTC (5-cyano-2,3-ditolyl tetrazolium chloride) is a permeant, colorless, non-fluorescent redox dye which has been widely used to determine the respiratory activity of microorganisms (Winding et al., 1994; Christensen et al., 1980; Kobayashi et al., 2012; Rodriguez et al., 1992; Cook and Garland, 1996, Itturiaga et al., 2001). Generally, CTC acts as redox partner instead of the terminal electron acceptor, oxygen (Creach et al., 2003) and is enzymatically reduced via electron transport process to a detectable, red fluorescent, insoluble CTC-formazan derivative (CTF), which accumulates intracellularly. CTC-loaded, healthy and respiring *Acanthamoeba* will reduce CTC to CTF while at the same time, dead or mitochondrially inactive cells will show minimal reduction and subsequently, diminished fluorescence.

CTC staining has been (Rodriguez et al., 1992; Itturiaga et al., 2001) reported to be toxic to cell therefore, CTF represents an index of respiratory activity for a specific period of observation. CTC was dissolved in deionized water to prepare 25 mM stock solution.

Briefly, trophozoites were grown in a 6-well plate, treated with 75 µg/mL (EC_{90}) G-418 in Neff's saline buffer and incubated at 37°C for a prescheduled period of time (0 to 6 hours). Later amoebae were removed from plates and centrifuged at 500 g for 5 minutes. Cells were washed again with Neff's saline buffer, centrifuged at 500 g for 5 minutes and 5 mM (final concentration) of CTC applied. Cells were incubated at 37°C in the dark for 30 minutes and finally washed once again with 1 mL Neff's saline buffer to remove excess dye. Cells were fixed with 4% paraformaldehyde for 20 minutes in the dark at room temperature. Finally 20-50µL of the final samples were applied to labelled slides with mounting media. Slides were left in the dark overnight to dry out at 4°C and observed by confocal microscopy the next day. Slides were examined under an

epifluorescence microscope Nikon A1R; (IMPACT - Image analysis, Multiphoton and confocal technologies, CIP, The University of Edinburgh, Scotland, U.K.) Pixel size: max. 4096 x 4096 pixels; A1-DU4 4 detections units; Epi-Filter rhodamine red; Excitation/Emission (nm): 480/630 by NIS Elements software. For the fluorescence spectrophotometric analysis 100µL of the sample were diluted in a cuvette containing 1900 µL ddH_20 (approx. 5 ×10^4 mL^{-1} cells). Emission signal intensity was measured in a LS55 ElmerPerkins luminesce spectrometer when excited at 480 nm. Fluorescence data were analysed with Biolight Luminescence system, BL studio 1.04.01. Experiments were repeated at least 3 times and data were expressed as the mean ± SE, student's paired t-test, one tail distribution, P<0.05, (Excel, Microsoft office).

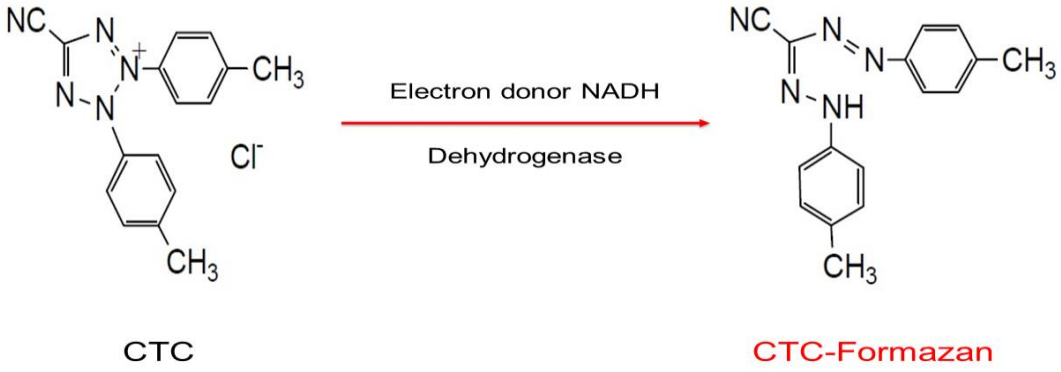

Figure 3.2: CTC reduction to red CTF

3.6.5 Plasma membrane permeability

SYTOX Green Nucleic Acid Stain is a bright, high-affinity nucleic acid stain that easily penetrates cells with compromised plasma membranes. However, it is incapable of crossing intact membranes of live cells. Cells with compromised cell membrane will

absorb higher amounts of the dye so analogously will present a higher fluorescence signal, while live and healthy cells present minimal fluorescence intensity.

Briefly, after culture to confluency at room temperature, trophozoites were treated with 75 µg/mL G-418 in Neff's saline buffer and incubated at 37°C for prescheduled periods of time (0 to 6 hours). Later amoebae were removed from plates and centrifuged at 500 g for 10 minutes. Cells were washed again with Neff's saline buffer and centrifuged at 500 g for 5 minutes and 2µM (final concentration) of SYTOX Green Nucleic Acid Stain was applied. Cells were incubated at 37°C in the dark for 30 minutes and finally washed twice with 1 mL Neff's saline buffer to remove excess dye. Positive control of compromised cell membranes was created by treatment with 2.5% of Triton X-100 for 1 minute and gentle agitation. For fluorescence spectrophotometric analysis 100µL of the sample were diluted in a cuvette containing 1.9 mL ddH_2O (5×10^4 mL^{-1} cells) and the emission signal intensity measured at 523 nm in a LS55 ElmerPerkins luminesce spectrometer with excitation at 504 nm. Fluorescence data were analysed with Biolight Luminescence system, BL studio 1.04.01. Experiments were repeated at least 3 times and data were expressed as the mean ± SE, student's paired t-test, one tail distribution, $P<0.05$, (Excel, Microsoft office)

3.6.6 Mitochondrial membrane potential ΔΨm

Mitochondrial membrane potential (ΔΨm) was monitored using JC-1 dye, tetra-ethyl-benzimidazolyl-carbocyanine iodide, a lipophilic cation which accumulates in energized mitochondria, to measure the mitochondrial membrane potential. At low concentrations and with a low ΔΨm, JC-1 is largely a monomer that emits green fluorescence at 530 ± 15 nm. At high concentrations and high ΔΨm, the dye JC-aggregates yield a red to orange coloured emission at 590 ± 15 nm. Consequently, a reduction in the aggregate fluorescence is indicative of depolarization and MOM permeabilization, while an upsurge indicates hyperpolarization.

As previously described *Acanthamoeba* trophozoites were treated with 75 µg/mL G-418 for predefined periods of time, harvested and washed twice with N.S.B. After centrifuging at 500 x g cells were suspended in N.S.B containing 6µM JC1 and left for 20 minutes at 37ºC in the dark. Later, trophozoites were washed twice in NSB with centrifugation for 5 minutes at 500 x g and used immediately for JC-1 measurement. Cells were analyzed by fluorescence microscopy using FITC (490-540 nm) and JC-1 (580-610 nm) emission filters and spectrophotometrically at 488nm nm. The Data are expressed as the mean value of three experiments ± SE. The ratio of the reading at 610 nm to the reading at 540 nm was considered as the relative ΔΨm value. Data obtained with the JC-1 spectrophotometer give a relative measure of mitochondrial membrane potential and could not be used for absolute measurements of membrane potential in millivolts.

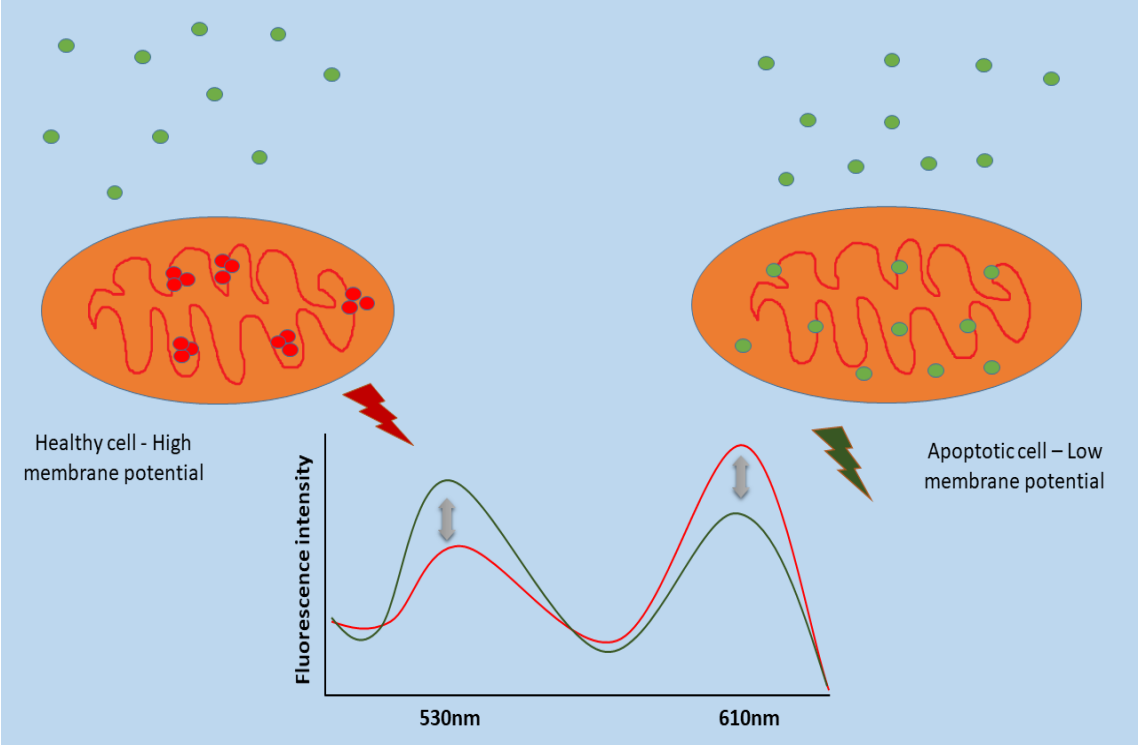

Figure 3.3: Mitochondrial membrane potential depolarization based on JC-1 fluorescence signal. J aggregates emit maximally at 610 nm, while the monomer emits maximally around 530 nm. Decreased intensity of J-aggregates signal indicates low ΔΨm and MOM permeabilization.

3.7 Molecular biology techniques

3.7.1 DNA extraction from *Acanthamoeba* (J. Lorenzo- Morales et al., 2005)

DNA extraction from *Acanthamoeba* was performed following a modified phenol chloroform technique. Briefly, amoebae were collected in Eppendorf tubes and centrifuged at 500 g for 10 minutes. Supernatant was discarded and cells were re-suspended and washed once with 1 mL of N.S.B. Supernatant was discarded and 500 µl of lysis buffer (30 mM Tris-HCl pH 7.4, 5 mM EDTA, 100 mM NaCl and 1% SDS) were added to the pelleted cells in addition to 10 µl of proteinase K (1 mg/ml). The mixture was incubated at 60ºC for at least 2 hours with occasional agitation. Later, the mixture was heated to 95ºC for 10 minutes to denature protein kinase K.

500 µl of buffered phenol, pH7.8, were added into the mixture and mixed gently and the sample was centrifuged at 10000 g for 10 minutes at 4ºC. The aqueous phase was transferred to a new tube and an equal volume of phenol pH7.8 was added and these steps repeated once. Later, the aqueous phase was transferred carefully to a new clean tube and was treated with 500 µl chloroform and mixed gently. The sample was centrifuged at 10000 g for 10 minutes at 4ºC and the aqueous phase was transferred to a new tube in order to repeat the chloroform step and centrifuged once again. Finally the top phase was transferred to a new tube where 500 µl of ice-cold isopropanol and 100 µl of 3 M sodium acetate were added. The mixture was mixed gently and left overnight at -20ºC. The next day, the sample was centrifuged at maximum speed for 30 minutes at 4ºC, supernatant was discarded and tubes were left to dry out at room temperature. The pellet was resuspended in 30µl of ddH_20. Lastly, the DNA concentration was determined using a NanoDrop 2000 (Thermo Fisher Scientific).

3.7.2 PCR for 18S rDNA amplification

For the identification of the newly isolated amoeba (GS isolate), the 18S rDNA fragment was amplified by PCR. Two pairs of primers were used (see table 3.1): JDP1

and JDP2, specific for the ASA.S1 region and Euk 18S for the whole 18S gene (Corsaro et al., 2010; Weekers et al., 1994; Dyková et al., 1999; Schroeder, 2001).

Primer	Fragment	Species	Size (bp)	Sequence
JDP1	ASA.S1F	*Acanthamoeba*	500	GGCCCAGATCGTTTACCGTGAA
JDP2	ASA.S1R	*Acanthamoeba*	500	GACTCCCCTAGCAGCTTGTGAG
Euk18sF	18s rDNA	*Acanthamoeba*	2000	GACTGGTTGATCCTGCCAG
Euk18sR	18s rDNA	*Acanthamoeba*	2000	TGATCCTTTCGCAGGTTCAC

Table 3.1: 18S rDNA primers information

The PCR reactions were performed using Promega's GoTaq Green Master Mix containing 20-30 ng of DNA in V_{final} = 50µl or by using components separately (Table 3.2).

Components	Final Volume	Final Concentration
Go Taq reaction buffer	10µl	1X (1.5mM $MgCl_2$)
PCR Nucleotide Mix, 10mM each	1µl	0.2mM each dNTP
upstream primer	2µl	1µM
downstream primer	2µl	1µM
GoTaq® DNA Polymerase (5u/µl)	0,25 µl	1.25u
template DNA	Approx. 10 µl	10-20ng
Nuclease-Free Water to	50µl	

Table 3.2: PCR components: final volume and concentration

Amplification conditions were as follows: one denaturing initial cycle at 95°C for 5 minutes, 35 cycles at 95°C for 1 minute, followed by 58°C (annealing) for 1 min, followed by 72°C for 2 minutes (extension), finalizing with 7 min of 72°C final elongation.

3.7.3 PCR purification

For better quality and purity, PCR products were purified with QIAquick PCR Purification Kit (QIAGEN) and QIA quick Gel Extraction Kit (QIAGEN) following the manufacturer's instructions.

3.7.4 DNA and RNA electrophoresis

DNA and RNA electrophoresis were performed on a BIO-RAD horizontal electrophoresis unit, in 0.8%, 1.0%, 1.5%, 1.8%, 2.0% agarose gel at 80 or 90 V with TAE buffer in room temperature. RNA electrophoresis was performed in 4℃. Gels were stained either before or after electrophoresis with 1X SYBR-Safe (Invitrogen). A Track-it 100 bp ladder (Invitrogen) was used to determine the size of the fragments. DNA fragments were later extracted from agarose gel and purified using QIAquick Gel Extraction Kit (QIAGEN) following the manufacturer's instructions.

3.7.5 18S rDNA Sequencing

Sequencing was performed by Edinburgh Genomics at The University of Edinburgh using an ABI 3730 capillary sequencing instrument. The sequencing was performed using the original PCR primers which were provided along with the samples.

3.7.6 *Acanthamoeba* RNA extraction

Extraction of *Acanthamoeba* (GS isolate) RNA was performed using RNeasy Mini Kit (QIAGEN) following manufacturer's instructions. The RNA was extracted under diverse treatment conditions depending on the experiment (Table 3.3). Generally, amoebae were collected by centrifugation at 500 g for 10 minutes in 1.5 mL sterile tubes. Supernatant was discarded and pellet was re-suspended in lysis buffer. Final RNA volume was 30 µl from which 5 µl were kept from each sample for quality and quantity analysis. Samples were kept at -20°C for a limited period of time before further processing.

3.7.7 *Acanthamoeba* RNA quantification and qualification

Quality analysis was performed after running the samples (approx. 2µl RNA+1µl loading dye +2µl ddH_20+) in a 1.2% agarose pre-stained gel at 4^{o}C while the quantity was measured with a Qubit 2.0 fluorimeter using a RNA BR assay kit. Briefly, 10 µL standards or diluted RNA were mixed with Qubit® Working Solution and incubated for 2 minutes at room temperatures. The two standards have 0 ng/µL and 10 ng/µL RNA, respectively. The relative fluorescence was plotted against the two concentrations in order to obtain the calibration curve. 2µl of each initial sample was diluted in 198 µl of Qubit working solution and incubated at room temperature for 2 minutes. Concentration values were finally calculated by the fluorimeter built-in software using a simple equation. Each sample concentration was given in ng/mL. Recommended concentration per sample was set to 37 ng/ml.

3.7.8 Illumina RNA sequencing workflow

Illumina RNA sequencing provides accurate, quick and large-scale sequencing in a minimum time followed by high accuracy data collection. It is divided into 4 major phases including sample preparation, cluster generation or clustering, sequencing and data analysis.

3.7.8.1 *Acanthamoeba* cDNA libraries and sample preparation

After RNA isolation, the samples contain many RNA types such as ribosomal RNA (rRNA), precursor messenger RNA (pre-mRNA), mRNA, miRNA and numerous types of non-coding RNA (ncRNA). Non-removal of the rRNA, which comprises approximately 90% of the whole RNA, before cDNA library construction will result in limited detection of less abundant RNAs and subsequently to weakened detection of expressed genes. Taking into consideration the fact that efficient removal of rRNA is a crucial first step for a successful transcriptome profile analysis, the downstream process is focused on enriching mRNA by selecting poly-adenylated (poly-A) RNAs, before library construction. This is mainly achieved by modified poly-T oligos which target the 3' poly-A tail of mRNA. After cDNA synthesis adapters are attached to the DNA fragments. These adapters include sequence binding site, indices and regions complementary to flow cell oligos (Chaitankar et al., 2016), (Figure: 3.4).

3.7.8.2 Clustering

Clustering is a process were every DNA fragment is isothermally amplified after attachment to flow cell's complementary sequence (Figure 3.4). Briefly, once libraries

have been set, hundreds of millions of DNA templates are hybridized to an eight-line flow cell that comprises a layer of covalently attached (immobilized) oligonucleotides complementary to the oligo-adapters that were introduced in the library cDNA stage (Corney et al., 2013; Fedurco et al., 2006; Chaitankar et al., 2016). Afterwards, high-fidelity DNA polymerases extend primers from 3'-ends while a denaturing stage removes the original template, leaving the copies immobilized on the cell surface. Later DNA templates are looped to complementary neighbor oligos forming a bridge. DNA polymerases replicate the templates from the hybridized oligos, forming dsDNA bridges, which are finally denatured to form dsDNA. Bridge amplification is repeated approximately 20 to 25 times and results in clusters of DNA replicates in which 50% represent the forward and 50% the reverse orientation. Repetition of the process by cycles of isothermal amplification and denaturation generate millions of copies, comprising approximately 2,000 molecules (Corney et al., 2015). The flow cell encloses more than 200 million clusters, with approximately 103 molecules per cluster (Figure 3.4; 3.5).

A lower or higher cluster density could result in unexpected reads and subsequently in erroneous comparisons and faulty outcomes. Reaching an ideal cluster density is therefore crucial, as it will define the number of reads obtained. Finally, the reverse strands are cleaved and removed and only the forward strands are used for sequencing.

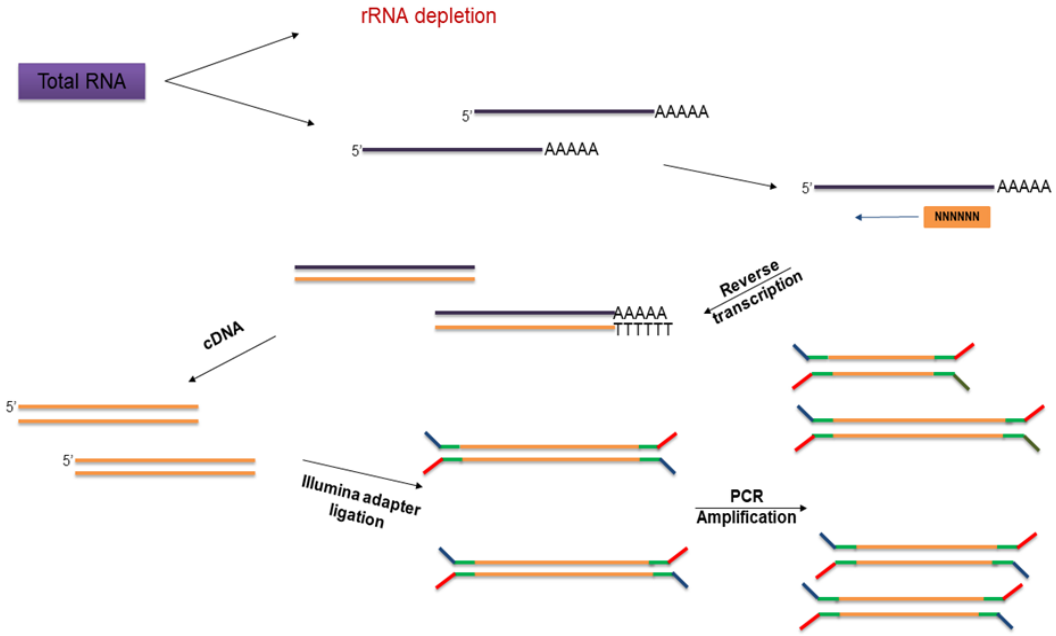

Figure 3.4: cDNA library preparation and illumina adapter's ligation.

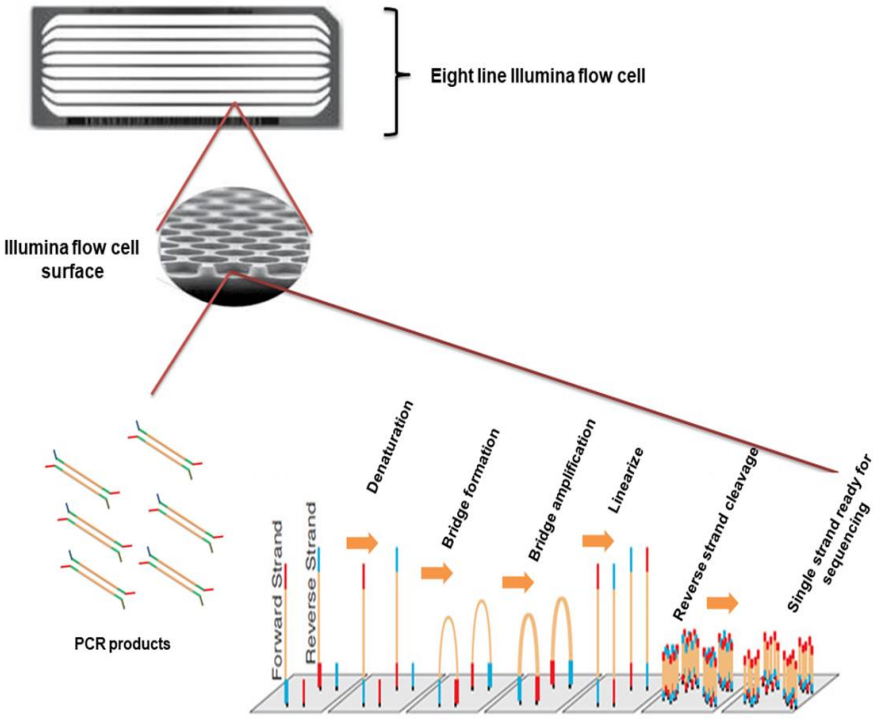

Figure 3.5: Simplified clustering procedure.

3.7.8.3 Sequencing

During sequencing, solutions of fluorescent labeled and reversible terminated nucleotides are added to run across the lanes of the flow cell, allowing their incorporation to the new DNA strand composition (Chaitankar et al., 2016). Briefly, a single predetermined fluorescent color corresponds to a specific nucleotide which in turn is imaged by laser excitation. Later, the fluorescent derivative is cleaved and washed off, allowing the incorporation of the next nucleotide. Fluorescence signals are recorded constantly by a camera, where powerful processors and programs convert fluorescence images to unreadable fastq files that under specific processing could lead later to readable DNA sequences. Pair end (PE) sequencing is also feasible in which both ends of the DNA template are sequenced resulting in two reads per fragment. This is achieved by a second round of bridge amplification where the forward strand is cleaved and washed away instead of reverse. This method was followed in this experiment and both reads were processed computationally. PE sequencing results in increased map-ability for repetitive regions and allows identification of splicing variants and chimeric transcripts.

3.7.8.4 Data analysis

Data analysis workflow, which is the final stage of Illumina RNA sequencing workflow, are explained thoroughly and methodically in bioinformatics tools and methods.

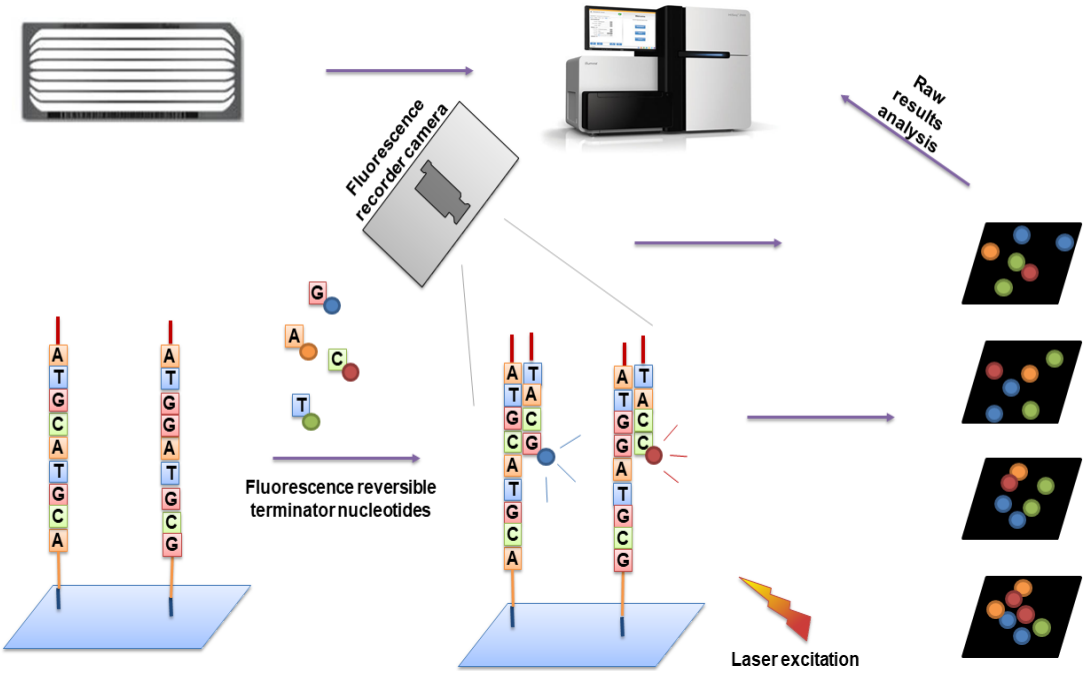

Figure 3.6: Illumina sequencing and data processing workflow.

3.8 Cytochrome c detection by western blotting

Detection of *Acanthamoeba* cytochrome c release, was achieved by western immunoblotting. Abcam's Cytochrome c Releasing Apoptosis Assay Kit (ab65311) provided an effective way for detecting cytochrome c translocation from mitochondria to cytosol during *Acanthamoeba* cell death. Manufacturers' instructions were followed.

Briefly, *Acanthamoeba* trophozoites were cultured routinely in T-25 flasks for 2 days at room temperature to confluency. Flasks were washed twice and EC_{90} G-418 were

applied in Neff's saline buffer. Cells were incubated at 37ºC for a predetermined period (0, 1, 3, 6 hours). After treatment *Acanthamoeba* cells were collected in Eppendorf tubes and centrifuged at 500 g for 5 minutes (~ 5 x 10^5/mL). Cells were washed once with N.S.B. and supernatant was removed. 1 mL of 1X Cytosol Extraction Buffer Mix containing DTT and Protease Inhibitors was used to re-suspend the pellet and the sample was incubated in ice for 10 minutes. Approximately 4-6 cycles of freeze–thaw were conducted using dry ice to freeze *Acanthamoeba* suspension (~4 min) and a tube thermal incubator set at 37ºC (~3 min). Cell homogenization was monitored under a microscope by applying 2-3µL of cell suspension onto a coverslip.

Later, the sample mix was centrifuged at 10,000 g for 30 minutes at 4ºC to separate the cytosolic and mitochondrial fractions. Supernatant was collected in a new Eppendorf tube and labeled as Cytosolic fraction. Pellet was re-suspended in 100 µL Mitochondrial Extraction Buffer Mix that contained DTT and protease inhibitors and the mixture was vortexed for 10 to 15 seconds and labeled as mitochondrial fraction. All samples were stored overnight at -20ºC before further processing.

3.8.1 SDS PAGE

1.0 millimeter, 16% separating and stacking gels were prepared as table 3.4 indicates. 10% w/v ammonium persulfate was prepared on the day of the experiment. Gels were left around 30 to 40 minutes to polymerize. A small amount of ethanol (~1mL) was applied on the top of the bottom running gel in order to smooth gel surface, which was later rinsed with ddH_2O.

Approximately, 10 µg (Pierce BCA protein assay kit) of each cytosolic and mitochondrial fraction isolated from treated and untreated *Acanthamoeba* trophozoites from several time points were mixed with 2X loading buffer consisting of: 10% w/v SDS, 10 mM dithiothreitol or beta-mercapto-ethanol, 20 % v/v glycerol, 0.2 M Tris-HCl, pH 6.8, 0.05% w/v bromophenol blue. Later, the mixture was boiled in a boiling water bath for 5 minutes and loaded on a 15% SDS polyacrylamide gel (Table 3.4a; 3.4b). Electrophoretic

separation was carried out in 1X electrode buffer containing 25 mM Tris-HCl, 200 mM glycine and 0.1% (w/v) SDS in a BIO-RAD mini protean system, first at 60V and then at 120 V, at room temperature, until sample tracking dye reached the very bottom of the gel (~3 hours), Bio Rad precision plus protein dual colour standard was used to calculate protein MW. Finally, gels were stained using Coomassie blue for 45 minutes at room temperature and destained gradually with destaining solution (10% v/v acetic acid and 40% v/v methanol). Coomassie staining was mostly used after protein transfer to examine transfer efficiency.

a)

Chemicals	15% Separation gel
Tris buffer (1.5M, pH 8.8)	3.75 mL
Acrylamide/Bis-acrylamide (30%/0.8% w/v)	8.0 mL
10% (w/v) SDS	150 µl
10% (w/v) APS	100 µl
ddH_2O	3.2 mL
TEMED	10 µl
V_{final}	15mL

b)

Chemicals	Stacking gel
Tris buffer (0.5M, pH 6.8)	3.78 mL
Acrylamide/Bis-acrylamide (30%/0.8% w/v)	2 mL
10% (w/v) SDS	150 µl
10% (w/v) APS	75 µl
ddH_2O	9 mL
TEMED	10 µl
V_{final}	15 mL

Table 3.3: Running (a) and stacking (b) gel composition.

3.8.2 Protein transfer

Proteins were transferred from polyacrylamide gel to a 0.4mm PVDF membrane by electric current through an orientated scaffold of sponges and filters. More specifically, a freshly transfer buffer (Tris-Glycine-Methanol; TGM) was created containing 25 mM Tris, 192 mM glycine and 10% methanol and stored at 4ºC. After electrophoresis, gels were washed twice in TGM for 5 minutes at room temperature to remove SDS and salts, while PVDF membranes were soaked in 100% methanol for 1 minute at RT. The protein gel was then placed between PVDF membrane and filters as shown in figure 3.6. Bubbles between the gel and the membranes were carefully removed by rolling out, as they result in inhibition of protein transfer. The whole construction was moved into a TGM buffered tank and transfer carried out at 55V for 1 hour at 4ºC (Figure 3.7).

After protein electro-transportation, PVDF membranes were stained with Ponceau S for 5 minutes at RT and gels were also stained with Coomasie blue to examine transportation efficiency. PVDF membranes were later gradually destained with ddH_2O excess. Membranes were later rinsed with TBS once for 5 minutes and gently agitation to remove excess methanol. Membranes were blocked after incubation at room temperature and for 60 minutes with 3.5% non-fat dried milk and washed twice with TBS + 0.1% Tween-20.

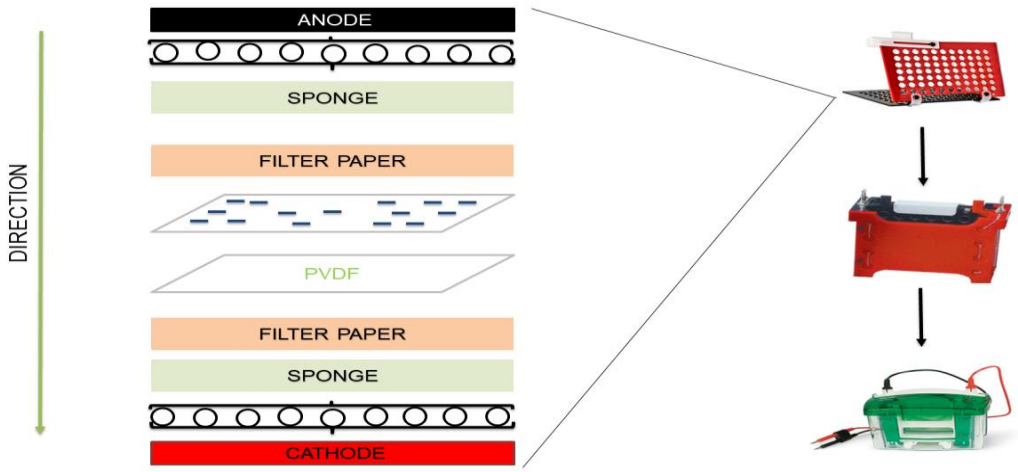

Figure 3.7: Protein transfer sandwich and Bio-Rad electrophoresis units for western blot.

3.8.3 Cytochrome c immuno-detection

Abcam's polyclonal rabbit anti-cytochrome c antibody (ab90529) was used at a final concentration of 2 µg/mL (~1:200) in 3.5% w/v skimmed dried milk, in NSB, V_{final} = 20 mL. PVDF membranes were incubated at 4℃, overnight with agitation and washed twice the next day for 5 minutes with TBS-T (TBS-0.1% Tween-20). Later a secondary fluorescent antibody was used to identify rabbit polyclonal anti-cytochrome c. Odyssey Goat anti-rabbit IgG IRDye 680 was diluted in 3.5% w/v skimmed dried milk, in NSB to 1 µg/mL, V_{final} = 20 mL and applied to protein membranes for 1 hour at room temperature, in the dark with gentle agitation. After the secondary antibody solution was discarded, membranes washed twice for 5 minutes with TBS + 0.1% Tween-20 and left to dry at room temperature in the dark.

3.8.4 Visualization

Membranes were observed with a LI-COR Odyssey Classic imager scanner and analyzed by win Image studio 5.2 analysis software.

3.9 Bioinformatics

3.9.1 Basic local alignment search tool (BLAST)

Protein and nucleotide BLAST was performed using the NCBI. Results were analyzed to identify species, search for homologous genes and compare protein sequences (Pearson, 2013).

3.9.2 Sequence alignments and phylogeny tree

Nucleotide sequences were obtained by DNA sequencing, GenBank and AmoebaDB, while protein sequences were obtained by Uniprot and AmoebaDB (Aurrecoechea et al., 2011). MEGA 7 was the main software used to align sequences with the Muscle algorithm (Edgar, 2004; Kumar et al., 2016; Hall, 2013). Maximum likelihood phylogeny tree construction was also performed by MEGA 7.

No	Species and strain	GenBank accession No	GENOTYPE
1	***Acanthamoeba castellanii*** **CDC:0981:V006**	**U07400**	**T1**
2	***Acanthamoeba palestinensis*** **Reich ATCC 30870**	**U07411**	**T2**
3	***Acanthamoeba griffini*** **S-7**	**U07412**	**T3**
4	***Acanthamoeba castellanii*** **Neff**	**U07416**	**T4**
5	***Acanthamoeba castellanii*** **Ma**	**U07414**	**T4**
6	***Acanthamoeba divionensis*** **strain AA1**	**AY351645**	**T4**
7	***Acanthamoeba lugdunensis***	**AF005995**	**T4**
8	***Acanthamoeba*** **sp. KA/E2**	**AF005998**	**T4**
9	***Acanthamoeba*** **sp. KA/E15**	**AY148961**	**T4**
10	***Acanthamoeba triangularis***	**AF316547**	**T4**
11	***Acanthamoeba lenticulata***	**U94741**	**T5**
12	***Acanthamoeba palestinensis***	**AF019063**	**T6**
13	***Acanthamoeba astronyxis***	**AF019064**	**T7**
14	***Acanthamoeba tubiashi***	**AF019065**	**T8**
15	***Acanthamoeba comandoni***	**AF019066**	**T9**
16	***Acanthamoeba culbertsoni Lilly*** **A-1**	**AF019067**	**T10**
17	***Acanthamoeba hatchetti*** **BH-2**	**AF019068**	**T11**
18	***Acanthamoeba healyi***	**AF019070**	**T12**
19	***Acanthamoeba sp.*** **UWC9**	**AF132134**	**T13**
20	***Acanthamoeba*** **PN15**	**AF333607**	**T14**
21	***Acanthamoeba jacobsi***	**AY262364**	**T15**

Table 3.4: List of *Acanthamoeba* genotypes and GenBank accession numbers used for the phylogenetic tree construction.

3.9.3 mRNA seq bioinformatics tools and workflow

mRNA sequencing was performed to evaluate gene expression in EC_{90} G-418 treated amoebae, which presented characteristics of apoptosis and regulated cell death, versus untreated *Acanthamoeba* populations at four different time points (0, 1, 3, 6 hours after G-418 treatment) during the cell death process. RNA was isolated as previously described. *Acanthamoeba* trophozoites from the GS isolate, which belongs to genotype T4, was used for the experimental procedure. mRNA sequencing was conducted by Edinburgh Genomics and resulted in approximately 750 GB of raw data. Several bioinformatics tools were used in order to analyze the raw paired reads that were produced from the illumina sequencer (Figure 3.8).

3.9.3.1 Quality control of RNA seq raw reads

Modern sequencers can generate thousands or millions of sequences in a single run. Before the downstream analysis of the information that is encoded in these sequences it is vital to examine the quality of the raw data to ensure that there are no issues or biases that can affect the final outcome. Nowadays most sequencers create quality reports as part of their analysis but those results are limited. In order to assess the raw reads quality, the FastQC tool with a simple command from a Linux terminal was used. Each sequencing run ended with two fastq files; one produced from the forward read and the other one from the reverse reads.

Cautious and profound observation of the quality control results of all 96 FASTQ files revealed that no further pre-processing of the data was needed. Quality controls include per base sequence quality, per tile sequence quality, adaptor presence, occurrence of duplicated reads (potential sequencing errors), sequence length distribution, GC content, per base N content and overrepresented k-mers.

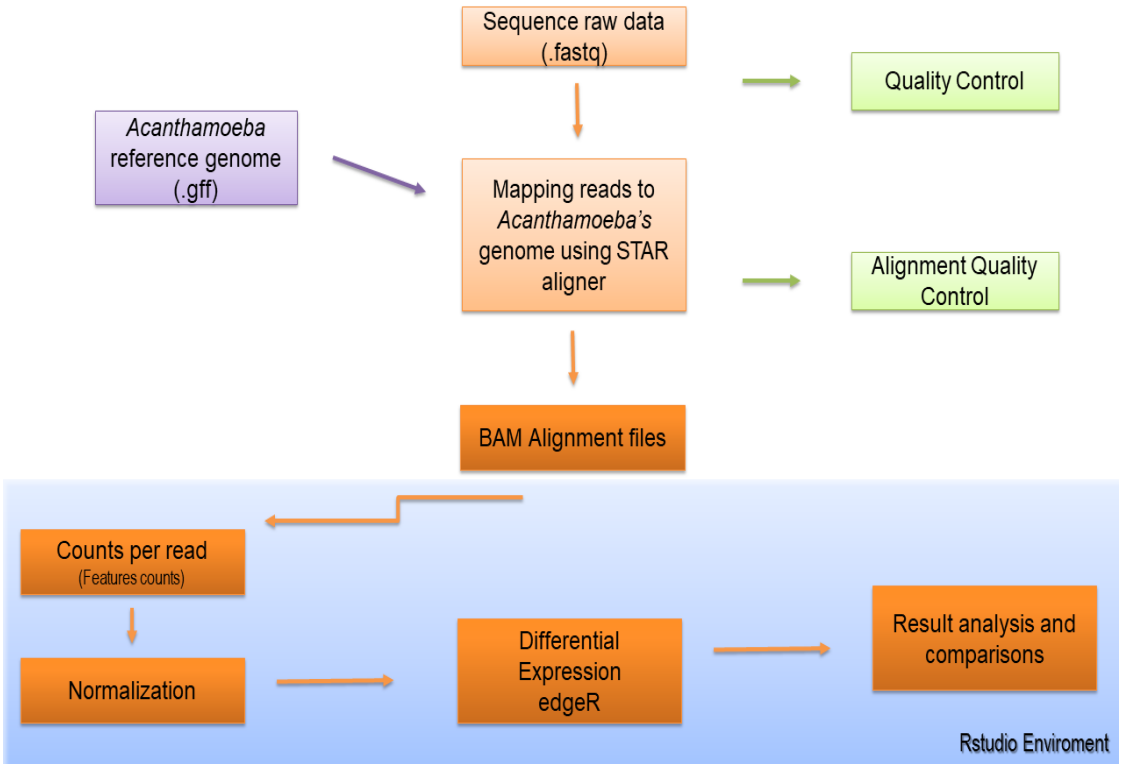

Figure 3.8: RNA seq data workflow.

3.9.3.2 Mapping reads to genome

Alignments were produced by the STAR aligner, resulting in BAM files. STAR is a fast and accurate aligner that detects canonical and uncanonical splice junctions and chimeric sequences (Haas et al., 2017). Reads were aligned to *Acanthamoeba's* reference genome (obtained from ENSEMBL Protists) which was previously indexed with STAR. The mapping quality was measured during the alignment and at the end of the process aggregated. The mapping rate and number of uniquely mapped reads aligned to reference genome was monitored using SAM tools. Later, alignments (final BAM files) were visualized using the IGV genome browser program to further confirm the quality of

the alignment (Robinson et al., 2013). By this method, gene deletions and insertions were also identifiable.

Bias identifications that were taken under consideration at this point were intron coverage, intergenic reads and 3' bias. Abundance of immature transcripts and incomplete poly (A) enrichment could result in increased intron coverage, while a high percentage of intergenic reads predicts genomic contamination. Finally, 3' high representation regions could indicate potential RNA degradation. IGV was the main program by which this evaluation was conducted.

Acanthamoeba's genome was indexed under the parameters:

$ STAR –runMode genomeGenerate –genomeDir –genomeFastaFiles Acanthamoeba_castellanii_str_neff.Acastellanii.strNEFF_v1.dna.nonchromosomal.fasta \–sjdbGTFfile Acanthamoeba_castellanii_str_neff.Acastellanii.strNEFF_v1.37.gtf

While, raw reads were aligned to genome using parameters:

$ STAR – genomeDir (files directory) –readFilesIn \ {RawRead(experimentcondition1a1)_1.fastqRawRead(experimentcondition1a1)_2.fastq } -- outFilterType BySJout – outFilterMultimapNmax 20 –outSAMunmapped Within\ --outFileNamePrefix Acanth_exp.condition_ --outSAMtype BAM SortedByCoordinate

3.9.3.3 Differential Expression analysis

Further analysis of the aligned reads was conducted in Rstudio 1.1.383 environment using various R-supported libraries and packages including, readr, statmode, bplyr, rtracklayer, Rsubread, limma and edgeR, in order to read, process, analyze and visualize inserted BAM aligned files.

Reads generated from RNA sequencing (BAM files) were quantified by featureCounts using *Acanthamoeba*'s GFF file (*Liao* et al., 2014). Later, data values were normalized using the trimmed median of M values (TMM) which is available in EdgeR (Robinson and Oshlack, 2010). By this means, observed count values of each sample were adjusted to a common value all across sequencing experiment libraries.

Differentially expressed (DE) genes were identified by setting standards of a fold change (fc _threshold) of < 2 and an FDR threshold of < 0.001 after biological coefficient of variation and moderated tagwise dispersion have been estimated. Later, genes of interest were selected for further analysis. Limma-voom was used with "makeContrasts" and "topTags" functions in order to recognize DE genes (Ritchie et al., 2015).

During DE analysis, various groups were created in order to categorize the aligned reads from the different time points and treatment conditions. Plots were also generated in Rstudio 1.1.383 using packages and libraries such as ggplot2, lattice and heatmap. Analytical outline of the script used for the analysis can be found in appendix 1.

Chapter 4

Molecular phylogeny of *Acanthamoeba*

4.1 Introduction

Acanthamoeba spp. are free-living amoebae, evenly distributed in the natural environment extending from soil to almost every aquatic habitat (Rodríguez-Zaragoza 2008). They also play an important central environmental role in bacterial diversity and their population regulation. The genus of *Acanthamoeba* is classified within the phylum Amoebozoa, subphylum Lobosa and the order Centramoedida (Cavalier-Smith et al., 2016).

Amoeboid microorganisms are phylogenetically fairly diverse, with some being more closely genetically related to plants or metazoans than to each other. Historically, classification of *Acanthamoeba* has been relied on morphological features (Pussard and Pons, 1977; Jonckheere, 1983, Costas and Griffiths, 1985), however currently, *Acanthamoeba* is classified into 20 different genotypes T1-T20 based exclusively on structural analysis of the SSU gene sequence (Corsaro, 2011, 2015).

Phylogeny refers to the evolutionary history of a taxonomic group of organisms, with particular reference to lines of ancestry and relations between an extensive set of organisms. The affiliation between taxa is usually demonstrated through molecular sequencing data and morphological data matrices.

Phylogenetic analysis is a process of elucidation of the evolutionary relationship among a group of organisms and is represented by a diagrammatic schema composed of nodes and branches, widely known as a phylogenetic tree. In modern molecular phylogenetic analysis the DNA sequence of a mutual gene or protein is used to evaluate the evolutionary relationship of species. Phylogeny is thus essential in understanding

biodiversity, genetics and evolution among groups of organisms. More precisely, diversity and phylogeny of *Acanthamoeba spp*. could assist to the development of a more congruent, precise and comprehensive classification, which in turn might provide an improved understanding of microorganism's physiology and patho-physiology.

The main purpose of the isolation and genotype identification, which this chapter describes, was initially the evaluation of the catholicity of the G-418 aminoglycoside effect on a wild strain, not previously isolated and cultured in axenic conditions. It was reported by Köhsler et al., that *Acanthamoeba* strains that have been cultured in axenic conditions for years gradually lose their ability to encyst (Köhsler et al., 2008). Encystment is perhaps not the only biological process that could have been lost during continuous cultivation and due to this observation, a new wild strain isolate, preferably belonging to the T4 genotype, which is the most widely distributed, was required.

Briefly*, Acanthamoeba* isolation was performed as previously described in 3.3.1 and the new axenic strain was labelled as 'GS strain', after George Square gardens, Edinburgh. Genomic DNA exctraction of the new isolate was conducted (3.7.1) and PCR amplification was performed under specific 18S rRNA primers, in order to determine the isolate T-type (3.7.2). PCR products were subsequently electrophoresed (3.7.4) and purified (3.7.3) before sent to Edinburgh Genomics for DNA sequencing (3.7.5). Later, retrieved sequences were aligned against multiple and different *Acanthamoeba* genotype 18S rRNA sequences (3.9.2) retrieved from GenBank (Table 3.5), using the MUSCLE algorithm. Finally, maximum like-hood phylogeny tree construction was performed by MEGA 7 (3.9.2) based on MUSCLE alignment.

4.2 Results - Phylogeny

The identification, classification and phylogenetic analysis of the *Acanthamoeba spp*. (GS isolate), which was isolated from George Square gardens, Edinburgh and was described analytically in materials and methods (3.4; 3.7), was conducted by 18S rRNA,

partial and simultaneously 18S rRNA (SSU) gene amplification (3.7.5) and subsequent sequence comparison analysis. Initially, PCR amplification of the ASA.S1 fragment which contains the diagnostic fragment ASA.S1, was reproduced by the JDP1 and JDP2 specific primers (3.7.2) and used successfully to identify the isolate as an *Acanthamoeba* genus.

Retrieved ASA.S1 sequence and homology search showed 94 – 98% identity to *Acanthamoeba* T4 genotype deposited in Genbank database. The T4 genotype is one of the most frequent *Acanthamoeba* genotypes isolated from all environments and it is simultaneously the most common genus associated to human diseases (Maciver et al., 2013).

A more precise classification of the isolate was performed by analysing the total 18S gene (SSU) of the isolated strain by phylogenetic analysis. SSU 18S rDNA gene is expected to show variation even among strains of the same species (Nassonova, 2010). The GS isolate 18S rRNA retrieved sequence was aligned with 20 different 18S rRNA sequences from different *Acanthamoeba* genotypes ranging from T1 to T15 (table 3.4), retrieved from GenBank, using MUSCLE aligner (3.9.2). Maximum likelihood phylogenetic analysis revealed that the GS isolate was clustered into pathogenic T4 genotype (Figure 4.1) and more genetically and evolutionarily close to *Acanthamoeba castellani* T4 Neff's strain. Meanwhile, the closest genotypes to T4 were found to be genotype T3 and T11, which parenthetically are all categorized to morphogroup II. Genotypes T7, T8 and T9 from morphogroup I are clustered in the same clade (Figure 4.1; Figure 4.2). Additionally, genotypes T5, T10, T12 and T15 from morphogroup III, were also found to be evolutionarily close.

Classification based on the ASA.S1 fragment was also performed (Figure 4.2) in order to combine the phylogenetic trees. As expected the outcome was close enough to full 18S gene (SSU) analysis. However slight variations were easily distinguishable mostly due to ASA.S1 enormous variability. 72 different *Acanthamoeba* genotypes and sequences were retrieved from GenBank for the tree construction. Genotype cluster of T4, T3 and T11 found again to be the most closely related as also genotypes T5, T10 and T12.

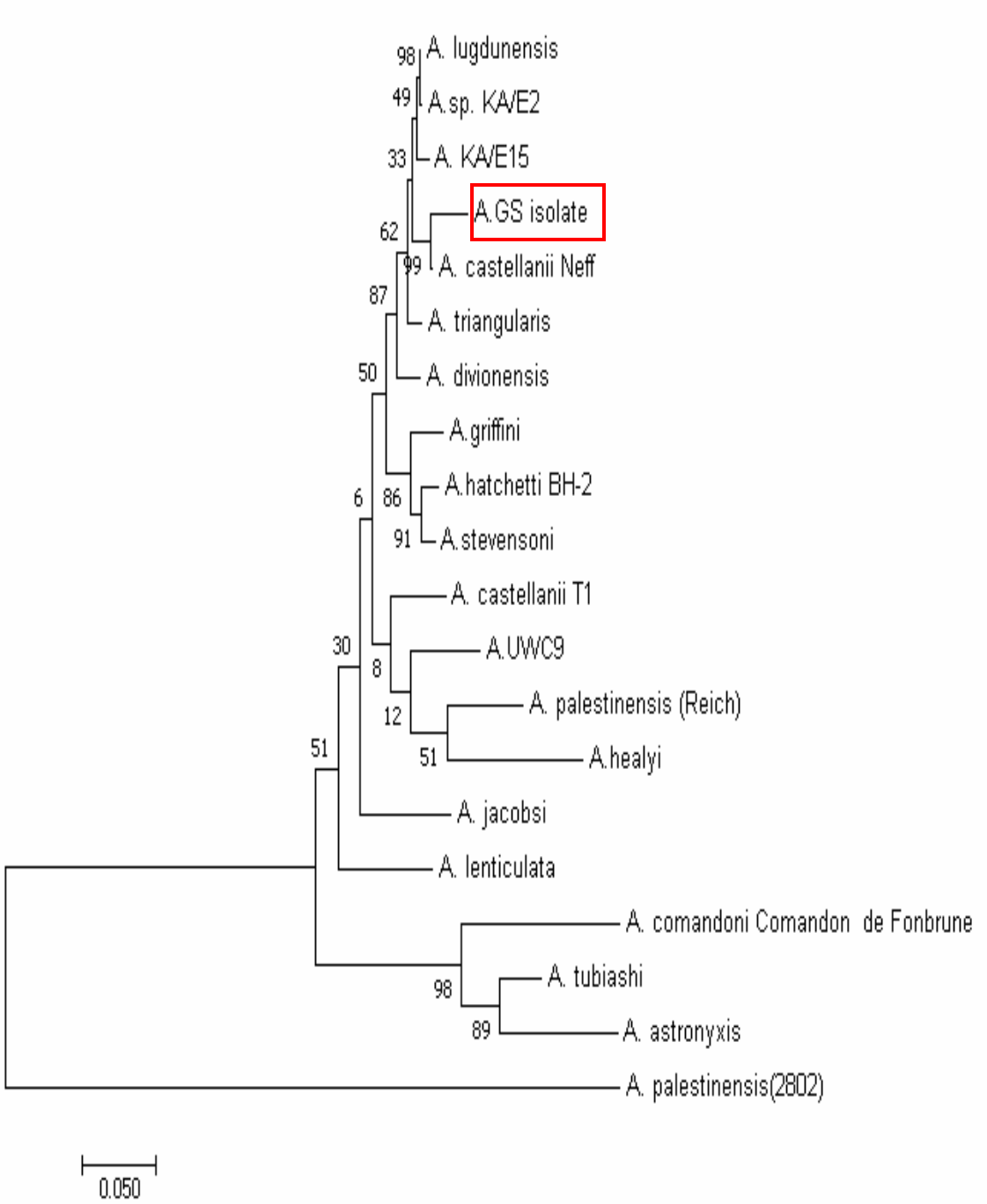

Figure 4.1: Phylogenetic tree of isolated the *Acanthamoeba* strain (*Acanthamoeba* GS isolate is highlighted in a red box) based on the full 18S rDNA gene, maximum likelihood method, 100 bootstrap replications, MEGA 7, (Kimura, 1980; Kumar 2016; Felsenstein, 1985).

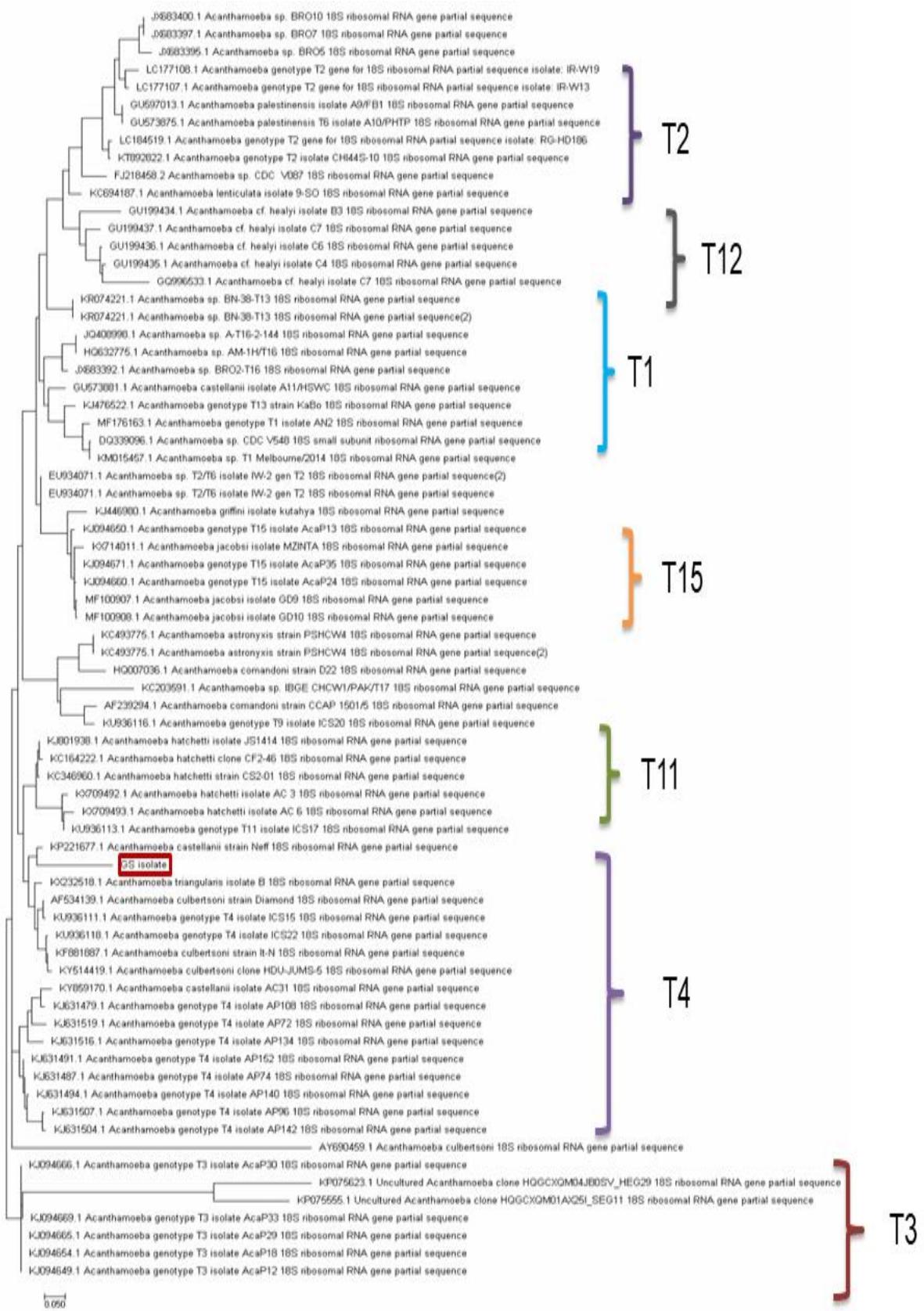
JX683400.1 Acanthamoeba sp. BRO10 18S ribosomal RNA gene partial sequence
JX683397.1 Acanthamoeba sp. BRO7 18S ribosomal RNA gene partial sequence
JX683395.1 Acanthamoeba sp. BRO5 18S ribosomal RNA gene partial sequence
LC177108.1 Acanthamoeba genotype T2 gene for 18S ribosomal RNA partial sequence isolate: IR-W19
LC177107.1 Acanthamoeba genotype T2 gene for 18S ribosomal RNA partial sequence isolate: IR-W13
GU597013.1 Acanthamoeba palestinensis isolate A9/PB1 18S ribosomal RNA gene partial sequence
GU573875.1 Acanthamoeba palestinensis T6 isolate A10/PHTP 18S ribosomal RNA gene partial sequence
LC184519.1 Acanthamoeba genotype T2 gene for 18S ribosomal RNA partial sequence isolate: RG-HD186
KT892822.1 Acanthamoeba genotype T2 isolate CH44S-10 18S ribosomal RNA gene partial sequence
FJ218458.2 Acanthamoeba sp. CDC V087 18S ribosomal RNA gene partial sequence
KC894187.1 Acanthamoeba lenticulata isolate 9-SO 18S ribosomal RNA gene partial sequence
T2
GU199434.1 Acanthamoeba cf. healyi isolate B3 18S ribosomal RNA gene partial sequence
GU199437.1 Acanthamoeba cf. healyi isolate C7 18S ribosomal RNA gene partial sequence
GU199436.1 Acanthamoeba cf. healyi isolate C6 18S ribosomal RNA gene partial sequence
GU199435.1 Acanthamoeba cf. healyi isolate C4 18S ribosomal RNA gene partial sequence
GQ996533.1 Acanthamoeba cf. healyi isolate C7 18S ribosomal RNA gene partial sequence
T12
KR074221.1 Acanthamoeba sp. BN-38-T13 18S ribosomal RNA gene partial sequence
KR074221.1 Acanthamoeba sp. BN-38-T13 18S ribosomal RNA gene partial sequence(2)
JQ400998.1 Acanthamoeba sp. A-T16-2-144 18S ribosomal RNA gene partial sequence
HQ632775.1 Acanthamoeba sp. AM-1H/T16 18S ribosomal RNA gene partial sequence
JX683392.1 Acanthamoeba sp. BRO2-T16 18S ribosomal RNA gene partial sequence
GU573881.1 Acanthamoeba castellanii isolate A11/HSWC 18S ribosomal RNA gene partial sequence
KJ476522.1 Acanthamoeba genotype T13 strain KaBo 18S ribosomal RNA gene partial sequence
MF176163.1 Acanthamoeba genotype T1 isolate AN2 18S ribosomal RNA gene partial sequence
DQ339096.1 Acanthamoeba sp. CDC V540 18S small subunit ribosomal RNA gene partial sequence
KM015467.1 Acanthamoeba sp. T1 Melbourne/2014 18S ribosomal RNA gene partial sequence
T1
EU934071.1 Acanthamoeba sp. T2/T6 isolate IW-2 gen T2 18S ribosomal RNA gene partial sequence(2)
EU934071.1 Acanthamoeba sp. T2/T6 isolate IW-2 gen T2 18S ribosomal RNA gene partial sequence
KJ446980.1 Acanthamoeba griffini isolate kutahya 18S ribosomal RNA gene partial sequence
KJ094650.1 Acanthamoeba genotype T15 isolate AcaP13 18S ribosomal RNA gene partial sequence
KX714011.1 Acanthamoeba jacobsi isolate MZINTA 18S ribosomal RNA gene partial sequence
KJ094671.1 Acanthamoeba genotype T15 isolate AcaP35 18S ribosomal RNA gene partial sequence
KJ094660.1 Acanthamoeba genotype T15 isolate AcaP24 18S ribosomal RNA gene partial sequence
MF100907.1 Acanthamoeba jacobsi isolate GD9 18S ribosomal RNA gene partial sequence
MF100908.1 Acanthamoeba jacobsi isolate GD10 18S ribosomal RNA gene partial sequence
T15
KC493775.1 Acanthamoeba astronyxis strain PSHCW4 18S ribosomal RNA gene partial sequence
KC493775.1 Acanthamoeba astronyxis strain PSHCW4 18S ribosomal RNA gene partial sequence(2)
HQ007036.1 Acanthamoeba comandoni strain D22 18S ribosomal RNA gene partial sequence
KC203591.1 Acanthamoeba sp. IBGE CHCW1/PAK/T17 18S ribosomal RNA gene partial sequence
AF239294.1 Acanthamoeba comandoni strain CCAP 1501/5 18S ribosomal RNA gene partial sequence
KU936116.1 Acanthamoeba genotype T9 isolate ICS20 18S ribosomal RNA gene partial sequence
KJ801938.1 Acanthamoeba hatchetti isolate JS1414 18S ribosomal RNA gene partial sequence
KC164222.1 Acanthamoeba hatchetti clone CF2-46 18S ribosomal RNA gene partial sequence
KC346960.1 Acanthamoeba hatchetti strain CS2-01 18S ribosomal RNA gene partial sequence
KX709492.1 Acanthamoeba hatchetti isolate AC 3 18S ribosomal RNA gene partial sequence
KX709493.1 Acanthamoeba hatchetti isolate AC 6 18S ribosomal RNA gene partial sequence
KU936113.1 Acanthamoeba genotype T11 isolate ICS17 18S ribosomal RNA gene partial sequence
T11
KP221677.1 Acanthamoeba castellanii strain Neff 18S ribosomal RNA gene partial sequence
GS isolate
KX232518.1 Acanthamoeba triangularis isolate B 18S ribosomal RNA gene partial sequence
AF634139.1 Acanthamoeba culbertsoni strain Diamond 18S ribosomal RNA gene partial sequence
KU936111.1 Acanthamoeba genotype T4 isolate ICS15 18S ribosomal RNA gene partial sequence
KU936118.1 Acanthamoeba genotype T4 isolate ICS22 18S ribosomal RNA gene partial sequence
KF881887.1 Acanthamoeba culbertsoni strain It-N 18S ribosomal RNA gene partial sequence
KY514419.1 Acanthamoeba culbertsoni clone HDU-JUMS-5 18S ribosomal RNA gene partial sequence
KY859170.1 Acanthamoeba castellanii isolate AC31 18S ribosomal RNA gene partial sequence
KJ631479.1 Acanthamoeba genotype T4 isolate AP108 18S ribosomal RNA gene partial sequence
KJ631519.1 Acanthamoeba genotype T4 isolate AP72 18S ribosomal RNA gene partial sequence
KJ631516.1 Acanthamoeba genotype T4 isolate AP134 18S ribosomal RNA gene partial sequence
KJ631491.1 Acanthamoeba genotype T4 isolate AP162 18S ribosomal RNA gene partial sequence
KJ631487.1 Acanthamoeba genotype T4 isolate AP74 18S ribosomal RNA gene partial sequence
KJ631494.1 Acanthamoeba genotype T4 isolate AP140 18S ribosomal RNA gene partial sequence
KJ631507.1 Acanthamoeba genotype T4 isolate AP96 18S ribosomal RNA gene partial sequence
KJ631504.1 Acanthamoeba genotype T4 isolate AP142 18S ribosomal RNA gene partial sequence
T4
AY690459.1 Acanthamoeba culbertsoni 18S ribosomal RNA gene partial sequence
KJ094666.1 Acanthamoeba genotype T3 isolate AcaP30 18S ribosomal RNA gene partial sequence
KP075623.1 Uncultured Acanthamoeba clone HQGCXQM04JB0SV_HEG29 18S ribosomal RNA gene partial sequence
KP075555.1 Uncultured Acanthamoeba clone HQGCXQM01AQ25I_SEG11 18S ribosomal RNA gene partial sequence
KJ094669.1 Acanthamoeba genotype T3 isolate AcaP33 18S ribosomal RNA gene partial sequence
KJ094665.1 Acanthamoeba genotype T3 isolate AcaP29 18S ribosomal RNA gene partial sequence
KJ094664.1 Acanthamoeba genotype T3 isolate AcaP18 18S ribosomal RNA gene partial sequence
KJ094649.1 Acanthamoeba genotype T3 isolate AcaP12 18S ribosomal RNA gene partial sequence
T3
0.050

Figure 4.2: Phylogenetic tree of isolated *Acanthamoeba* strain (*Acanthamoeba* GS isolate-red box) based on partial analysis of 18S rDNA ASA.S1 fragment, maximum likelihood method, 100 bootstrap replications, MEGA 7, (Kimura, 1980; Kumar 2016; Felsenstein, 1985).

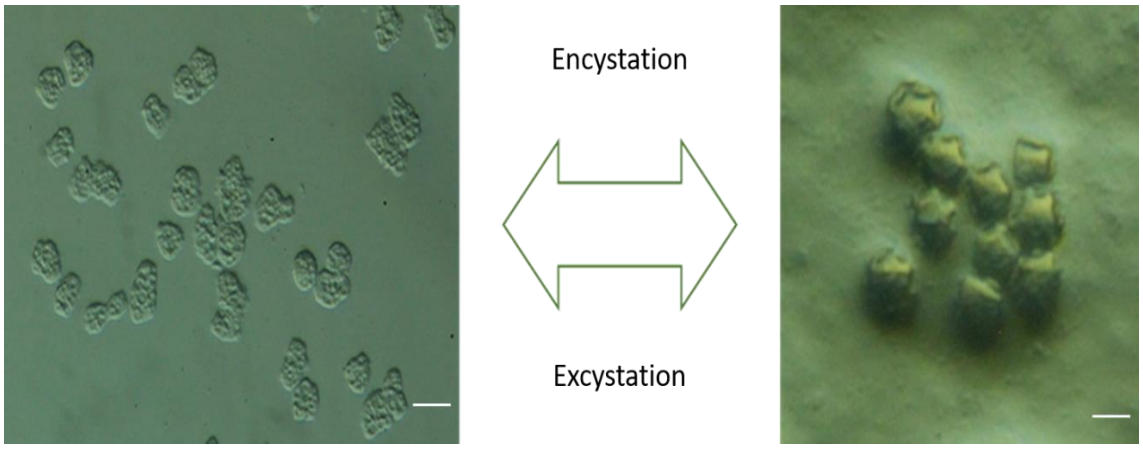

Figure 4.3: Morphology of GS isolated *Acanthamoeba* trophozoites (left) and cyst morphology (right). Morphologically GS isolate was categorized in the second morphogroup as represented by stellate endocysts with crumpled ectocysts forms. Scale bar 20 µm.

4.3 Discussion

Over the previous years, taxonomy and classification of *Acanthamoeba* was based entirely on trophozoite and cyst morphological features and sometimes on iso-enzyme profiling (Pussard and Pons, 1977; Jonckheere, 1983, Costas and Griffiths, 1980, 1985), rendering this categorization fairly misleading and inadequate. Based on this former misidentification and classification, misconceptions and constant alterations in *Acanthamoeba* systematics were constantly occurring. However, recently molecular and phylogenetic studies have been trying to compose all the different information and to subsequently represent a more consistent phylogeny for *Acanthamoeba spp.* (Stothard et al., 1998; Corsaro et al., 2011, 2015).

In this chapter, it was shown that both phylogenetic analyses, either based on the ASA.S1 fragment or on the full length of 18S rDNA gene, categorized the GS isolate in the T4 genotype cluster and more precisely genetically close to *Acanthamoeba castellanii* T4 genotype. Nevertheless, it is safer to assume that phylogeny based on the full size of the 18S rDNA gene was of higher phylogenetic value since more information is enclosed in the full-sized gene rather in a small portion of it.

On the other hand, phyogeny based on the ASA.S1 fragment comprises a quick and quite convenient method due to the abundance of ASA.S1 sequences recorded in databases (Corsaro, 2011). For instance, a quick examination of the GenBank database reveals approximately 2000 records of *Acanthamoeba* 18S rDNA genes. Interestingly, only 10% of the records are near to the full size of the gene, or at least close to the GTSA.B1 fragment, which is the minimal requirement for acceptable classification and genotyping (Schroeder-Diedrich, 1998; Schroeder, 2001).

ASA.S1 fragment certifies high genus specificity for *Acanthamoeba* identification and simultaneously is obtainable from all genotypes. This, combined with the fact that it is highly archiveable in gene databases, renders it ideal for diagnostic applications. However, it should not be considered as evidence for a new genus classification. In 2015, Corsaro argued that analysis of the ASA.S1 fragment is an insufficient method of

Acanthamoeba genus identification and classification and therefore the full length of the 18S rDNA gene should be used instead for such approaches. He proposed that an even bigger fragment (GTSA.B1 approx. 1600 bp) should be used as minimal identification requirement and simultaneously, the entire length of SSU should be analysed and compared for adequate classification (Corsaro, 2015).

Acanthamoeba categorization and phylogeny remain essential. The species identification and classification approaches have to be further improved, despite the numerous molecular characteristics that have been used for the microorganism taxonomic purposes hitherto, as there is large amount of erroneous information recorded in databases, which after processing, deliver mainly imprecise associations among species, genotypes and Acanthamoebidae morphogroups. For instance, members of T19 and the T20 genotype have been reported in both morphogroups II and III (Magnet, 2015; Fuerst, 2015; Corsaro, 2015).

Undoubtedly, a more reliable classification and taxonomy will become feasible over the coming years since much more information from molecular phylogeny and sequence analysis will be become available and accessible. Simultaneously, the use of the full 18S rDNA gene sequence in the species categorization will allow a much simpler comprehension and elucidation of *Acanthamoeba* evolution.

Chapter 5

Acanthamoeba cell death

5.1 Introduction

There are many pathways and mechanisms that can lead to cell death. Some of these include the use of chemicals or radiation, which in turn mediate stress signal production and transmission. The kind of signal or the concentration of a potential cell death inducer agent is particularly variable and differs from cell to cell. Some agents might be able to cause apoptosis in a specific cell type, necrosis or autophagy in another and simultaneously be effectless in a third one.

In the case of *Acanthamoeba,* induction of cell death was a tricky process not only because the microorganism is characterized by increased tolerance to several amebicide drugs and chemical substances, but mainly due to its ability to form resistant double-wall cysts, under unfavourable conditions. By this mean, ways of mediating cell death, including exclusively environmental stresses that could have led to cyst transformation including lack of nutrients, had been excluded from the beginning.

In this chapter, *Acanthamoeba* cell death was evaluated and characterized after treatment with various concentrations of G-418 in Neff's saline buffer, AX2 media and PBS at 37°C and room temperature; also numerous concentrations of Polymyxin b were tested, in various buffers and temperatures, as previously described in Methods, with the Trypan blue exclusion assay (3.4). PMB has previously been reported to have an impact on *Acanthamoeba* viability (Wright et al., 1985; John et al., 1990) while G-418 was never before used to treat microbial infections. It was however used for transfected *Acanthamoeba* trophozoites with resistance to G-418 selection (Peng et al., 2005). Furthermore, G-418 has been reported to induce programmed cell death in *Entamoeba*

histolytica (Villalba et al., 2007). Numerous substances including known inhibitors were also used to block or delay PMB- and G-418-mediated cell death in order to identify signs of programmed cell death.

5.2 Results

Generally, Polymyxin b (PMB) and G-418 aminoglycoside managed to induce cell death in *Acanthamoeba* trophozoites. However, there were remarkable differences in the way death was delivered by these drugs. G-418 induced cell death was characterized as a more selective and accurate procedure with a more defined morphology, while PMB-induced cell death was considered more accidental and imprecise. Initially, the two most important findings were the morphology of the dying and dead trophozoites, which was significantly dissimilar and the time frame in which cell death was occurring. Furthermore, an additional but important difference between the two substances and the way by which death was induced was that G-418 was able to induce extended cell death only under specific conditions, whereas PMB was characterized as a more versatile death inducer.

5.2.1 Polymyxin b induced cell death

Polymyxin b in concentrations ranging from 5μg/mL to 100μg/mL induced a concentration-dependent and rather acute cell death in *Acanthamoeba* trophozoites (Figure 5.1a). More specifically, 5μg/mL PMB reduced viability to approximately 4.23% after 360 minutes, while 10 μg/mL produced ananalogous effect in viability rate after 180 minutes. PMB at 100μg/mL had an even more acute effect on trophozoites, as it reduced more than 94% of *Acanthamoeba* viability in the first hour of treatment, compared to control trophozoites. Notably, it was observed that the effects of PMB varied significantly even between different isolates of the same genotype, as has already been reported (Khan, 2015).

It was observed that trophozoites with the highest percentage death rates were detected when incubated in NSB and at 37ºC, while the lowest percentage death rates were obtained when incubated in AX2 medium and at room temperature (Figure: 5.1a,b).

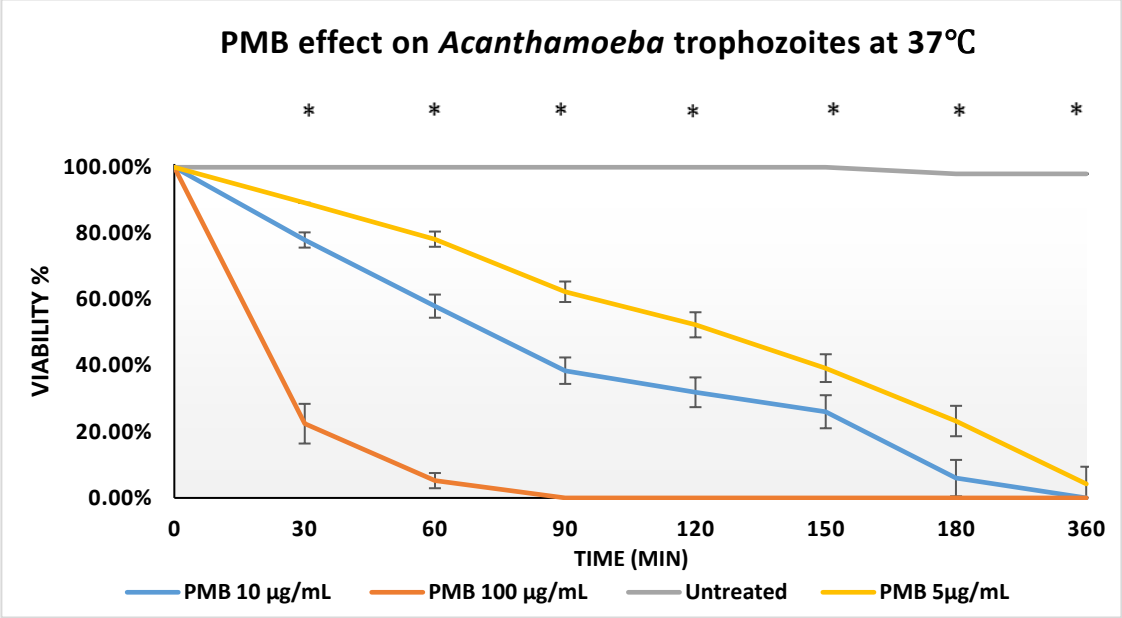

Figure 5.1a: The diagram demonstrates Neff's strain trophozoites viability of Polymyxin b treated and untreated population, related to minutes of incubation. Cells were incubated at 37°C in Neff's amoeba Saline buffer. Significance is indicated (*), ($P<0.05$, paired t-test; one tail distribution).

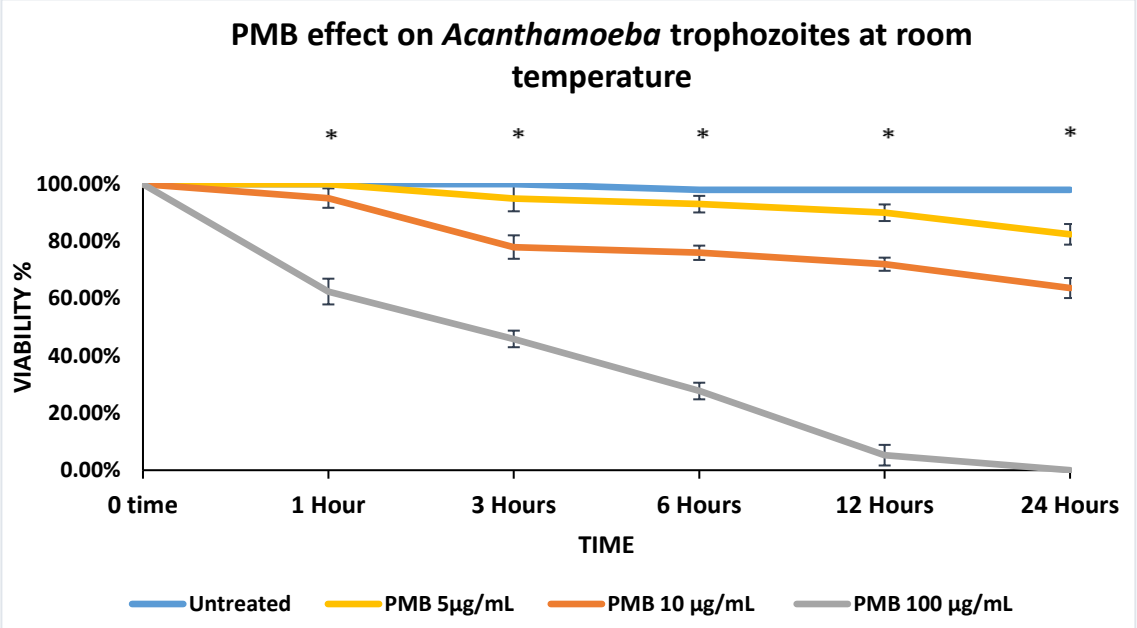

Figure 5.1b: The diagram represents *Acanthamoeba* Neff's strain viability during treatment with PMB in AX2 media at room temperature, Significance is indicated (*), ($P<0.05$, paired t-test; one tail distribution).

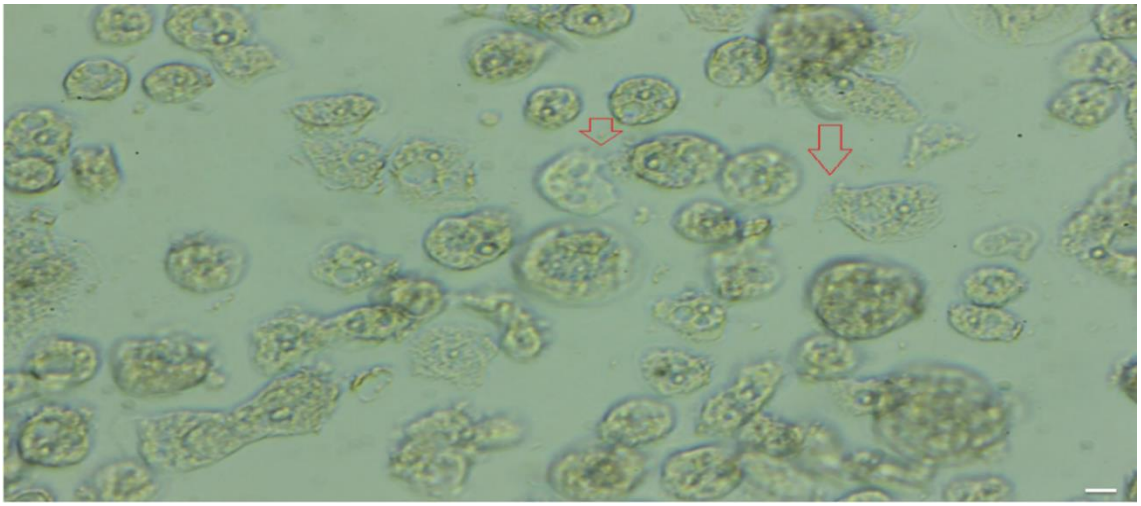

Figure 5.2: Characteristic effect of PMB on *Acanthamoeba* GS strain trophozoites in Neff's amoeba saline. The agent seems to create rupture in *Acanthamoeba* membrane leading to the release of cytosolic particles. Red arrows indicate trophozoites with compromised membranes, Scale bar 10µm.

During treatment with 10µg/mL PMB in NSB, no significant biochemical variation in intracellular calcium levels or any fluctuations in pH was noticed, at least in the first 60 minutes of incubation (Figure 5.3; 5.4). Later measurements of calcium intracellular levels were not feasible due to low numbers of cells. Control trophozoites were found to contain approximately 28 nM of intracellular free calcium while at the same time PMB treated trophozoites had similar concentrations, ranging from 27 to 31 nM.

Similarly, intracellular pH did not show any notable difference between control and treated cells, as control *Acanthamoeba* trophozoites showed parallel pH values to PMB-treated cells. The intracellular pH of untreated *Acanthamoeba* ranged from 7.5 to 7.7 while intracellular pH of treated Acanthamoeba was 7.5-7.6 (Figure 5.4).

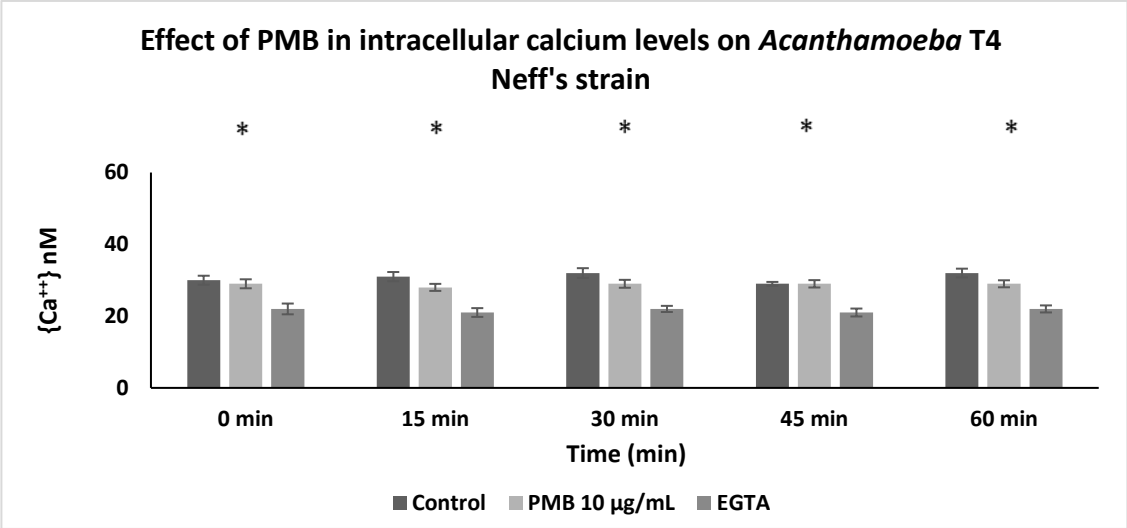

Figure 5.3: The histogram shows intracellular calcium levels of 10 µg/mL PMB-treated and untreated *Acanthamoeba* trophozoites, for 90 min after PMB induction, in NSB at 37ºC. Values are expressed as the means of 3 independent experiments, error bars represent SE, Significance is indicated (*), ($P<0.05$, paired t-test; one tail distribution).

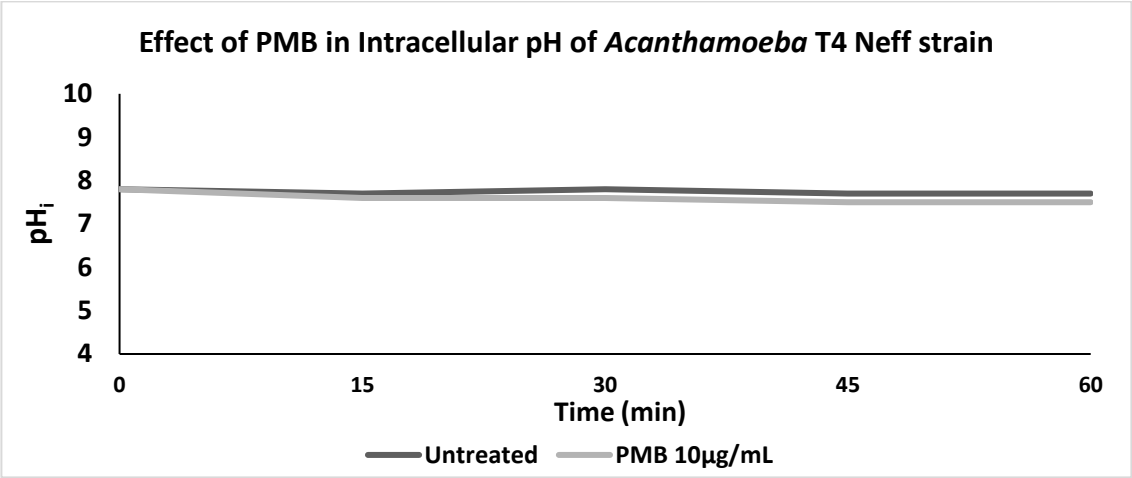

Figure 5.4: The diagram shows the intracellular pH variation of 10 µg/mL PMB treated and untreated *Acanthamoeba* trophozoites for 90 min after aminoglycoside induction, in NSB at 37ºC. Error bars represent SE, Significance is indicated (*).

5.2.2 G-418 aminoglycoside-induced cell death

It was observed that maximal percentage death rates after treatment with G-418 were shown in *Acanthamoeba* trophozoites incubated in NSB and at 37ºC (Figure 5.5), while minimal percentage death rates and high viability levels were noticed in AX2 room temperature (Figure 5.6; Figure 5.7 a,b). EC_{50} and EC_{90} of G-418 at 37ºC and in NSB media, for 24 hours was calculated at 32 ± 3 µg/mL and 75 ± 5 µg/mL respectively (Appendix 2; Figure 2.1).

It was also noticed that the tested concentrations of G-418 aminoglycoside mediate cell death only when cells are incubated in Neff's saline buffer and at 37ºC. For instance, incubation in slightly different saline buffer, such as PBS, showed viability rates over 78% (Figure 5.7 a,b) after 24 hours at 37ºC when treated with G-418 100 µg/mL, while trophozoites incubated in NSB with G-418 100 µg/mL for 24 hours at 37ºC showed 0% viability.

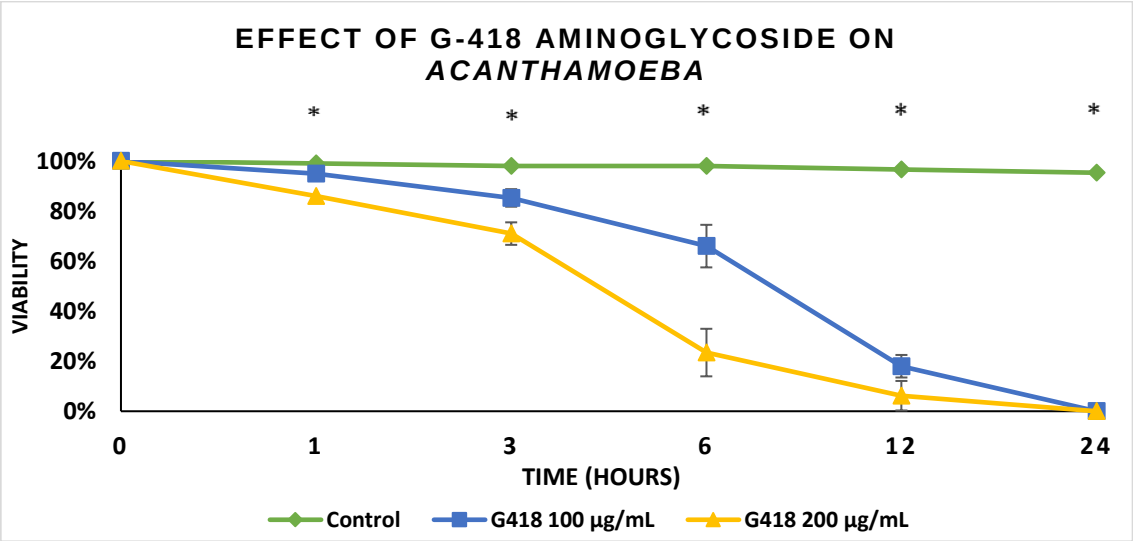

Figure 5.5: The diagram demonstrates the viability of G-418 treated and untreated populations of *Acanthamoeba* trophozoites, relative to hours of incubation. Cells were incubated at 37°C in Neff's amoeba saline buffer. Values are expressed as the mean of 3 independent experiments, error bars represent SE, Significance is indicated (*), ($P<0.05$, paired t-test, one tail distribution).

Furthermore, after treatment with 100 µg/mL G-418 and incubation in NSB, PBS, AX2 or non-glucose AX2 at room temperature for 48 hours, trophozoites did not show any signs of death, as viability was preserved at very high levels in all media, in many cases more than 93% (Figure 5.6).

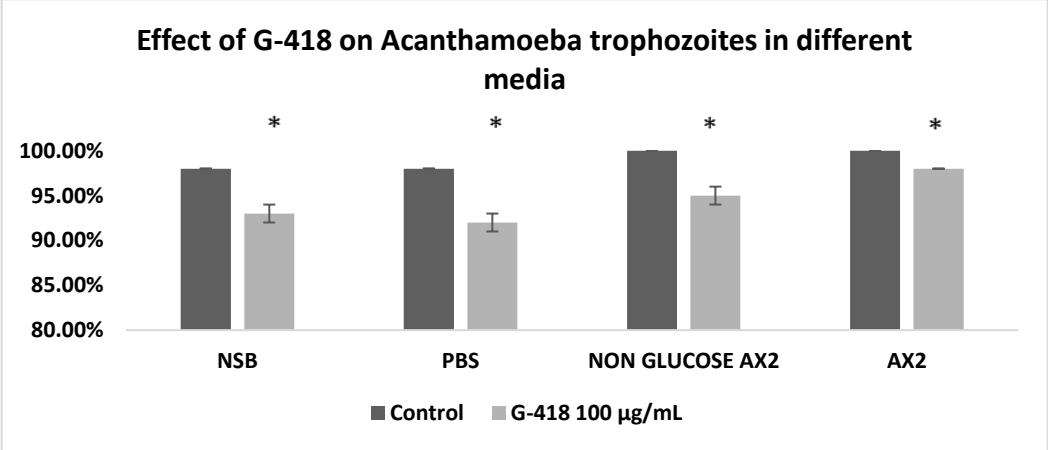

Figure 5.6: The histogram shows the viability of *Acanthamoeba* trophozoites after 48 h treatment with 100 µg/mL G-418 at room temperature. Values are expressed as the mean of 3 independent experiments, error bars represent SE, Significance is indicated (*), (P<0.05, paired t-test, one tail distribution).

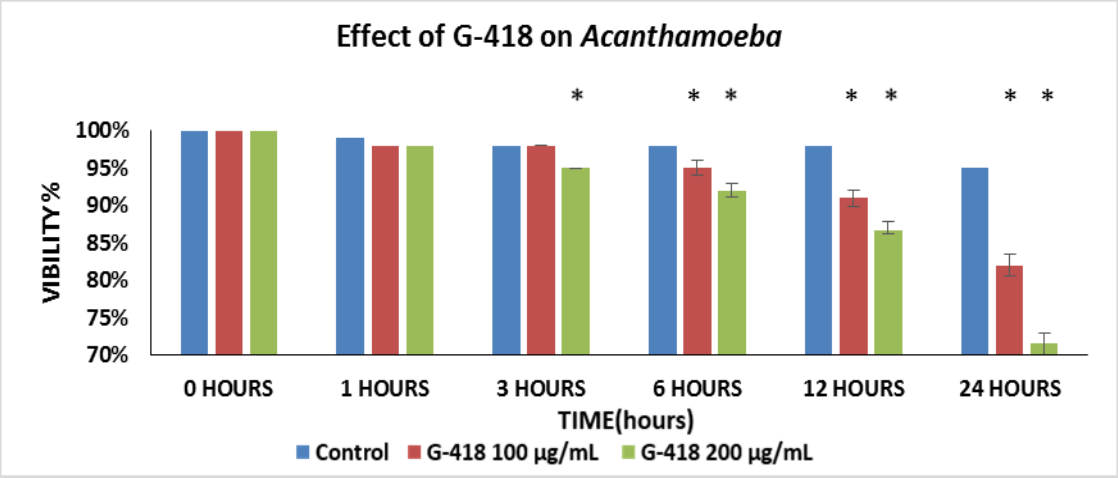

a)

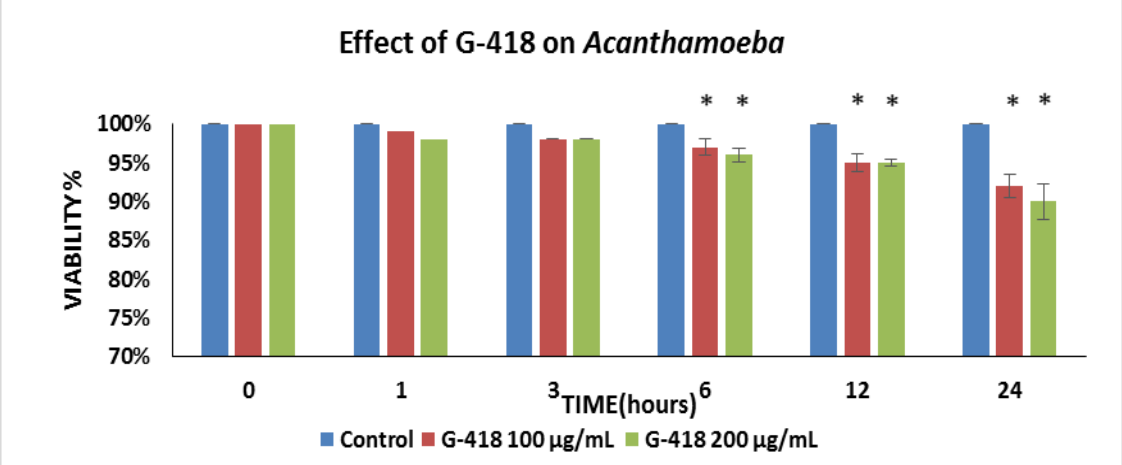

b)

Figure 5.7 a, b: The histograms show *Acanthamoeba* trophozoite viability on treatment with different concentrations of G-418 aminoglycoside at 37°C in three different media a) PBS b) AX2. Values are expressed as the means of 3 independent experiments. Error bars represent SE, Significance is indicated (*), P<0.05, paired t-test, one tail distribution.

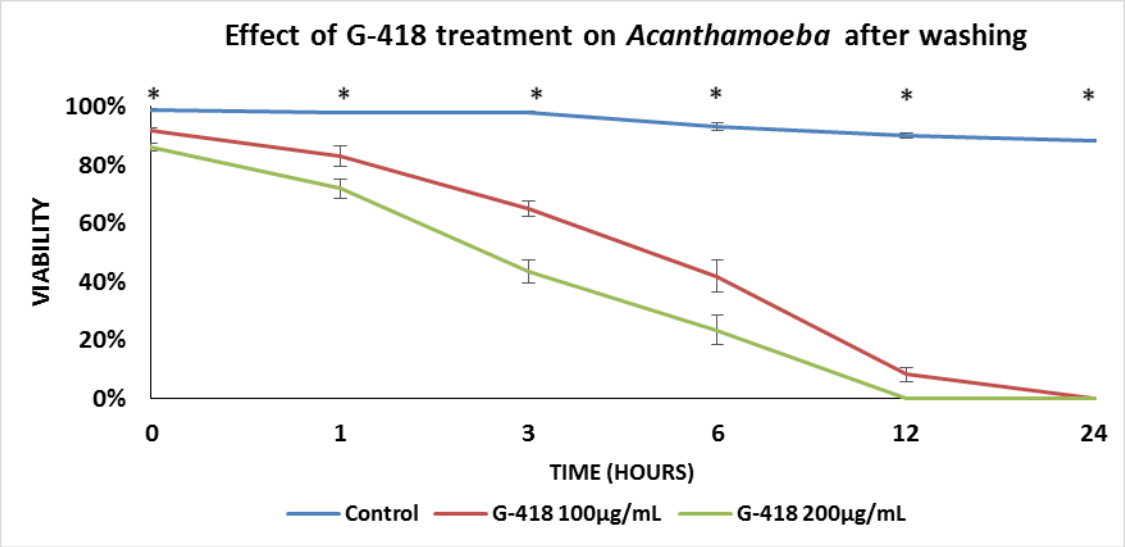

Figure 5.8: The diagram shows *Acanthamoeba* trophozoite viability after 1 hour of treatment with 100 µg/mL and 200µg/mL G-418. Values are expressed as the means of 3 independent experiments. Error bars represent SE, Significance is indicated (*), P<0.05, paired t-test, one tail distribution.

It was also observed that G-418 induced cell death was not a direct effect of the aminoglycoside, since after its removal *Acanthamoeba* trophozoites continued to 'die' with approximately analogous percentages (Figure 5.8), compared to amoebae from which G-418 was not removed (Figure 5.5).

5.2.2.1 G-418 aminoglycoside-induced cell death inhibition or delay

Based on previous observations, several apoptotic inhibitor substances have been used to block or partially inhibit G-418 induced death, including cysteine protease inhibitors such as Z-VAD-FMK (1-10μM) and E-64 (1-20 μM), calmodulin inhibitors such as N-(6-Aminohexyl)-5-chloro-1-naphthalenesulfonamide hydrochloride (W7), inhibitors of mitochondrial Ca^{2+} uniporters and MTP opening such as cyclosporin A (Petrinilli et al., 1993) and ruthenium red (Hoon et al., 2003) and finally cycloheximide (Sanchez et al.,1997), a known protein synthesis blocker, has been also tested, in addition to G-418, on *Acanthamoeba* cells.

None of the aforementioned inhibitors managed effectively to block the phenomenon, as after treatment with a combination of G-418 and various concentrations of different inhibitors, *Acanthamoeba* trophozoites maintained their death percentages over time (Figure 5.9). However it was noticed that some substances, including 2.5% DMSO, caffeine and lovastatin, were able to partially block or delay the death process when administered in combination with G-418.

More precisely, treatment with 100 μg/mL G-418 and 2.5% DMSO diminished cell death rates up to 25% after 24 hours of incubation (Figure 5.10). Combined treatment with caffeine and G-418 also conspicuously decreased death rates. More precisely, after treatment with a combination of 100 μg/mL G-418 and 1mM caffeine, viability of *Acanthamoeba* trophozoites dropped to approximately 65% after 24 hours, representing a significant increase compared to the viability of G-418 treated cells (Figure 5.10). Finally, it was observed that loavastatin delayed the phenomenon of cell death, as after 24 hours, cells treated with a combination of 100 μg/mL G-418 and 1mM lovastatin showed approximately 20% viability compared to cells treated only with G-418, which population had completely died after 24 hours (Figure 5.10).

It should also be noted that equivalent concentrations of the inhibitors and substances that have been used to block or delay the cell death induction have also been

administered to *Acanthamoeba* trophozoites as controls and subsequently viability was measured, with no significant variations and implications.

Finally, *Acanthamoeba* trophozoites treated with 100 µg/mL G-418 and various concentrations of ruthenium red (10µM is shown as example), in contrast to 2.5 % DMSO, caffeine and lovastatin treatments, showed a quite sharp death outburst with the majority of the cells found to be dead after 3 hours of treatment. At the same time, concentrations of ruthenium red alone (1-200 µM) did not affect trophozoite viability (Figure 5.11).

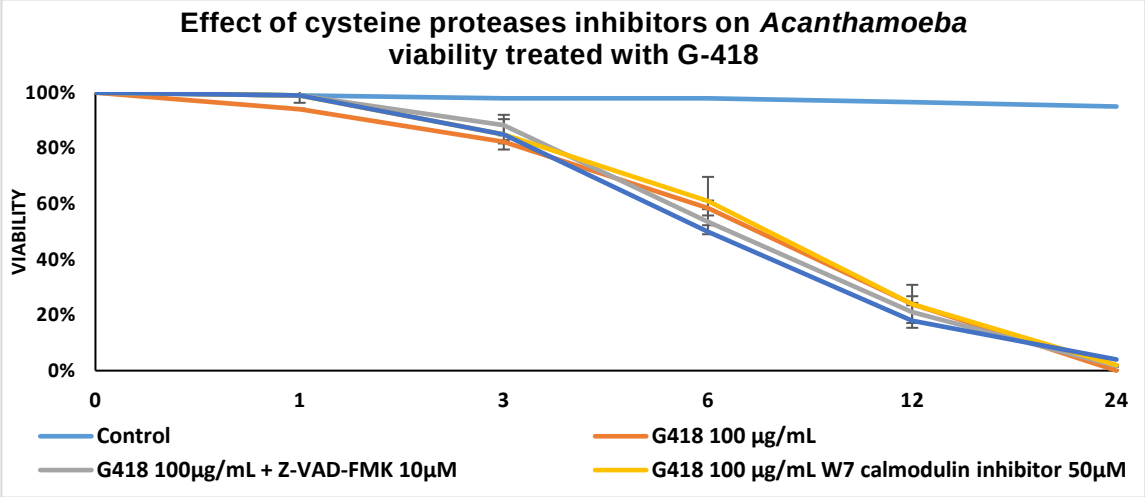

Figure 5.9: Effect of cysteine protease inhibitors on the viability of *Acanthamoeba* treated with 100µg/mL G-418, over time. Values are expressed as the means of 3 independent experiments, error bars represent SE. Significance is indicated (*), P>0.05, paired t-test one tail distribution.

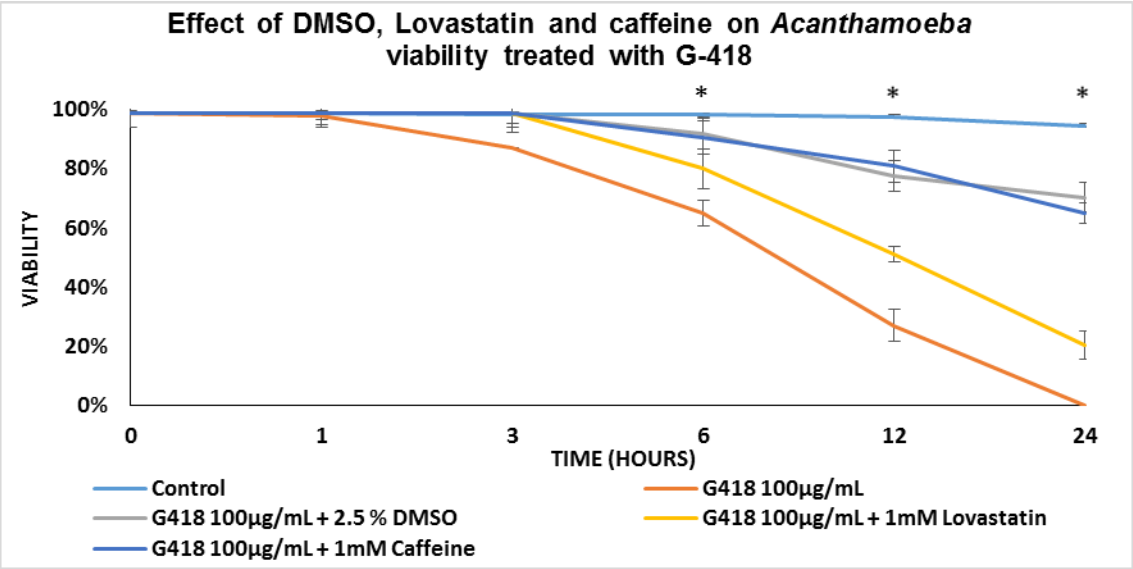

Figure 5.10: Effect of 2.5% DMSO, Lovastatin and Caffeine on the viability *of Acanthamoeba* treated with 100µg/mL G-418, over time. Values are expressed as the means of 3 independent experiments, error bars represent SE, Significance is indicated (*), P<0.05, paired t-test one tail distribution.

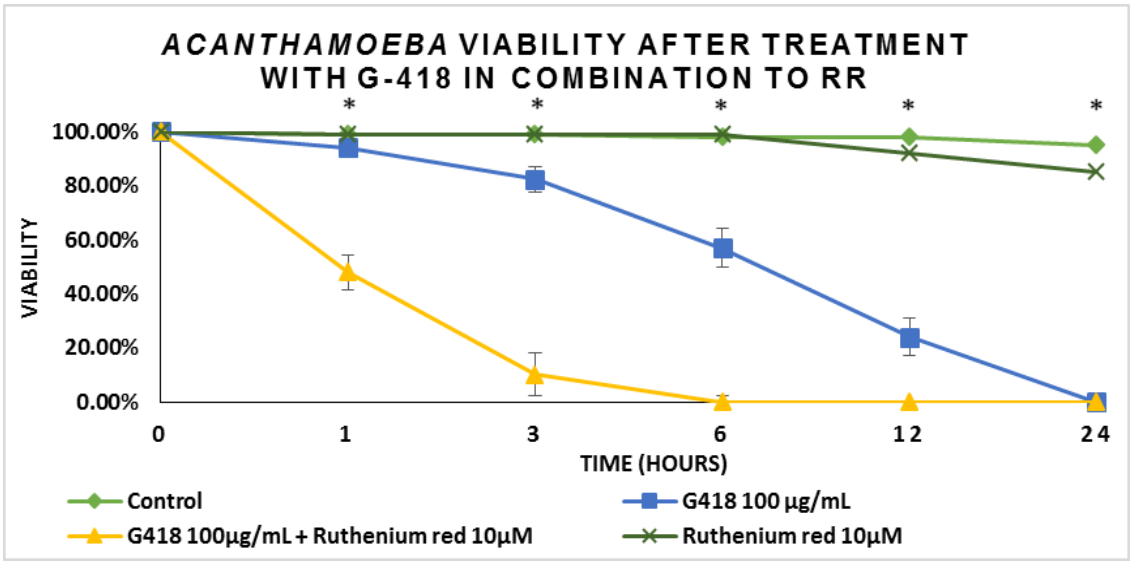

Figure 5.11: Effect of Ruthenium red on the viability *of Acanthamoeba* treated with 100µg/mL G-418, over time. Values are expressed as the means of 3 independent experiments. Error bars represent SE, Significance is indicated (*), P<0.05, paired t-test one tail distribution.

5.3 Discussion

Generally, there are two fundamental routes by which cells die (Galluzzi et al., 2018). The first includes the activation of regulated pathways and enzyme-protein interactions that are stimulated by a plethora of death signals (RCD or regulated cell death) and the second is by mechanical or physical membrane trauma (ACD or accidental cell death) which render the cell incapable of maintaining its own homeostasis.

After comparison of many factors including specific drug characteristics, viability results, biochemical alterations during cell death, morphology of dead cells, environmental settings and time of occurrence it was concluded that Polymyxin b mediates accidental cell death (ACD) in *Acanthamoeba* trophozoites under these described conditions and used concentrations. ACD is characterized as a virtually immediate and uncontrollable type of cell death and results in physical disassembly of the plasma membrane, as is induced by chemicals such as drugs, by physical stress such as high temperatures and by osmotic forces, or by mechanical cues.

More precisely, Polymyxin b-induced cell death initially involved selective plasma membrane injury and disassembly as microscopy shown. Secondarily, *Acanthamoeba* trophozoites swelling was also noticed due to membrane breakage, but not a generalized rise in cell membrane permeability. However, the membrane was becoming more permeable during time, potentially due to ATP depletion and finally physical disruption of the whole cell membrane structure occurred, as shown in Figure 5.2. Analysis of biochemical markers such as the intracellular calcium concentration and intracellular pH homeostasis did not reveal any variations during treatment with PMB, which is taken as additional evidence for the accidental cell death scenario. Furthermore, several substances and inhibitors that were used did not block or even delay the imminent induction of death by PMB.

On the other hand, G-418 aminoglycoside-induced cell death was more selective and also more difficult to trigger. Based on observations, temperature stress was an essential factor in G-418 mediated death, as identical drug concentrations failed to induce

trophozoite death in many media, including NSB, at room temperature. Moreover, G-418 mediated cell death was more easily induced and in comparatively higher rates when cells were incubated in NSB. Neff's saline buffer contains 36 μM $CaCl_2$ compared to PBS, so provides an extra source of extracellular [Ca^{2+}], which in turn could be critical in cell death signal transduction. In the natural environment, where *Acanthamoeba* thrives as a free-living amoeba and especially in soil habitats, calcium concentration is higher than in PBS buffer whereas traces of calcium are only existent. This observation might explain the inability of *Acanthamoeba* to udergo cell death after treatment with G-418 in analogous buffers, under the same experimental conditions, since microorganism might have been evolved and adapted to pump calcium from its natural environmental habitat.

At the time, features such as death morphology, selectivity of G-418 mediated cell death and observed biochemical features such as intracellular calcium rise and pH fluctuations (extended details are in the next chapter) during treatment with G-418 were used to support the hypothesis that G-418 mediated cell death could be more controlled than the ACD phenomenon described earlier after Polymyxin b induction. Another sign pointing in that direction was the evidence that after treatment for 1 hour with G-418 at 37ºC in NSB and subsequent washing of the aminoglycoside, *Acanthamoeba* cells continued to die, with almost similar death percentages, supporting the theory that the aminoglycoside is crucial to triggering a sequence of intracellular events, but that its presence is not required for completion of the phenomenon.

Since *Acanthamoeba* G-418 mediated cell death was characterized by numerous apoptotic features, which are described thoroughly in the next chapters (6and7), it was a logical step to attempt blockage or inhibition of molecules that might be responsible for the apoptotic appearance of the amoebic cells. Therefore, cysteine protease inhibitors, including membrane-permeant Z-VAD-FMK and E-64, were administered in combination to G-418 without, however, any notable variation in viability rates and only minor changes in trophozoite death morphology.

Caffeine has been reported to flatten and to attenuate ER stress (Hosoi et al., 2014; Teng et al., 2017) and subsequently calcium release. Although in low concentrations caffeine has reported to induce programmed cell death in *Acanthamoeba*

(Martín-Navarro et al., 2017), in higher concentrations, with parallel treatment of G-418 and over a limited time span, caffeine had a positive effect on trophozoite viability, as cell death rates were notably decreased. This effect was hypothesised to be a direct consequence of caffeine repression of ER stress.

Mitochondria are considered one of the downstream checkpoints in calcium signalling. Both cyclosporin A (Oka et al., 2008; Fournier et al., 1987) and ruthenium red (Lehninger, 1970; Storey and Lambert., 2017) have been reported to prevent calcium-related mitochondrial dysfunction and subsequent cell death induction. Various concentrations of both mitochondrial calcium influx inhibitors were administered in combination with G-418 at 37°C.

Results shown that treatment with cyclosporin A did not have any significant inhibitory effect on cell death whereas, micromolar concentrations of ruthenium red not only failed to induce resistance against cell death induction but dramatically increased death rates in a shorter time. Furthermore, the morphology of dying or dead *Acanthamoeba* cells changed radically when cells where incubated with G-418 in the presence of ruthenium red, which, interestingly, had no effect on *Acanthamoeba* viability when administered to control amoebae. This observation made feasible the scenario supporting the idea that *Acanthamoeba* could undergo more than one forms of regulated cell death. This prompt, mitochondria-driven cell death phenomenon was completely distinguishable from the already noticed G-418 apoptotic morphology or membrane breakage appearance after treatment with Polymyxin B, however due to massive and catastrophic effects on trophozoites, further study was extremely difficult and was not attempted.

Concentrations of lovastatin were also used to partially inhibit *Acanthamoeba* cell death expansion after the ascertainment of significant upregulation of Ras genes in transcriptomic analysis of G-418 treated amoebae. As was shown, lovastatin partially inhibited and delayed cell death during 24 of continuous observation, however Ras signalling has been considered to play a secondary auxiliary role in *Acanthamoeba* regulated cell death, since many characteristic morphological features remained obvious.

DMSO (Dimethyl sulfoxide), is a significant polar aprotic but simple solvent that dissolves both polar and non-polar substances. Initially, chemical compounds such as cycloheximide and cyclosporin A, which were used to inhibit the cell death phenomenon, were dissolved in DMSO, providing incorrect data regarding *Acanthamoeba* cell death features. Later, inhibitory effects were noticed after combined treatment, but were actually based neither on cycloheximide nor cyclosporin, but on DMSO.

It has been reported that low concentrations of DMSO, including 2.5%, are able to alter nuclear actin structure and consequently nuclear formation in various cell types, including amoebae and mammalian cells (Fukui and katsumaru, 1980). Furthermore, it was suggested that such nuclear actin alteration could function significantly in regulation of gene replication and/or transcription through its contractile nature (LeStourgeon et al., 1975). Alterations in regulation of gene expression could easily explain some of the morphological features that appear during the phenomenon and reveal a gene-related dependency of cell death.

It was shown that treatment with G-418 aminoglycoside and simultaneous heat stress at 37℃ leads to high percentages of mediated cell death that can be partially delayed or blocked. These observations did not clarify either a precise death pathway or any important signalling and execution molecule during *Acanthamoeba* cell death, however it established that the observed phenomenon was more controlled than a random accidental side-effect of G-418 and the temperature stress condition.

Parallel inhibitory and death blockage experiments that were performed on *Acanthamoeba* trophozoites treated with various concentrations of PMB did not reveal any blockage or delay of cell death induction, strengthening even more the accidental cell death model of the PMB effect on amoebae, which was proposed.

Chapter 6

Apoptotic morphological features of *Acanthamoeba* programmed cell death

Introduction

6.1 Apoptotic hallmarks of *Acanthamoeba* programmed cell death

Each form of cell death is characterized by a certain set of morphological features that are distinguishable from other types of cell death. The majority of cells undergoing apoptosis represent a parallel and a very analogous pattern of morphological characteristics that are basically under the control of the same intracellular pathways. Furthermore, the agents or the environmental conditions that have been applied in order to induce apoptosis are hardy indicative of these features' occurrence, although it should be mentioned that in some cases different stimuli can trigger some of the morphological alterations or the experimental conditions can partially regulate the full extent of the phenomenon (Häcker, 2000). It should consequently be acknowledged, that there are slight changes during the development of apoptotic morphology.

Cell shrinkage, rounding up formations, retraction of pseudopods, cellular pyknosis and chromatin condensation into sharply delineated masses, karyorrhexis, mitochondrial dysfunction, DNA fragmentation and plasma membrane blebbing are the predominant signatures of apoptotic cell death. These phenotypic features distinguish apoptosis from other types of cell death including autophagic cell death, necroptosis, accidental cell death and necrosis (Kerr et al., 1974; Galuzzi et al., 2018).

Although these signs have been used to identify apoptotic cell death, a phenotype lacking one or more of those features does not indicate the absence of apoptosis. For

example, the absence of DNA fragmentation and lack of apoptotic body formation have been reported in many studies associated to apoptosis, especially those conducted *in vitro* (Yuste et al., 2001).

The main objective of this chapter is to present a key set of *Acanthamoeba* apoptotic morphological characteristics that have been also described in noumerous cells that undergo apoptosis and programmed cell death. These features have been observed during treatment with G-418 and include cell shrinkage, trophozoite rounding up formations after a period of time, loss of dry mass, the appearance of apoptotic like bodies, chromatin condensation, chromatin fragmentation and simultaneous maintenance of the outer membrane integrity, at least at the first stages of the process.

Briefly, *Acanthamoeba* trophozoites were observed under optical (3.5.1), high contrast quantitive (3.5.2; 3.5.3) and confocal microscopy (3.5.4) after treatment with EC_{90} G-418 for predefined periods of time. Hoechst 33342 staining (3.6.3) was used to stain amoebae nuclear DNA and to track diffrences in chromatin condensation bettween control and EC_{90} G-418 treated cells, while Sytox green (3.6.5) stain was used to examine alterations in plasma membrane permeability between G-418 treated and untreated amoebae during the phenomenon. Changes in cell size, sphericity and loss of mass were detected by high contrast quantitive (3.5.2; 3.5.3) microscopy. Finally, apoptotic-like body formations were observed by optical microscopy (3.5.1).

6.2 Results

6.2.1 Cell shrinkage

As it was revealed by high-contrast microcopy (3.5.3), *Acanthamo*eba trophozoites treated with G-418 EC_{90} and incubated at 37℃ showed a reduction in cell size and dry mass in comparison to untreated trophozoites during treatment for 20 hours

(Figure 6.2; Figure 6.3). Both untreated and treated populations started with identical values of cell density and relative dry mass (Figure 6.1 a; b).

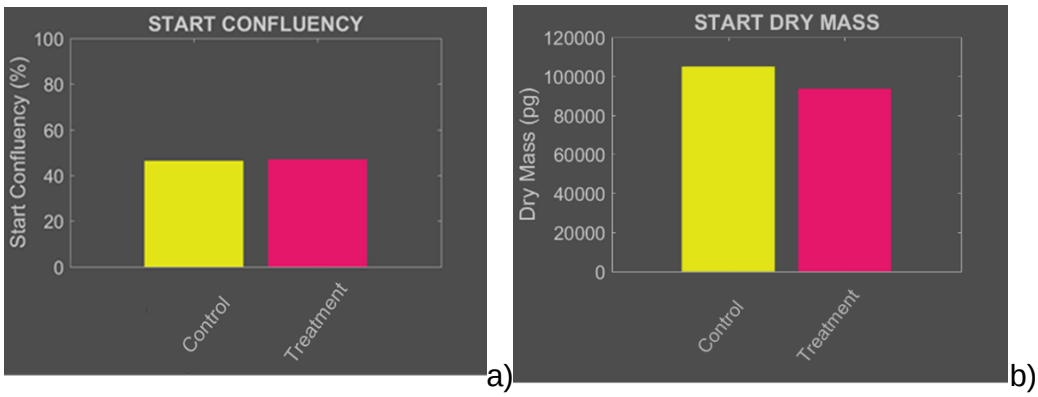

a) b)

Figure 6.1: *Acanthamoeba* confluency and trophozoite starting dry mass. The diagrams are indicative a) of the initial percentage of cells and b) the starting dry mass.

More precisely, it was observed that dry mass per cell was decreased from 260 pg to 80 pg in G-418 treated cells while at the same time control *Acanthamoeba* trophozoites indicated a smaller decrease, from 300 pg to 200 pg (Figure 6.2 b). Density per cell also showed a dramatic decrease, from 0.8 pg to 0.5 grams/cm^3 in G-418 treated cells, compared to untreated amoebae which showed a minor reduction (Figure 6.2 a). Notably, this reduction in cell size and mass in treated amoebae was a progressive procedure taking place over time and not an immediate effect, induced directly either by temperature stress or pharmacological treatment which for instance, is particularly observed during *Acanthamoeba* transformation from a trophozoite to a pseudocyst, when cell size reduction is also observed.

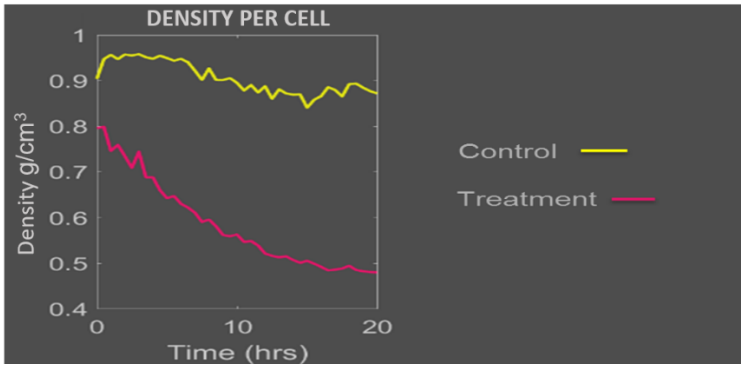

a)

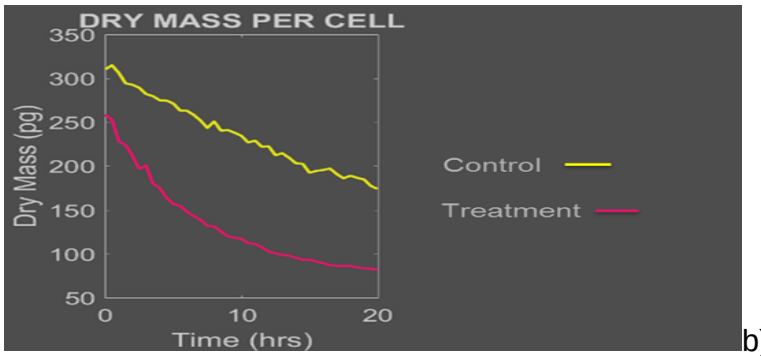

b)

Figure 6.2 a, b: The diagrams show the reduction in mass density per cell a) and in the dry mass per cell b), during treatment for 20 hours with G-418 EC_{90}. Values are expressed as the means of 3 independent measurements.

Covered cell area of *Acanthamoeba* trophozoites, which is indicative of cell size, was also measured and found to be reduced in cells treated with G-418. For instance, it was found that the mean coverage area was approximately 250 μm^2 per untreated cell, while it was decreased to 180 μm^2 per cell in G-418 treated amoeba (Figure 6.3 a).

Another interesting fact that came out of the analysis was the determination of the mean velocity of locomotive *Acanthamoeba* trophozoites. Mean speed was found to be lessened in both control and treated trophozoites during the time of incubation at 37℃. More precisely, control cells showed a small reduction in their mean velocity, from 0.002 μm/s to 0.0014 μm/s, while at the same time G-418 treated cells, showed a three-fold decline from 0.0015 μm/s to 0.0005 μm/s during a period of 20 hours (Figure 6.4).

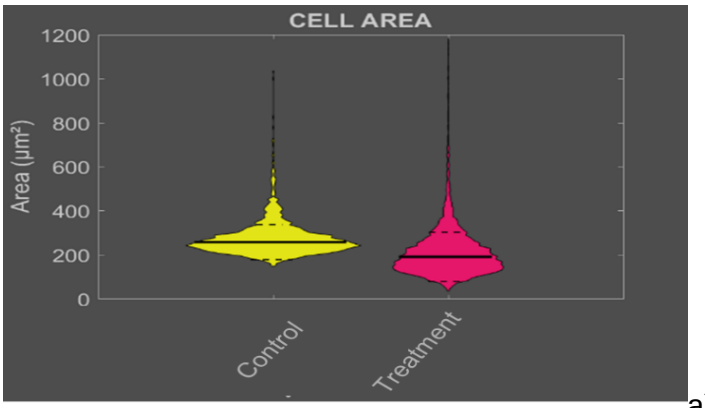

a)

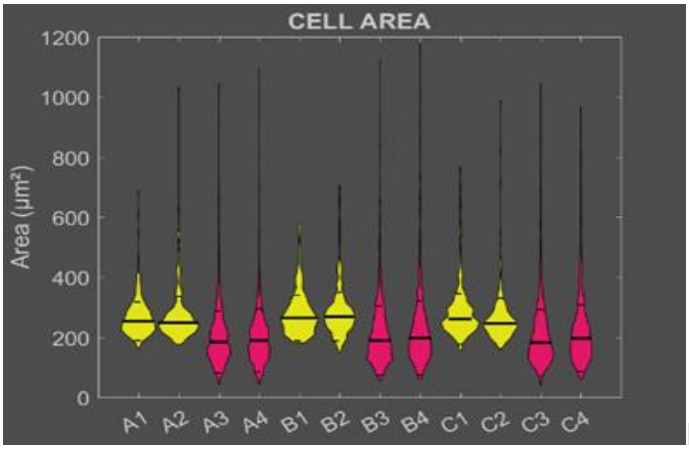

b)

Figure 6.3 a) b): The diagrams illustrate the mean cell area coverage measured in μm^2 of G-418 EC_{90} treated and untreated *Acanthamoeba* trophozoites during a period of 20 hours. A1-C4 represent the 12 wells of a 12 well plate. Columns 1 and 2 represent control trophozoites and 3 and 4 G-418 treated amoebae.

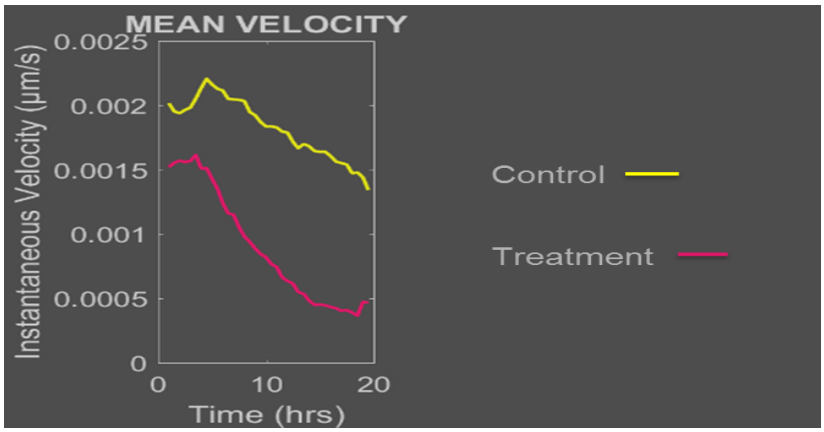

Figure 6.4: The diagram represents the mean velocity of G-418 treated and untreated trophozoites during a period of 20 hours. Values are expressed as the mean of 3 independent measurements.

Morphological analysis of the treated trophozoites showed that during treatment with G-418, the finely coordinated intracellular structure of *Acanthamoeba* was completely lost (Figure 6.5). In addition, a more circular formation and retraction of pseudopods were also seen, compared to the control population of trophozoites in which neither loss of internal integrity nor pseudopod retraction occurred. Most of the morphological phenomena developed and were observed after 3 hours of incubation, while before this time, the morphology of treated and untreated trophozoites was almost identical.

A plethora of small particles that were emerging from dead cells were also detected and could be considered as apoptotic body formations (Figure 6.5 B2; C2). The occurrence of these formations was noted roughly 6 hours after initiation of G-418 treatment. The final stage of G-418 induced cell death seemed to be characterized by complete cell lysis and membrane rupture (Figure 6.5). Analogous alterations in trophozoite morphology were not detected during treatment with Polymyxin b, an additional clue that further supported the difference in mechanism of death induction by these two substances.

6.2.2 Chromatin alterations

Fluorescence microscopy (3.5.4) combined to Hoechst staining (3.6.3) revealed that treatment with G-418 altered the typical morphology of *Acanthamoeba* trophozoite nuclei. After almost 3 h of incubation with G-418 EC_{90}, trophozoites did not show any morphological differences from the controls and the nucleus was characterized by dense regional chromatin with a central 'endosome/body' (Figure 6.6 A; B; C). Furthermore the nuclear membrane appeared to be intact. After 4 hours of incubation treated trophozoites nuclei appeared more condensed compared to untreated trophozoites and also the nuclear membrane seemed to have lost integrity (Figure 6.6 D). After 5 hours of incubation the first signs of fragmented chromatin were obvious (Figure 6.6 E). Furthermore the characteristic chromatin ring condensation was obvious in many nuclei (Figure 6.7). After 6 hours of treatment nuclear chromatin seemed finely fragmented into several pieces which were eventually distributed in the cytoplasmic area (Figure 6.6 F; G; H). At the same time the nuclear morphology of the control untreated trophozoites remained unaltered.

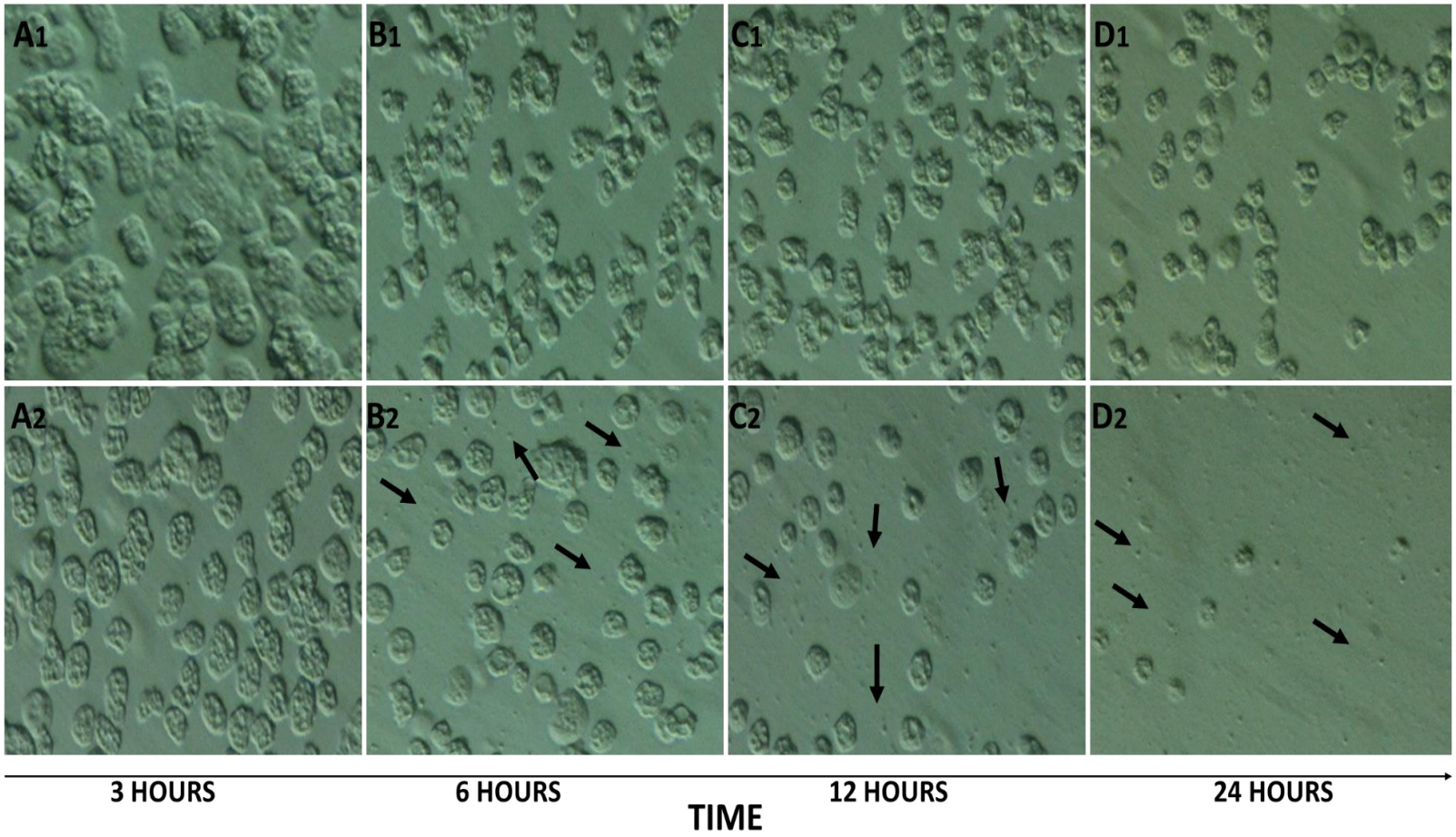

Figure 6.5: Morphology of G-418 treated and untreated *Acanthamoeba* trophozoites under light microscopy. Arrows indicate microscopic round cellular formations that look like apoptotic bodies formations. Images are representative of 3 independent experiments.

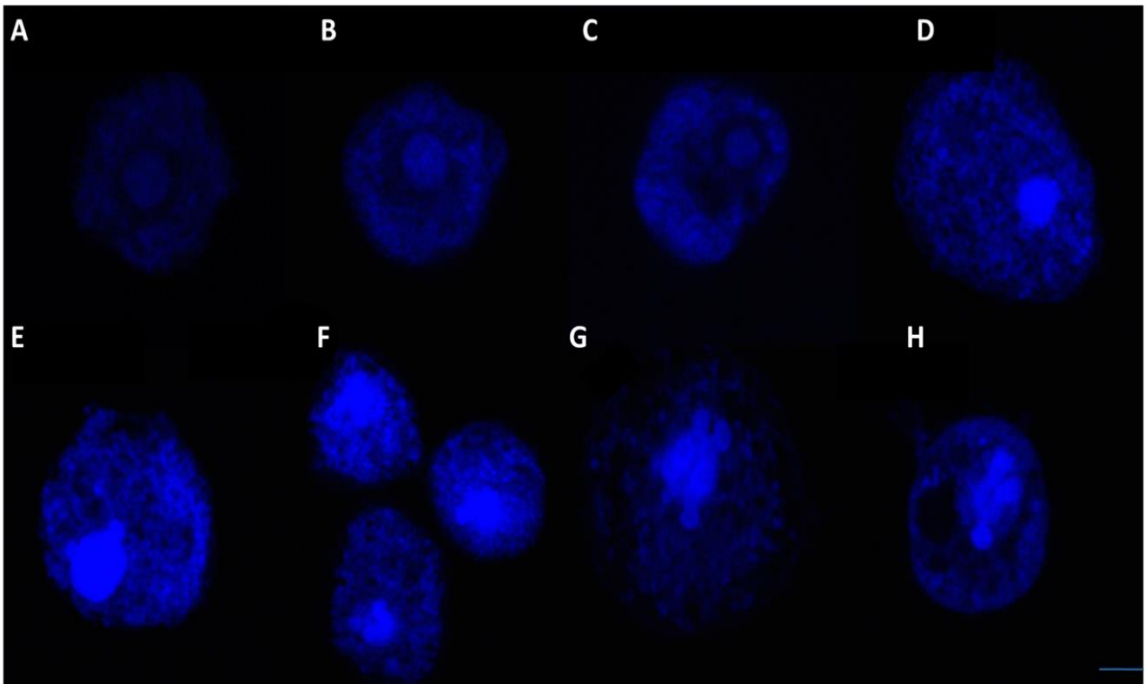

Figure 6.6: Representative Hoechst 33345 staining time course of *Acanthamoeba* apoptotic chromatin condensation. A-H correspond to 1-8 hours of G-418 treatment. Images are representative of three independent experiments. Scale bar 5μM.

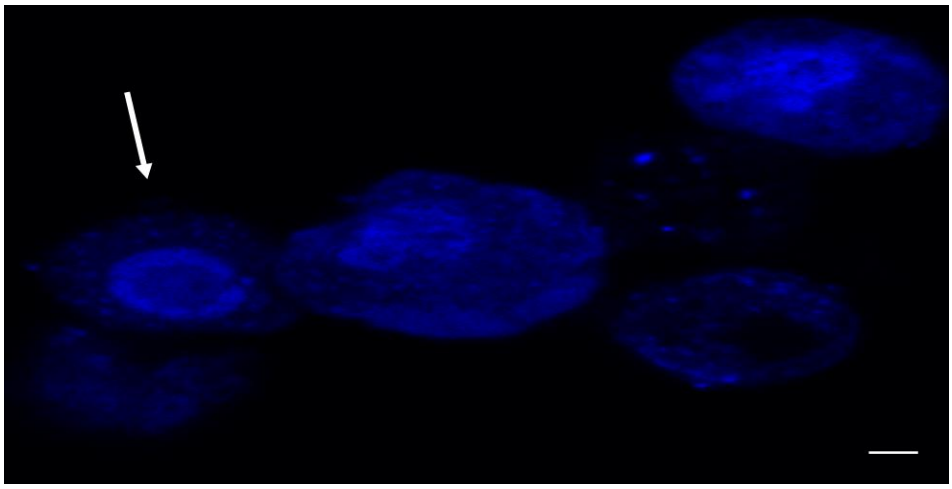

Figure 6.7: Characteristic sign of ring condensation formation after 6 hours of G-418 treatment. Some of the neighbouring cells have already formed distinct chromatin bodies. Scale bar 5μm.

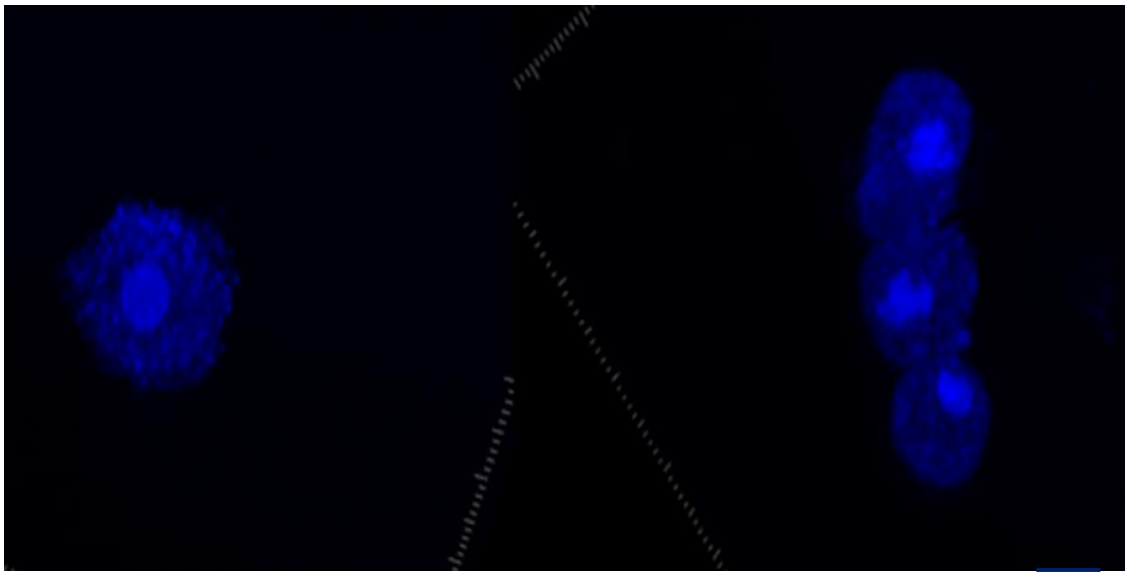

Figure 6.8: Typical 3D representation of the altered chromatin morphology observed in untreated (left) and G-418 treated cells after 6 hours of treatment. Images are representative of three independent experiments. Scale bar 10µm.

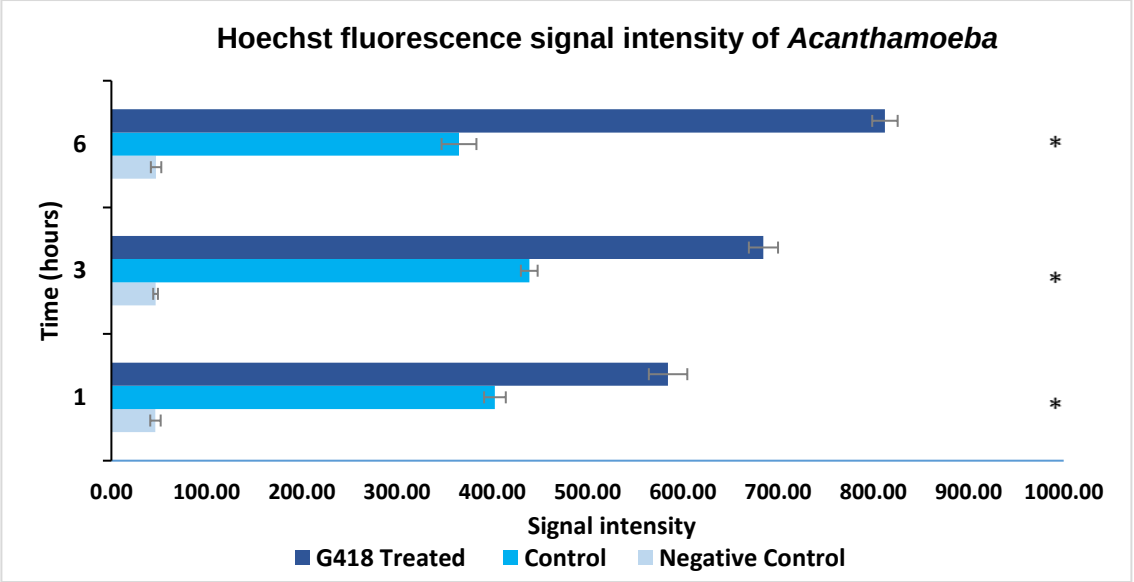

Figure 6.9: The diagram shows Hoechst signal emission intensity from various *Acanthamoeba* trophozoites when excited at 350nm, measured in a spectrofluorimeter at 3 different time points (1-3-6 hours). Values are representative of three independent

experiments. Error bars represent S.E., Significance is indicated (*), (P< 0.05, student t-test, one tail).

In 2017, Navarro et al. have reported signs of programmed cell death in *Acanthamoeba* trophozoites when treated with caffeine. Treatment of *Acanthamoeba* GS strain with 10μM caffeine for 24 hours in NSB at room temperature also revealed signs of apoptotic chromatin fragmentation compared to untreated trophozoites, suggesting that chromatin condensation and fragmentation are not specific characteristics of G-418 treatment. More than 60% percent of the examined nuclei showed the characteristic apoptotic features, although the phenomenon was not so intense as with G-418 treatment (Figure 6:6; Figure 6.8).

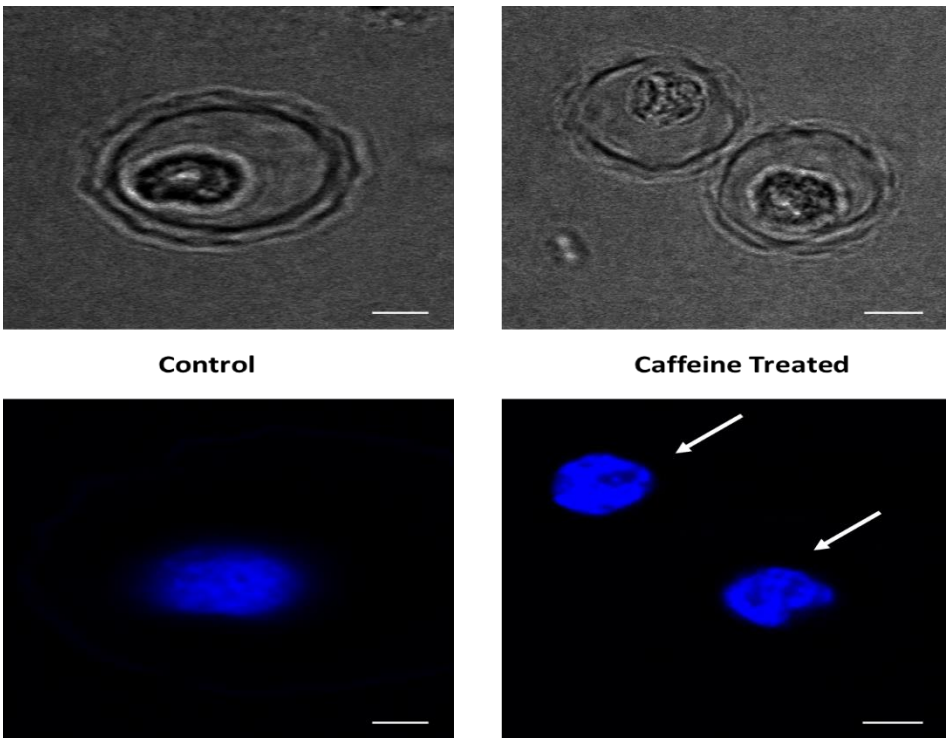

Figure 6.10: The figures illustrate the medium chromatin fragmentation observed after 24h treatment with caffeine, IC_{50}= 10μM. Images are representative of three independent experiments.

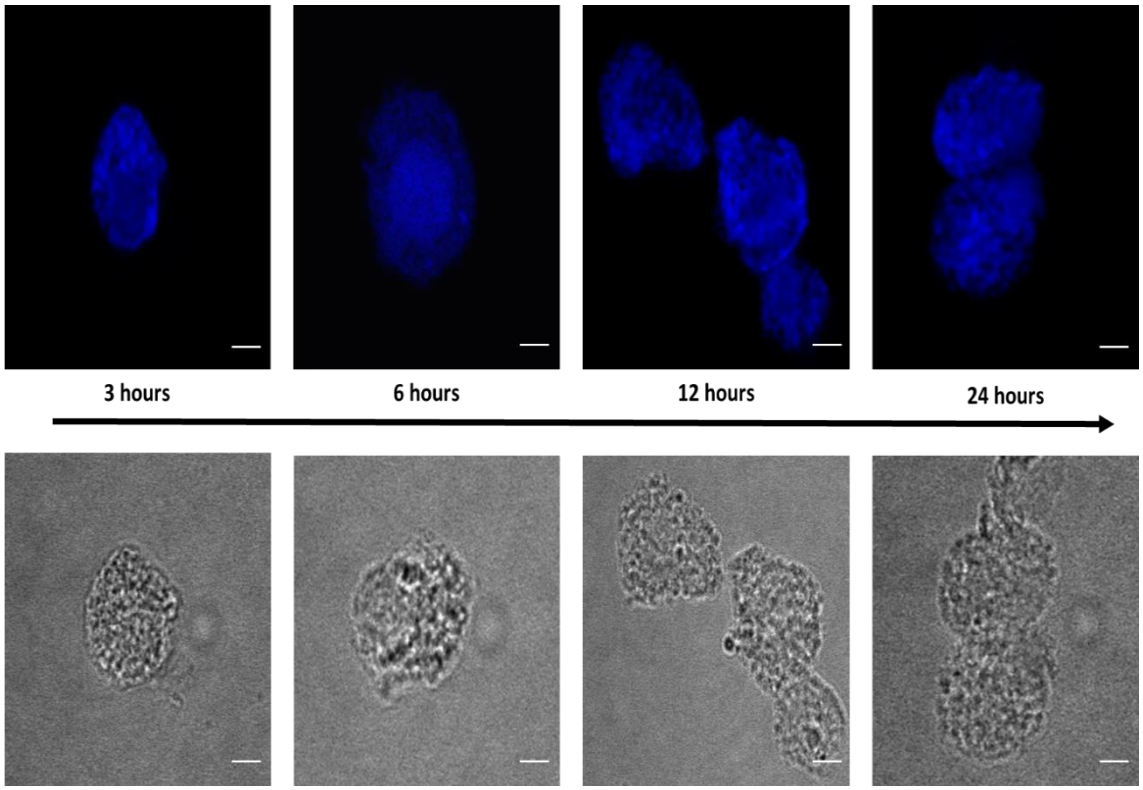

Figure 6.11: Illustration of *Acanthamoeba* nuclei alterations during treatment with G-418 and 2.5% DMSO. Scale bar 5μm. Images are representative of three independent experiments.

Administration of 2.5% DMSO to G-418 treated *Acanthamoeba* cells resulted in considerably decreased chromatin condensation and percentage of fragmentation (Figure 6.11). Furthermore, amoebae incubated with a combination of 2.5% DMSO and G-418 accumulated significantly decreased Hoechst staining compared to trophozoites treated only with G-418. Also notable was the increased difficulty of staining trophozoites nuclei after the induction of G-418 in 2.5% DMSO, despite the fact that there was no obvious alteration in outer membrane morphology that could provide an extra barrier to the already permeant Hoechst stain. In addition, 2.5% DMSO also resulted in decreased chromatin condensation and fragmentation after caffeine treatment in NSB.

6.2.3 DNA Fragmentation

DNA fragmentation and formation of a ladder motif were not observed in numerous cases by DNA electrophoresis (3.7.4) including variable incubation time points and different treatments (Figure 6.12).

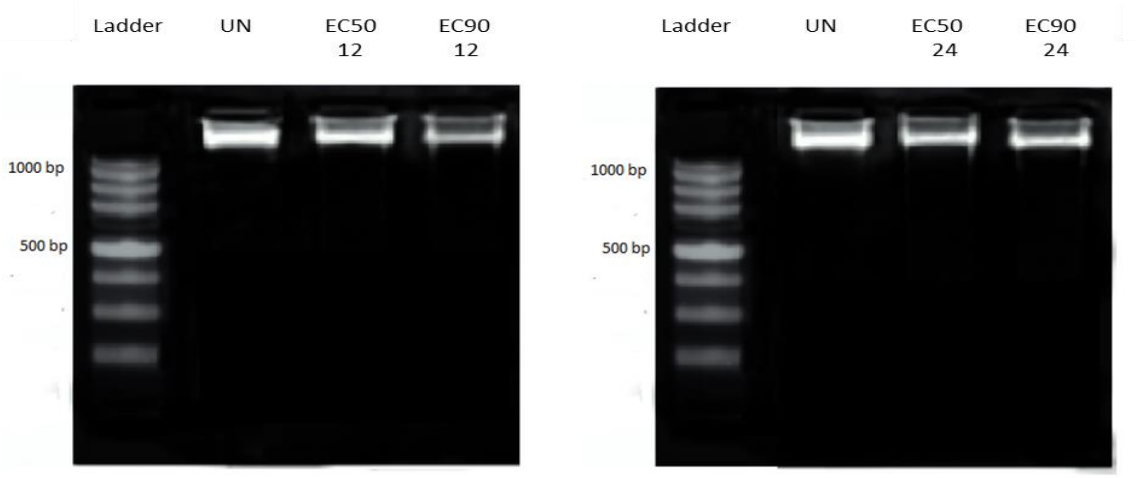

Figure 6.12: Representative 1.8% agarose DNA gel electrophoresis of EC_{90} and EC_{50} G-418 treated *Acanthamoeba* trophozoites. Images are representative of 3 independent experiments.

6.2.4 Membrane permeability

Acanthamoeba trophozoites treated with G-418 EC_{90} did not show increased outer cellular membrane permeability at least in the first stages of treatment and cell death induction. More precisely, treated trophozoites showed fluorescence intensity levels similar to of those that were untreated. After 6 hours of treatment with G-418 EC_{90}, trophozoites exhibited slightly higher fluorescence than control cells. The positive control was characterized by a high fluorescence intensity, as expected, while cells untreated with Sytox green (negative control) showed almost zero fluorescence (Figure 6.12). Furthermore, outer cellular membrane disruption and permeability was observed and analyzed under fluorescence microscopy (3.5.4) (Figure 6.13) and confirmed previous spectrophotometry (3.6.5) results.

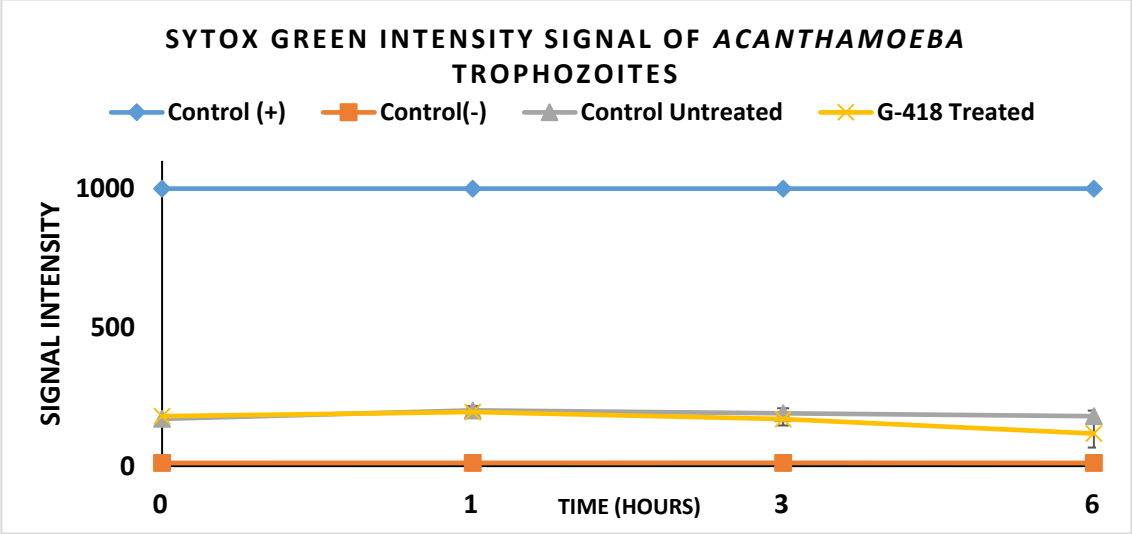

Figure 6.13: SYTOX green signal intensity of different *Acanthamo*eba populations during G-418 treatment. The diagram represents SYTOX green fluorescence intensity of EC_{90} G-418 (75 µg/mL) treated and untreated *Acanthamoeba* trophozoites at 1, 3 and 6 hours of incubation. Positive amoebae were previously treated with Triton 2.5% and negative cells represent SYTOX green fluorescence of unloaded *Acanthamoeba* trophozoites. Error bars represent SE.

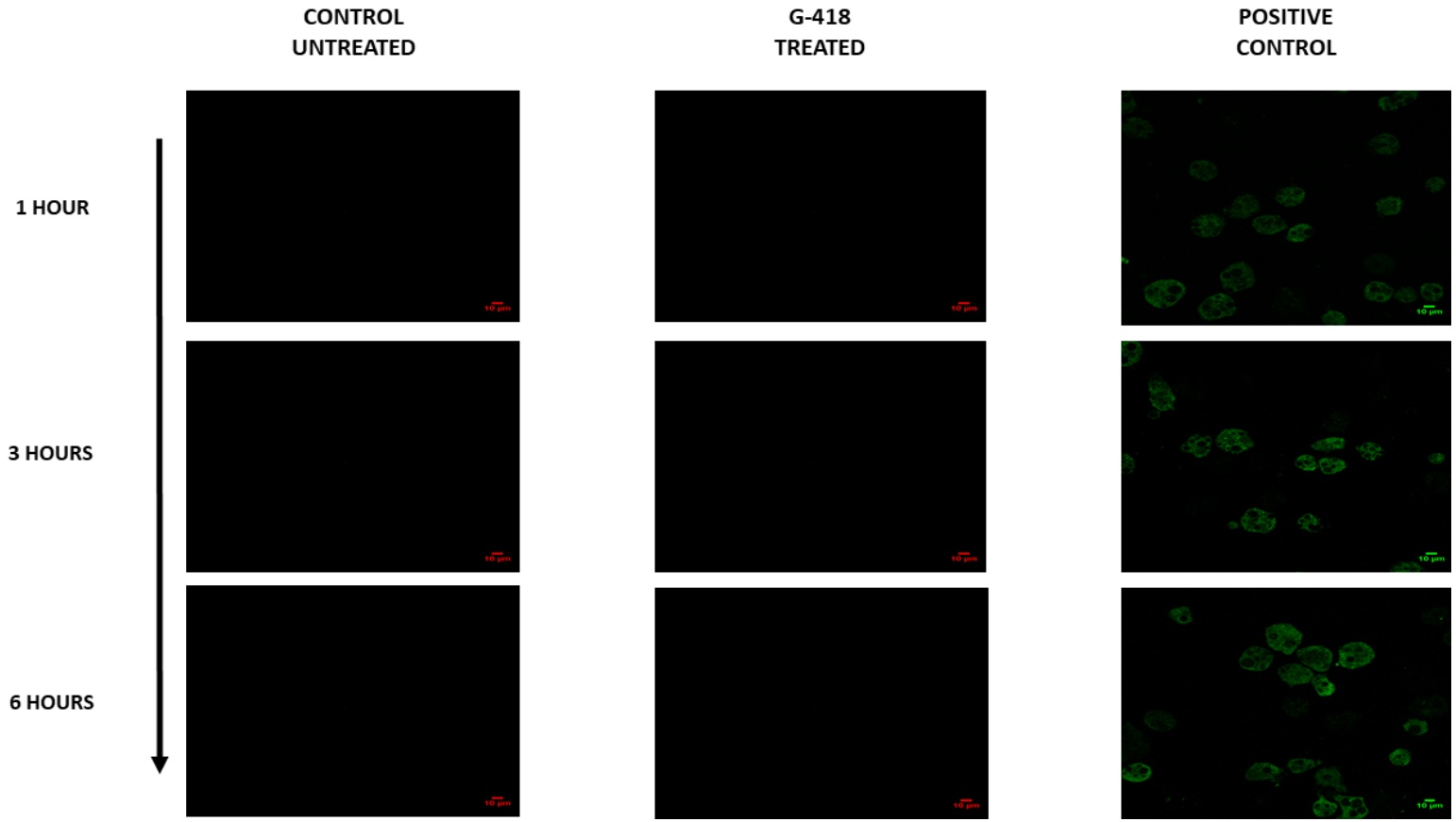

Figure 6.14: Microscopic representation of SYTOX green fluorescence intensity in untreated *Acanthamoeba* (left); 75 µg/mL G-418 treated (middle) and positive control (right) compared to hours of treatment. Positive cell were previously treated with Triton 2.5% and negative cell represent SYTOX green unloaded *Acanthamoeba* trophozoites. Images are representative of 3 independent experiments. Scale bar 10µm.

6.3 Discussion

Apoptotic procedures are the predominant forms of cell death and occur under a wide range of physiological and pathological circumstances. Apoptotic features have been already described in unicellular protists and in a plethora of multicellular organisms, as previously stated. The apoptotic process includes numerous morphological features like cell shrinkage, chromatin condensation, nuclear DNA fragmentation and formation of apoptotic bodies. To allow the extensive morphological alterations that occurring during apoptosis and other forms of regulated cell death, cells experience a sequence of intense events such as cytoplasmic membrane alterations and nuclear rearrangements. Some of these distinguishable apoptotic characteristics have been also observed and analyzed in *Acanthamoeba* G-418 mediated cell death.

Reduction of cell volume throughout apoptotic cell death has been regarded as a passive procedure, occurring in order to enable cell breakage into smaller, apoptotic bodies, assisting their subsequent deconstruction and engulfment by neighboring cells or macrophages. Conversely, studies based on the decreased cellular volume role during apoptosis have led to a novel understanding of how and why cells shrink (Bortner et al., 2002). It has been reported that cells with decreased cellular volume exhibit chromatin condensation and fragmentation and simultaneously an approximately 4-fold elevation of caspase-3-like activity, compared to cells that have undergone apoptosis but do not present a shrunken phenotype (Bortner et al., 1997). Furthermore, cells with shrunken phenotype had a lower K^+ intracellular concentration, which is subsequently co-responsible for the apoptotic nuclease and caspase activation (Dallaporta et al., 1998). The morphology of G-418 treated *Acanthamoeba* trophozoites indicates such characteristics including cell shrinkage and apoptotic-like bodies' formations, as microscopy studies revealed. Interestingly, these characteristics, including cell shrinkage and granule appearance, did not occur or were not observed during treatment with polymyxin b, as was discussed in previous chapters.

Dynamic alterations in the compaction of nuclear chromatin are one of the most distinguishable phenomena of apoptotic implementation. In healthy and untreated

Acanthamoeba trophozoites, the genomic DNA is packaged into the nuclei, several micro-meters in length. Throughout treatment with G-418 aminoglycoside, microorganism's DNA attains a greater level of condensation and is packed with nuclear proteins, forming distinct chromatin apoptotic bodies. Experimental analysis exposed at least three different stages of chromatin condensation including chromatin shrinkage/chromatin ring condensation, assembly of chromatin apoptotic bodies and finally nuclear collapse and disassembly. The notable degree of compaction and the fragmented chromatin bodies formation, along with the fact that apoptotic chromatin condensation does not comprise the formation of separate chromosomes, suggests that *Acanthamoeba* has a precise method for the induction of apoptotic chromatin condensation.

It was also shown that chromatin condensation and fragmentation in *Acanthamoeba* trophozoites was not only limited to G-418 treatment. Micromolar concentrations of caffeine produced similar morphological effects, however these were not as intense and distinctive. This observation might be indicative of a well conserved death pathway in *Acanthamoebidae* parasites.

Administration of 2.5% DMSO in combination with G-418 had already shown to greatly decrease death rates in *Acanthamoeba* trophozoites. Examination of amoebae nuclei which had been treated with 2.5% DMSO and G-418 revealed that a much lower percentage of Hoechst staining had accumulated in the nucleus and simultaneously in many cases there was great difficulty in distinguishing between the cytoplasm and nucleus. This effect was potentially due to micronuclei actin microfilament rearrangement, a consequence of 2.5% DMSO stress (Fukui and katsumaru, 1980). This DMSO-mediated nuclear membrane modification seems to provide a protection against cell death either by blocking apoptotic signals that are directed to nuclei or by regulating gene expression (LeStourgeon et al., 1975).

DNA fragmentation has been reported in many cases as a late-stage characteristic of apoptosis. In G-418 treated *Acanthamoeba* trophozoites, despite the fact that they presented extended nuclear condensation and fragmentation, DNA electrophoresis failed to identify any DNA fragments or reveal a DNA ladder motif. The

absence of such a feature has been described previously in numerous systems, including various mammalian cells, associated with apoptosis (Schulze-Osthoff et al., 1994; Sakahira, et al., 1999; Yuste et al., 2001). Lack of DNA fragmentation might be a consequence of extended nuclease function, since overexpression has been confirmed through transcriptomic analysis and is discussed in the next chapters.

Experimental data also revealed that membrane integrity is not compromised immediately after incubation with G-418. For instance, even after 6 hours of incubation, when other interesting phenomena were reported to have taken place, including chromatin condensation and fragmentation, trophozoite membranes remained impermeable, as Sytox green dye-loaded trophozoites emitted a low intensity fluorescence signal comparable to control untreated amoebae. At the same time, a positive control of *Acanthamoeba* trophozoites treated with 2.0% Triton X-100 (compromised membranes) showed high fluorescence intensity levels, as expected.

Based on morphological criteria, it was shown that *Acanthamoeba* cells, despite the fact that they failed to demonstrate an oligonucleosomal fragmentation pattern, present most of the morphological apoptotic hallmarks that have been used to describe the phenomenon of apoptosis such as cell shrinkage, chromatin condensation and nuclear fragmentation, maintenance of the membrane integrity during the phenomenon and finally the presence of small round particles that could be characterized as apoptotic-like bodies.

Chapter 7

Apoptotic biochemical features of *Acanthamoeba* programmed cell death

Introduction

7.1 Biochemical hallmarks of apoptosis

Apoptosis is characterized by numerous of morphological and biochemical features that enable differentiation among various types of cell-death. Biochemical characteristics of apoptosis are considered phenomena that occur throughout apoptosis and include intracellular ion fluctuations, caspase activation, mitochondrial dysfunction, mPTP opening and release of pro-apoptotic mitochondrial factors such as cytochrome c, AIF and EndoG.

Intracellular variations in the levels of $[Ca^{2+}]_c$ can regulate and initiate apoptotic cell death. The excess of $[Ca^{2+}]_{c,}$ which is primarily based on ER stress and membrane calcium channels, is accumulated in mitochondria where it leads to mitochondrial dysfunction and mitochondrial membrane permeabilization by triggering the opening of the mitochondrial permeability transition pore (Orrenius et al., 2003).

Intrinsic apoptosis or mitochondrially-regulated pathway of apoptosis is a subcategory of apoptotic cell death that is characterized by these features and is mainly regulated by mitochondria and proteins that regulate the mitochondrial permeability transition pore. In mammalian cells, in mitochondrial dysfunction, cytochrome c is released and forms a multi-protein compound known as apoptosome which in turn initiates the activation of the proteolytic caspase cascade through caspase 9. AIF and EndoG have also been reported to translocate from mitochondria to nucleus where they

mediate DNA fragmentation not only in multicellular organisms (Yang et al., 2017; Wei et al., 2017) but also in parasitic protozoans such as *Dictyostelium discoideum* (Arnout et al., 2001) and *Leishamnia* spp (Rico et al., 2009). Intrinsic apoptosis is also subdivided into caspase- independent and caspase-dependent pathways, based on caspase activation and functionality during the phenomenon.

This chapter reports a set key of biochemical apoptotic characteristics that have been observed in *Acanthamoeba* cells during treatment with G-418 and have been also described in numerous cells that undergo apoptosis and programmed cell death. These features include increase of intracellular calcium concentration, extensive mitochondrial dysfunction and release of mitochondrial proapoptotic factors such as cytochrome c.

Briefly, alterations in intracellular calcium ion concentration in *Acanthamoeba* trophozoites after treatment with EC_{90} G-418 were evaluated by fluorescence and sprectrophotometry techniques (3.6.1). Mitochondrial dysfuction was first evaluated by measuring trophozoite respiration rates based on CTC formazan accumlation (3.6.4), while disruption in outer mitochondrial membrane potential was detected with the use of the JC-1 stain (3.6.6). Finally, cytochrome c detection was performed after western blotting (3.8).

7.2 Results

7.2.1 Intracellular calcium concentration

Variations in cytosolic $[Ca^{2+}]_c$ after G-418 EC_{90} treatment at 37ºC were measured for a period of 150 minutes by spectrofluorometric analysis in a LS 55 Perkin Elmer luminesce spectrometer, using the fluorescent probe Fura 2-AM, a ratiometric dye that binds to free Ca^{+2} (3.6.1). It was observed that the levels of calcium in untreated *Acanthamoeba* trophozoites remained stable at 25 nM throughout the predifined time period. However, in trophozoites treated with G-418, $[Ca^{2+}]_c$ concentration rose from 25

± 3.6 nM at the beginning, to 45 ± 3.8 nM at 30 minutes, 54 ± 4.2 at 60 minutes, with a maximum of 62 ± 4.5 nM ($P<0.05$) at 90 minutes after G-418 induction (Figure: 7.1). 1mM EGTA (final concentration) was used as a negative control which suscefully diminished calcium concentration in both control and treated *Acanthamoeba* cells. Generally, the levels of intracellular calcium was significantly higher in the trophozoites treated with the aminoglycoside in a period of 180 minutes whereas at the same time the amount of intracellular Ca^{2+} in the control amoebae remained stable.

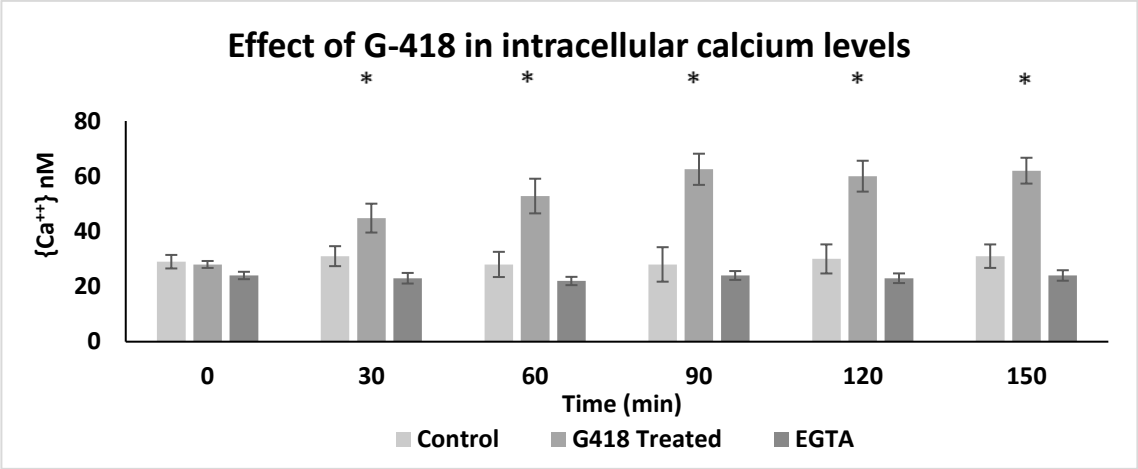

Figure 7.1: Intracellular calcium fluctuations after EC_{90} G-418 induction. Negative control column represents treated amoebae after the addition of 10μM EGTA. Values represents the mean of 3 independent experiments. Errors bars represent standard error, Significance is indicated (*), $P<0.05$ t-test; one tail distribution.

7.2.2 Mitochondrial dysfunction

Mitochondrial dysfunction was primarily evaluated using the mono-tetrazolium redox compound, 5-cyano-2,3-ditolyl tetrazolium chloride (CTC), which produces a fluorescent formazan (CTF) when it is chemically or biologically reduced and is

simultaneously deposited intracellularly (3.6.4). CTF is an excellent indicator of the cell's respiratory activity and it can be detected either spectrophotometrically or microscopically. More specifically, it was observed that in CTC- loaded, G-418 treated *Acanthamoeba* trophozoites, formazan production was decreasing during time of incubation, implication towards mitochondrial dysfunction (Figure 7.2), whereas at the same time, CTC-loaded untreated trophozoites shown stable formazan production implication of stable respiratory and metavolic activity. Interestingly, after 6 hours of incubation with the aminoglycoside, formazan production in *Acanthamoeba* trophozoites diminished considerradly reaching negative control fluorescence levels indicative of negligible mitochondrial activity. CTC unloaded trophozoites were used as a negative control (3.6.4).

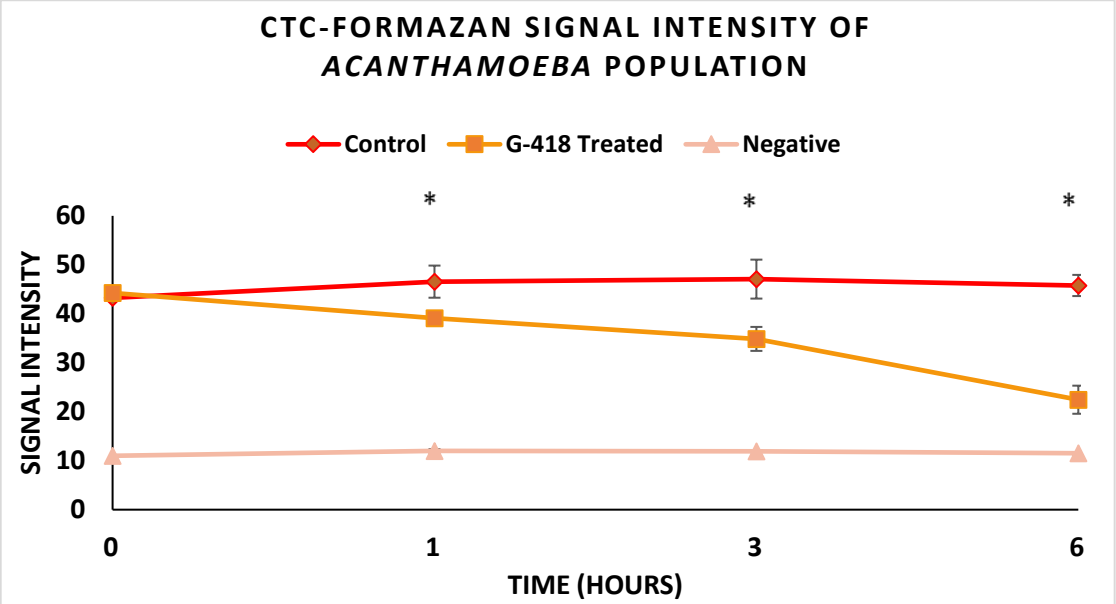

Figure 7.2: The diagram shows CTC reduction to detectable red formazan after G-418 induction in treated and control untreated *Acanthamoeba* trophozoites when excited at 350nm. The negative control represent fluorescence of *Acanthamoeba* trophozoites without CTC loaded. Values are representative of 3 independent experiments. Error bars represent standard error, significance is indicated (*), P<0.05 t-test; one tail distribution.

Fluorescence microscopy (3.6.4) confirmed previous spectrophotometry results as G-418 treated, CTC- loaded *Acanthamoeba* trophozoites showed decreased levels of intracellular red formazan accumulation (E1;E2;E3, Figure 7.3) compared to untreated cells during incubation time (B1;B2;B3, Figure 7.3). CTF fluorescence is shown to be greatly diminished 3 hours after G-418 treatment (E2, Figure 7.3) while after 6 hours is not even easily distinguishable (E3, Figure 7.3) indicative of defective mitochondrial function.

Mitochondrial function was further evaluated by the use of the JC-1 dye (3.6.6) during G-418 treatment. Experimental analysis revealed that the mitochondrial deficiency of the G-418 treated *Acanthamoeba* trophozoites, which was also previously detected, is based largerly upon changes occurring on mitochondrial membrane potential disturbance ($\Delta\Psi m$), rather than in mitochondrial breakage.

JC-1 ratio of 603nm/540nm fluorescence intensities indicates the relative amount of the dye that exist as monomer or aggregate, which in turn indicates mitochondrial potential status. More precisely, it was found that the JC-1 fluorescence ratio was stable in untreated trophozoites loaded with JC-1 during 6 hours of incubation, while at the same time the fluorescence ratio of the G-418 treated, JC-1 loaded *Acanthamoeba* showed a noticeable fall, indicative of mitochondrial permeabilization (Figure 7.4). Analysis of the readings in Fig. 7.4 has shown a remarkable decrease in $\Delta\Psi m$ ranging from 24% at the first hour to 58% at three hours and to 70% at six hours compared to control amoebae cells. These differences were also detected by fluorescence microscopy (3.6.6) where it is obvious that J-aggregate fluorescence, which is marker of healthy and functional mitochondria, is decreased dramatically throughout G-418 treatment (Figure 7.5).

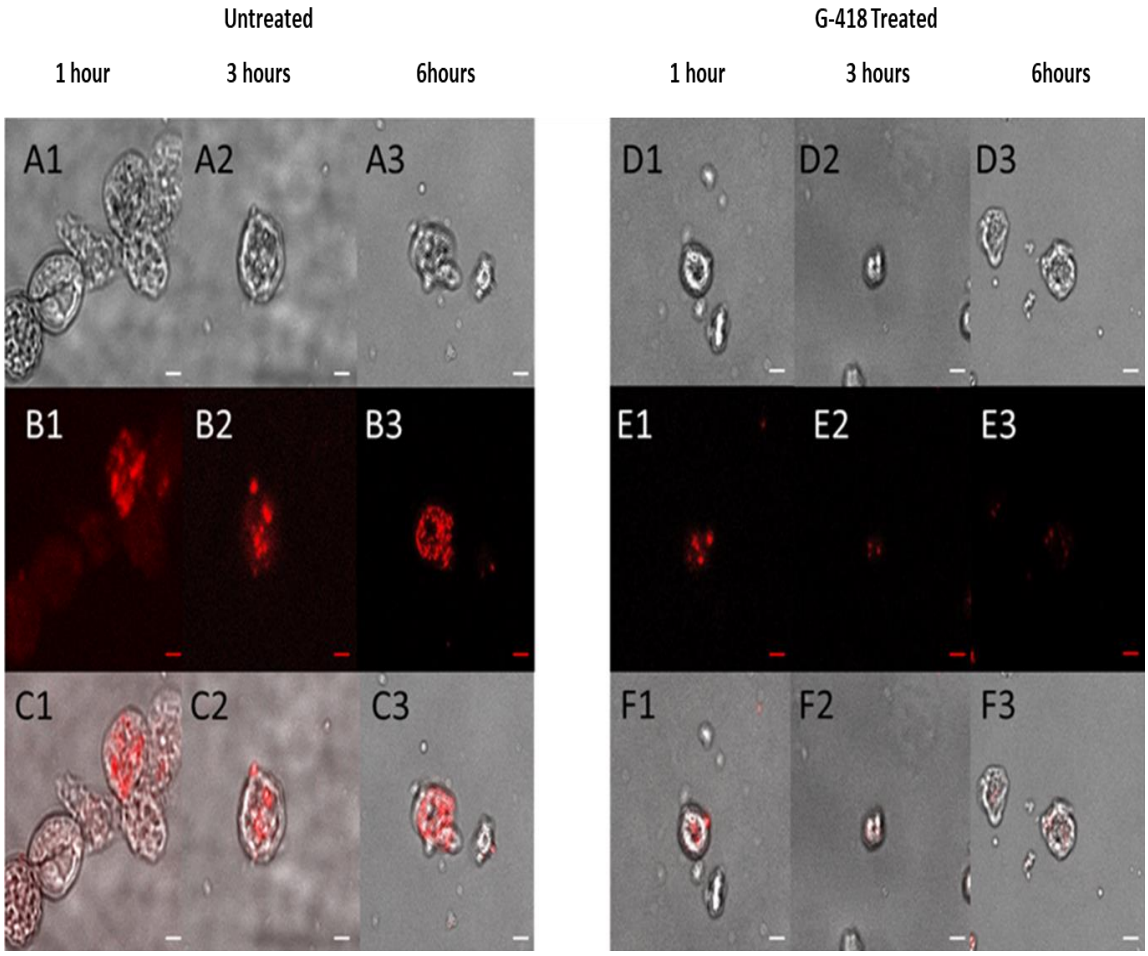

Figure 7.3: Illustration of formazan reduction during the 6-hour period of incubation. Signal intensity of the CTC reporter indicates respiration activity. The left column shows fluorescence intensity of untreated trophozoites while the right column shows fluorescence intensity of EC_{90} G-418 treated amoebae at 1, 3 and 6 hours. (A1, A2 and A3, B1, B2 and B3 and so on) after G418 induction. A1-A3 and D1-D3 phase contrast), B1-B3 and E1-E) formazan fluorescence, C1-C3 and F1-F3 phase and merge fluorescence. Images are representative of three experiments. Scale bar 5µm.

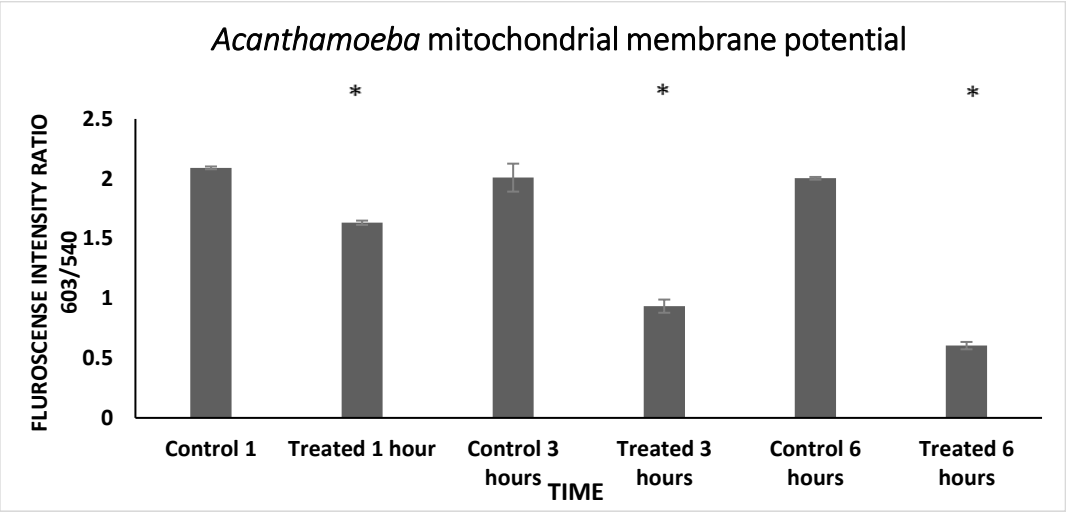

Figure 7.4: Graphical representation of the ΔΨm fluctuations during a period of six hours. Errors bars represent standard error, Significance is indicated (*), P<0.05 t-test; one tail distribution.

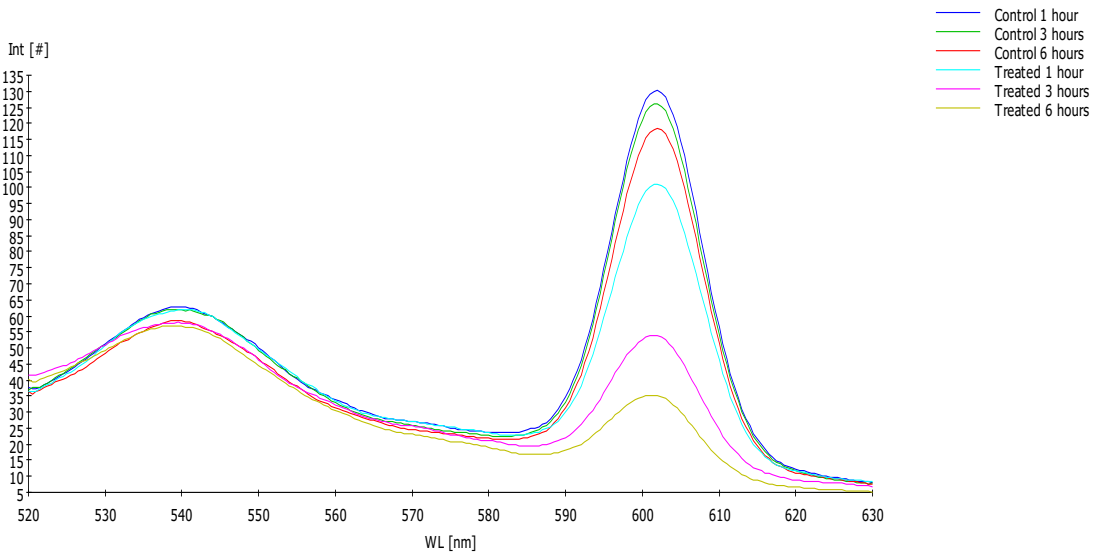

Figure 7.5: Diagram of JC-1 dye loaded on *Acanthamoeba* showing the different signal intensities of the JC-1 monomer at 540 nm and J-aggregate at 603 nm.

Fluorescence microscopy also revealed these findings, as green fluorescence, indicative of the JC-1 monomer and indicative of a low ΔΨm, was easily distinguishable after 3 hours of treatment with G-418 EC_{90} (Figure 7.5) and became even more intense after 6 hours of treatment. At the same time, untreated cells maintained very low and insignificant green and high red fluorescence, which is indicative of high ΔΨm and healthy mitochondria.

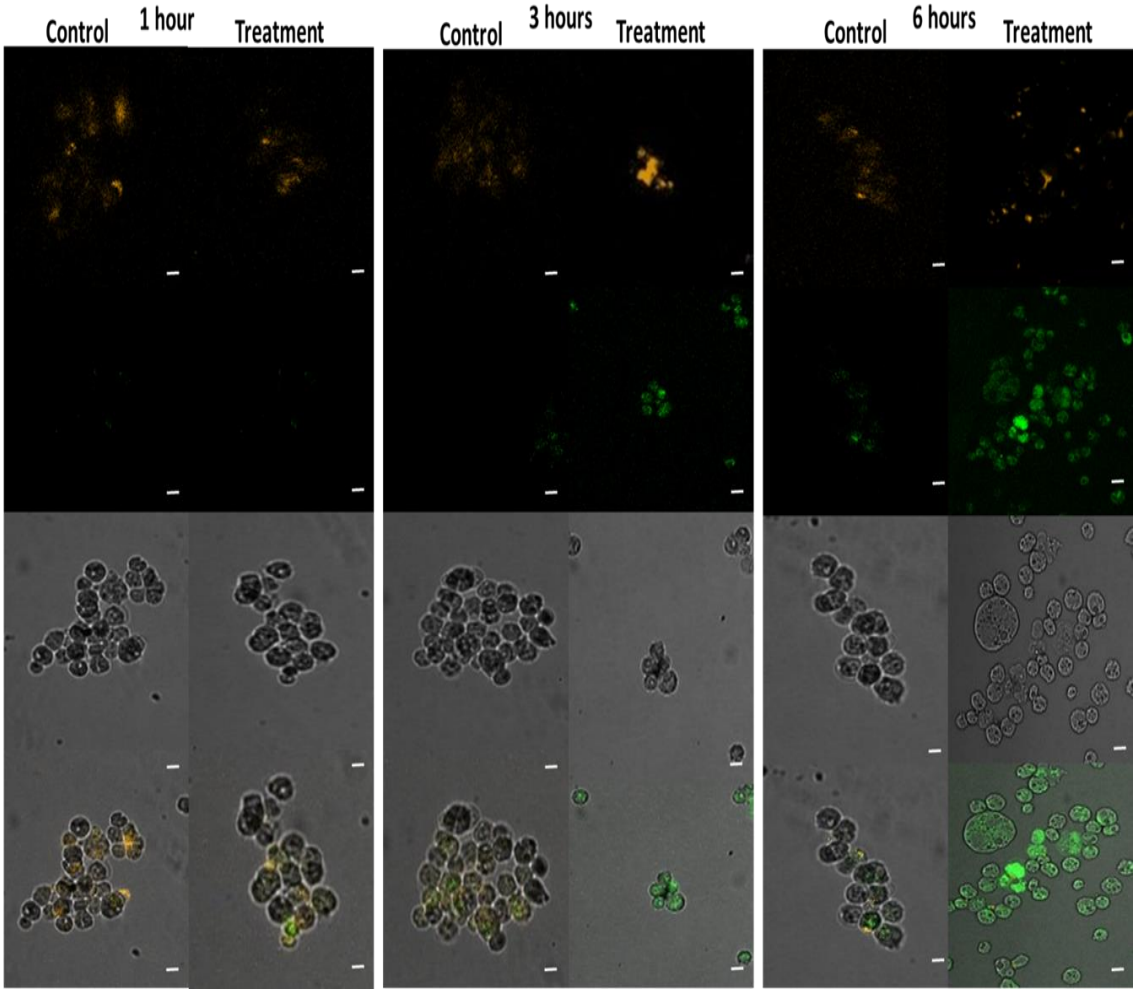

Figure 7.6: Fluorescence microscopy of G-418 treated and untreated Acanthamoeba trophozoites loaded with JC-1. Images are representative of 3 independent experiments. Scale bar 10μm.

7.2.3 Cytochrome c detection

Cytochrome c detection in *Acanthamoeba* trophozoites during treatment with G-418 aminoglycoside was evaluated by fluorescent western blotting (3.8). After protein separation by electrophoresis (3.8.1), lysates were transferred from polyacrylamide gel to a PVDF membrane (3.8.2). The PVDF membrane was later stained with Ponceau S in order to evaluate transfer efficiency (Figure 7.7). After membrane immunoblotting (3.8.3) and visualization (3.8.4), it was observed that after 3 hours of treatment with EC_{90} G-418, cytochrome c was detectable in the cytosolic fraction of the treated *Acanthamoeba* cells, implying its release from mitochondria, whereas there was no cytochrome c release in control amoebae (Figure 7.8). A band of slightly higher molecular weight was detected at approximately 22 kDa, instead of 12-15 kDa as was initially expected. The same band is also observed in the mitochondrial fraction of treated and untreated cell lysates (Figure 7.9).

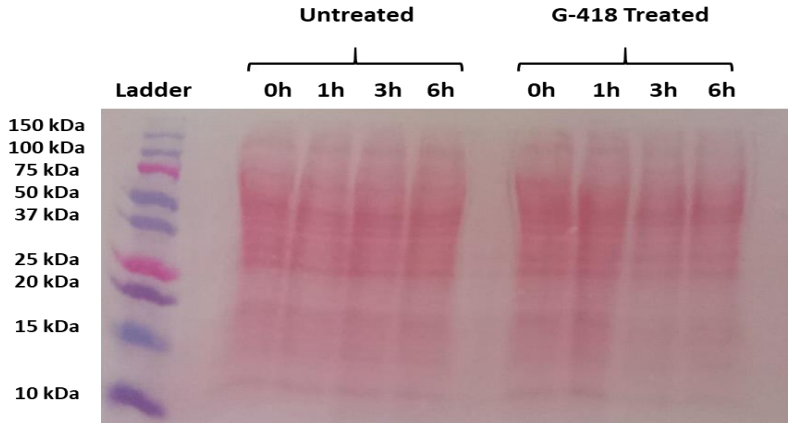

Figure 7.7: PVDF membrane after protein transfer and Ponceau S 0.1% staining. On the far left are protein molecular weight markers. On the left, are shown lysates from untreated *Acanthamoeba* trophozoites at different times; on the right are shown lysates from treated amoebae.

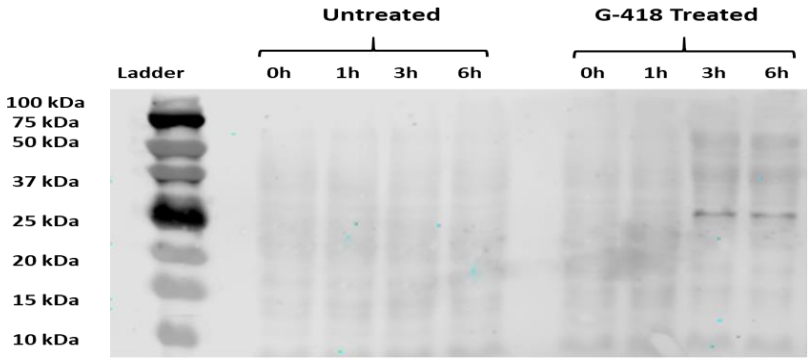

Figure 7.8: Representative western blot image from cytosolic fraction of *Acanthamoeba* cytochrome c at 4 different time points. On the far left are BIO-RAD precision protein molecular weight markers.

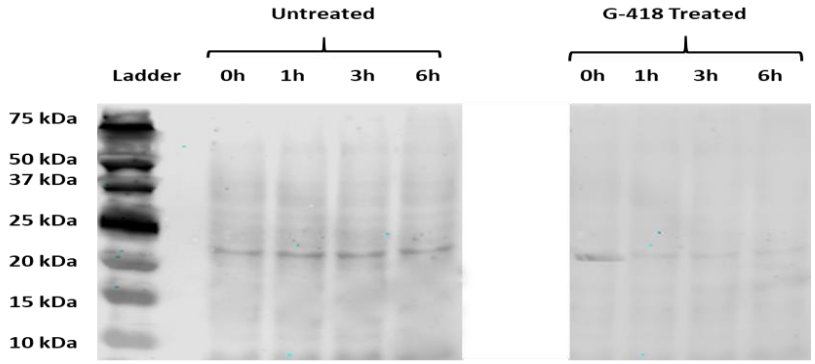

Figure 7.9: Representative western blot image from mitochondrial fraction of *Acanthamoeba* cytochrome c at 4 different time points. On the far left are BIO-RAD precision protein molecular weight markers.

7.3 Discussion

As well as distinctive morphological features, apoptosis is characterized by a number of biochemical alterations comprising fluctuations in intracellular ions and cation levels, mitochondrial dysfunction, release of ROS, activation of caspases and DNA fragmentation.

Increase of intracellular calcium levels has been reported in many programmed cell death studies, in early and late stages of apoptosis, in almost every kind of cell (Kruman et al., 1998; Tombal et al., 1999; Lynch et al., 2000). In this study, it was shown that during treatment with G-418, levels of *Acanthamoeba* intracellular calcium were increased considerably. It could be safely suggested though, that the rise in $[Ca^{2+}]_c$ can be considered one of the first steps of *Acanthamoeba's* programmed cell death induced by the aminoglycoside and simultaneously as a trigger or effector of the downstream phenomena that are taking place.

Excess of intracellular calcium might be due to endoplasmic reticulum stress, since G-418 aminoglycoside has been previously reported to cause such an effect (Jin et al., 2004) and also caffeine, which is considered as an ER repressive factor, partially inhibited G-418 mediated cell death.

Increased levels of calcium in the cytosol could cause mitochondrial calcium overload (Scorrano et al., 2003), which in turn could lead to MOM permeabilization and release of pro-apoptotic factors and proteins into the cytosol. MOM permeabilization was successfully detected in G-418 treated *Acanthamoeba* trophozoites with the use of the JC-1 fluorescent dye. As was shown, treated amoebae are characterized by a low mitochondrial ΔΨm, which allows release of mitochondrial apoptotic factors including AIF, EndoG and cytochrome c, whereas untreated cells under the same conditions showed high ΔΨm and functional mitochondria without any detectable MOM permeabilization. Mitochondrial dysfunction was also evaluated by measuring the level of respiration. Characteristically, fluorescence intensity readings indicative of mitochondrial respiration suggested gradual mitochondrial dysfunction and dysregulation

during treatment with G-418. More precisely, it was found that after 6 hours of treatment, *Acanthamoeba* trophozoite respiratory activity had almost disappeared, a phenomenon that is considered a natural outcome of MOM permeabilization.

The side-effects of mitochondrial outer membrane permeabilization are not limited to organelle dysfunction, but also include the release into cytosol of many pro-apoptotic factors, including cytochrome c, EndoG and AIF. Afterwards, AIF and EndoG translocate to the nucleus where they mediate chromatin and DNA fragmentation. On the other hand, cytochrome c upon its release is reported to bind to Apaf1, forming the apoptosome, which in turn is responsible for activation of caspases and their downstream lytic effect.

Western blotting revealed the presence of cytochrome c in the microorganism's cytosol after treatment of *Acanthamoeba* with G-418 aminoglycoside. More precisely, it was shown that after roughly 3 hours of incubation, cytochrome c was translocated from *Acanthamoeba* mitochondria to cytosol, whereas in untreated trophozoites, no such translocation was observed. However, it is yet unclear whether and how cytochrome c release might play a vital and leading role in the completion of apoptosis. The Abcam's polyclonal antibody reacted to a protein at approximately 25 kDa, close to double that of the 12.9 kDa size expected from the encoding sequence of the conserved *Acanthamoeba* cytochrome c gene (Amoebadb.org). *Acanthamoeba* cytochrome c protein comprises an exposed cysteine residue (appendix 2, fig: 2.2) and as it is known that cytochrome c has a strong tendency to polymerize through domain-pair exchange (Hirota et al. 2010). Subsequently, the 25 kDa band that is recognised by the anti-cytochrome c antibody might be a homodimer of *Acanthamoeba* cytochrome c.

In the majority of cells and systems, cytochrome c release from mitochondria is considered among the most significant checkpoints of the apoptotic procedure. Based on its high conservation rate among species and due to its primary importance, it would be safe to assume a strong association between cytochrome c release and *Acanthamoeba* programmed cell death. However since the microorganism lacks most of the machinery required to mediate cytochrome c-dependent cell death reported in mammalian cells, including caspases and Apaf1, we have to consider the possibility of an alternative death pathway, which applies in the case of *Acanthamoeba* and feasibly to other unicellulars

that resemble Acanthamoebadoid and can likewise undergo regulated cell death. In this case, cytochrome c release from mitochondria and its subsequent translocation to cytosol could not be considered a random consequence of MOM permeabilization, but a major event in programmed cell death execution.

AIF is also a protein highly conserved among species that plays an undeniably significant role in apoptotic processes. In this study, there was not enough evidence to support the involvement of AIF in G-418 mediated cell death, however AIF participation in the phenomenon could possibly explain some of the apoptotic features, including chromatin fragmentation. AIF could like cytochrome c be released from mitochondria during MOM permeabilization and might be subsequently translocated to the nucleus where its apoptotic function could develop. Further studies need to be conducted on that assumption, since AIF has been described in many unicellular protozoans as has already been stated.

Furthermore, identified intracellular calcium increase, as well as mitochondrial dysregulation, might cause hyperactivation of RAS and MAPK signaling pathways since rise of $[Ca^{2+}]_c$ is considered a significant Ras signaling activator agent (Yoshiki et al., 2010; Rosen et al., 1994; Cullen and Lockyer, 2002). Transcriptomic analysis of treated and untreated *Acanthamoeba* trophozoites, which is thoroughly analyzed in next chapters, has revealed an excessive upregulation of Ras and MAPKs genes during treatment with the aminoglycoside, indicating an active role for these molecules during G-418 cell death. However, it is not fully substantiated that this increase originates directly from the rise in $[Ca^{2+}]_c$.

Chapter 8

RNA seq analysis of *Acanthamoeba* programmed cell death

8.1 Introduction

RNA-seq is a high-throughput sequencing, revolutionary tool in transcriptomics that enables the quantification, detection, identification and profiling of the constantly altering, total cellular transcriptome over time, for similar or diverse groups or treatments, which leads to precise identification of differentially expressed genes (DEGs). Identification and quantification analysis of the DEGs is critical for the understanding of cell behaviour and phenotypic variation. Differential examination of gene and transcript expression using high-throughput RNA sequencing is complicated by several sources of measurement variability and is characterized by various statistical challenges.

Overall, RNA-Seq technology is an advantageous technique for differential expression analysis comprising five distinct stages. Initially, isolated RNA samples are converted into complementary cDNA sequences with adaptors attached to one or both ends and are sequenced from a high throughput platform to obtain short sequences of 30-400bp from one end (single-end) or both ends (pair-end). Later, the produced sequences are mapped to a genome using a sequencer aligner such as Bowtie, TopHat or STAR and the levels of gene expression are further estimated by bioinformatics tools including cufflinks or featureCounts. The fourth stage includes normalization of the reads and identification of the DEGs by EdgeR or Deseq2. Finally, the significance of the complete data is assessed biologically.

The purpose of the RNA seq analysis in this study was initially to determine if there are differences in the transcriptomic profiles of the G-481 treated trophozoites compared to untreated cells during pre-determined periods of time. Secondly, to identify

programmed cell death-associated genes that might control the course of the phenomenon and how the expression of these genes is regulated. Thirdly, to assess biologically the extent of “death” gene expression or respective repression that might determine the fate of *Acanthamoeba* cells. Furthermore, it would be feasible to associate some of the features that have already been observed on a gene-wise basis, upon expression analysis.

For this reason, transcriptomic comparisons were conducted at four different time points including times of 0, 1, 3, 6 hours after cell death induction by G-418 and two different conditions, comprising treated and untreated *Acanthamoeba* trophozoites under the same environmental conditions (37ºC) and in the same media (NSB) as previously described (3.9). Briefly, total RNA from both *Acanthamoeba* population was isolated at different time points as described (3.7.6). RNA samples were later quantitatively and qualitatively evaluated (3.7.7) before sent for sequencing (3.7.8) to Edinburgh Genomics.

Retrived sequences from RNA-seq were analyzed as previously described in 3.9.3. Briefly, all retrieved sequences were initially set to quality control analysis (3.9.3.1) before aligned to *Acanthamoeba* reference genome (obtained by ENSEMBL Protists database) using STAR aligner (3.9.3.2). Differential expression analysis and detection of differentially expressed genes (DE) were conducted in Rstudio 1.1.383 environment by using a plethora of R-supported programmes, libraries and packages, comprising readr, statmode, bplyr, rtracklayer, Rsubread, limma and edgeR, in order to read, process, analyze and visualize inserted BAM aligned files (3.9.3.3).

Differentially expressed (DE) genes were later identified by setting criteria of a fold change (fc _threshold) of < 2 and an FDR threshold of < 0.001 after biological coefficient of variation and moderated tagwise dispersion had been estimated. Transcript of the code used in Rstudio1.1.383, can be found in appendix 1.

8.2 Results

8.2.1 RNA quality

mRNA from 8 samples of *Acanthamoeba castellanii* GS isolate strain was sequenced in 2 HiSeq 4000 75PE lanes with three replicates for each treatment 0, 1, 3 and 6 hours after aminoglycoside treatment. The initial concentration of the 24 samples was verified with QUBIT (3.7.7) using fluorescent probes and simultaneously RNA quality by electrophoresis (3.7.4), (Figure 8.1).

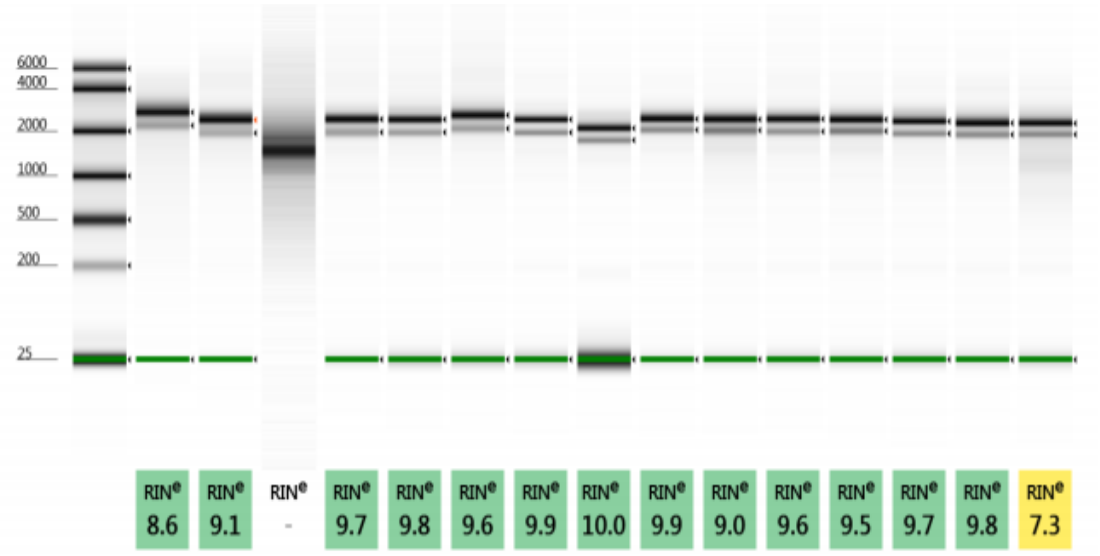

Figure 8.1: Representative RNA electrophoresis of *Acanthamoeba* RNA samples showing RNA quality. A molecular size ladder is positioned on the left. Also the RNA Integrity Number (RIN) is noted. Samples with RIN number around 8 or greater are considered to be the least degraded. Values over 7 are considered acceptable and if under 7 usually repetition of isolation is required. Sample 3 shows characteristics of degradation and it was resubmitted.

8.2.2 Quality control of the obtained sequences

Each sample resulted in the generation of 4 fastq files, individually containing approximately 18 million sequences. Each of the 96 files passed the FastQC analysis separately and was checked for abnormalities and low-quality scores (3.9.3.1). Quality control and filtering of raw reads is considered one of the most significant phases in the pre-processing of sequencing reads. Duplication levels are usually flagged in RNA seq because different transcripts will be presented at significantly dissimilar levels in the initial sample. In order to be able to observe lowly expressed transcripts it is consequently common to greatly over-sequence highly expressed transcripts and this usually leads to multiple duplicates-copies, hence the warning (Figure 8.2).

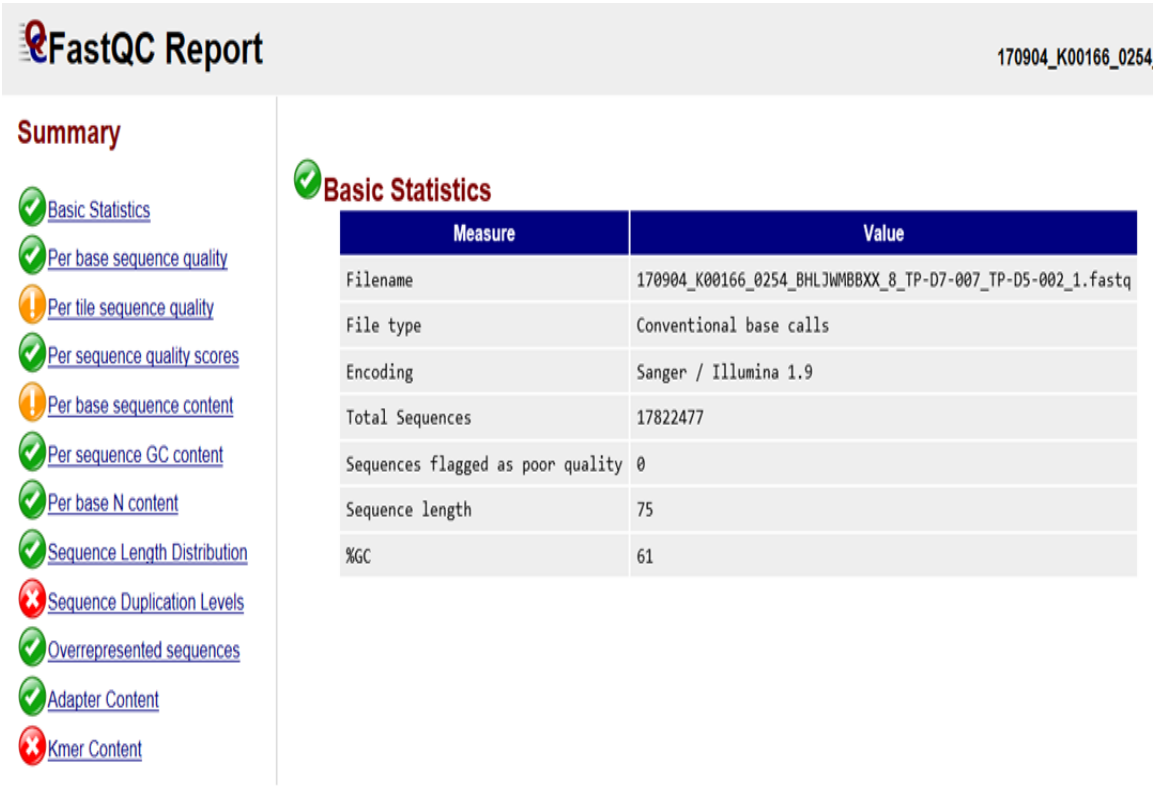
FastQC Report

170904_K00166_0254

Summary

- Basic Statistics
- Per base sequence quality
- Per tile sequence quality
- Per sequence quality scores
- Per base sequence content
- Per sequence GC content
- Per base N content
- Sequence Length Distribution
- Sequence Duplication Levels
- Overrepresented sequences
- Adapter Content
- Kmer Content

Basic Statistics

Measure	Value
Filename	170904_K00166_0254_BHLJWMBBXX_8_TP-D7-007_TP-D5-002_1.fastq
File type	Conventional base calls
Encoding	Sanger / Illumina 1.9
Total Sequences	17822477
Sequences flagged as poor quality	0
Sequence length	75
%GC	61

Figure 8.2: Representative summary of FastQC Reports, including basic statistics, per base sequence quality, per tile sequence quality, per sequence quality scores, per base sequence content, per sequence CG content, per base N content, sequence length distribution, sequence duplication levels, overrepresented sequences, adapter content and Kmer content. In basic statistics are noted the total number of sequences, sequences flagged with poor quality, sequence length and the GC percentage.

8.3 Differential expression analysis results

8.3.1 Exploring differences between libraries

Generally, Multidimensional scaling or MDS plotting is a visualization of the similarity level of individual cases of a dataset and is characterized as one of the most significant descriptive plots to examine gene expression analysis (3.9.3.3). In this case, the points of the plot represent the different treatment conditions and time points of *Acanthamoeba* genes' differential expression. The points are organized in such way that their proximity distances correlate to their similarities. For instance, similar cases are represented by points closer to each other and respectively dissimilar cases are more distant.

The plot also gives an initial idea of the extent to which differential expression can be identified before performing formal examinations and simultaneously, is both an analysis step and a quality control stage to examine the overall differences between the expression profiles of the different samples (Chen et al., 2016).

MDS plot generated by limma on R-studio environment, shows 3 different distinct groups. Group 1 (blue circle, Figure 8.3) includes samples from time 0 of both G-418 treated and untreated cells, the second group (green circle, Figure 8.3) represents

samples from untreated cells at 1, 3 and 6 hours and finally the third group includes all the samples from the treated cells which can also be further subdivided to 3 sub-groups based on incubation time (yellow circle, Figure 8.3).

The individual subgroups of these clusters are suspected to have low transcriptional dissimilarity and high transcriptional similarity amongst them. Also, over dimension 2 it seems that the difference among the samples including control *Acanthamoeba* populations at 0 and 1, 3, 6 hours is smaller compared to variation over other samples. Simultaneously, the largest transcriptional variance seems to be among control amoebae at 0 hours' time point and treated amoebae at 6 hours' time point, over dimension 1.

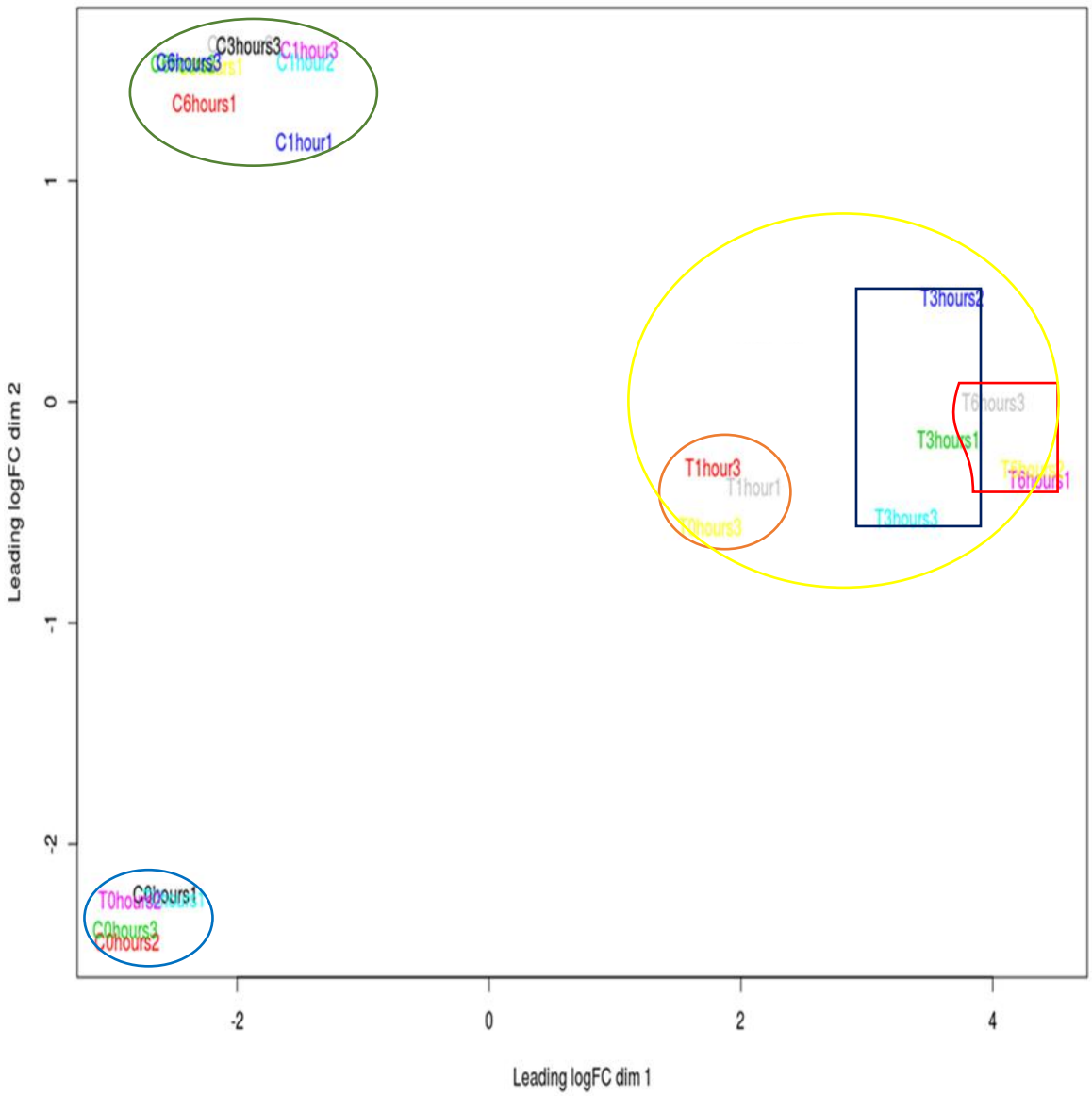

Figure 8.3: MDS plot made by limma using the plotMDS function, in R studio showing the variation of the samples that have been clustered in unsupervised and general manner. Distances on the plot correspond to the leading fold-change, which is the average log_2-fold-change for the 500 genes that are most divergent among each pair of samples by default.

8.3.2 Dispersion estimation

8.3.2.1 Biological coefficient variation

The comparison of gene expression in two or more groups of samples requires knowledge of the normal variation or dispersion in order to decide whether an observed value is outside or inside the “normal” dispersion limits and to assess differential expression. The value of dispersion for individual genes is called tagwise dispersion and is estimated using model-based approaches.

EdgeR estimates an empirical Bayes moderated dispersion for each individual gene. It also estimates a common dispersion, averaged over all genes which is a global dispersion and a trended dispersion where the dispersion of a gene is predicted from its abundance (Chen et al., 2016). EdgeR uses the negative binomial distribution to model the read counts for each gene in each sample. The dispersion parameter of the negative binomial distribution accounts for variability between biological replicates and it determines the variance of each gene. Subsequently, the common dispersion model is used for each gene variation modeling (3.9.3.3).

The biological coefficient variation of some genes, especially those with low expression levels, can be much higher than the common dispersion. The common dispersion has been estimated to be around 0.1 for the same cell lines from EdgeR authors, however in this case, there was a higher rate among comparisons, as common dispersion fluctuated around 0.2, betraying higher variation among samples (Figure 8.6). This indicates that the “true” abundance for a gene can vary up to 20% between samples. Generally, the higher the estimate of the common dispersion the higher the variability among replicates.

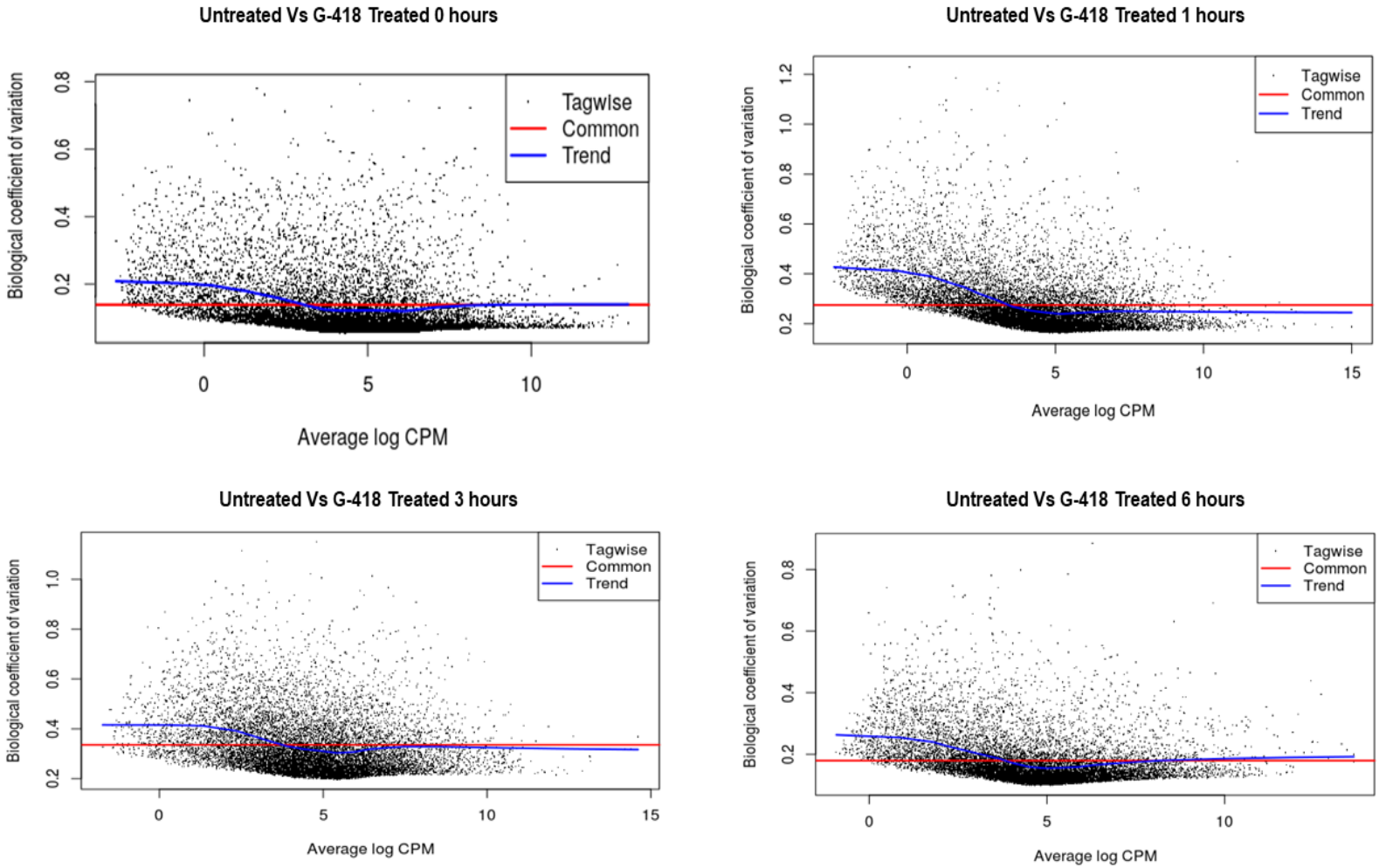

Figure 8.4: Scatterplot of the biological coefficient of variation (square-root dispersion) against the average abundance of each gene. The plot shows the square-root estimates of the common, trended and tagwise dispersions.

8.3.3.2 Moderated tagwise dispersion

RNA seq experiments are usually characterized by 3 samples per condition in two groups. Effect of this fact is that the gene dispersion estimation is based on four to five degrees of freedom that in turn leads to decreased and sometimes unreliable estimations. Conversely, common dispersion is based on several thousand observations, which renders it very trustworthy. In this case, in order to improve and further stabilize tagwise dispersion estimation, values are "squeezed" towards the common value, resulting in an outcome where estimates larger than the common value get smaller and estimates smaller than the common value get larger, respectively (Figure 8.7).

8.4 Differentially Expressed Genes analysis

Comparisons among samples from untreated and G-418 treated cells were performed at 4 different time points (0, 1, 3 and 6 hours) and revealed a significant number of differentially expressed genes. More precisely, at 0 hours gene expression did not show any difference between treated and untreated trophozoites, as was expected. After one hour of incubation with the aminoglycoside, treated amoebae showed 2604 D.E. genes with a fold change of at least 2 and a maximum FDR threshold of 0.001 among untreated and treated amoebae (Figure 8.7; 8.8). DE genes were increased to 2833 (229 more) after 3 hours (FDR_threshold ≤ 0.001; Fc_threshold ≥ 2). Interestingly after 6 hours the number of DEGs reached the number of 7803 which is approximately 50% of Acanthamoeba genes under the same parameters (Figure 8.7; 8.8). When the FDR value, was increased to 0.05 (5% possibility of being falsely differentially expressed) the DEGs increased dramatically to 5460 after thefirst hour, 6886 at 3 hours and 8275 after 6 hours (Figure 8.9).

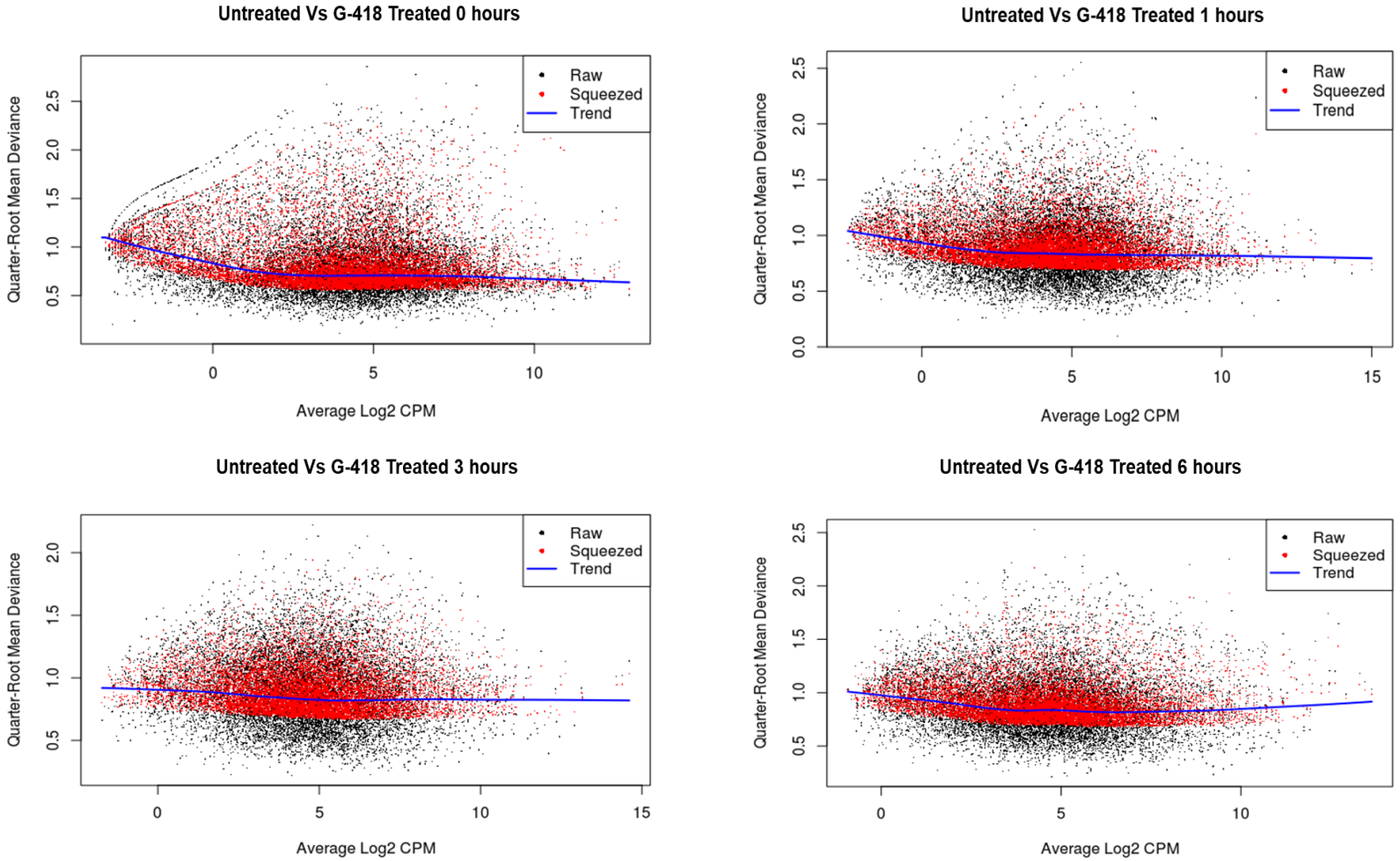

Figure 8.5: Moderated tagwise dispersion estimation among comparisons made between untreated and treated amoebae during time.

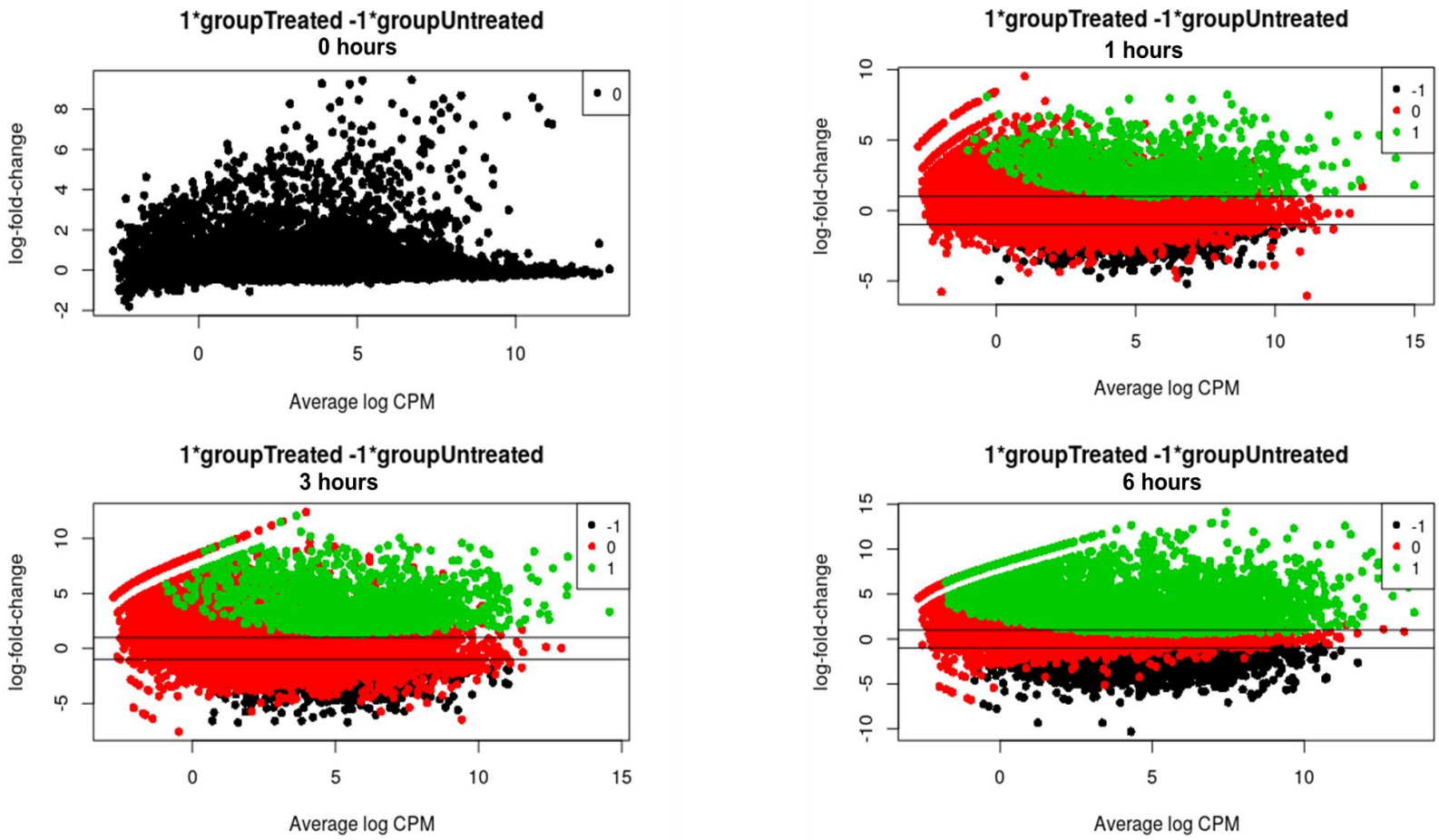

Figure 8.6: Scatter plots of DEGs showing log-fold change against average log-CPM. Green dots represent upregulated genes, black downregulate genes and red genes that do not alter significantly. Horizontal lines represent logfold change of 1. CPM were set at least 2 and maximum FDR at 0.001.

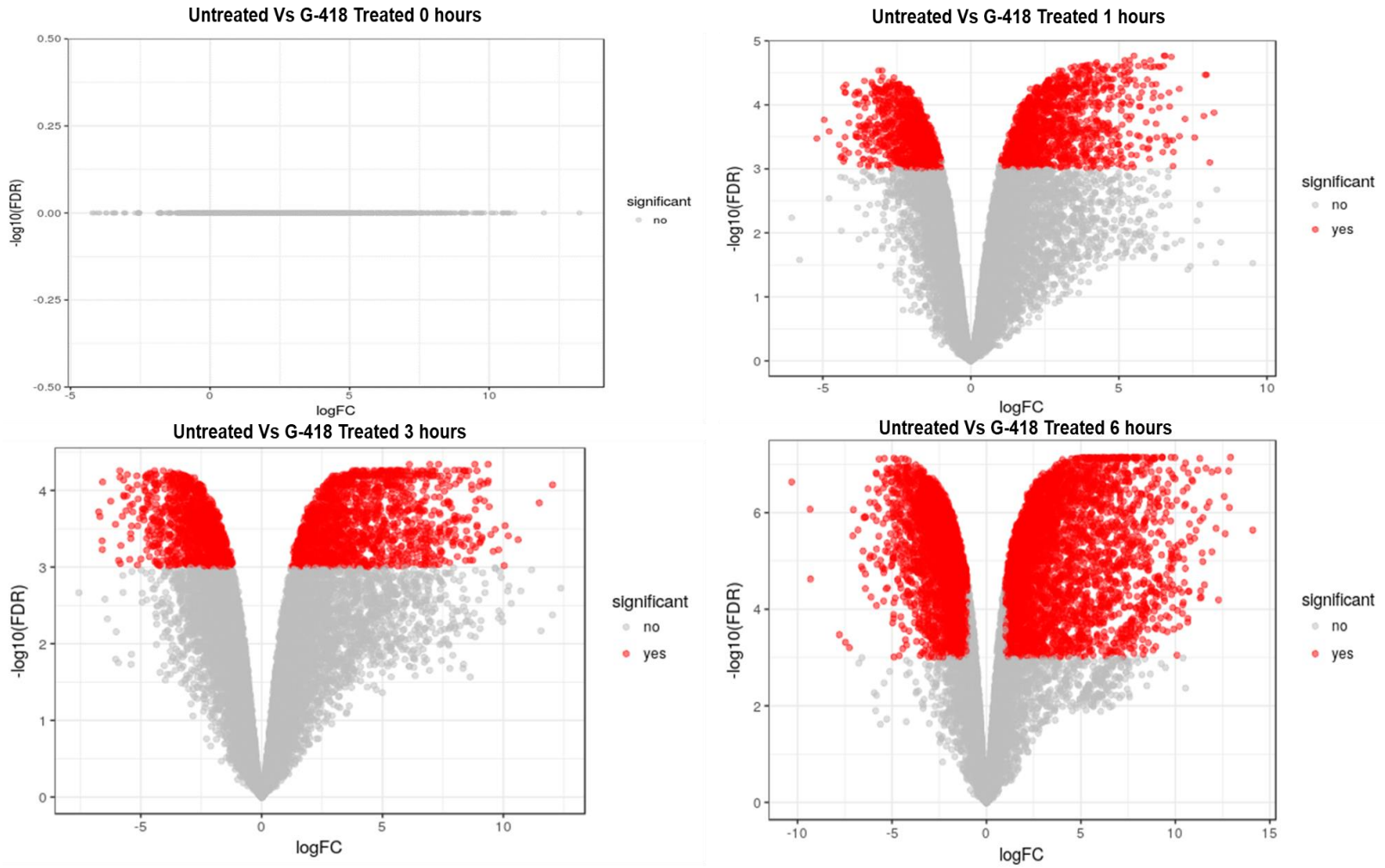

Figure 8.7: Volcano plots of differentially expressed genes at 0, 1, 3 and 6 hours of incubation. Parameters as CPM were set at least 2 and maximum FDR at 0.001. Significant DEGs are shown by red dots.

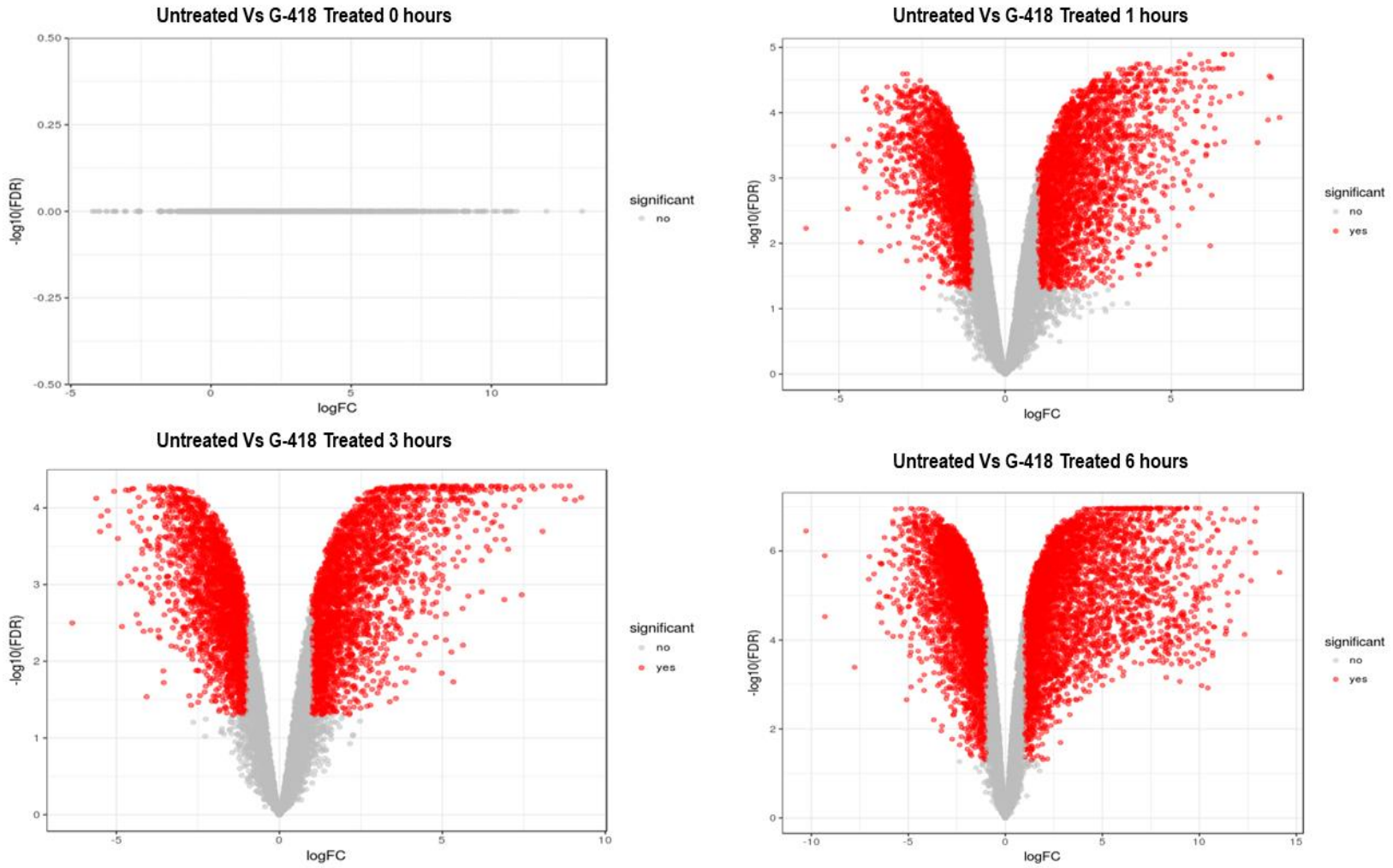

Figure 8.8: Volcano plots of differentially expressed genes at 0, 1, 3 and 6 hours of incubation. Parameters as CPM were set at least 2 and maximum FDR at 0.05. Significant DEGs are shown by red dots.

At the same time comparison among untreated amoebae was also performed in order to identify the level of DEGs and variation among samples. As was already known from the MD plot (Figure 8.5), genes from control samples at 0 and 1 hour have been mapped as far distinct from each other. Analysis revealed that there are 1035 differentially expressed genes with a fold-change of at least 2 and a maximum FDR threshold of 0.001, between trophozoites from 0 hours and trophozoites from 1 hour. This however is easily explained based on stress produced by temperature variation (0 hours at RT; 1 hour at 37^{o}C).

Later the number dropped to 826 DEGs when comparing control trophozoite samples from 1 and 3 hours (Figure 8.6) and finally only 1 gene was found to be differentially expressed by at least 2-fold and with a maximum FDR threshold of 0.001, among trophozoites from 3 hours and trophozoites from 6-hour control cells (Figure 8.10).

As was also expected, the BCV was significantly lower in comparisons of untreated cells, fluctuating around 0.1 which is the standard value for similar cell lines, compared to the BCV values generated by the control versus treated comparisons that have been previously made (Figure 8.6), suggesting a lower gene variation along time.

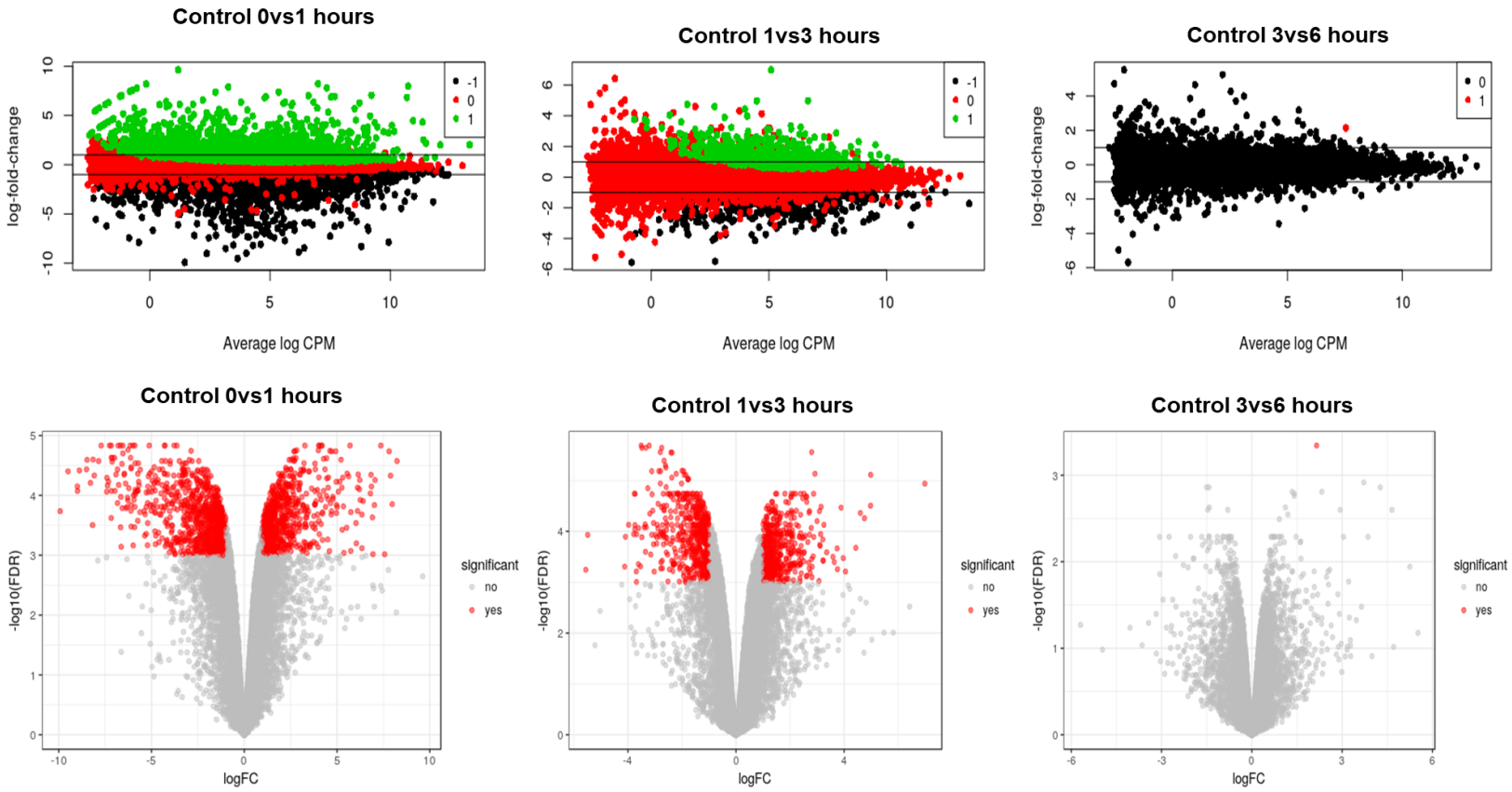

Figure 8.9: Diagrams showing significant DEGs expression between untreated *Acanthamoeba* cells at three different time point comparisons. Green dots represent upregulated genes, black downregulated genes and red genes that do not significantly alter. Horizontal lines represent logfold change of 1. In the top right and lower right figures, the red dot represents the only upregulated gene and black dots genes that do not significantly alter. CPM were set at least 2 and maximum FDR at 0.001

ID	LogFc	LogCPM	FDR	Protein Description	Homology
ACA1_143990	6.56241104	9.231606	1.71E-05	RAS subfamily	
ACA1_127590	5.51468797	6.531113	1.71E-05	Unknown	WH2 Domain motif
ACA1_072360	6.77214573	11.93665	1.78E-05	UBX protein domain	ubiquitin-regulatory protein
ACA1_171970	5.20049777	5.97979	2.01E-05	Hypothetical protein	Aminoglycoside phosphotransferase
ACA1_080730	5.36183087	13.75772	2.01E-05	Heat shock protein	
ACA1_276490	4.25039989	6.257151	2.16E-05	Vesicle-associated membrane protein	
ACA1_127660	5.86165494	5.15034	2.16E-05	Hypothetical protein	CsbD stress family
ACA1_087450	3.9246563	7.054655	2.37E-05	RAS subfamily	
ACA1_129230	5.3759211	10.30634	2.37E-05	Hypothetical Protein	E3 ubiquitin-protein ligase
ACA1_171980	4.01482487	8.067635	2.37E-05	RAS subfamily	
ACA1_091850	3.79271576	8.016228	2.46E-05	Hypothetical Prt	Unknown
ACA1_143980	6.52937406	7.656538	1.71E-05	RAS subfamily	
ACA1_140060	4.29211614	10.85629	2.46E-05	ATPase	
ACA1_090170	6.50123816	7.688336	2.46E-05	RAS subfamily	
ACA1_081860	4.60364504	6.391337	2.46E-05	Ser/Thr kinase	MAPK
ACA1_089990	5.12600337	11.22629	2.50E-05	RAS subfamily	
ACA1_374380	3.71078782	14.33886	2.50E-05	Heat shock protein	
ACA1_093820	5.89326929	8.338743	2.50E-05	Hypothetical Protein	Unknown
ACA1_265510	3.50492894	6.598706	2.50E-05	Palmitoyl Thioesterase	
ACA1_256400	6.18975249	7.813812	2.53E-05	RAS subfamily	

Table 8.1: List of the 20 greatest DEGs between treated and untreated *Acanthamoeba* after 1 hour (FDR ≤ 0.001 and fold change ≥ 2). Protein description retrieved from www.amoebadb.org and homology based on Uniprot blast are also shown.

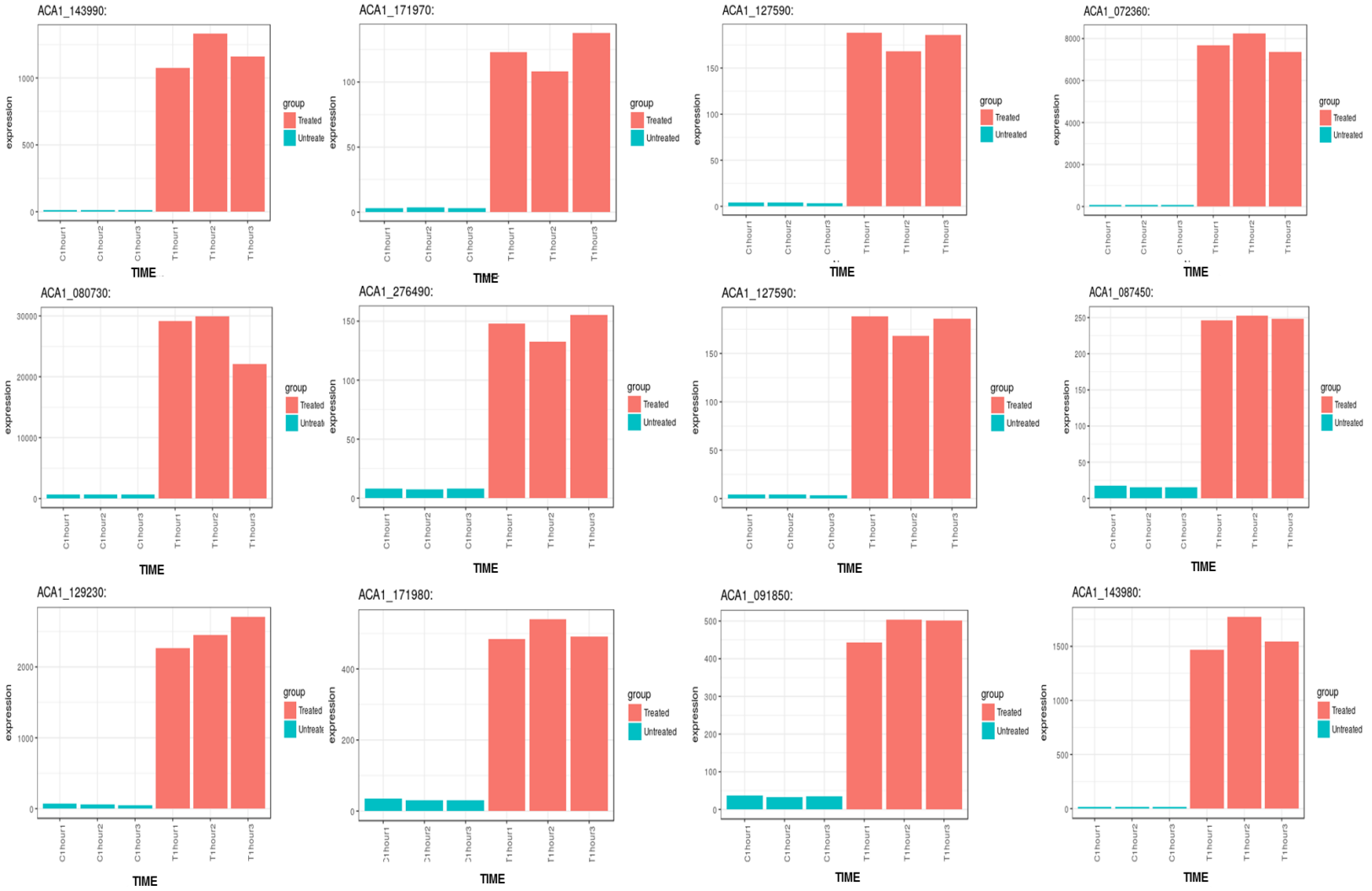
ACA1_143990:
ACA1_171970:
ACA1_127590:
ACA1_072360:
ACA1_080730:
ACA1_276490:
ACA1_127590:
ACA1_087450:
ACA1_129230:
ACA1_171980:
ACA1_091850:
ACA1_143980:
expression
TIME
group
Treated
Untreated
C1hour1
C1hour2
C1hour3
T1hour1
T1hour2
T1hour3

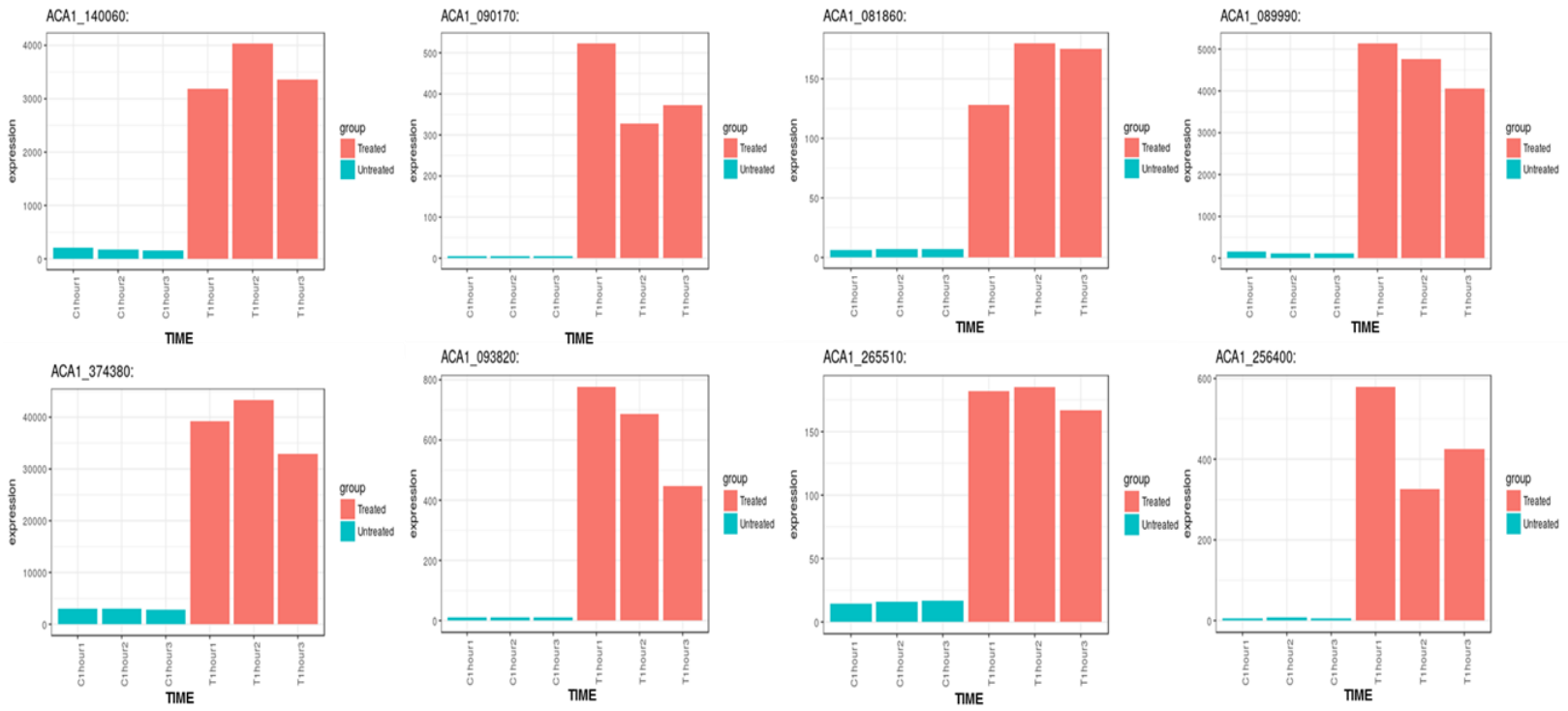

Figure 8.10: Expression profile analysis of the 20 largest DEGs in treated *Acanthamoeba* trophozoites after one hour of incubation based on EdgeR. The expression is presented in CPM. Red histograms represent expression profiles analyzed from each treated sample while blue histograms represent expression profiles analyzed from each untreated sample.

ID	LogFc	LogCPM	FDR	Protein Description	Homology
ACA1_072360	8.817264	11.94299	4.56E-05	UBX Domain protein	
ACA1_089990	7.314984	11.71435	4.56E-05	RAS subfamily	
ACA1_220460	9.365788	7.360668	4.56E-05	Hypothetical protein	Unknown
ACA1_070460	6.11124	12.07162	4.56E-05	Chaperone DnaJ	
ACA1_044470	8.166822	6.780263	5.44E-05	Hypothetical protein	Unknown
ACA1_093820	7.972137	9.100271	5.44E-05	Hypothetical protein	Transcriptional regulator cudA
ACA1_142420	5.645899	9.428149	5.44E-05	Tyrosine Phosphatase	
ACA1_208850	5.342992	6.311283	5.44E-05	Carboxylesterase	
ACA1_281310	7.072855	4.581416	5.54E-05	Hypothetical protein	Unknown
ACA1_108580	5.75193	4.528487	5.54E-05	Hypothetical protein	Unknown
ACA1_230450	4.960556	8.470046	5.54E-05	Hypothetical protein	Unknown
ACA1_391420	5.626383	10.24228	5.54E-05	Hypothetical protein	Unknown
ACA1_063570	8.350433	13.11957	5.54E-05	Hypothetical protein	Unknown
ACA1_065000	6.424787	9.89528	5.54E-05	Hypothetical protein	Unknown
ACA1_333240	5.758967	5.876957	5.54E-05	Hypothetical protein	Unknown
ACA1_255680	6.112366	10.49178	5.54E-05	Protein Kinase	
ACA1_365840	6.66442	6.94374	5.54E-05	Hypothetical protein	Serine endopeptidase
ACA1_091980	5.079199	8.996453	5.54E-05	Synaptobrevin	
ACA1_127650	8.442011	2.860586	5.54E-05	Hypothetical protein	Unknown
ACA1_159040	7.657217	9.873746	5.54E-05	Hypothetical protein	Unknown
ACA1_163390	4.189563	7.612113	5.54E-05	Hypothetical protein	ubiquitin-like protein

Table 8.2: List of the 20 greatest DEGs between treated and untreated *Acanthamoeba* after 3 hours (FDR ≤ 0.001 and fold change ≥ 2). Protein description retrieved from www.amoebadb.org and homology based on Uniprot blast is also mentioned.

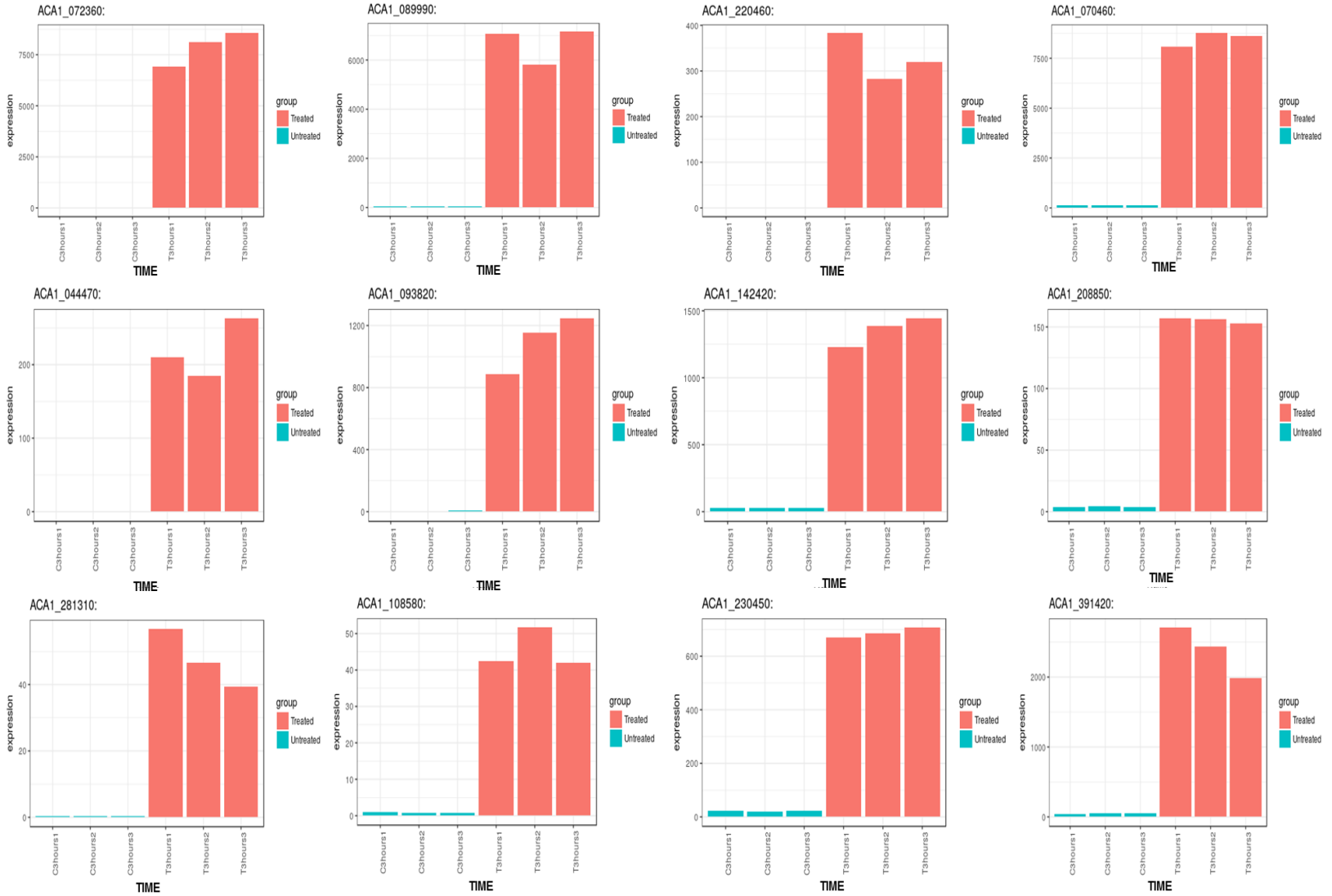
ACA1_072360:
ACA1_089990:
ACA1_220460:
ACA1_070460:
ACA1_044470:
ACA1_093820:
ACA1_142420:
ACA1_208850:
ACA1_281310:
ACA1_108580:
ACA1_230450:
ACA1_391420:
expression
TIME
group
Treated
Untreated
C3hours1
C3hours2
C3hours3
T3hours1
T3hours2
T3hours3

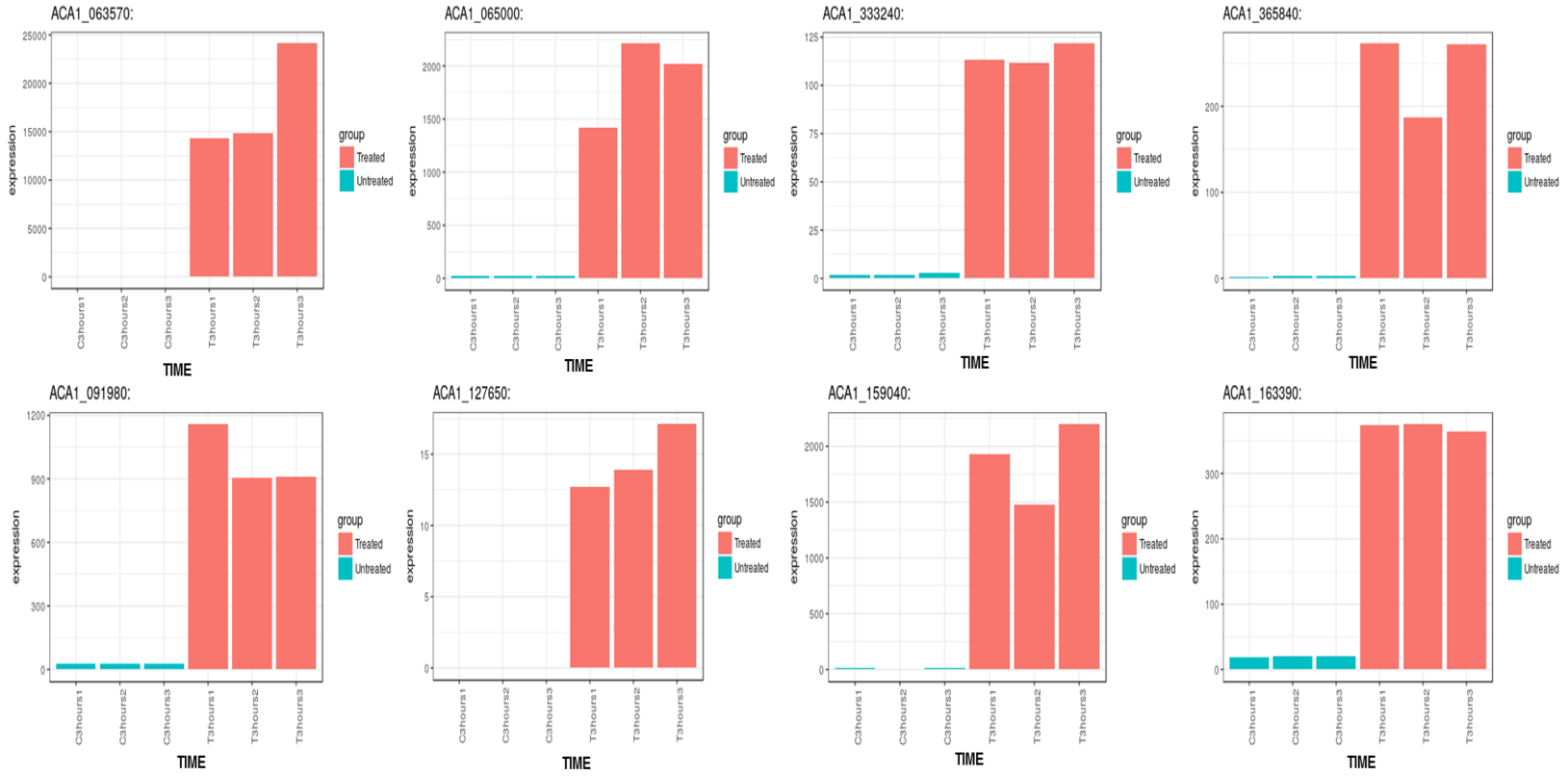

Figure 8.11: Expression profile analysis of the 20 biggest DEGs in treated *Acanthamoeba* trophozoites after 3 hours of incubation based on EdgeR. The expression is presented in CPM. Red histograms represent expression profiles analyzed from each treated sample while blue histograms represent expression profiles analyzed from each untreated sample.

ID	LogFc	LogCPM	FDR	Protein Description	Homology
ACA1_093170	7.97695	6.892021	7.15E-08	Kelch domain protein	
ACA1_097200	7.881855	8.610867	7.15E-08	MIF4G domain protein	
ACA1_378880	7.740856	6.574794	7.15E-08	Hypothetical protein	Unknown
ACA1_292170	8.487559	5.362409	7.15E-08	Hypothetical protein	Unknown
ACA1_220440	7.449845	5.427786	7.15E-08	Hypothetical protein	Unknown
ACA1_208730	7.764392	9.930901	7.15E-08	Carboxylesterase	
ACA1_153680	9.297893	8.209998	7.15E-08	Amz2 protein	Peptidase
ACA1_184390	7.094239	8.769101	7.15E-08	Hypothetical protein	Unknown
ACA1_069740	8.97882	4.964736	7.15E-08	Betalactamase	
ACA1_019200	6.129931	5.685494	7.15E-08	Hypothetical protein	Unknown
ACA1_167050	6.239263	8.949428	7.15E-08	RAS subfamily	
ACA1_069180	6.979725	7.356811	7.15E-08	Hypothetical protein	Kinesin like protein
ACA1_065030	7.133178	8.979023	7.15E-08	Hypothetical protein	Translation factor
ACA1_255680	6.768984	10.5653	7.15E-08	Protein kinase	
ACA1_246080	8.07252	4.048879	7.15E-08	ATPase	
ACA1_281310	9.298831	4.732681	7.15E-08	Hypothetical protein	Unknown
ACA1_063520	5.953535	8.49215	7.27E-08	zinc finger	
ACA1_275680	7.945333	7.433191	7.27E-08	Hypothetical protein	Unknown
ACA1_023100	9.973223	8.547317	7.27E-08	Hypothetical protein	Endonuclease
ACA1_095540	5.556857	6.10838	7.27E-08	F box protein domain	

Table 8.3: List of the 20 most DEGs between treated and untreated *Acanthamoeba* at 6 hours (FDR ≤ 0.001 and fold change ≥ 2). Protein description retrieved from www.amoebadb.org and homology based on Uniprot blast is also mentioned.

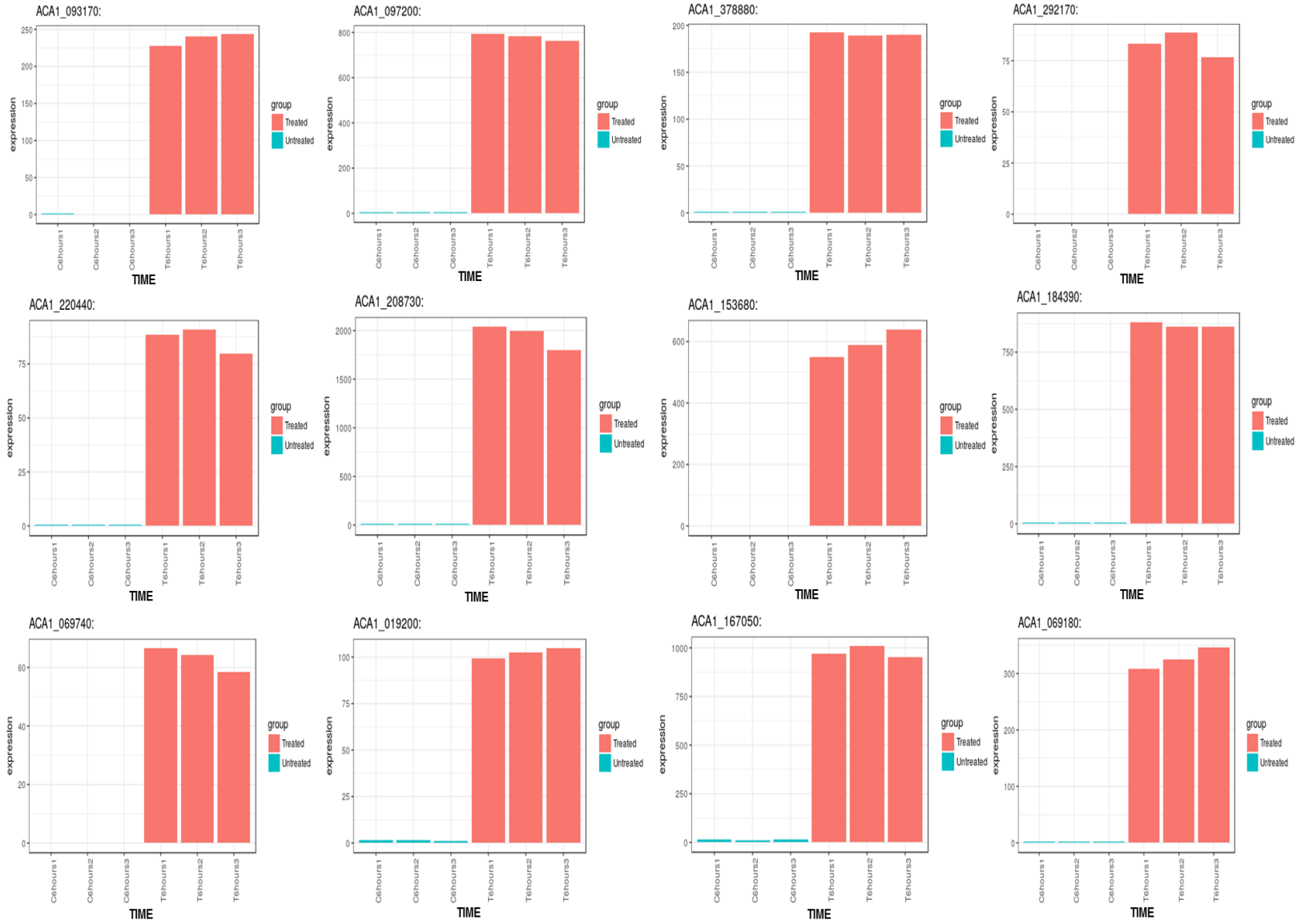
ACA1_093170:
ACA1_097200:
ACA1_378880:
ACA1_292170:
ACA1_220440:
ACA1_208730:
ACA1_153680:
ACA1_184390:
ACA1_069740:
ACA1_019200:
ACA1_167050:
ACA1_069180:
expression
TIME
group
Treated
Untreated
C6hours1
C6hours2
C6hours3
T6hours1
T6hours2
T6hours3

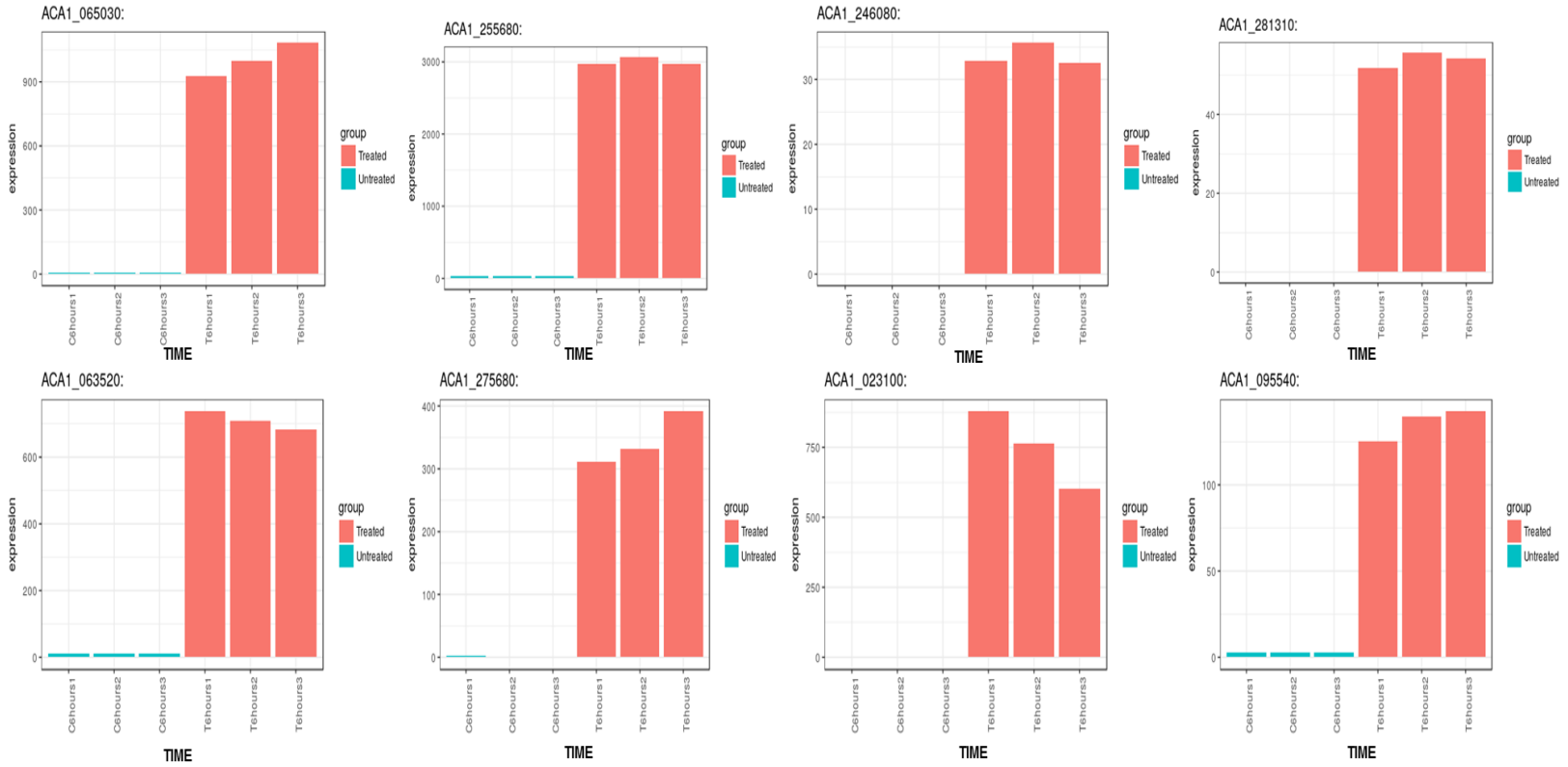

Figure 8.12: Expression profile analysis of the 20 largest DEGs in treated *Acanthamoeba* trophozoites after six hours of incubation based on EdgeR. The expression is presented in CPM. Red histograms represent expression profiles analyzed from each treated sample while blue histograms represent expression profiles analyzed from each untreated sample.

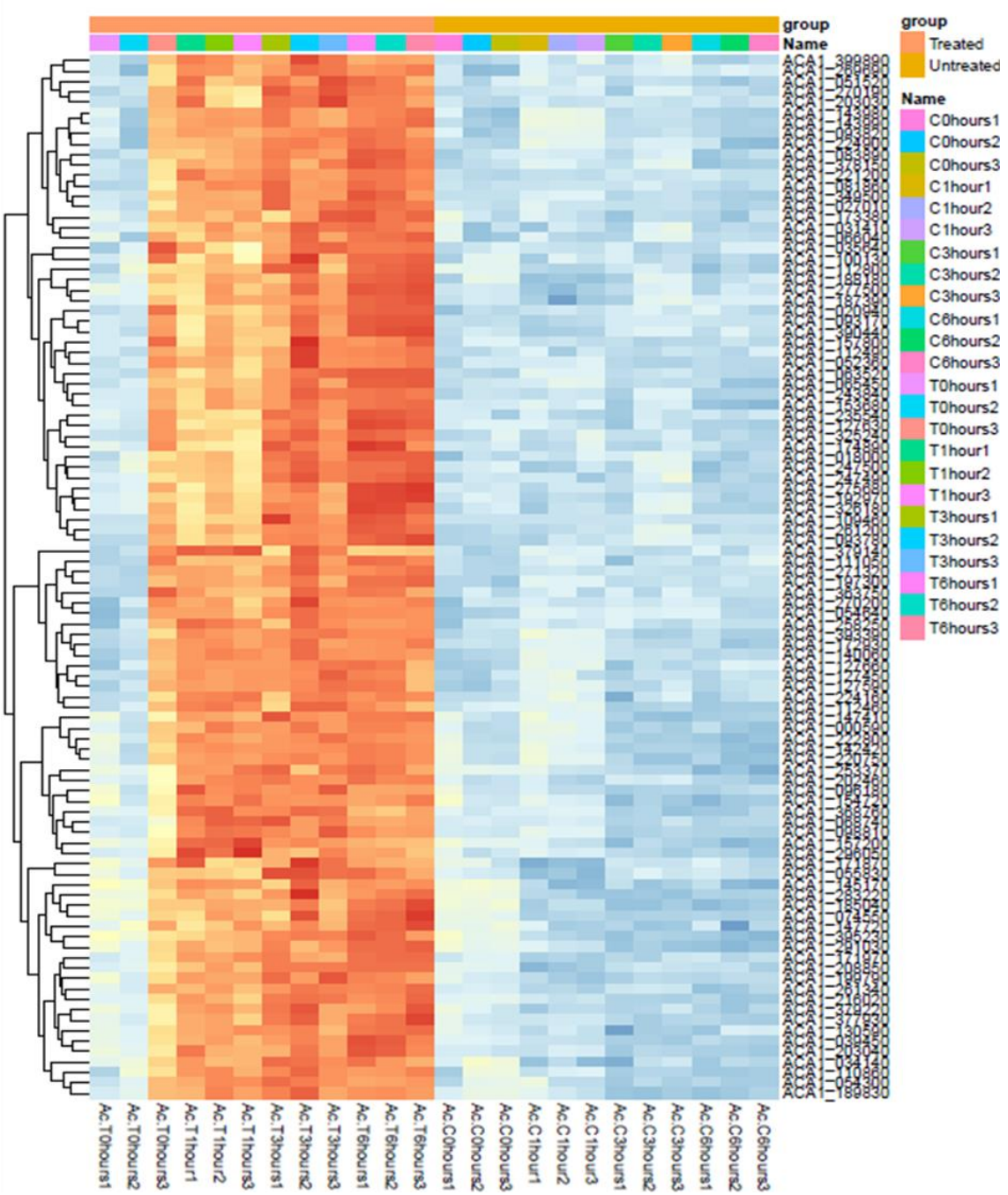

Figure 8.13: Heatmap of differentially expressed genes of all treatment conditions against time. Warmer-darker colors represent higher expression. Genes were identified as differentially expressed (FDR < 0.001) by EdgeR and expressed (CPM > 2).

8.5 Discussion

The identification of differentially expressed mRNAs, consequently genes through RNA seq sequencing has been used to assist understanding not only of gene function but also of the fundamental molecular mechanisms of individual biological systems and organisms. RNA seq analysis has also been used to analyse gene expression and differentiation in many biological processes from cell proliferation (Yang et al., 2015; Ramaker et al., 2018) to apoptosis (Wang et al., 2016) and many physiological and pathophysiological conditions from cancer (Lin et al., 2018) to autoimmune disorders (Giannopoulou et al., 2015; Ma et al., 2015).

In this study, RNA was isolated from two distinct conditions after 4 different periods of time, sequenced and analysed using various bio-informatics tools, including aligners, read-abundance counters and differential expression analysers. In this first chapter of RNA seq analysis were initially shown the numerous and fundamental quality controls which were performed in almost every step and guaranteed a strong base, which eventually led to assumptions and differentially-expressed gene analysis results that were as safe as possible. It was also shown how dispersion and gene variation was estimated and how CPM and FDR differentiates DEGs analysis and also affects the number of DEGs.

From the first stages of RNA analysis it was obvious that there were significant transcriptomic differences between control amoebae and G-418 treated *Acanthamoeba* trophozoites while simultaneously, isolated mRNA from treated trophozoites showed further differentiation between isolates at different times (Figure 8.5). At the same time transcriptomic profiles of the untreated amoebae changed slightly during the period of incubation, indicating minor transcriptomic alterations between them.

More precisely, it was found that at zero time there was no difference in transcriptomic profiles between G-418 treated and control trophozoites, as downstream analysis revealed no genes that are differentially expressed. This observation also verified that the two *Acanthamoeba* populations shared the same gene expression level

and started from the same trascriptomic point. Subsequently, there was not any genetic predisposition that could compromise the outcome.

Interestingly, 1 hour after treatment, the comparison between treated and untreated cells revealed 2604 genes that were marked as differentially expressed at maximum FDR threshold at 0.001 and lowest fold change of at least 2. Paradoxically, despite the fact that in both conditions are found highly expressed genes related to heat shock proteins (HSPs), some of them are expressed in only one condition associated to G-418 treatment, such as ACA1_374380 and ACA1_080730 (Table 8.1). However many of them, including proteins with characteristic domains that are categorized as HSPs, are expressed in both conditions and were not marked as differentially expressed.

Heat shock proteins comprise mainly anti-apoptotic agents that interact with a great variety of intracellular proteins and scaffolds (Kenedy et al., 2014). More precisely, it has been reported that higher expression of heat shock proteins mediates cell survival while inhibiting partially, directly and indirectly stimulation of pro-apoptotic proteins, such as BAX proteins, which in turn lead to MOM permeabilization and release of pro apoptotic factors such as cytochrome c, AIF and EndoG (Stankiewicz et al., 2009; Gotoh et al., 2004). Furthermore, HSPs have been effectively associated with reduced stimulation of caspases (Lanneau et al., 2008), whereas also an additional protective role of HSPs includes their ability to prevent ubiquitination and subsequent proteasomal degradation (Andrieu et al., 2010).

However, HSPs have been also reported as pro-apoptotic proteins that interact with a variety of cellular proteins, including pro-caspases and caspases that are directly involved in apoptosis (Samali et al., 1999; Lau et al., 1997; Xanthoudakis et al., 1999). Simultaneously, HSPs have been reported to promote apoptosis through decreased activity of the Akt pathway (Basso et al., 2002). It is clear therefore, that their expression levels can partially determine the fate of the cell in response to death stimuli, although it is as yet unclear how this is being achieved. *Acanthamoeba* G-418 treated cells showed extended expression of heat shock proteins, suggesting their role in the death process, although is unclear whether HSPs act as pro-apoptotic signals or execute a desperate cell attempt to bypass or supress cell death and increase the fraction of cells surviving.

An essential role of HSPs function is to act as co-chaperones, which in turn control the multifunctional abilities of each distinct HSP (Kennedy et al., 2014). These co-chaperones include proteins that contain domains like DnaJ, Cys-rich Zn-finger, tetratricopeptide repeat (TPR), U-box and BAG-family proteins (Takayama et al., 2003). Interestingly, many proteins with these characteristics were also found to be upregulated, including ACA1_070460 and ACA1_080730 (Table 8.1). It is nevertheless unknown in which direction these regulator proteins might lead.

Thorough investigation revealed that as well as the DEGs related to heat shock genes were entities related to Ras subfamily genes (Table 8.1). At least 20 different Ras subfamily genes were identified among the 50 most differentially expressed genes at 1 hour after cell death induction, including ACA1_181840, ACA1_143990, ACA1_087450, ACA1_171980, ACA1_143980, ACA1_090170, ACA1_089990, ACA1_256400 and ACA1_227760 (Table 8.1). Generally, Ras proteins function as on/off regulators for signal transduction. Simultaneously, Ras family proteins are vital for intracellular signalling through pathways that regulate crucial cellular procedures such as actin cytoskeletal integrity, cell adhesion, differentiation, proliferation and finally cell death (Kauffmann et al., 1997). According to cell type and external stress conditions, Ras signalling could mediate either cell death or cell survival.

Implication of Ras signaling pathways in the unicellular cell death phenomenon is not something entirely new. Ras signaling has been reported to accelerate signs and progression of programmed cell death in *Candida albicans,* although Ras activation is not itself sufficient to kill cells (Phillips et al., 2006). Increased Ras signaling has been also linked to the caspase-independent cell death pathway (Kitanaka et al., 1998; Elgendy et al., 2011). Based on the plethora of Ras genes that have been found to be upregulated in *Acanthamoeba* G-418 treated cells and not in control amoebae it would be safe to assume that Ras signaling plays a significant role in cell death progression. Probably Ras signaling may sensitize *Acanthamoeba* trophozoites to PCD induced by a combination of stimuli, including temperature stress and G-418 treatment, although it has reported that high level expression of Ras alone could mediate cell death likewise (Joneson et al., 1999).

An additional interesting fact from this initial analysis was the identification of ubiquitination-related genes. Ubiquitination is the basic signal in a cell that allows the regulation of intracellular protein levels and simultaneously participates in significant cellular biological procedures including apoptosis, DNA repair and replication, transcription and cell cycle progression, by mediating the cell's selective proteolysis by 26S proteasomes (Broemer and Meier, 2009). The ubiquitin-proteasome scaffold involves primarily E3 ligases and deubiquitinating enzymes (Gupta et al., 2018) and is considered to be the basic intracellular, non-lysosomal protein degradation system in eukaryotic cells. Many proteins and molecules associated with regulated cell death processes have been recognised as proteasome substrates, suggesting ubiqutination's energetic and essential role in the death processes (Jesenberger and Jentsch, 2002).

G-418 treated trophozoites seem to show high levels of ubiquitination as both of these requirements appear to be fulfilled, based on gene expression analysis. More precisely ACA1_072360 and ACA1_129230, which represent proteins with deubiquitinating enzyme domains and E3 ligases respectively, were found to be highly expressed in treated amoebae (Table 8.1) whereas at the same time their expression in control amoebae remained basal. Increased ubiquitination has been also described in various systems (Wojcik, 1999; Orlowski, 1999) related to apoptotic and regulated cell death. Simultaneously over recent years, ubiquitin E3 ligases have emerged as essential controllers of the apoptotic phenomenon as protein levels of many pro- and anti-apoptotic molecules could be under the control of the ubiquitin-dependent degradation system (Broemer and Meier, 2009).

Protein kinases and protein phosphatases regulate various cellular processes including differentiation, proliferation, cell cycle regulation, survival and cell death (Li et al., 2006). Ser/Thr kinases, by phosphorylation, activate or deactivate specific downstream effectors, including transcriptional factors and cytoplasmic proteins, in order to achieve cellular responses to stimuli (Cuadrado et al., 2010). MAPK and Jun N-terminal kinases have been also associated with apoptotic cell death in different cell types (Callsen and Brune, 1999; Chen, 2000) and have simultaneously been shown to be essential for both cell proliferation and cell death. Although the activation of kinases that leads to cell proliferation or cell death is quite dependent on the signal, the nature of the

cell and the external stress conditions involved in such circumstances is a crucial parameter and might result in variable outcomes (Liu and Lin, 2005; Lin and Dibling, 2002). MAPKs have been also linked to mitochondrial apoptotic pathways through both enhancing transcription of pro-apoptotic genes and directly by activating them (Cuadrado et al., 2010).

MAPKs genes, including ACA1_081860, have been found in the top 20 of the largest DEGs (Table 8.1) between treated and untreated trophozoites, indicating an important role of MAPKs in the phenomenon of *Acanthamoeba* cell death. Even more upregulated MAPKs genes were identified during analysis, including ACA1_058060, ACA1_064490 and ACA1_39920, which are discussed more analytically in the next chapter.

Transcriptional comparison among genes 3 hours after initial treatment revealed even more DEGs, however the majority of them were classified as hypothetical proteins and additional BLAST enquiry also failed to identify orthologous genes with at least 30% resemblance. More precisely, 2833 genes were marked as differentially expressed with maximum FDR threshold at 0.001 and lowest fold change of at least 2. However, some genes remained highly expressed including Ras subfamily genes such as ACA1_098990 (Table 8.2) and ubiquitination related genes like ACA1_072360 and ACA1_129230 in both comparisons (1 hour and 3 hours).

A tyrosine phosphatase gene, specifically ACA1_142420, was found to be among the highest DEGs when compared to untreated *Acanthamoeba* transcriptome after three hours of treatment (Table 8.2). The role of protein-tyrosine phosphatases as controllers of anti-apoptotic stimuli is commonly accepted (Halle et al., 2007), however individual protein-tyrosine phosphatases were suggested to either enhance or counteract a diversity of cell survival stimuli, ultimately favouring either cell survival or cell death.

Comparison among DEGS after 6 hours after treatment revealed a plethora of differentially expressed genes. Analysing however the 20 highest DEGs at this condition (Table 8.3) revealed that the majority of them were classified as hypothetical proteins and additional BLAST enquiry also failed to identify homologous genes with at least 30%

resemblance. More precisely, 7803 genes were marked as differentially expressed at maximum FDR threshold at 0.001 and lowest fold change of at least 2.

More than 50% of *Acanthamoeba* genes were found to be differentially expressed 6 hours after G-418 treatment. Ras subfamily genes such as ACA1_167050, ubiquitination related genes such as ACA1_063520 and ACA1_095540 and MAPKs such as ACA1_255680 occupy a position among the top 20 DEGs. It is obvious that Ras signalling, ubiquitination and MAPK interactions are common to G-418 treated cells as were identified at the top of every comparison between treated and untreated amoeba cells.

One of the most interesting observations, made based on 6 hours DEGs comparison, was the identification of a highly expressed protein with the zinc-binding loop region of a homing endonuclease. ACA1_023100 is described as a hypothetical protein according to the amoeba database (www.amoebadb.org), however further analysis and protein blast (Uniprot) showed homology to HNH endonucleases. Nucleases and more specifically endonucleases are crucial enzymes that as well as their physiological functions mediate also DNA fragmentation and chromatin condensation. HNH endonucleases have not been widely considered as DNA engineering tools as they are characterized by a lack of the modular DNA-binding motif found in ZF or TALE proteins. Moreover, moderate sequence degeneracies are tolerated by HNH endonucleases, increasing by this means the possibility of off-target binding (Gimble and Wang, 1996; Argast et al., 1998). HNH endonucleases are able to cleave one or both strands of the DNA double helix (Galburt and Stoddard, 2002), thus are quite heterogeneous and apparently very flexible and adjustable in performing various functions.

It is interesting that nuclear fragmentation, which has been already detected and discussed in previous chapters, after G-418 induction in *Acanthamoeba* trophozoites is placed chronologically approximately five to six hours after aminoglycoside treatment. Consequently, there may be a closer association between these two events. It should be mentioned though that numerous endonucleases and other enzymes that could have led in that direction have been found to be upregulated during the cell death phenomenon as is thoroughly described in next chapter.

An additional significant observation that was recovered from the analysis was the fact that at the top of DEGs in every comparison were ATPase genes, including ACA1_140060 and ACA1_246080, which were continuously higher expressed in G-418 treated trophozoites compared to untreated amoebae, suggesting a highly energy-dependent ongoing procedure.

Chapter 9

Gene profile analysis of *Acanthamoeba* programmed cell death

9.1 Introduction

There is an abundance of evidence to suggest that a variety of cell death modalities operate in mammal cells and higher eukaryotes in response to various death stimuli. The question that arises is whether the situation is the same in parasitic protozoans, including *Acanthamoeba spp*. Despite the great evolutionary divergence among multicellular and unicellular organisms and the clear molecular and biochemical differences, previous reviews have shown extended similarities in cell death machinery between multicellular and unicellular organisms. However, numerous genes that have been recognised as being regulators of metazoan apoptotic pathways are not always present in parasitic protozoal genomes, suggesting different pathways.

Analysis of the top differentially expressed genes provided some very useful insights regarding programmed cell death in *Acanthamoeba* G-418 treated cells and identified some very valuable information on gene profiling of G-418 treated amoebae. However, in a phenomenon that resembles apoptosis it is crucial to proceed to a more profound analysis and examination of other gene profiles with lower expression but possibly more significant to the final outcome.

Accordingy, in this chapter, genes associated with apoptosis in other models were inspected and analysed biologically. These genes comprise *Acanthamoeba's* metacaspase, genes related to autophagy, ser/thr kinases and phosphatases, Ras family genes, deoxyribonucleases, endonucleases, calpains, cathepsins and glutathione S-transferases corresponding to the amoeba database (http://www.amoebadb.org). This chapter actually constitutes a RNA-Seq screen of the G-418 aminoglycoside-induced programmed cell death response in *Acanthamoeba.* Gene expression and comparisons

between control and treated amoebae were performed as described in 3.9.3, using the EdgeR, in R studio 1.1.383 environment (transcript can be found in Appendix 1).

9.2 Results

9.2.1 *Acanthamoeba* metacaspase expression

Acanthamoeba metacaspase (Acmcp) has not been yet annotated in the *Acanthamoeba* reference genome, however a quick blast enquiry reveals ACA1_087710 as the most prominent match. ACA1_087710 is described as "ICElike protease (caspase) p20 domain containing protein" in the amoeba database, however it obviously refers to Acmcp. Phylogenetic analysis of ACA1_087710 was also performed, relating the protein more closely to *Saccharomyces cerevisae* metacaspase, rather than trypanosomal and *Leishmania* metacaspases (Appendix 2; figure 2.3). Individual differential expression analysis of *Acanthamoeba* metacaspase revealed an increasing trend in trophozoites treated with the aminoglycoside with time (Figure 9.1). As expected, at zero time, the expression profile of Acmcp was found roughly similar between treated and untreated trophozoites. Notably, in control populations, metacaspase expression showed a gradual decline during incubation, while at the same time, in G-418 treated trophozoites, Acmcp showed an up to 12-fold increase in transcriptomic abundance with time, revealing a impending role for metacaspase during *Acanthamoeba* cell death. The highest levels of *Acanthamoeba's* metacaspase mRNA were observed at 6 hours after treatment (Figure 9.1).

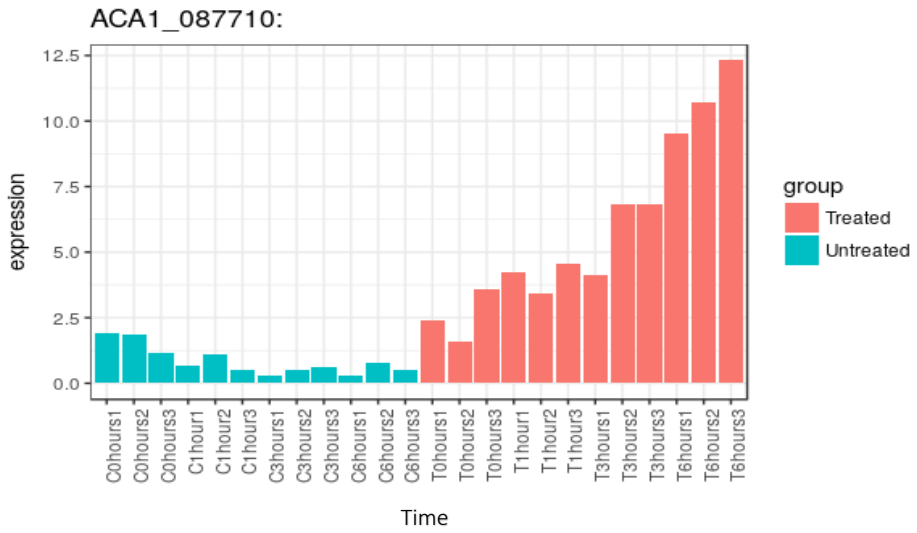

Figure 9.1: Expression profile analysis of *Acanthamoeba* metacaspase. The diagram illustrates Acmcp expression over time, between untreated and G-418 treated trophozoites. Expression is shown in CPM. Red colour indicates treated cells, blue untreated.

9.2.2 Protein kinase gene expression

Phosphorylation is responsible for causing a functional alteration of a target protein mainly either by shifting an enzyme's activity or its interaction with other proteins. Many protein kinases (PKs), which are the principal effectors of phosphorylation, are known to regulate many cellular processes, particularly those associated with signal transduction. PKs genes have been identified and their expression profile during treatment was analysed. Some representative kinase groups that were examined comprised non-specific PKs, serine/threonine protein kinases, mitogen-activated protein Kinases (MAPK), MAP2K, MAP3K, calcium/calmodulin-dependent protein kinases and tyrosine kinases.

9.2.2.1 Ser/Thr kinases gene expression

Representative analysis of ser/thr kinases genes has shown an important and widespread increase in G-418 treated trophozoites, suggesting increased phosphorylation compared to control cells. More precisely, the majority of the ser/thr kinases were found to be upregulated, marking a significant increase including indicative genes like ACA1_253460, ACA1_082010, ACA1_081860, ACA1_068390 and ACA1_123760. At the same time, a very small percentage of ser/thr genes were found to be downregulated during treatment including genes like ACA1_376760 and ACA1_372850 (Figure 9.2).

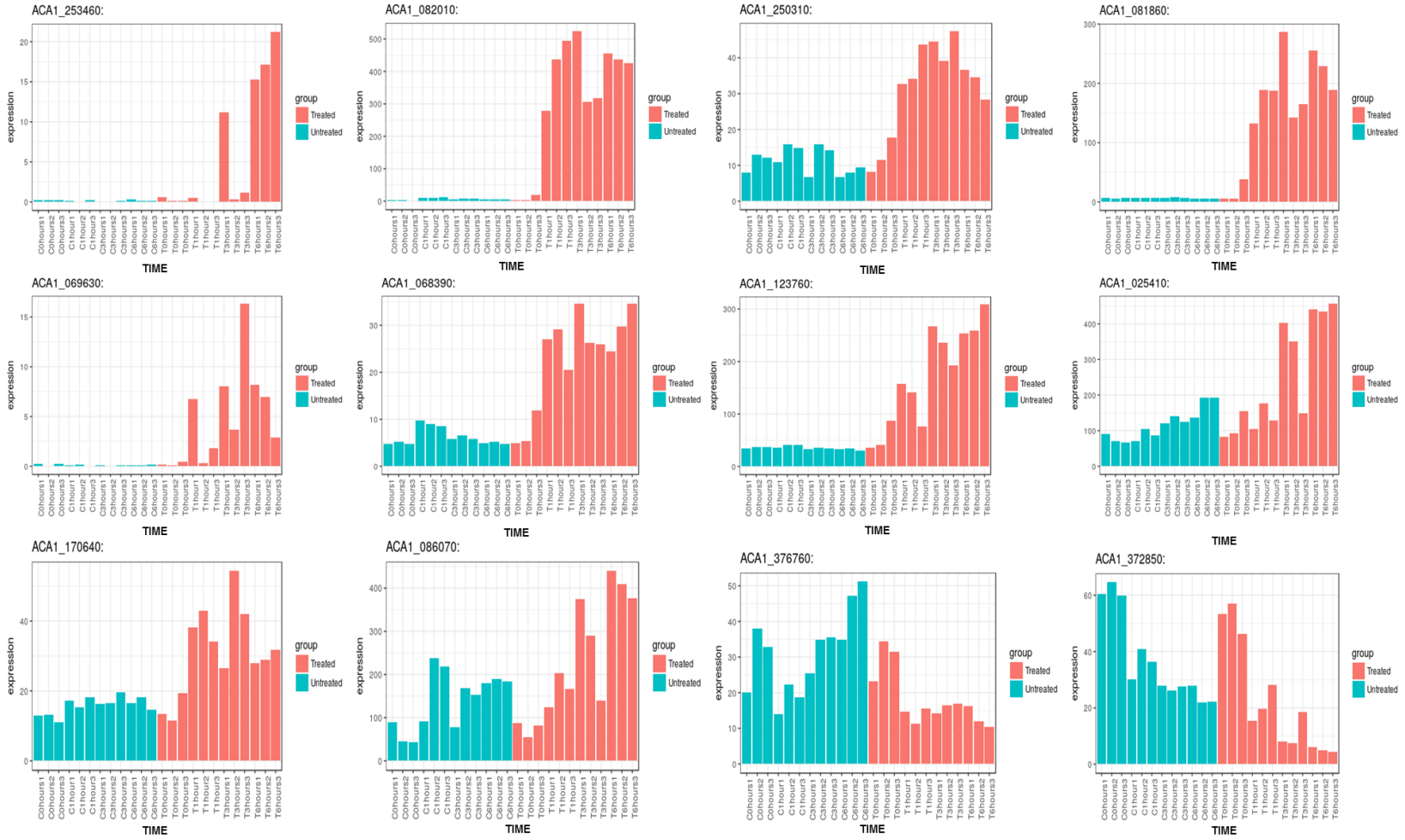

Figure 9.2: Expression profile analysis of *Acanthamoeba* ser/thr protein kinases. The diagrams illustrate representative Ser/Thr PKs expression during time, between untreated and G-418 treated trophozoites. Expression is shown in CPM. Red colour indicates treated cells, blue untreated.

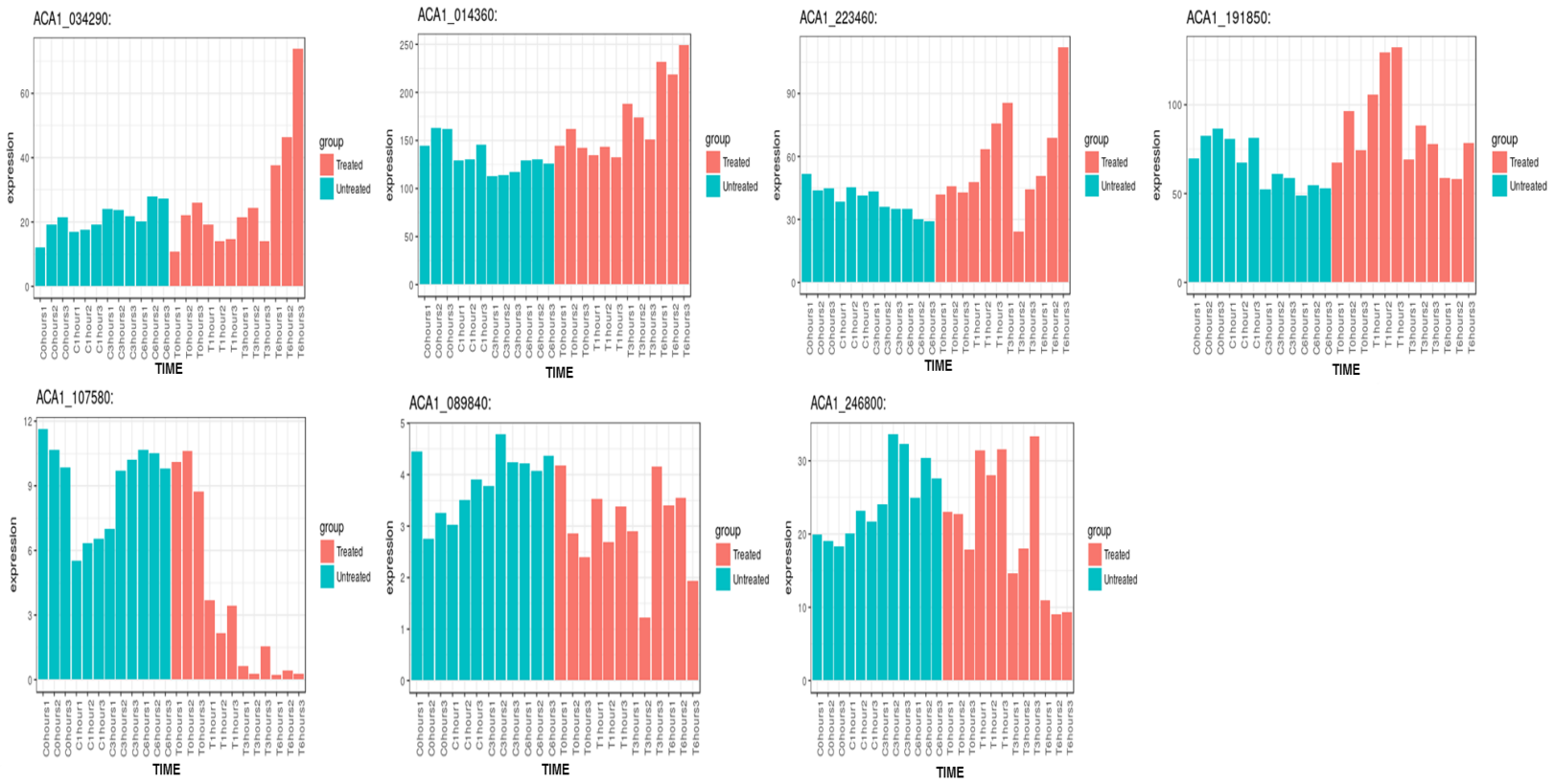

Figure 9.3: Expression profile analysis of *Acanthamoeba* Calcium-Calmodulin-dependent protein kinases. The diagrams illustrate calcium dependent PKs expression during time, between untreated and G-418 treated trophozoites. Expression is shown in CPM. Red colour indicates treated cells, blue untreated.

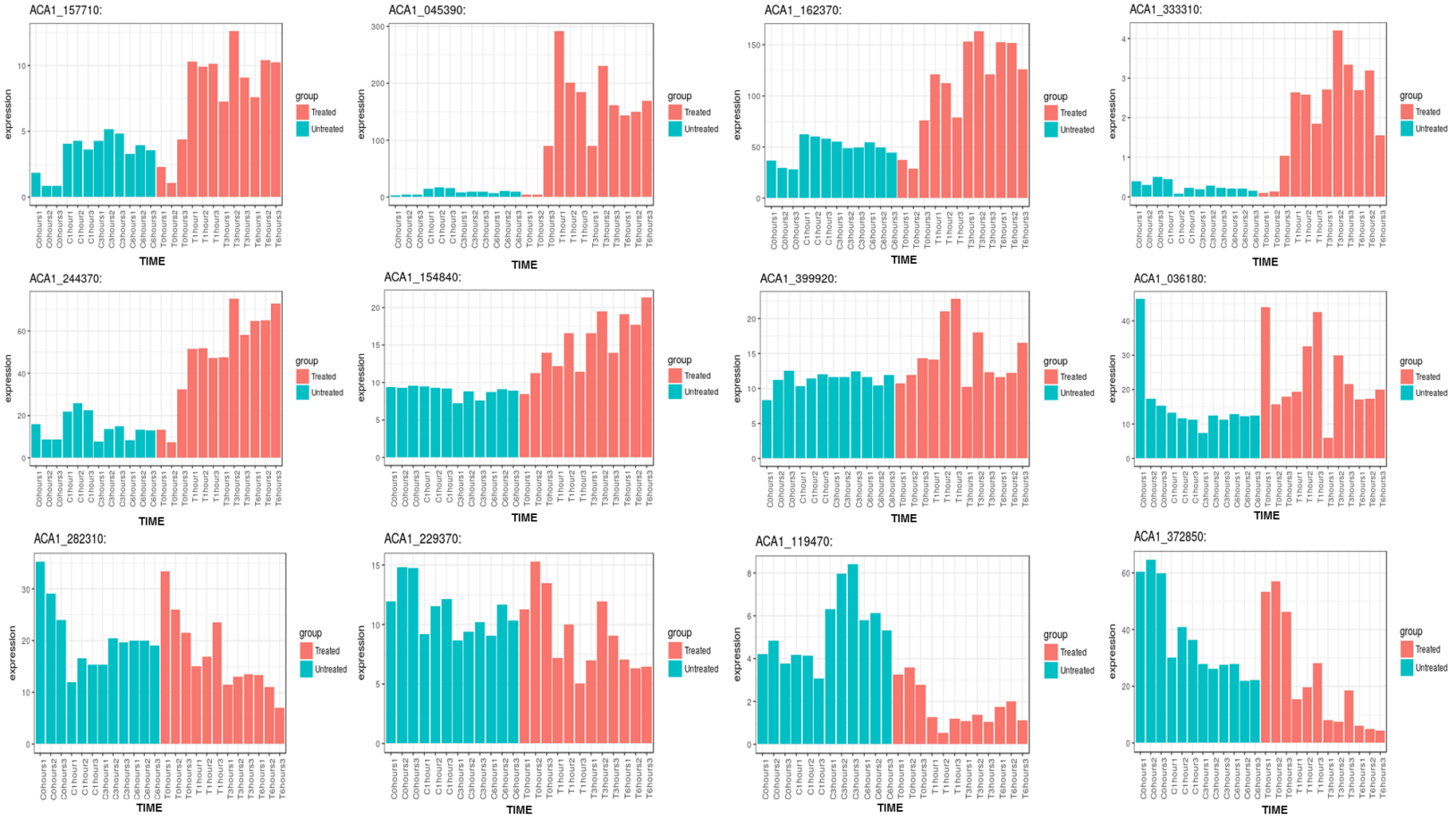

Figure 9.4: Expression profile analysis of *Acanthamoeba* MAPKs. The diagrams illustrate mitogen activated protein kinases expression over time, between untreated and G-418 treated trophozoites. Expression is shown in CPM. Red colour indicates treated cells, blue untreated.

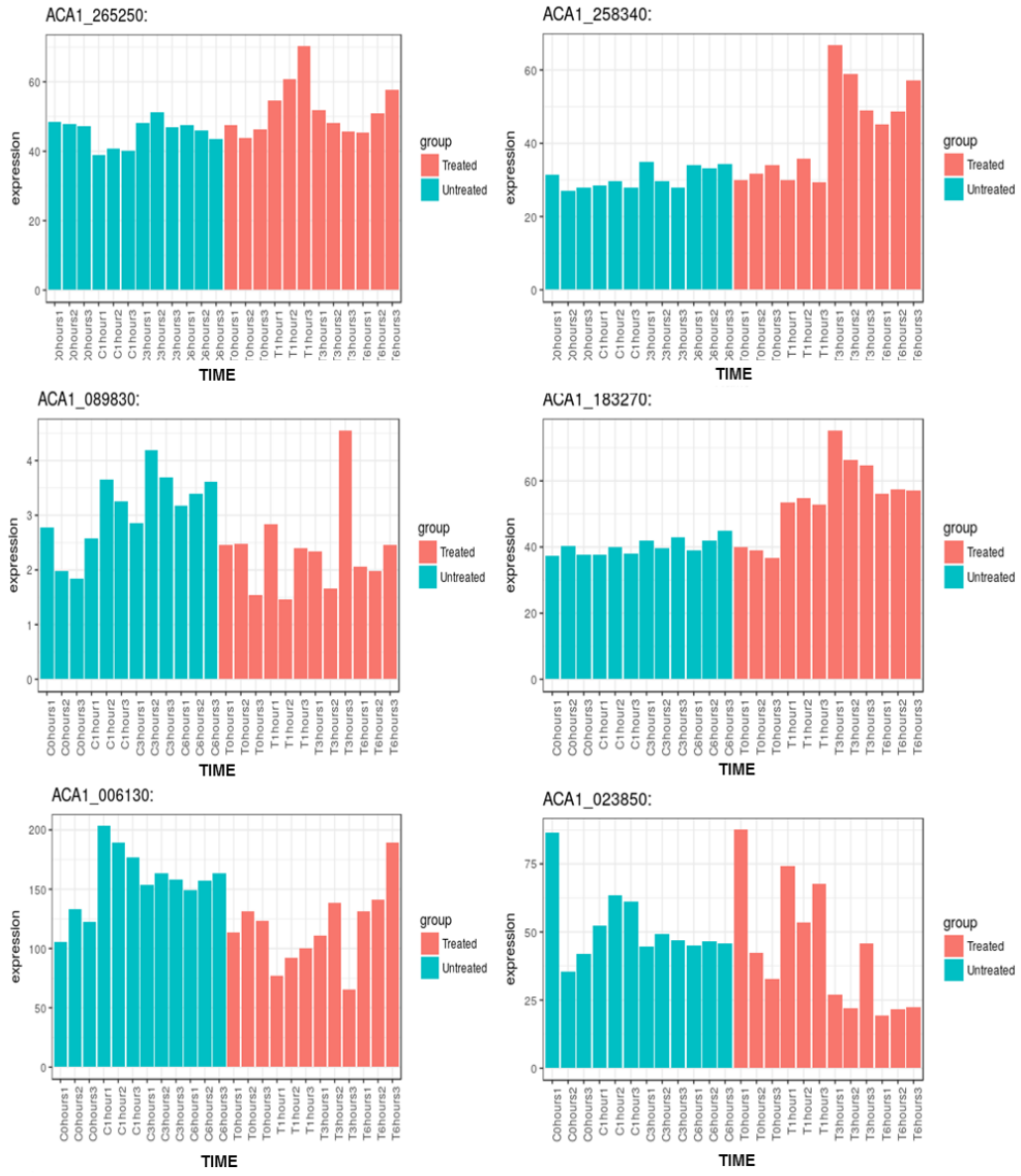

Figure 9.5: Expression profile analysis of *Acanthamoeba* TKs. The diagrams illustrate tyrosine kinases expression over time, between untreated and G-418 treated trophozoites. Expression is shown in CPM. Red colour indicates treated cells, blue untreated.

Calcium-calmodulin-dependent protein kinases including ACA1_034290, ACA1_014360, ACA1_222460 and ACA1_119850 were found to be partly upregulated (Figure 9.3) in treated *Acanthamoeba* cells, while ACA1_107580 was found to be downregulated. At the same time Ca^{2+}/Calmodulin gene expression remained stable in untreated amoebae. Also, calcium-calmodulin-dependent protein kinases like ACA1_ 089840 and ACA1_246800 showed a profile expression pattern with fluctuations (Figure 9.3)

At least 12 genes were identified as mitogen-activated protein kinases and subsequent quantification analysis has revealed a significant increase in their expression levels. For instance, genes including ACA1_045390, ACA1_399920, ACA1_244370, ACA1_162370, ACA1_154840, ACA1_333310 (MAP3K), ACA1_157710 and ACA1_036180 showed increased expression levels in treated amoeba cells while their expression levels remained roughly unaffected in untreated cells (Figure 9.4). However, MAPK genes such as ACA1_372850, ACA1_282310, ACA1_229370 and ACA1_119470 showed a decreased trend during incubation in treated cells, compared to untreated where expression levels remained stable (Figure 9.4).

Finally, after analysis of tyrosine kinase genes including ACA1_006130, ACA1_183270, ACA1_265250, ACA1_023850, ACA1_258340 and ACA1_089830, no significant alteration in gene expression profile was observed in both G-418 treated and untreated *Acanthamoeba*. ACA1_ and 183270 ACA1_258340, however, were found to be slightly upregulated during treatment, though not enough to be compared with alterations in ser/thr protein kinase expression.

9.2.3 Protein phosphatase expression

Many protein phosphatases (PPs), which are the principal effectors of dephosphorylation, have been identified and their expression profile was analysed. In total, 42 different ser/thr protein phosphatase genes were analysed. Further analysis

showed that 16 out of 42 genes were significantly downregulated (Figure 9.6) during treatment with G-418, including ACA1_058340, ACA1_295970, ACA1_209530, ACA1_296330, ACA1_233880, ACA1_397190, ACA1_005830, ACA1_026840, ACA1_073120, ACA1_329670, ACA1_033640, ACA1_062340, ACA1_062340, ACA1_060990, ACA1_316340 and ACA1_234820. At the same time 17 ser/thr phosphatases genes, including ACA1_251050, ACA1_173990, ACA1_199950, ACA1_052860, ACA1_068700, ACA1_114840, ACA1_342920, ACA1_107440, 379840, ACA1_193150, ACA1_211150, ACA1_211140, ACA1_087940, ACA1_063870 and ACA1_058340, were found to show no significant difference in their profile of expression between G-418 treated and untreated *Acanthamoeba* trophozoites. 9 Ser/thr PPs genes including ACA1_151330, ACA1_087940, ACA1_256940, ACA1_121740 (Figure 9.6), ACA1_269730, ACA1_246770, ACA1_191840, ACA1_321950 and ACA1_251170, were found to be upregulated in G-418 treated cells compared to untreated amoebae, where their expression remained stable.

11 additional tyrosine protein phosphatase genes were also examined and their expression profiles analysed. Specifically, ACA1_394730, ACA1_191870, ACA1_367320, ACA1_121530 and ACA1_212830 did not significantly alter their profile expression during treatment with G-418. Between treated and untreated *Acanthamoeba*. ACA1_068510, ACA1_214010 and ACA1_138490 were found to have increased expression levels in G-418 treated, compared to untreated trophozoites while ACA1_053250 and ACA1_103200 were found to be downregulated during treatment with the aminoglycoside (Figure 9.7).

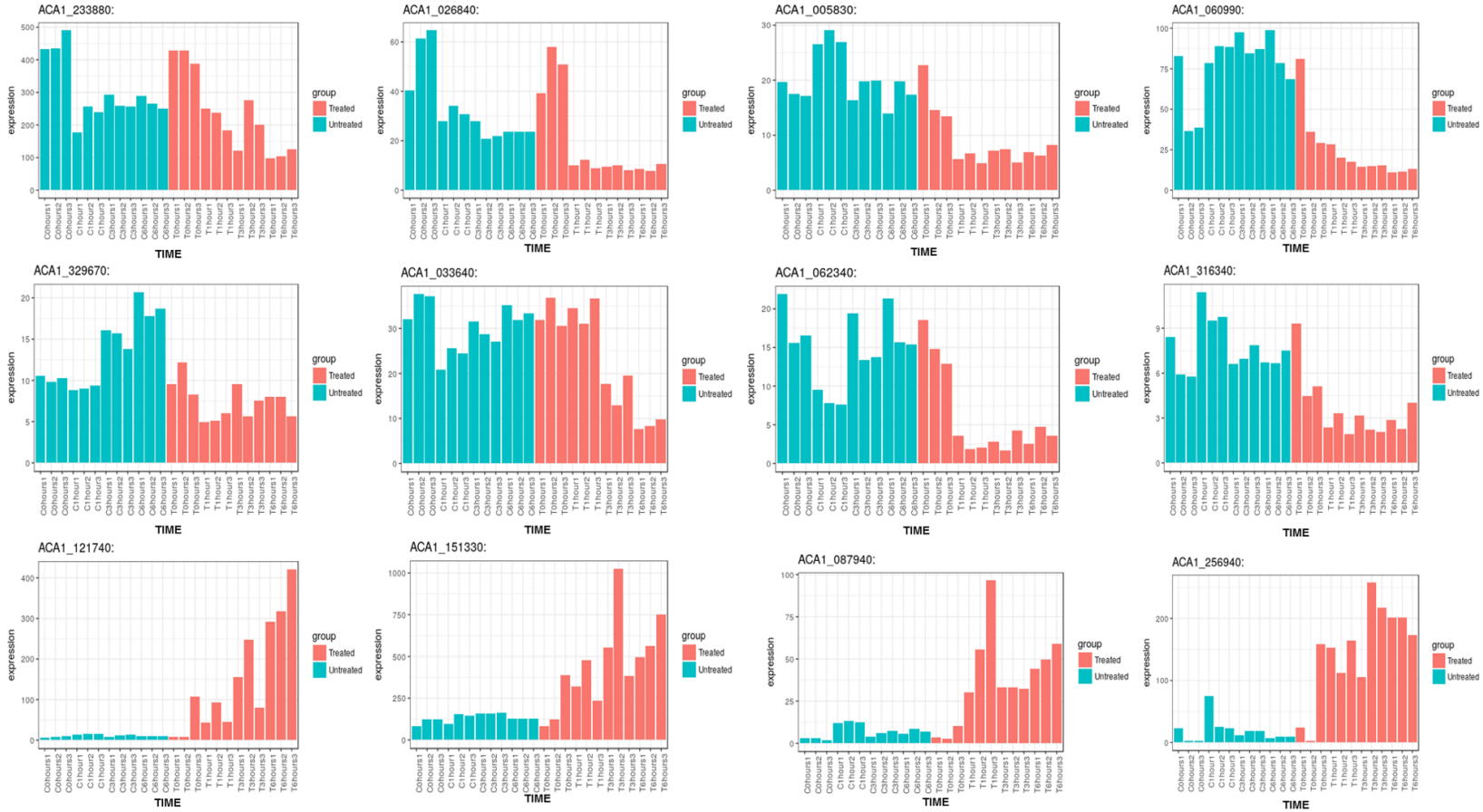

Figure 9.6: Expression profile analysis of *Acanthamoeba* ser/thr protein phosphatases. The diagrams illustrate ser/thr protein phosphatases expression during time, between untreated and G-418 treated trophozoites. Expression is count in CPM. Red colour indicates treated cells, blue untreated.

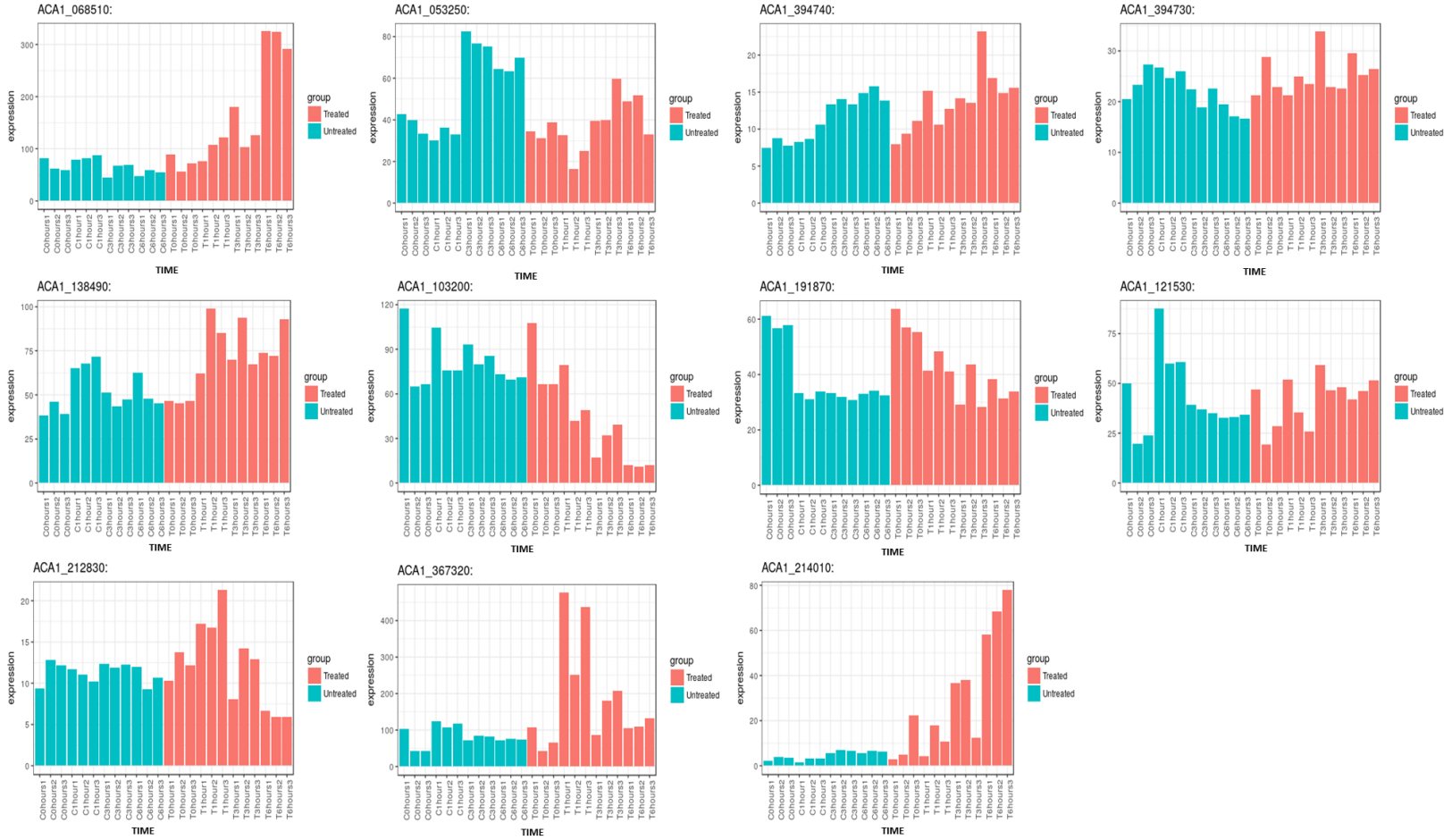

Figure 9.7: Expression profile analysis of *Acanthamoeba* tyrosine protein phosphatases. The diagrams illustrate tyrosine protein phosphatase expression over time, between untreated and G-418 treated trophozoites. Expression is shown in CPM. Red colour indicates treated cells, while blue untreated.

9.2.4 *Acanthamoeba* calmodulin gene expression

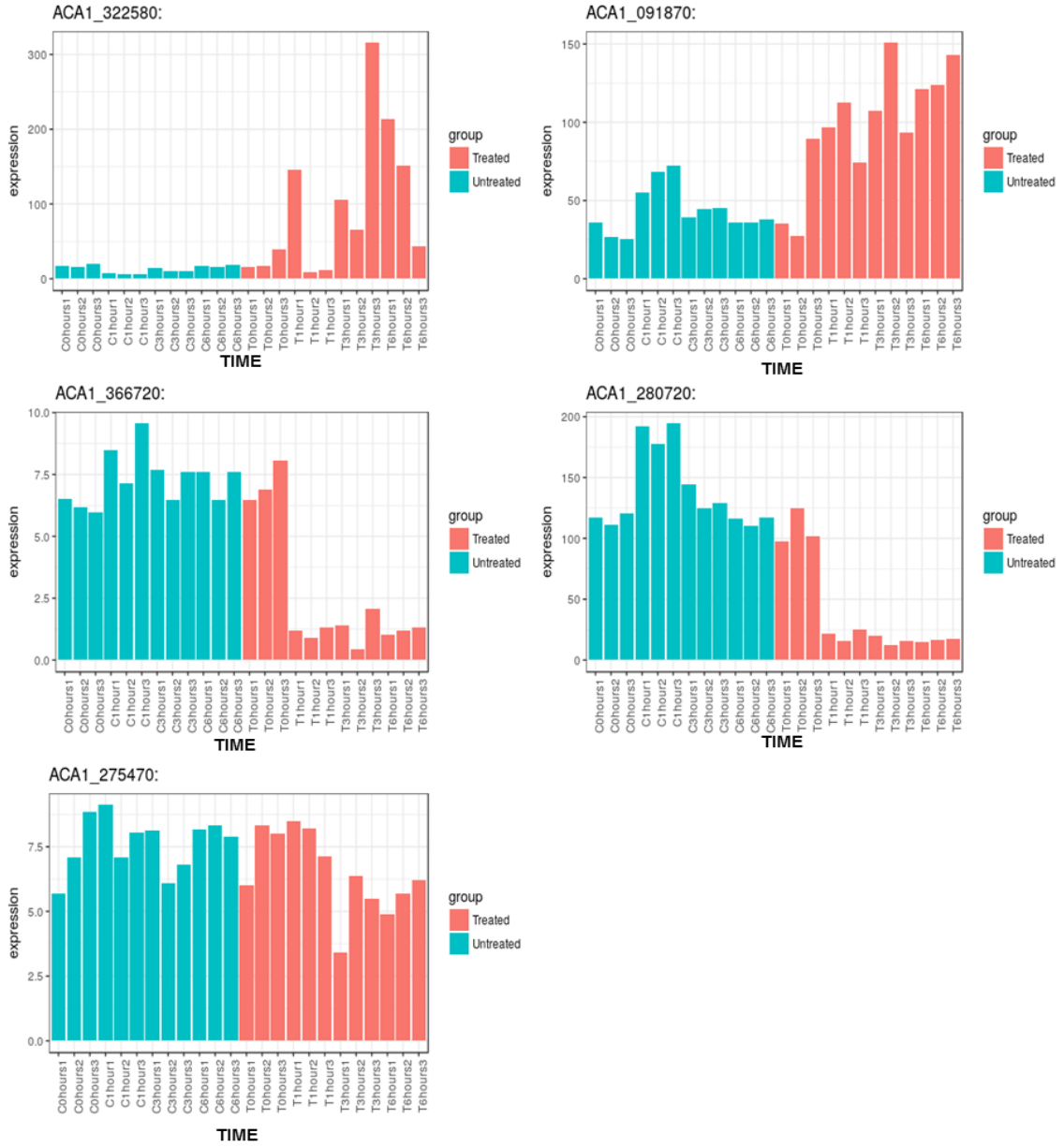

Figure 9.8: Expression profile analysis of *Acanthamoeba* calmodulin proteins. The diagrams illustrate calmodulin proteins expression over time, between untreated and G-418 treated trophozoites. Expression is shown in CPM. Red colour indicates treated cells, blue untreated.

At least 5 different genes were identified as calmodulin proteins based on the amoeba database and their expression profile was examined and analysed. More precisely, two out of five genes including ACA1_322580 and ACA1_091870 were found to be significantly upregulated in G-418 treated *Acanthamoeba* trophozoites during time of incubation (Figure 9.8), two out of five comprising ACA1_280720 and ACA1_366720 were found to be downregulated, compared to control untreated amoebae which showed roughly stable calmodulin expression. Finally, at least one calmodulin gene (ACA1_275740) out of five was found with no significant variation among treated and untreated cells (Figure 9.8).

9.2.5 *Acanthamoeba* endonuclease expression

At least 26 different genes were identified as endonucleases and endonuclease/exonuclease/phosphatase family proteins using the Amoeba database (www.aboebadb.org). RNA seq analysis revealed that the majority of them (15 genes) including ACA1_031650, ACA1_068120, ACA1_012980, ACA1_201500, ACA1_270220, ACA1_364760, ACA1_151290, ACA1_000200, ACA1_369100, ACA1_060660, ACA1_363260, ACA1_088850, ACA1_280690, ACA1_074530 and ACA1_390420 were upregulated in G-418 treated trophozoites compared to untreated amoebae (Figure 9.9a).

Furthermore 10 genes, including ACA1_175470, ACA1_338400, ACA1_083100, ACA1_157850, ACA1_201190, ACA1_383700, ACA1_090080, ACA1_358490 and ACA1_260140, were found to maintain or slightly differentiate their expression profile levels among treated and untreated cells (Figure 9.9b). And finally, only one gene (ACA1_041990) was found to be downregulated in G-418 treated amoebae over time, when compared to control cells (Figure 9.9b).

Figure 9.9a: Expression profile analysis of *Acanthamoeba* endonucleases and endonuclease/exonuclease/phosphatases family proteins. The diagrams illustrate endonucleases family proteins upregulated expression over time, between untreated and G-418 treated trophozoites. Expression is shown in CPM. Red colour indicates treated cells, blue untreated.

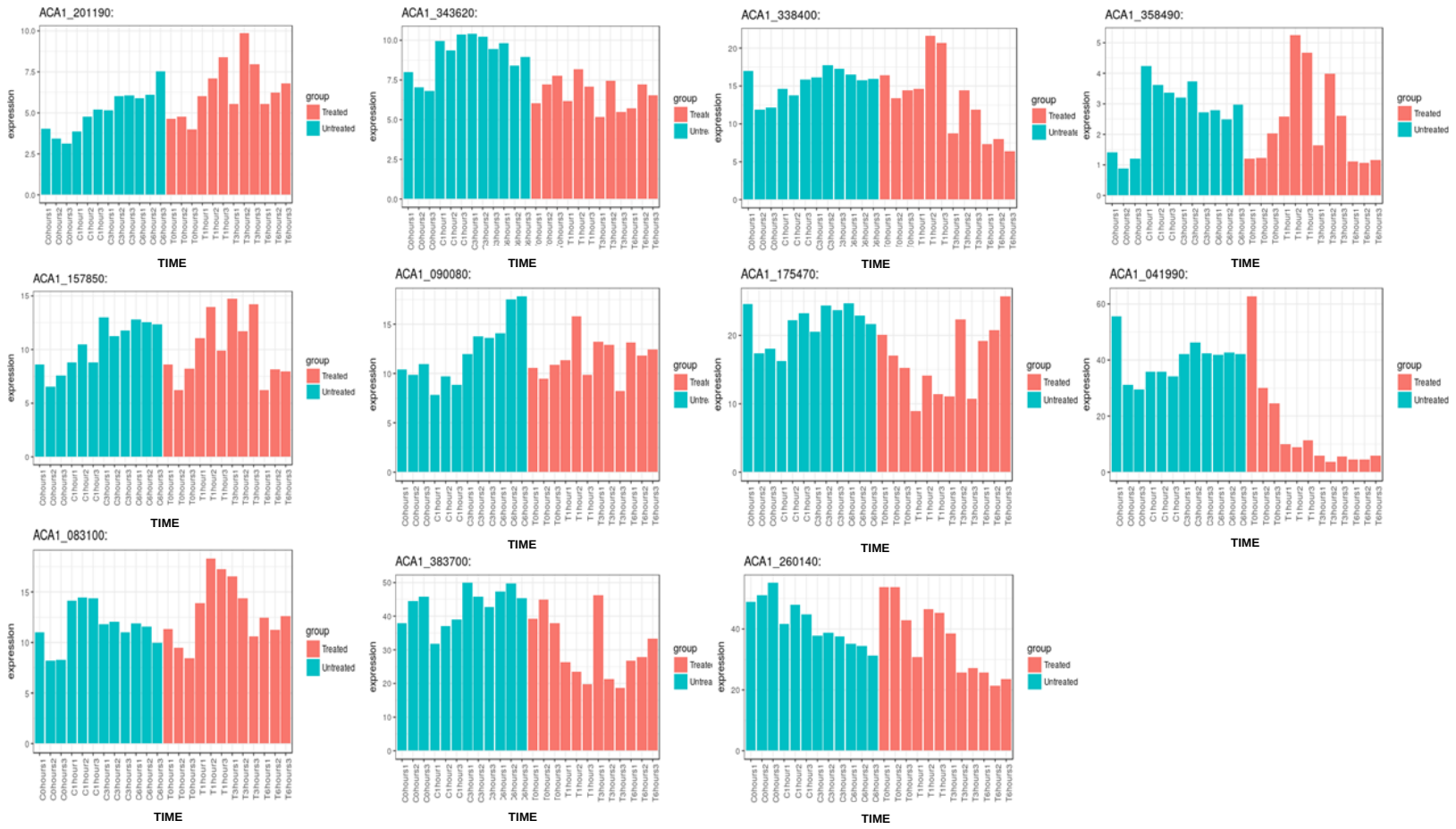

Figure 9.9b: Expression profile analysis of *Acanthamoeba* endonucleases and endonuclease/exonuclease/phosphatases family proteins. The diagrams illustrate endonuclease family proteins with unaltered and downregulated expression over time, between untreated and G-418 treated trophozoites. Expression is shown in CPM. Red colour indicates treated cells, blue untreated.

9.2.6 *Acanthamoeba* deoxyribonuclease expression

Acanthamoeba encodes at least 3 different deoxyribonucleases, including ACA1_041920, ACA1_041940 and ACA1_041950. Interestingly, RNA seq analysis revealed that both ACA1_041920 and ACA1_041940 maintained their expression levels over time among G-418 treated trophozoites and control cells, while at the same time ACA1_041950 showed a significant increase during incubation in G-418 treated cells, ranging from 2- to 3- fold change when compared to control amoebae (Figure 9.10).

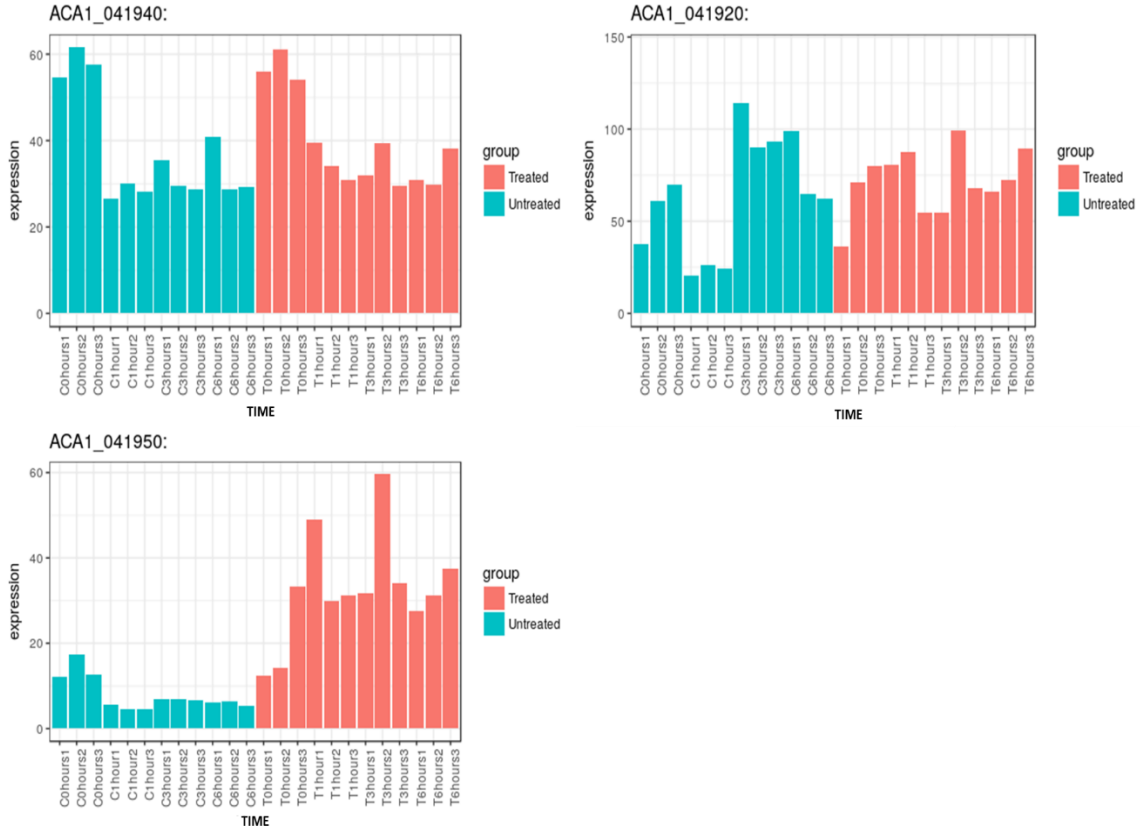

Figure 9.10: Expression profile analysis of *Acanthamoeba* deoxyribonucleases. The diagrams illustrate deoxyribonucleases with unaltered or upregulated expression over time, between untreated and G-418 treated trophozoites. Expression is shown in CPM. Red colour indicates treated cells, blue untreated.

9.2.7 *Acanthamoeba* cysteine proteases

Notably, an important number of cathepsins including ACA1_022730, ACA1_181520, ACA1_317670, papains of the cysteine protease family including ACA1_018960, ACA1_27050, ACA1_066290, ACA1_022680, ACA1_079690, ACA1_322170 and other cysteine proteases comprising ACA1_115390, ACA1_304310, ACA1_155530, ACA1_087440 and ACA1_051490 were found to be upregulated during treatment with G-418 (Figure 9.11).

Simultaneously, a small proportion of cysteine proteases were found to be downregulated with time in treated amoebae including ACA1_093370, ACA1_322370, ACA1_244230 (cathepsins); ACA1_159080, ACA1_198340 (papain-like proteases); ACA1_296310 and ACA1_277940 (other cysteine proteases).

9.2.8 *Acanthamoeba* serine proteases

At least 6 diferent serine proteases including ACA1_321400, ACA1_061760, ACA1_128830, ACA1_273880, ACA1_277790 and ACA1_155550 were identified in amoebadb and their expression profile was analyzed. Interestingly two out of six proteases, including ACA1_321400 and ACA1_128830, which have been also described as encystation-mediating enzymes (Moon et al., 2012), have been found to be upregulated up to two or three times in G-418 treated amoebae whereas their exression in untreated cells remained low and stable (Figure 9.12). Conversely, ACA1_061760, ACA1_155550 and ACA1_2777790 were found to be downregulated up to two or three times in G-418 treated *Acanthamoeba* over time, while their expression in healthly trophozoites remained stable and at a high level. ACA1_273880 did not show any difference in its expression levels during treatment between treated and untreated amoebae (Figure 9.12).

Figure 9.11: Expression profile analysis of *Acanthamoeba* cysteine proteases. The diagrams illustrate cathepsins, papains and other cysteine proteases found to be upregulated over time, between untreated and G-418 treated trophozoites. Expression is shown in CPM. Red colour indicates treated cells, while blue untreated.

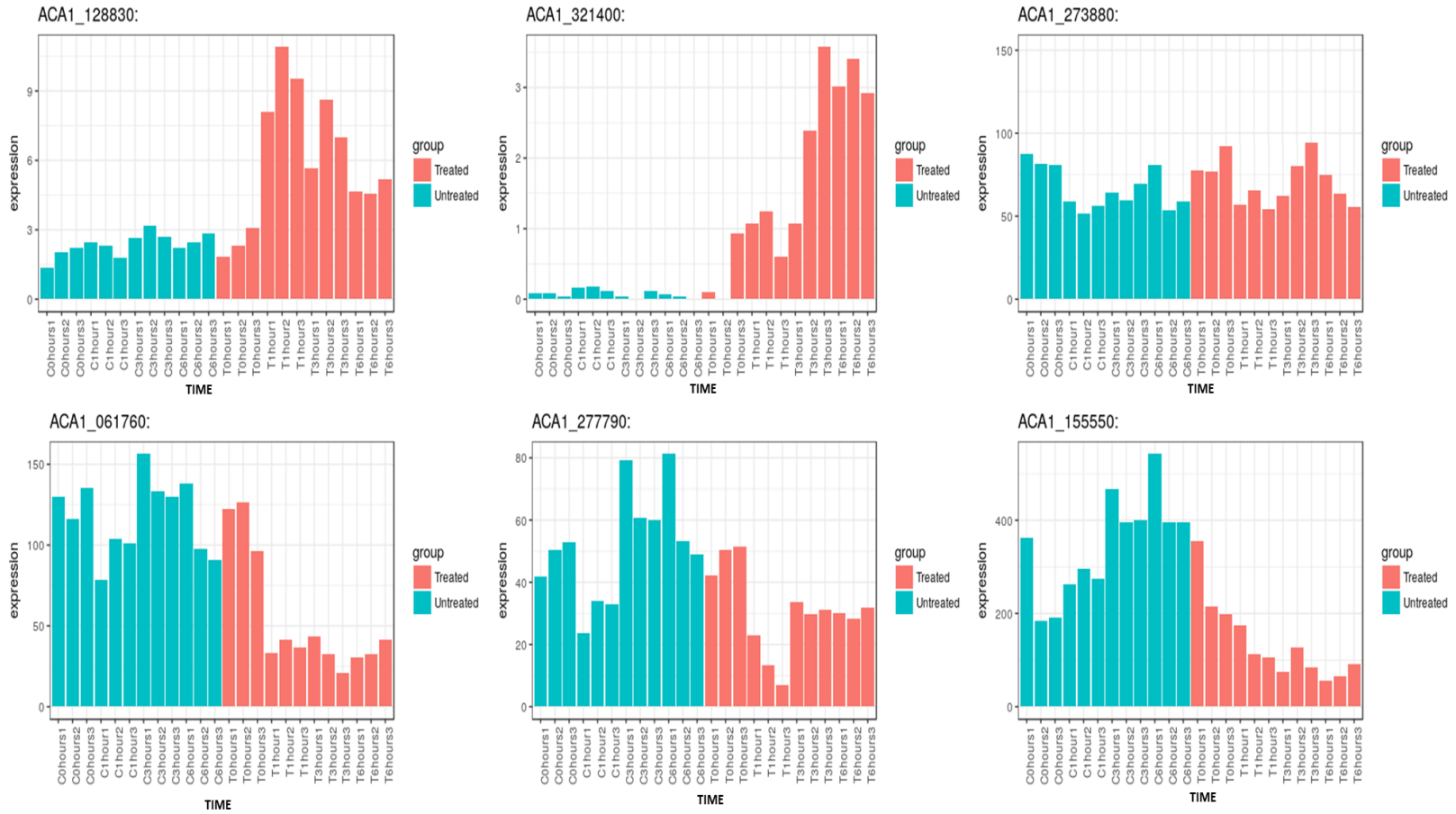

Figure 9.12: Expression profile analysis of *Acanthamoeba* serine proteases. The diagrams illustrate serine proteases found to be differentially expressed over time, between untreated and G-418 treated trophozoites. Expression is shown in CPM. Red colour indicates treated cells, blue untreated.

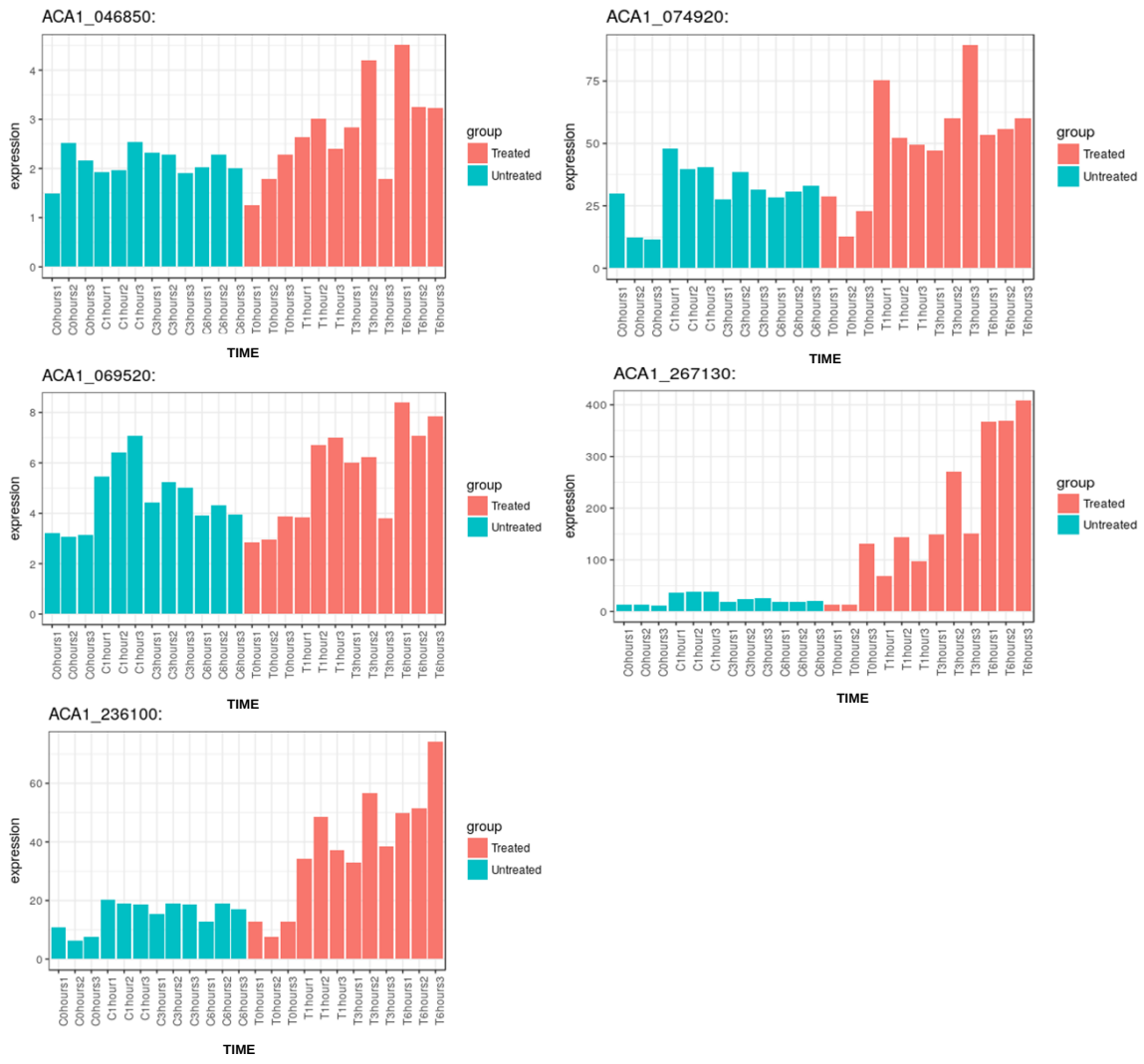

Figure 9.13: Expression profile analysis of *Acanthamoeba* ubiquitin proteases. The diagrams show ubiquitin proteases found to be significantly upregulated during time, between untreated and G-418 treated trophozoites. Expression is shown in CPM. Red colour indicates treated cells, blue untreated.

9.2.9 *Acanthamoeba* Ras family gene expression

In total, 104 Ras family genes were examined during incubation with G-418 in treated and untreated *Acanthamoeba* trophozoites as previous analysis has shown a close involvement of Ras signalling in the process. More than 50% (57 genes) of the Ras related genes were found to be significantly upregulated in treated amoebae whereas in many cases, including ACA1_143990, ACA1_256400 and ACA1_070190, their expression was not even detectable in control trophozoites (Figure: 9.14). The highest differential expression was detected in genes comprising ACA1_075010, ACA1_256400, ACA1_382920 and ACA1_089990.

Conversely, only 14 Ras related genes were found to be slightly downregulated in G-418 treated trophozoites including ACA1_326130, ACA1_036440, ACA1_360180, ACA1_227760, ACA1_286140, ACA1_054110, ACA1_20130, ACA1_057550, ACA1_090060, ACA1_090100, ACA1_21240, ACA1_164860, ACA1_365410 and ACA1_399850. Finally after analysis, 33 Ras family genes, were found to have no significant variation in their expression levels between treated and untreated *Acanthamoeba* trophozoites.

9.2.10 *Acanthamoeba* autophagy regulator gene expression

At least 17 different genes were identified as autophagy-related genes using the amoeba database (http://amoebadb.org/amoeba/) and their expression analysis was analysed and further biologically evaluated. Interestingly, a plethora of autophagy related genes including ACA1_181960, ACA1_322340, ACA1_051880 (ATG8), ACA1_140190 (ATG4), ACA1_292820, ACA1_331710 (ATG27), ACA1_200420 (ATG27) and ACA1_382080 (ATG12) showed an increase in their expression levels while at the same time, ACA1_163910, ACA1_142580, ACA1_055340 (ATG2) and ACA1_040500 (ATG16) were found to be downregulated in treated amoebae, compared to untreated *Acanthamoeba* trophozoites (Figure 9.15).

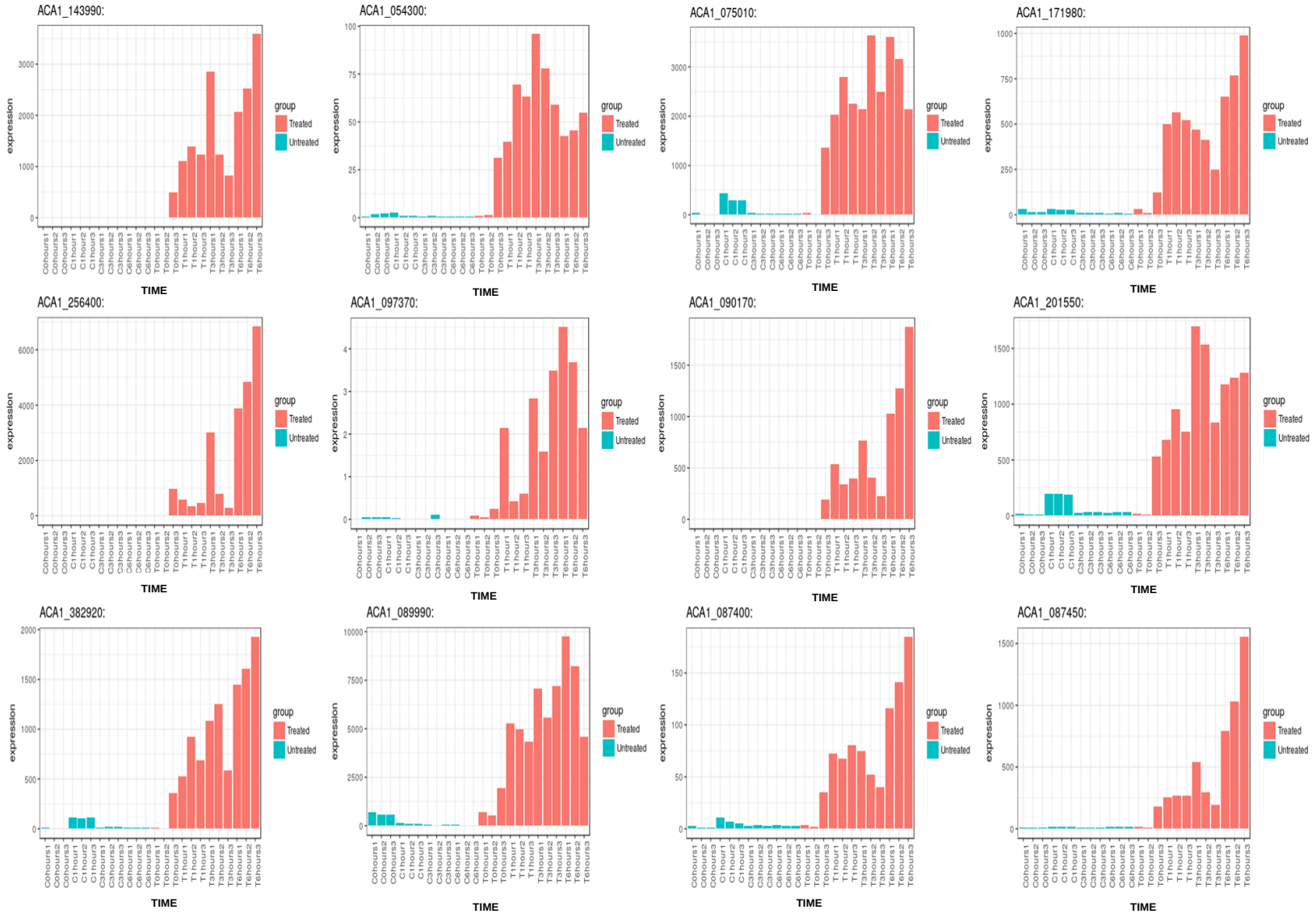
ACA1_143990:
ACA1_054300:
ACA1_075010:
ACA1_171980:
ACA1_256400:
ACA1_097370:
ACA1_090170:
ACA1_201550:
ACA1_382920:
ACA1_089990:
ACA1_087400:
ACA1_087450:
expression
TIME
group
Treated
Untreated

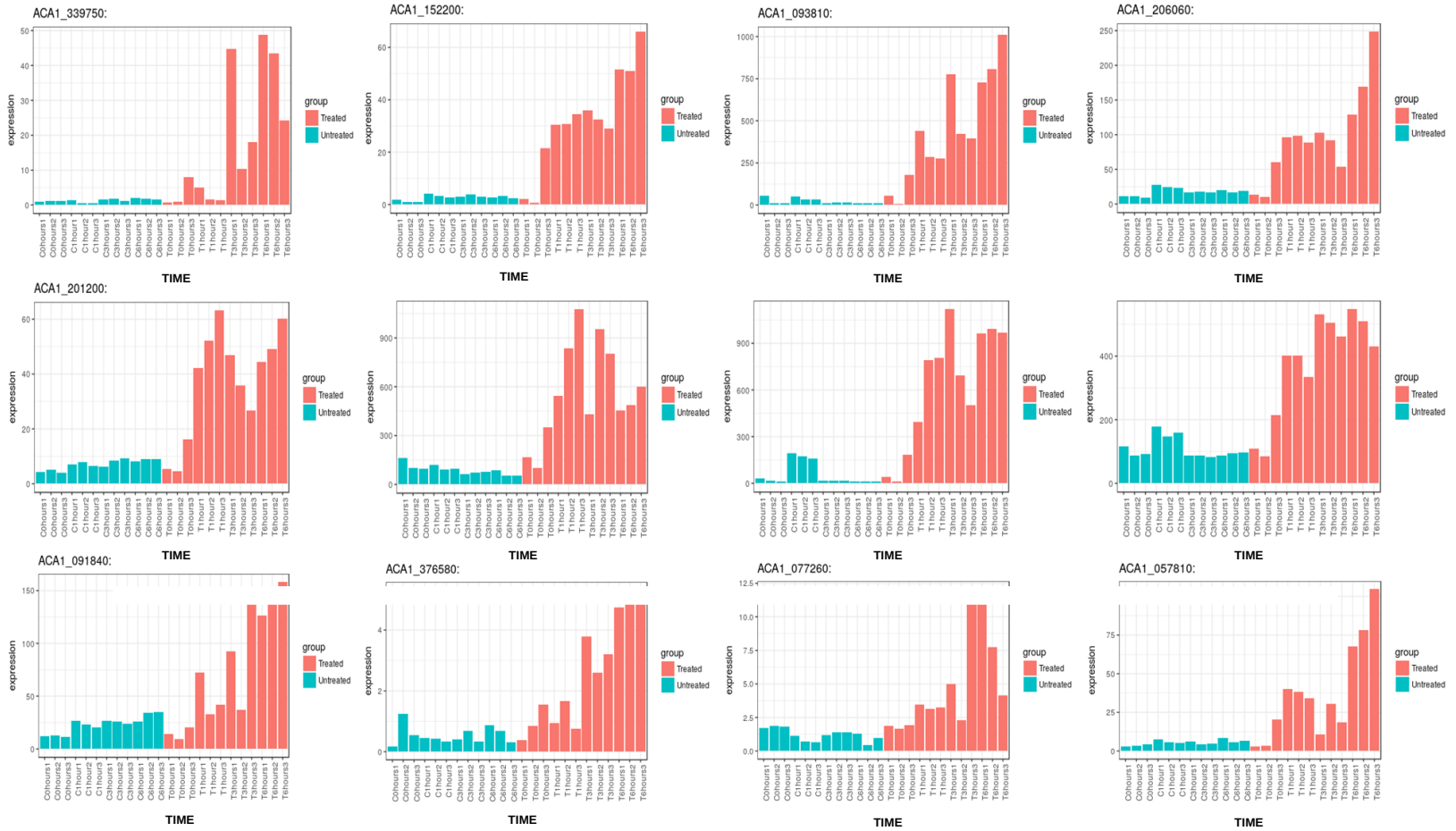

Figure 9.14: Expression profile analysis of *Acanthamoeba* Ras family genes. The diagrams illustrate representative Ras family genes, found to be significantly upregulated over time, between untreated and G-418 treated *Acanthamoeba* trophozoites. Expression is shown in CPM. Red colour indicates treated cells, blue untreated.

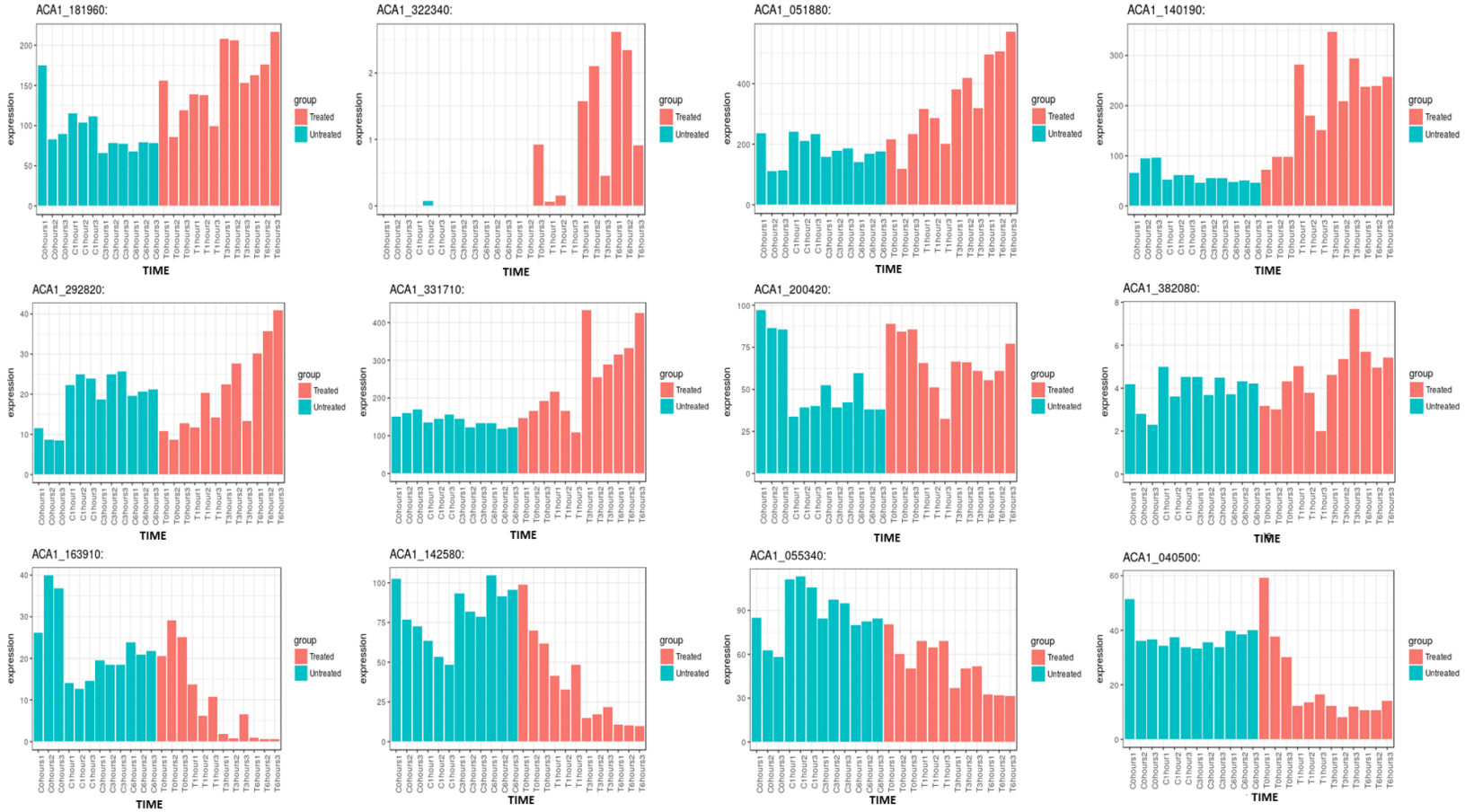

Figure 9.15: Expression profile analysis of *Acanthamoeba* autophagy regulator genes. The diagrams illustrate representative autophagy regulator genes including ATG 2, ATG 4, ATG 8, ATG 9, ATG 12, ATG16 and ATG 27, found to be differentially expressed over time, between untreated and G-418 treated trophozoites. Expression is shown in CPM. Red colour indicates treated cells, blue untreated.

9.2.11 *Acanthamoeba* ubiquitin-related gene expression

Ubiquitination is a complex intracellular process that involves a plethora of proteins including ubiquitin fusion enzymes, ubiquitin activation enzymes, ubiquitin conjugating enzymes, many ubiquitin ligases, ubiquitin-specific proteases, proteasome proteins and ubiquitin hydrolases. During the analysis, more than 90 genes related to ubiquitination according to the amoebae database were analysed and their profile analysis was analysed biologically.

More precisely, the majority of genes related to ubiquitination steps, including activation, conjugation and ligation, performed by ubiquitin-activating enzymes (E1s), ubiquitin-conjugating enzymes (E2s) and ubiquitin ligases (E3s), were found to be upregulated, comprising ACA1_068730, ACA1_043250, ACA1_155480, ACA1_072330, ACA1_261410 related to ubiquitin-activating enzymes and ACA1_065120, ACA1_128500, ACA1_187890, ACA1_052770, ACA1_112540, ACA1_276870, ACA1_ 217720, ACA1_390500 related to ubiquitin-conjugating enzymes and finally ACA1_129500, ACA1_065270, ACA1_110430 and ACA1_ 174250 related to E3 ubiquitin related ligases. Additionally, at least 7 proteins with characteristic Ubox domain were also found to be upregulated including ACA1_058270, ACA1_289330, ACA1_210680, ACA1_261610, ACA1_088750, ACA1_063500 and ACA1_ 088750 (Figure 9.16).

Genes related to ubiquitin-specific proteases, including ACA1_236100, ACA1_074920, ACA1_267130 and ACA1_069520 and ubiquitin hydrolase genes including ACA1_291510, ACA1_178540, ACA1_371700, ACA1_378160, ACA1_169550, ACA1_072350 and ACA1_038220 were found to be significantly upregulated in G-418 treated *Acanthamoeba* trophozoites compared to untreated cells, where their expression showed minor and insignificant variations. Finally, all genes related to proteasomes by reference to the amoeba database, including ACA1_291470, ACA1_170940, ACA1_159830, ACA1_194920, ACA1_264010, ACA1_128490, ACA1_291480, ACA1_177560, ACA1_260270, ACA1_389440 and ACA1_069610, were found to be downregulated in G-418 treated *Acanthamoeba* trophozoites (Figure 9.17).

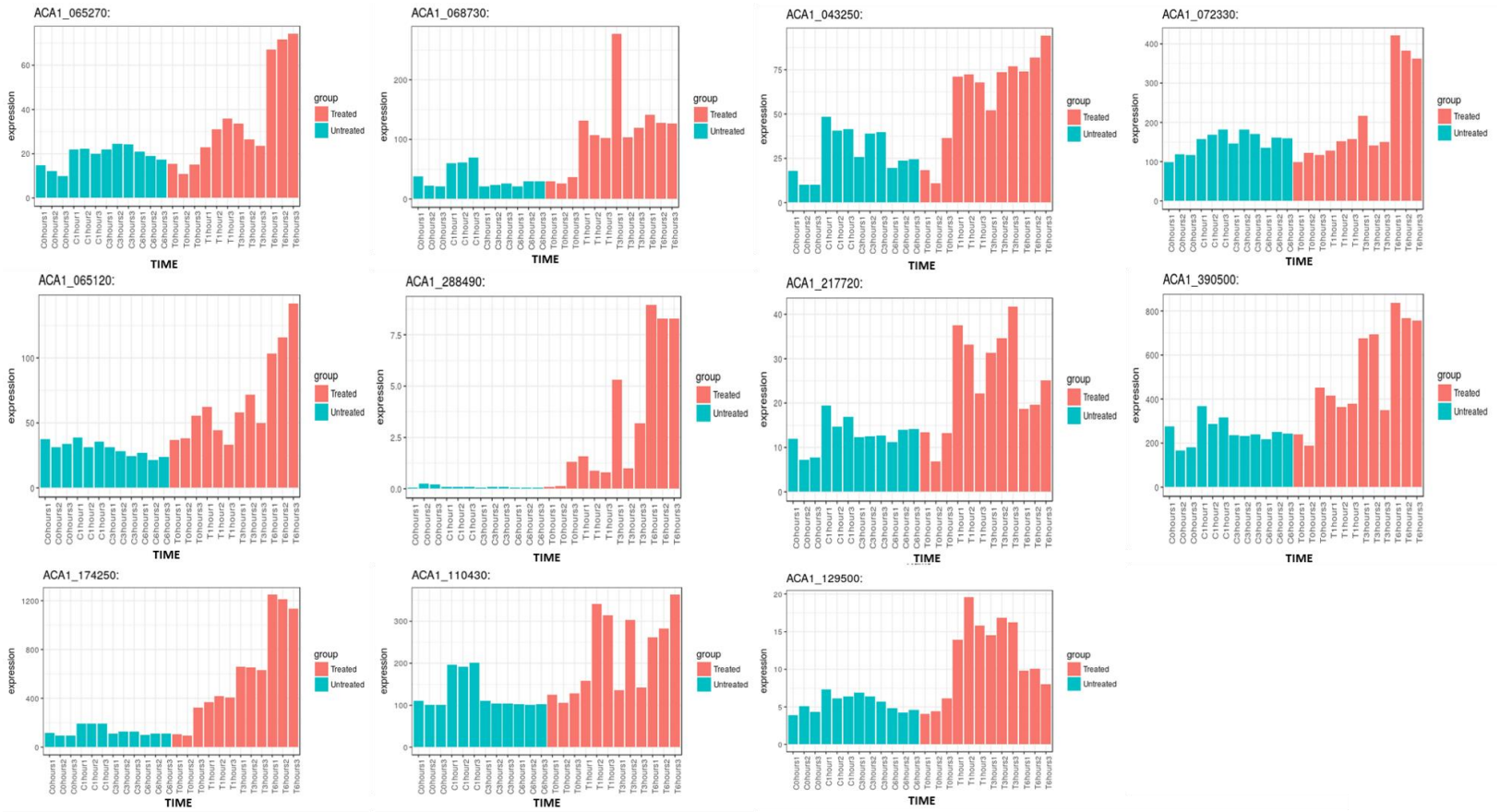

Figure 9.16: Expression profile analysis of *Acanthamoeba* ubiquitination related genes. The diagrams illustrate representative ubiquitin fusion enzymes and ubiquitin activation enzymes in the first row, ubiquitin conjugating enzymes in the second row and ubiquitin E3 ligases in the third, which were found to be differentially expressed and precisely upregulated over time, between untreated and G-418 treated trophozoites. Expression is shown in CPM. Red colour indicates treated cells, blue untreated.

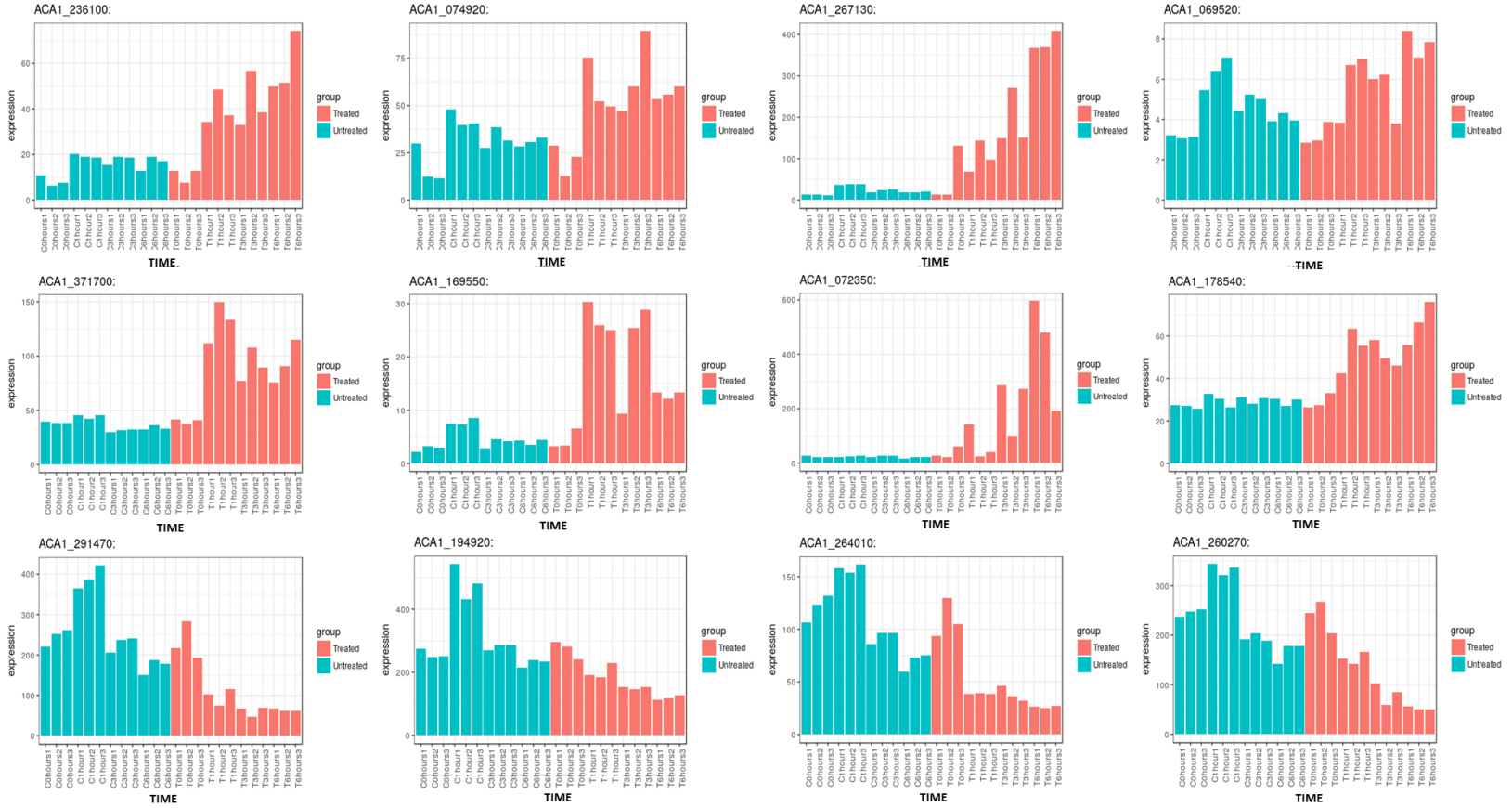

Figure 9.17: Expression profile analysis of *Acanthamoeba* ubiquitination proteasome-related genes. The diagrams illustrate representative ubiquitin proteases enzymes in the first row, ubiquitin hydrolases enzymes in the second row and proteasome related proteins in the third, found to be differentially expressed over time, between untreated and G-418 treated trophozoites. Expression is shown in CPM. Red colour indicates treated cells, blue untreated.

9.2.12 *Acanthamoeba* glutathione S-transferase gene expression

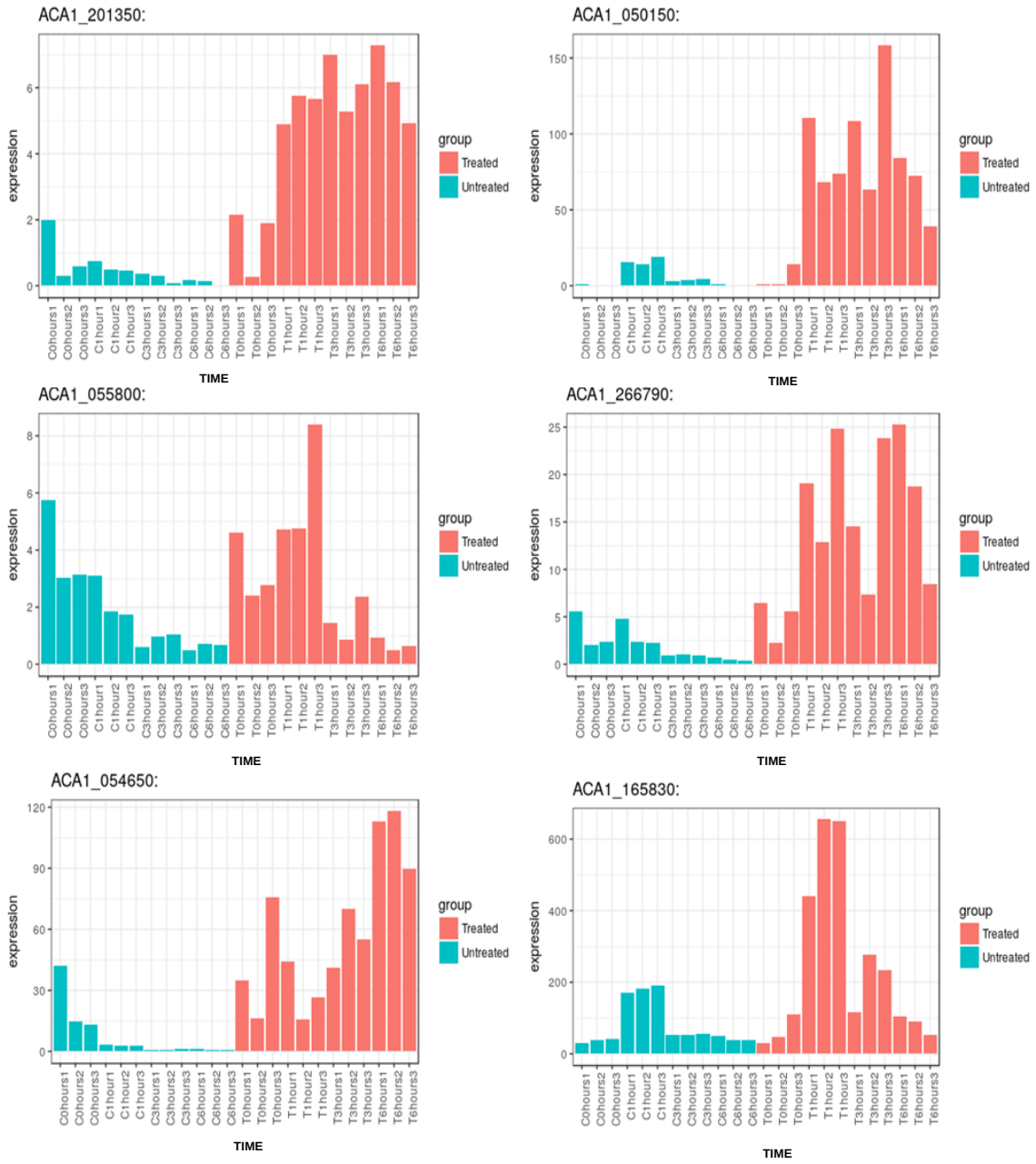

Figure 9.18: Expression profile analysis of *Acanthamoeba* glutathione S-transferase genes. The diagrams illustrate representative glutathione S-transferase genes found to

be differentially expressed over time, between untreated and G-418 treated trophozoites. Expression is shown in CPM. Red colour indicates treated cells, blue untreated.

Interestingly, all glutathione transferase genes, including ACA1_201350, ACA1_054650, ACA1_055800, ACA1_266790, ACA1_201350 and ACA1_050150, showed a remarkable increase in their expression levels during treatment with G-418, whereas at the same time, the expression levels in control *Acanthamoeba* trophozoites followed a decreasing trend (Figure 9.18).

9.2.13 *Acanthamoeba* cyst-specific gene expression

Overall, 6 genes related to *Acanthamoeba* encystation, namely ACA1_075240, ACA1_050400, ACA1_327930, ACA1_096350, ACA1_075210 and ACA1_399800, were identified and their expression profiles were analysed (Figure 9.19). More precisely genes ACA1_07510, ACA1_050400, ACA1_327930 and ACA1_075240 were found to be significantly upregulated during treatment with G-418 aminoglycoside, while at the same time their expression levels in control cells remained unchanged. ACA1_096350 showed a declining trend in both populations, although in G-418 treated cells there was a more prominent decrease compared to control amoebae. Finally, ACA1_399800 showed gradually rising expression in control trophozoites during incubation, whereas its expression in G-418 treated cells was significantly lower (Figure 9.19).

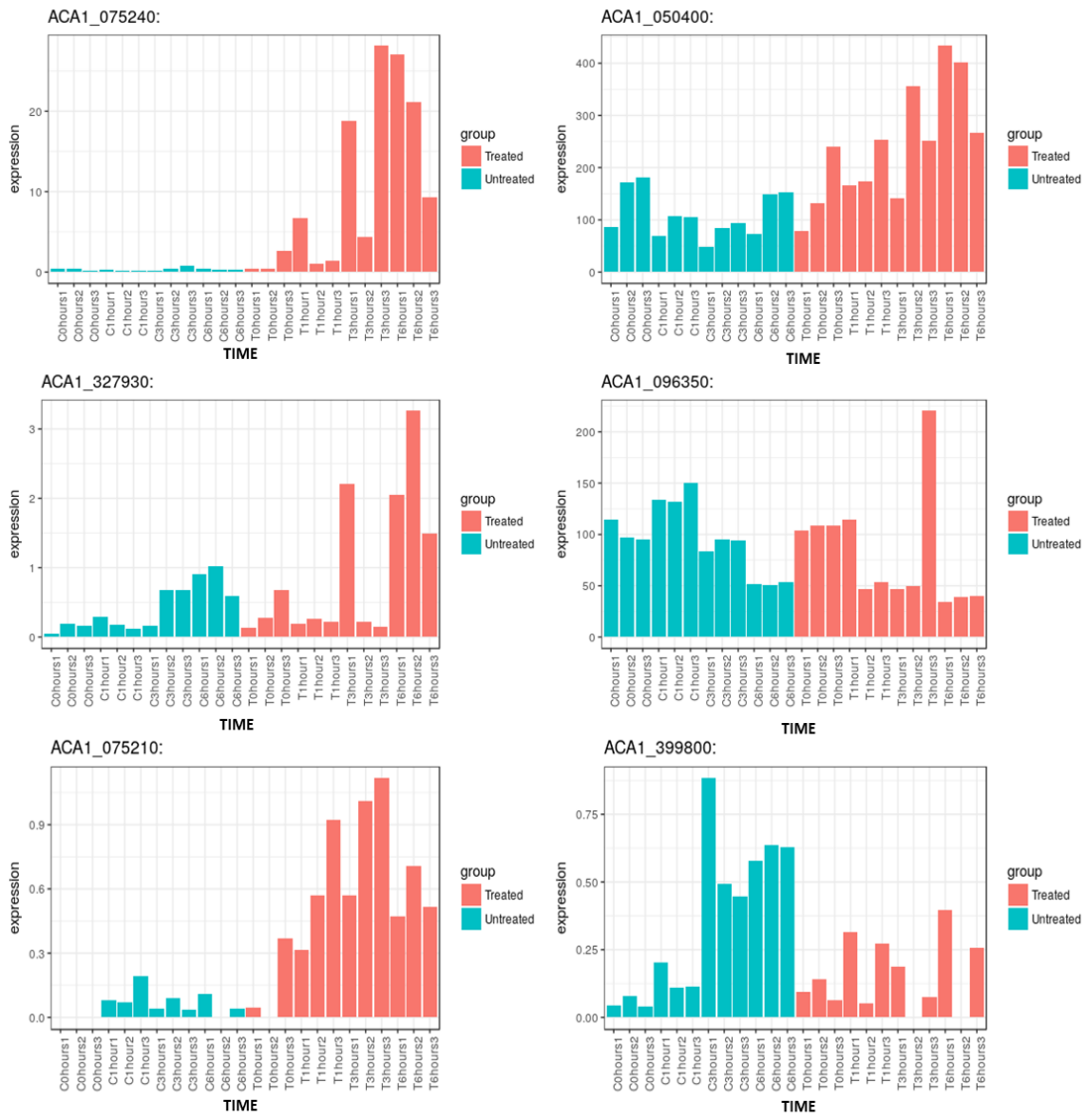

Figure 9.19: Expression profile analysis of *Acanthamoeba* cyst-specific genes. The diagrams illustrate representative cyst-specific genes found to be differentially expressed over time, between untreated and G-418 treated trophozoites. Expression is shown in CPM. Red colour indicates treated cells, blue untreated.

9.3 Discussion

In this chapter, the transcriptomic levels and the relative biological abundance of differentially expressed genes including MAPKs, phosphatases, various endonucleases, multiple proteases, autophagy-related genes and Ras family genes, which have all been previously associated with apoptotic processes by numerous studies in various systems and organisms, were analysed in depth. The analysis revealed a close relationship among many categories of the previous family genes suggesting their potential regulatory role in *Acanthamoeba* in G-418 mediated cell death.

Phosphorylation is a transient and reversible protein alteration used to regulate protein function. Two major categories of enzyme, protein kinases and protein phosphatases, play essential roles in protein phosphorylation regulation and are accordingly associated with a wide array of intracellular events, including cell survival and cell death. Phosphorylation also determines protein localization, enzymatic activities and protein stability and is thus considered an important regulator of cell death (Niemi and MacKeigan, 2013).

Mitogen-activated protein kinases are ser/thr protein kinases, classified in three different subcategories comprising extracellular signal response kinase 1/2, c-Jun NH_2-terminal kinase and finally p38. MAPKs are considered to be important regulators of evolutionarily conserved signalling pathways that play crucial regulatory roles in a plethora of cell biology and physiology aspects (Liu and Lin, 2005). ERKs have been initially associated with cell survival whereas, p38-MAPKs and JNKs were thought to be stress-responsive and thus involved in regulated cell death (Wada and Penninger, 2004). Furthermore, JNK and ERK hyper activation have been also proposed to trigger apoptosis and other forms of programmed cell death after many stimuli, including UV and gamma-irradiation, toxins, peroxide and pharmaceutical substances (Cangol and Chambar, 2010; Westwick et al., 1995; Chen et al., 1996).

The regulation of cell death pathways by MAPKs, however, is more complex than originally thought and often fairly debateable. Analysis of *Acanthamoeba's* ser/thr kinases

including MAPKs revealed a significant increase in their expression levels in G-418 treated trophozoites, which was observed at least one hour after G-418 treatment. At the same time, MAPK expression did not show any significant alteration in control amoebae. This finding is striking and could suggest that aminoglycoside pharmacological treatment is manipulative of MAPKs activity, which in turn could be used to sensitize trophozoites to imminent cell death. Furthermore, mitogen-activated protein kinase overexpression implies their significant role in the regulation of signalling transduction pathways, presumably by controlling cytoplasmic and nuclear events described earlier in G-418 mediated cell death.

Mitogen-activated protein kinase kinase kinase (MAP3K) is a ser/thr kinase that controls protein kinase pathways comprising stress-activated protein kinases (SAPK) and mitogen-activated protein kinases. MAP3K (ACA1_333310) is found to be significantly upregulated after 1hour of G-418 treatment and is reported to be activated in response to growth factor stimulation and by extended expression of activated Ras (Russel et al., 1995), which could stimulate MAP2K4/7-JNK or MAP2K1/2-ERK1/2 signalling pathways (Xia et al., 2000; Rosen et al., 1994), based on cell type and stimulus. In this case, it was already shown increased Ras levels that could have led into MAP3K overexpression and overactivation. For instance, after an apoptotic stimulus, MAP3K is reported to be cleaved in order to generate a soluble C-terminal catalytic fragment, which in turn contains the kinase domain and exhibits selectivity towards JNK activation (Schlesinger et al., 2002; Minden et al., 1994).

In this case, presumably, G-418 *Acanthamoeba* MAP3K overexpression could have led to cell death induction, either by increased MAP3K soluble C-terminal cytosolic fragments with characteristic kinase activity that induces apoptotic cell death, or by subsequent activation of the apoptotic JNK signalling pathway (Figure 9.13). Activation of the JNK signalling pathway could have initially mediated upregulation of *Acanthamoeba* pro-apoptotic genes either through transactivation of specific transcription factors or secondarily by regulating, through distinct phosphorylation events, the activities of the trophozoite mitochondrial anti- and pro-apoptotic proteins (Dhanasekaran and Reddy, 2008). However, these scenarios, likely as they may be, need to be further and more deeply evaluated by experimental procedures in order for

their participation in *Acanthamoeba* programmed cell death to be identified and thoroughly described.

Other important proteins of which the expression was found to be significantly upregulated in G-418 treated *Acanthamoeba* cells were the glutathione S–transferases (GSTs). GSTs are involved in cellular glutathiolation of a variety of endogenous and xenobiotic compounds by catalysing their conjugation with reduced glutathione (Turella et al., 2005). Their expression has been associated with cell proliferation, regulation and apoptosis by direct interaction with the c-jun N-terminal kinase (Holley et al., 2007). For instance, suppression of the glutathione S–transferase P1 gene leads to increased JNK activity, increased proliferation and reduced apoptosis in mouse embryonic fibroblasts (Ruscoe et al., 2001). Furthermore, under physiological conditions, glutathione S–transferase P1 monomer has been reported to inhibit JNK signalling by creating a glutathione S–transferases P1-JNK protein scaffold (Adler et al., 1999), while at the same time, under stress stimuli, glutathione S–transferase P1 dissociates from JNK and composes inactive dimers, allowing JNK downstream signalling (Holley et al., 2007).

Glutathione S–transferase expression levels were found to be significantly upregulated in G-418 treated trophozoites, which is indicative of their role in *Acanthamoeba* programmed cell death. Protein modulation by S-glutathiolation might inhibit activation of survival signals and therefore contribute to cell death induction (Circu et al., 2012). Furtermore, overexpression might leads to GST dimerization or polymerization and their subsequent dislocation from JNK kinases, which subsequently allow sustained JNK pathway hyperactivation and consequent cell death induction (Lu et al., 2007). However, GSTs have mostly been described as anti-apoptotic regulators of the JNK pathway and in this case, overexpression might represent the cell's desperate effort to avoid the apoptotic outcome of the JNK signalling pathway.

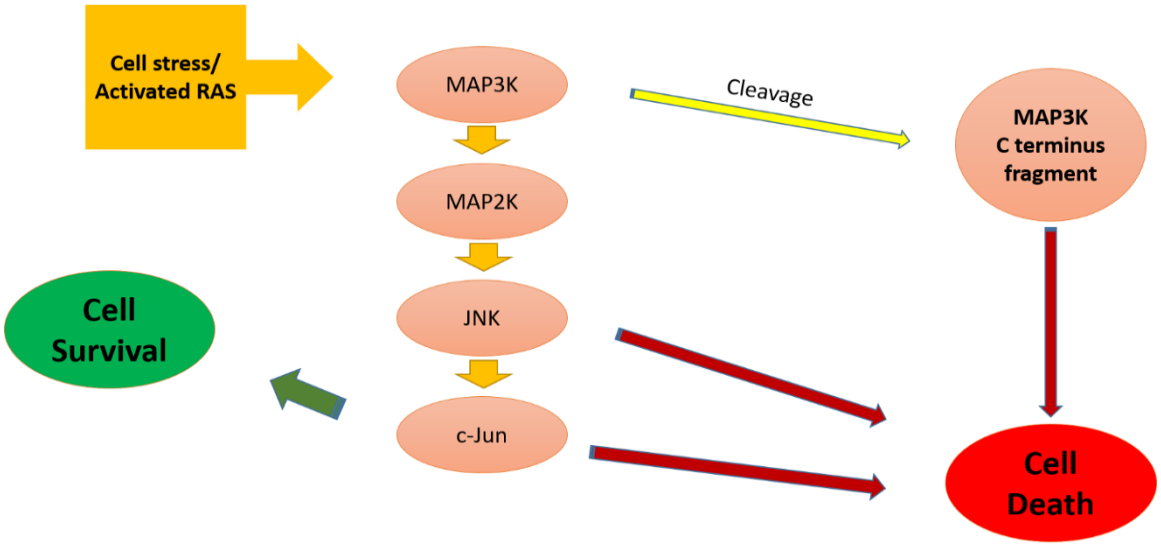

Figure 9.20: Representative downstream apoptotic MAPKs/JNK signalling pathway.

Extended Ras signalling was one the first characteristics that RNA-seq analysis revealed in G-418 treated trophozoites, as numerous genes related to Ras subfamily genes were found to be among the most differentially expressed genes in the two amoebae populations. Further and deeper analysis revealed that even more Ras subfamily genes were found to be significantly upregulated in G-418 treated *Acanthamoeba.* Furthermore, experiments using lovastatin as a Ras farnesylation inhibitor, in combination with G-418, revealed a delay in cell death expansion in *Acanthamoeba* trophozoites, suggesting that Ras signalling might accelerate the pathogen's programmed cell death development. Ras signalling pathways have already been reported to be involved in PCD in unicellular organisms including *Candida albicans* (Phillips et al., 2006).

A possible explanation for the observed extended Ras hyperexpression in G-418 treated *Acanthamoeba* trophozoites might be the after-effect of a prolonged increase in intracellular calcium (Rosen et al., 1994; Cullen and Lockyer, 2002; Yoshiki et al., 2010) which has already been detected. Furthermore, extended Ras expression might have led

to subsequent MAPK overexpression and MAPK downstream signalling overactivation as previously described, with a definitive purpose of cell death induction.

Contrary to the finding of ser/thr kinase overexpression, tyrosine protein kinases did not show any significant alteration in their expression profile levels between treated and untreated amoebae and subsequently their regulatory ability or association in G-418 mediated *Acanthamoeba* cell death. Generally, there is very little evidence of tyrosine phosphorylation reported in cell death regulation, as tyrosine kinases have been more closely related to cell cycle regulation including mitosis and proliferation (Howard et al., 2003).

Serine-threonine phosphatase family proteins are highly conserved and ubiquitously expressed among species and are involved in the regulation of several cellular functions, by dephosphorylation of signalling molecules initially initiated by protein kinases. Biological activities of phosphatases have been associated with cell cycle control, signal transduction, DNA replication, transcription and cell death (Bononi et al., 2004). More precisely, phosphatases have been linked to the regulation of the mitochondrial Bcl-2 proteins which are vastly responsible for the activation or the inhibition of the intrinsic apoptosis pathway (Ruvolo et al., 1999). The phosphatases' pro-apoptotic function is mediated by direct dephosphorylation of specific proteins such as anti-apoptotic Bcl-2 and pro apoptotic factor Bad (Bononi et al., 2004). Additionally, phosphatases are able to dephosphorylate and deactivate MEK1 and ERK-family kinases and hence to block mitogenic and survival signals (Aggarwal et al., 2011).

Analysis of *Acanthamoeba's* phosphatases expression revealed a downward motif in G-418 treated trophozoites (Figure 9.7). Initially, as was expected in control amoebae, phosphatases maintained their physiological levels of expression whereas in G-418 treated trophozoites the majority of phosphatase genes were found to be downregulated or to maintain their expression levels, while only 9 genes where found to be upregulated. A parallel trend was also observed in tyrosine phosphatases expression, where only 2 genes where found to be significantly upregulated during treatment with the aminoglycoside. Increased levels of individual PTPs could betray their specific role in the microorganisms "apoptotic" signal transduction, although substrates and signalling

pathways remain largely unknown. Distinct tyrosine phosphatases were suggested to either increase or decrease a plethora of cell survival stimuli, eventually favouring either cell survival or cell death respectively (Hale et al., 2007). Although regulation of particular signalling proteins and pathways including MAPKs, or PI3K is usually mediated by various phosphatases rather than a particular PTP enzyme (Hale et al., 2007).

Taking the majority of the data into consideration, it could be generally assumed that during G-418 cell death, phosphorylation is a more favoured process and prevails over dephosphorylation as means of signal transduction. However, the action of phosphatases should not be considered less important, as they may interact concertedly and collaboratively with protein kinases. Unfortunately, the genome of *Acanthamoeba* is not yet fully annotated and characterized in order to allow a deeper gene-specific analysis. Additionally, a more profound analysis would also clearly reveal the potential protein substrates of the overexpressed kinases and phosphatases, to subsequently allow a more comprehensive design of a new cell death signalling pathway, or identify an already described one.

The proteolytic intracellular machinery comprises several proteases localized in different cell compartments in order to maintain essential cellular procedures and to eliminate denatured or misfolded proteins. Other protein proteases, discrete from caspases, have been proposed to be associated with regulated cell death procedures and apoptosis. These proteins include granzymes A and B, calpains, lysosomal and granular proteases, papain-like proteases, cathepsins and serine proteases (Turk et al., 2000; Johnson, 2000; Wang, 2000; Leist and Jäätelä, 2001b; Bursch, 2001; Suzuki et al., 2001; Van Loo et al., 2002). It has also been proposed that cytoplasmic overexpression of numerous proteases, comprising those that are theoretically unlikely to be associated with cell death, could mediate apoptosis and other forms of regulated cell death (Williams and Henkart, 1994). Overall, proteases seem to play an important role in programmed cell death completion, although their role in the phenomenon's regulation has not yet been clarified in terms of defined molecular pathways.

In this study a surprisingly high number of endogenous proteases, including cathepsins and papain proteases, were found to be significantly upregulated in

Acanthamoeba trophozoites during treatment with G-418, while at the same time their expression was maintained at physiological levels in control amoebae (Figure 9.11). More precisely, the highest expression was observed after 6 hours of treatment with the aminoglycoside, suggesting their role to be as executioner molecules of the cell death process, rather than signalling molecules that mediate the phenomenon. The release of lysosomal proteases into the cytosol has been reported to induce apoptosis by mediating the proteolytic activation of mitochondrial Bid proteins and subsequent cytochrome c release by MOM permeabilization (Stoka et al., 2001). Moreover, *Acanthamoeba* intracellular proteases might be associated with the appearance of granules (apoptotic-like bodies formation), which have been observed under light microscopy and are obvious after 6 hours of incubation, their number increasing dramatically during incubation. Since *Acanthamoeba* lacks caspases, this phenotype might be the result of intracellular protease function.

Regardless of the fact that caspases are considered to be general orchestrators of characteristic apoptotic features, this observation might also lead to the assumption that in systems that lack caspases, similar apoptotic features can be also derived from overexpression or activation of generally silent intracellular proteases in cells undergoing apoptosis or any other form of regulated cell death.

The task of the efficient cellular protein degradation is predominantly accomplished by the lysosomes, where lytic enzymes including cathepsins, a group of cysteine proteases, undertake protein breakdown (Turk et al., 2007). Adequate and regulated lysosomal damage was shown to lead to apoptotic cell death, sometimes without the apparent activation of caspases, although the mechanisms are less well defined while at the same time enormous lysosomal rupture was associated with necrotic and accidental cell death (Bursch, 2001). Caspases and cathepsins, although both being cysteine proteases, differ in their enzymic specificity, their intracellular localization and their mechanism of action.

RNA analysis of G-418 treated *Acanthamoeba* cells showed a great number of upregulated genes coding for cysteine proteases, such as cathepsins and papain-like proteases. This finding strengthens the assumption that supports an energetic

involvement of the cathepsins and the papains in G-418 mediated cell death. In support of this theory, studies have shown re-localization of cathepsin D during apoptosis from lysosomes to cytosol (Li et al., 1998). However it is not clear if these cysteine proteases play an auxiliary role by activating or deactivating signalling molecules, for instance by cleaving important proteins or as signalling pathway executioners, which are simply needed for the final 'clean-up' and the total lysis of the dying cell.

Based on the expression profiles, the greatest increase of both cathepsin and papain mRNA is observed after 6 hours of treatment, when other important phenomena have already occurred. Subsequently, in G-418 treated *Acanthamoeba* trophozoites high protease expression levels might regulate the final stages of the cell death and simultaneously determine and define the ending cell death morphology. Apoptosis has been already characterized by high levels of cathepsins, based on mRNA measurements (Guenette et al., 1994; Sensibar et al., 1990), rendering this finding particularly significant for the characterization process.

Metacaspases are cysteine peptidases orthologous to caspase enzymes that are found only in plants, protozoa and fungi, organisms that are devoid of caspases (Uren et al., 2000). Metacaspases are characterized by a caspase-like histidine–cysteine catalytic dyad, although they differ from caspases, for instance, in their substrate specificity (Tsiatsiani et al., 2011). In several protozoa including *Acanthamoeba (Saheb* et al., *2014; Tryzna* et al*. 2008)*, *T. brucei (*Szallies et al., 2002)*, Coclodinium polykrikoides* (Wang et al., 2018) and *Leishmania*, (Vercammen et al., 2006) metacaspase genes have been identified and their role in regulated cell death has been studied. Metacaspases are from previous findings considered inextricably associated with programmed cell death processes and particularly important molecules in the phenomenon's completion.

More precisely, metacaspase Yca1 of *Saccharomyces cerevisiae* was found to be associated with PCD of aged cells and simultaneously when *S. cerevisiae* cells were subjected to diverse extracellular stresses including viral infections and temperature variations (Mandeo et al., 2002; Ivanovska and Hardwick 2005; Flower et al., 2005). Additionally, *S. cerevisiae* Yca1 null mutants, genetically modified to overexpress LmjMCA (*Leishmania* metacaspase) and subsequent H_2O_2 induced stress, led to

programmed cell death (Vercammen et al., 2006). Furthermore, in *P. falciparum*, (Meslin et al., 2007) PfMCA1 metacaspase has been reported to mediate apoptotic cell death characterized by DNA fragmentation and loss of transmembrane mitochondrial potential.

Metacaspases (MCAs) like caspases and other pro-apoptotic and apoptotic proteins have also been associated with cellular functions other than cell death regulation, including removal of unfolded proteins in *Saccharomyces cerevisiae* (Hill et al., 2014), involvement in cell cycle regulation in *T. brucei* and *L. major* (Ambit et al., 2008; Helms et al., 2006). *Acanthamoeba* metacaspase (Acmcp) is characterized by the Cys/His catalytic dyad and also a conserved area of up to thirty amino acids that is identifiable in almost all metacaspases (Saheb et al., 2014). In *Acanthamoeba,* metacaspase has been proposed to interact with the contractile vacuole and its overexpression has been reported to induce deficiencies in cellular osmolarity regulation (Saheb et al., 2013), although its potential cell death regulatory or executive ability has not ever studied in depth and should not be ruled out.

Interestingly, RNA-seq analysis revealed that Acmcp expression was increased by approximately 12-fold during incubation and treatment with G-418, while at the same time control amoebae showed a slight but significant reduction in Acmcp expression at the same period of time. This observation could strongly link and establish Acmcp as an important regulator of *Acanthamoeba's* programmed cell death. However the role of *Acanthamoeba* MCA in cell death is still an enigma mainly through lack of experimental procedures that could block Acmcp effectively, either by appropriate metacaspase inhibition or by molecular techniques (like siRNAs or null Acmcp mutants) and subsequent induction of cell death. Furthermore, its precise role and whether Acmcp act as a death signalling molecule or as death executioner agent remains largely unknown.

Generally, there are two types of serine protease-mediated, death-signalling caspase-independent pathways (Egger et al., 2002) that could also probably apply in *Acanthamoeba* programmed cell death and have been previously suggested. The first is perforation of the mitochondrial membrane mediated by serine proteases, as a result of mitochondrial regulator protein cleavage, which in turn leads to mitochondrial apoptotic

factor release and the second includes the direct proteolytic activation of serine proteases (Egger et al., 2002).

Two serine proteases, ACA1_321400 and ACA1_128830, which have been associated with *Acanthamoeba* encystation (Moon et al., 2012) have also been found to be significantly upregulated in G-418 treated trophozoites. Serine proteases have been proposed to mediate apoptosis-like cell death under caspase-inhibiting conditions (Egger et al., 2002) and might be involved in post-mitochondrial proteolytic and apoptotic events (Dong et al., 2000). Furthermore, many studies have reported that serine proteases and non-caspase proteases are crucial to chromatin degradation (Wright et al., 1994; Hughes et al., 1998; Moffitt et al., 2007), besides being also responsible for endogenous endonuclease activation (Torriglia et al., 2000). Considering these facts, including serine protease gene upregulation and their confirmed proteolytic action against a plethora of substrates, the assumption that renders serine proteases, especially ACA1_321400 and ACA1_128830, which presented the most interesting and characteristic expression profile in treated trophozites, as important executioners of *Acanthamoeba* programmed cell death might not be unsubstantial. However, further experimental processes including serine protease inhibition, are essential to support and further validate this theory.

Ubiquitination, which is the conjugation of ubiquitin to proteins and ubiquitin-dependent proteolysis, has arisen as a prominent means of regulating cellular processes including signalling, degradation of intracellular proteins, transcription, cell viability and cell death (Kwon et al., 2005; Bader and Steller, 2009; Jesenberger and Jentsch, 2002). Proteasomes are scaffold protein complexes that degrade ubiquitin-marked misfolded or damaged proteins by proteolysis, executed mainly by cysteine proteases and other proteases found in the proteasomes. Moreover, intracellular proteolysis has been proposed to occur in programmed cell death accompanied by increased expression of ubiquitin genes (Delic et al., 1993). The tagging reaction is catalysed by enzymes called ubiquitin ligases and leads to poly-ubiquitination and finally to degradation by proteasomes.

Ubiquitination was already considered to occur in *Acanthamoeba* G-418 treated cells, as genes related to ubiquitination were found among those with the highest DEGs,

during comparisons between control and G-418 treated amoebae. Furthermore, many genes related to the ubiquitination pathway, including ubiquitination activating enzyme genes, ubiquitin conjugation enzymes, ubiquitin E3 ligases, DUBs, ubiquitin carboxy terminal hydrolases and ubiquitin-related cysteine proteases, were also found to be significantly upregulated during treatment with G-418. These expression analysis results suggest that ubiquitination pathways are certainly involved in *Acanthamoeba* programmed cell death, however their regulatory affect remains only superficially analysed. Is widely known though, that regulatory molecules including caspase activators, apoptotic gene transcription factors and proteins of the Bcl-2 family, which control mitochondrial outer membrane permeabilization, are under the control of the ubiquitin/proteasome system (Neutzner et al., 2012).

The most likely scenario could be the one which supports the idea that ubiquitination and de-ubiquitination might regulate the quantity of cell's anti- and pro-apoptotic factors, as genes related to the proteasome scaffold, which is the final stage of ubiquitin protein degradation, were found to be downregulated in G-418 treated trophozoites compared to untreated amoebae. However it could be hypothesised that the ubiquitination/proteasome system is not principally responsible for the extended morphological proteolytic effect that was observed during treatment, but partially by lysing important regulatory molecules. Simultaneously, this assumption might also support the scenario that was previously analysed and supported the extended role of proteases as executioners, rather cell signalling molecules.

Autophagy is an evolutionarily conserved intracellular degradation process, predominantly executed by the autophagy-related (ATG) family of genes and commonly observed during apoptosis and other forms of regulated cell death, which simultaneously acts as both a protector and executioner these processes. For instance, ATG 12 has been previously associated with mitochondria-mediated apoptosis by interacting with Bcl-2 family proteins (Rubinstein et al., 2011). Furthermore, many autophagy-related genes, which are core components of the autophagy machinery, have been associated with these procedures and it has been proposed that expression of autophagy-related genes is essential for cell degradation and clearance, after the induction of apoptosis (Qu et al., 2007). For instance, after treatment with G-418, trophozoites showed higher expression

of ATG8, ATG12 and ATG5, which are involved in the autophagosome formation pathway (Ger van Zanbergen et al., 2010). Autophagosomes might function in the characteristic phenotype of *Acanthamoeba* cell death. Finally, there is no evidence that autophagy can mediate cell death, however reports imply that autophagy itself may be a mechanism of cell death (Lu et al., 2006; Kroemer and Levine, 2008).

During treatment with G-418 many ATG-related genes were found to be upregulated in *Acanthamoeba* trophozoites while their expression profile remained unchanged in control amoebae. This observation identified the essential role of ATG genes during *Acanthamoeba* cell death and simultaneously autophagy was closely associated with the phenomenon. The autophagy pathway is governed by numerous kinases including PI3k/Akt, MAPK and JNK (Sridharan et al., 2011; Byun et al., 2009) which were already found to be upregulated. It may not be then wrong to assume, based on previous studies on autophagy, that autophagy-related gene expression is dispensable for G-418 mediated cell death in *Acanthamoeba*, but at the same time could be vital for the generation of engulfment signals which are subsequently required for the phagocytic elimination of the intracellular compartments of the dying cells. This assumption and other data (Huang et al., 2013) might indicate that autophagy could differ and regulate the way which cells die and not just whether they die or not. It could also be hypothesized that under stress conditions autophagy is initially induced, in an effort to ease the stimulus and sustain cell viability, however if the stress persists or is strong enough, expression of ATG genes and the subsequent increase in autophagy levels might function as a molecular switch, to enable the activation of cell death processes.

Another assumption that could be made is that the overexpression of some ATG genes, autophagy and subsequent cell death occur through a caspase-independent mechanism, perhaps upon JNK activation, which contains a large number of nuclear and cytoplasmic target genes and transcription factors, in response to extended Ras signalling (Byun et al., 2009). Activation of JNK signalling could, as explained earlier, mediate c-Jun phosphorylation, pro-apoptotic gene expression and subsequent cell death induction.

Finally, an additional interesting fact that was observed during gene expression analysis was the identification of many genes with increased expression levels which have been reported to be upregulated and play crucial roles during encystation. Some of these genes include autophagy-related genes (Kim et al., 2015; Song et al., 2012; Moon et al., 2011, 2013), serine proteases (Moon et al., 2012) and even cyst-specific proteins. These results indicate that *Acanthamoeba* encystation and programmed cell death, which as has been described are both energy-dependent processes, may co-exist and even might have a similar basis, which could be potentially controlled by the same regulatory pathways and molecules. Furthermore, it could be hypothesised that encystation might be the microorganism's answer to extrinsic signals derived from the natural environment, including variations in the pH, osmolarity, temperature and nutrient deprivation, whereas programmed cell death is the microorganism's response to intracellular signals, including mitochondrial inadequacy, viral and bacterial infection, or genetic dysregulation.

Better understanding of how these processes, including *Acanthamoeba* encystation, autophagy and programmed cell death, are related is likely to be an important area of research and could provide basic understanding of basic biological processes, not only in *Acanthamoeba*, but in a wider-spectrum cell and cell death field. Simultaneously it will offer exceptional opportunities to counter harmful infections and diseases.

Chapter 10

Discussion

Acanthamoeba is a regulator of bacterial profusion and an opportunistic human pathogen, able to cause painful keratitis and granulomatous encephalitis among other diseases. It is widely distributed in the natural environment since has the ability to adapt to the most unimaginably harsh environments and it has been isolated in every continent including Antarctica. *Acanthamoeba* abundance is due partially to its adaptable life style, which enables the transformation of an active, feeding and infective trophozoite to a dormant and resistant double-walled cyst under unfavourable conditions, in a process called encystation.

Cell death and cell survival are ongoing and active processes whereby *Acanthamoeba* trophozoites, like other cells, are continuously required to integrate stress signals and consequently decide upon their fate. These decisions are conducted by an extensive variety of signalling pathways that are regulated by specific enzymes and more precisely by distinctive and evolutionarily conserved proteins. Initially such mechanisms might function as self-defence alternatives, although during evolution they might have evolved to serve other purposes that eventually will guarantee entire population or organism survival.

Apoptosis and other forms of regulated cell death have been extensively described and studied in multicellular organisms in which their existence regulates important organismal processes such as differentiation and development. On the other hand, forms of regulated cell death and unicellular organisms sound as if they cannot coexist. Oxymoron as it sounds, cell death mechanisms that share common characteristics with those of multicellular organisms have been reported in a plethora of yeast, bacteria and protozoans and it is also reported that some parasitic protists may have more than one apoptotic pathway (Tan and Nasirudeen, 2005; Brown and Hurd,

2013). This significant evidence implies that unicellular internal death-mediating mechanisms not only exist, but are taxonomically widespread.

The existence of cell death signalling pathways in unicellular organisms, which might be thought to have been evolved to maximize their own proliferation rates instead of death occurrence, might offer vital advantages and guarantee population survival in unfavourable conditions after all.

A likely explanation is that *Acanthamoeba* could undergo programmed cell death in order to gain a group benefit by regulating its density and by this means prevent either food source limitation or premature host mortality. At the same time, cell death mechanisms could shield *Acanthamoeba* viability from aggressive types of viruses and bacteria that could infect individual trophozoites and threaten the entire population's prosperity. Therefore, elimination of infected trophozoites through intracellular cell death programs could efficiently restrict or prevent pathogens from spreading.

The term apoptosis is used primarily to describe regulated cell death in multicellular organisms and has specific characteristics, comprising chromosomal condensation, nuclear DNA fragmentation, cell shrinkage, rounded up formations, loss of mitochondrial membrane potential and formation of apoptotic bodies. This study showed that most of the morphological features of apoptosis are observed during treatment of *Acanthamoeba* trophozoites with G-418 aminoglycoside. However, *Acanthamoeba* does not encode caspases, which are responsible for and interwoven with characteristic apoptotic cell morphology, so the term apoptosis might be inappropriate to describe the extent of the phenomenon, despite the fact that the same terminology has been used repeatedly to describe caspase-independent apoptotic pathways. The resemblance in the characteristic features but obvious variations in the underlying machinery across species has resulted in an argument, whether apoptosis, or a form thereof, is really the procedure being observed in unicellular organisms that lack caspases, including *Acanthamoeba*.

Biochemical evidence for a caspase-like execution pathway has been reported in many protozoan parasites, including *B. hominis* (Tan and Nasirudeen, 2005) and

Plasmodium spp (Al-Olayan et al., 2002), although caspases have not been found in unicellular organisms, as previously mentioned. However, there is no justifiable argument against the probability that other protein cascades involving more than one clan of cysteine proteases might regulate and operate the phenomenon of apoptosis in some unicellular microorganisms, including *Acanthamoeba*. Cysteine proteases different from caspases, comprising metacaspases, papains and cathepsins, seem to substitute for the role of caspases in parasitic protozoans, as has been previously implied (El-Fadili et al., 2010). Genes related to the cathepsin family, papain family, metacaspase and serine protease genes, were found to be significantly up-regulated during *Acanthamoeba* cell death, which indicates their involvement in cell death regulation and execution. Furthermore, cross-talk between different intracellular proteases could strengthen and at the same time accelerate cell death mechanisms. Complete identification and characterization of these protein protease scaffolds' role could undoubtedly provide new therapeutic approaches for the regulation of the cell death process not only in *Acanthamoeba* infections, but also in other systems and organisms likewise.

Mitochondria are categorized as major key points in many apoptotic pathways and various systems. In this study it was shown that during *Acanthamoeba* programmed cell death, mitochondrial activity was not only dramatically decreased, but simultaneously mitochondrial depolarization and a great decrease in ΔΨm of MOM was also observed. These alterations in mitochondrial physiology led subsequently to the release of apoptotic agents such as cytochrome c. This apoptotic event sequence seems to be triggered by a rise in intracellular calcium levels, which gradually mediated mitochondrial deficiency (Figure 10.1).

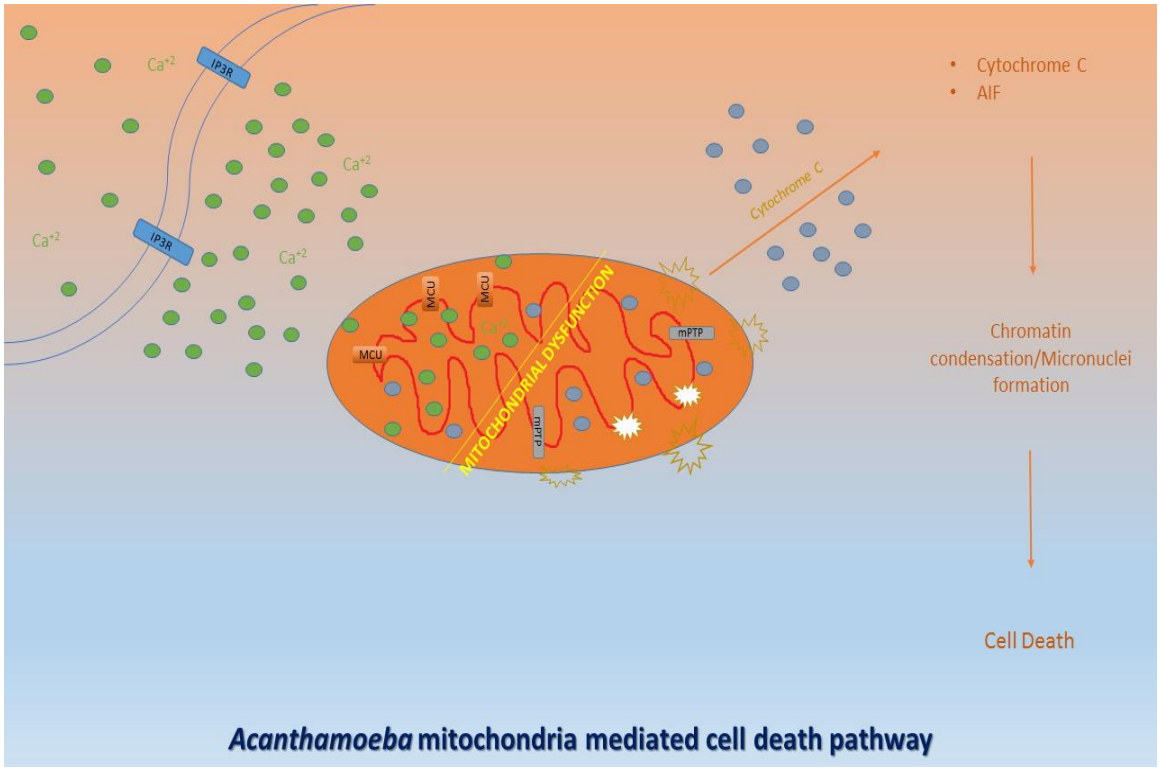

Figure 10.1: *Acanthamoeba* intrinsic or mitochondria mediated cell death pathway. The graphical diagram represents observed apoptotic events in *Acanthamoeba* trophozoites during treatment with G-418.

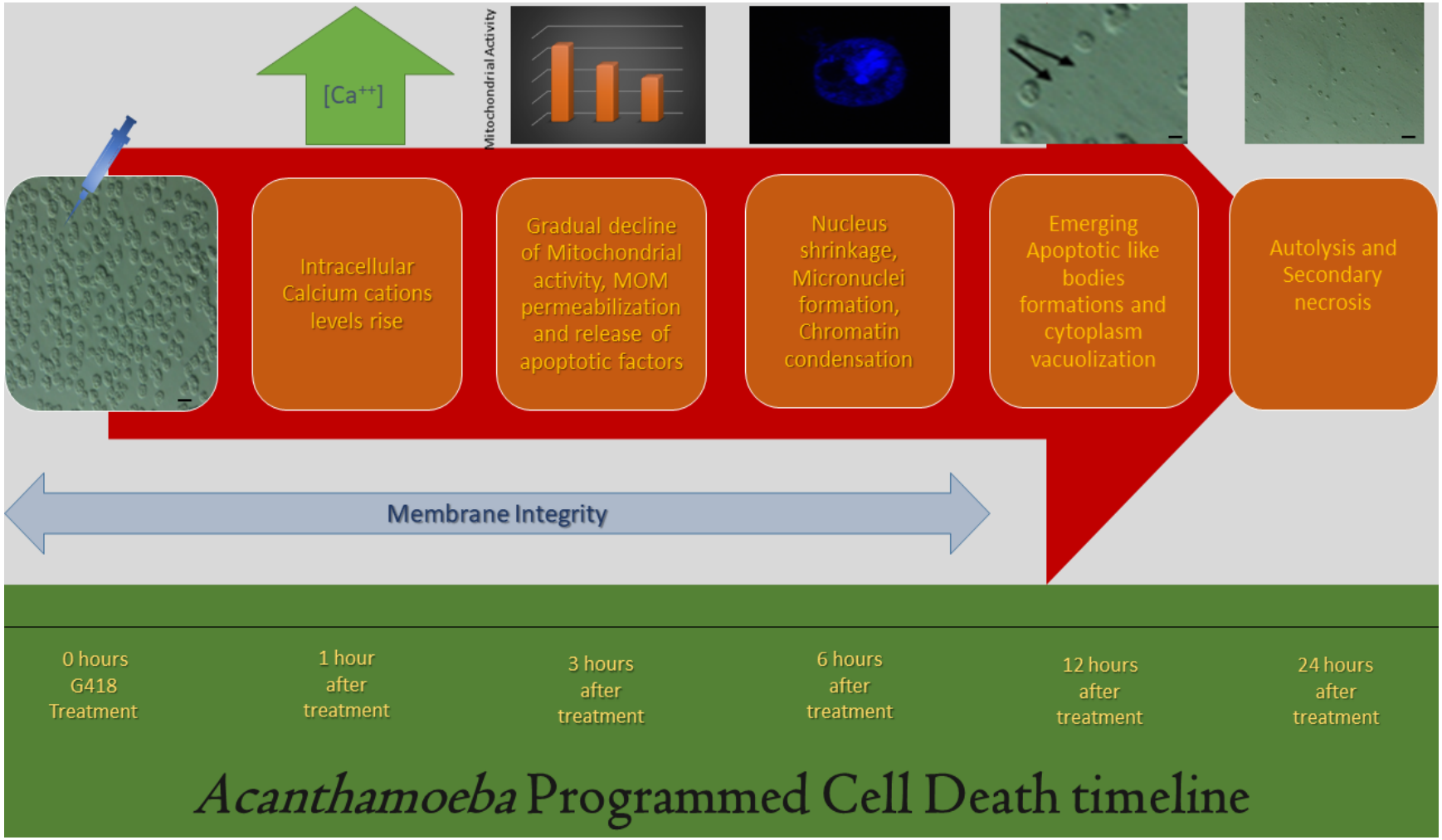

Figure 10.2: *Acanthamoeba* apoptosis-like cell death timeline. The graphical diagram represents some basic morphological and biochemical alterations occurring in *Acanthamoeba* trophozoites during treatment with EC_{90} G-418. Scale 10µm.

Transcriptomic analysis of G-418 treated trophozoites revealed that *Acanthamoeba* cell death could be a finely regulated phenomenon. Numerous proteins that could acts as initiators, regulators and orchestrators of the phenomenon have been found to be significantly differentially expressed between treated and control amoebic populations during treatment. Some of these proteins include kinases and phosphatases, heat shock proteins, autophagy related proteins, glutathione S-transferases, cysteine and serine proteases, endonucleases, Ras family proteins and ubiquitination-related proteins.

Altogether above protein families, have been proposed to play significant roles either as signalling molecules or as executioners in variable systems and organisms during apoptosis or other forms of regulated cell death. This study managed to associate many of those proteins to *Acanthamoeba* programmed cell death phenomenon although it is as yet unclear at which point or what is the exact function of each one of them. In order for their function to be fully disclosed, further and deeper experimental analysis is required. This investigation could primarly include genetically modified *Acanthamoeba* trophozoites (e.g. with knockout selected gene/genes) where further and precise observations of apoptotic features occurance might differentiates, from that which have been already described in the wild type and in this study.

Phenomenon characterization as apoptosis or apoptotic cell death might be the closest related term to describe the entire set of the morphological and biochemical alterations that were taking place during *Acanthamoeba* cell death and were analytically described in this study. However, apoptosis is inextricably linked and first described in metazoan regulated cell death, rendering the term not particularly suitable to define the full perspective of *Acanthamoeba's* programmed cell death. Interestingly, a plethora of genes related to autophagy were found also to be significantly upregulated during treatment and it would not have been irrational to consider autophagic cell death as an alternative. However, *Acanthamoeba* trophozoites failed to represent characteristic morphological and biochemical features of autophagic cell death despite the signs of an active autophagic ongoing procedure. This finding though might act as a confirmation of the crosstalk between programmed cell death and autophagy in *Acanthamoeba*.

Evidence obtained from the study of *Acanthamoeba's* programmed cell death, which shares a plethora of characteristics with apoptosis, could imply that the latter originated, not just prior to multicellularity, but even before the divergence of unicellular lineages. The perspective of the study supports the existence of simple regulated death pathways in *Acanthamoeba* and in lower eukaryotes in general. However, due to evolution and cellular complexity, these pathways are at present characterized by increased specificity of molecules and additional checkpoints that differ from organism to organism and cell to cell.

The initial management of *Acanthamoeba* Keratitis infenctions comprises combined dosages of diamidines such as hexamidine (1000 μg/ml) or propamidine isethionate (1000 μg/ml) and cationic antiseptics like chlorhexidine (200 μg/ml) each hour, for three continuous days (Russel et al., 1996; Dart et al., 2009), while after this initial aggressive approach treatment, dosages are reduced to every 3 hours until response to treatment is observed. Side effects attributed to usage of these drugs comprise mainly iris atrophy, cataract and peripheral ulcerative keratitis. Similarly, in *Acanthamoeba* granulomatous encephalitis, among 94 confirmed cases from 1955 to 2013 the mortality rate was as high as 85-90% (Zamora et al., 2014; Siddiqui et al., 2016). Administrative combined antibiotic therapy, including some of the substances as rifampin, azithromycin, fluconalozole, pentamidine, amphotericin and miltefosine, have shown some promising results, however all successful treatment cases were preceded by a timely prognosis.

It is more than evident that mortality and morbidity associated with *Acanthamoeba* diseases, especially those of *Acanthamoeba* granoulomatous encephalitis (AGE) and *Acanthamoeba* keratitis (AK), persisted at high levels. Conventional medicine has failed to present an efficient strategy against these infections so far, thus new therapeutic approaches need to be adopted and tested. Manipulation of *Acanthamoeba's* PCD pathways might be an alternative tactic against microbial infections with quite encouraging and promising outcomes, since targeted regulation of such pathways could be considered particularly efficient. Furthermore, regulation of cell death pathways, assures non existent or negligible side effects, compared to other methods.

This study suggested the presence of intracellular cell death pathways in *Acanthamoeba,* while at the same time identifying some key features that might be of high importance. For instance, it was shown that mitochondrial dysfunction plays an important role in microorganism cell death progress. Therefore, future treatment procedures could precisely target *Acanthamoeba* mitochondrial function in order to treat diseases caused by the microorganism. Apparently, mitochondrial dysfuntion was associated with an increase in intracellular [Ca^{2+}] which in its turn was potentially an aftereffect of endoplasmatic reticulum stress. Subsequently, another therapeutic alternative could comprise the disturbance of *Acanthamoeba's* ER homeostasis or the increase of intracellular Ca^{+2} concentration, in order to trigger death-signalling pathways.

Another possibility in *Acanthamoeba* disease management could be the use of genetically modified or wild-type *Acanthamoeba*-specific viruses. By this means, viruses could invade the microorganism, multiply using the host's machinery and lead to its lysis. If the potential virus implementation strategy is considered to threaten host morbidity, viruses could initially be genetically modified not to. Furthermore, genetically modified viruses designed to infect *Acanthamoeba* cells could act as genetic material transfer agents. For instance, as this study shown, plenty of apoptotic related genes, including metacaspase, genes related to autophagy, ser/thr kinases and phosphatases, Ras family genes, deoxyribonucleases, endonucleases, calpains, cathepsins and glutathione S-transferases were highly upregulated during cell death phenomenon. Transfer some of these genes into *Acanthamoeba* through genetically modified viruses and simultaneously, their expression under the regulation of a highly expressed promoter, could mediate microorganism programmed cell death or in the worst case scenario sensitize *Acanthamoeba* to programmed cell death or to a broader sprectrum of death stimuli, rendering its eradication easier and more efficient.

Manipulation and activation of *Acanthamoeba's* programmed cell death pathways as a therapeutic alternative will also guarantee minimal disease recurrence since almost all the members of the entire amoebal population will forced to undergo cell death. Current approaches do not favour this, but in some cases allow *Acanthamoeba* transformation to dormant double-walled cysts, higly resistant and

quite problematic to treat. This transformation renders short or long term excystation from cysts to trophozoites feasible when the conditions are optimal and accordingly *Acanthamoeba* reproduction, expansion and re-emerging infection. Theoretically, induction of cell death will not provide the opportunity for amoebic transformation since as this study has shown, stimulation of trophozoites towards cell death could be immediate and straightforward compared to encystation, which requires a significant amount of time.

Hypothetically, it seems that this kind of manipulation will provide an excellent therapeutic alternative not only to diseases caused by *Acanthamoeba* but to numerous other diseases caused by microorganisms whose eradication by currect conventional medicine is problematic. Furthermore, deep understanding of programmed cell death pathways in *Acanthamoeba* may reveal additional target molecules that in turn could be easily manipulated an extended range of pathophysiological conditions related to cell death programmes' efficiency and deficiency including tumor malignancies and autoimmune disorders, since the biological principles are highly conserved among different species and cells.

APPENDIX 1

Differential expression analysis R studio script (modified)

```
library(dplyr)
library(ggplot2)
library(GSEABase)
library(rtracklayer)
library(readr)
library(BiocInstaller)

biocLite("EGSEA")
biocLite("gage")
biocLite("KEGGREST")
biocLite("pathview")

library(Rsubread)
library(edgeR)
library(AnnotationDbi)
library(locfit)
library(statmod)
library(pheatmap)
library(KEGGgraph)
library(gageData)
library(DBI)
library(data.table)
library(GenomeinfoDb)
library(GSA)
library(KEGG.db)
library(KEGGdzPathways)
library(KEGGgraph)
library(limma)
library(locfit)
library(Rcurl)
library(lattice)
library(MASS)
library(Matrix)
library(mgcv)
library(nlme)
library(nnet)
library(parallel)
library(rpart)
```

```
rm(list =ls())

setwd('/ /')
data_dir <- 'BAM Alignments files'

geninfo <- 'groups.tsv'

targets <- read.delim(file.path(geninfo), stringsAsFactors = FALSE)

targets$Name <- make.unique(targets$ID)

rownames(targets) <- targets$Id

bam_dir <- file.path(data_dir)
bam_files <- list.files(bam_dir, full.names = TRUE, pattern = '.bam')
bam_files

gtf_file <- file.path('Acanthamoeba_castellanii_str_neff.Acastellanii.strNEFF_v1.37.gtf')

cat(readLines(gtf_file, n = 10), sep="\n")

gtf_content <- import (gtf_file, feature.type = 'gene')
gtf_content

annotation <- data.frame(elementMetadata(gtf_content), stringsAsFactors = FALSE)
rownames(annotation) <- annotation$gene_id

count_results <- featureCounts(files = bam_files, annot.ext = gtf_file,
isGTFAnnotationFile = TRUE, GTF.featureType = 'exon', GTF.attrType = 'gene_id',
strandSpecific = 2, isPairedEnd = FALSE, nthreads = 1)

colnames(count_results$counts) <- sub('.*(Ac.*)\\.bam', '\\1',
colnames(count_results$counts))

colnames(count_results$stat)[-1] <- sub('.*(Ac.*)\\.bam', '\\1',
colnames(count_results$stat)[-1])

raw_counts <- count_results$counts
head(raw_counts)
nrow(raw_counts)
length(which(rowSums(raw_counts>=1)>1))

count_results$stat
```

#visualization

```
stats <- data.frame(count_results$stat[, -1], row.names = count_results$stat[, 1])
stats <- stats[apply(stats, 1, function(x) any(x > 0)),]
stats <- reshape2::melt(t(stats))
stats$name <- targets[stats$Var1, 'Name']

ggplot(stats, aes(x = Var1, y = value, fill = Var2)) +  geom_bar(stat = "identity", position
= 'fill') + theme_bw() + theme(axis.text.x = element_text(angle = 90), legend.title =
element_blank()) + xlab("Sample") + ylab(NULL)
raw_counts <- raw_counts[rownames(annotation), rownames(targets)]


dgList <- DGEList(
  counts = raw_counts,
  samples=targets,
  group = targets$Group,
  genes = annotation)
dgList

dgList$samples$Name <- targets$Name


#Normalisation


dgList <- calcNormFactors(dgList)

dgList$samples


#Explore the data


plotMDS(
  dgList,
  gene.selection ='pairwise',
  col = as.integer(dgList$samples$group),
  labels = dgList$samples$group)


#Filter the data


dgList <- dgList[rowSums(cpm(dgList)>=0.1) >= 3 , ,
                 keep.lib.sizes=FALSE]
dgList <- calcNormFactors(dgList)

nrow(dgList)
```

#Explore the data

```
plotMDS(
  dgList,
  gene.selection ='pairwise',
  col = as.integer(dgList$samples$group),
  labels = dgList$samples$group)
```

#Plotting a function

```
plot_gene <- function(gene_id, inputDgList){
  expr <- cpm(inputDgList)
  plot_data <- cbind(inputDgList$samples, expression = expr[gene_id,])
  plot_data <- plot_data[order(plot_data$group),]
  plot_data$sample <- factor(rownames(plot_data), levels = rownames(plot_data))
  p <- ggplot(plot_data, aes(x= Name, y= expression, fill= group)) + geom_bar(stat =
"identity") + theme_bw() + theme(axis.text.x = element_text(angle = 90, hjust = 1)) +
  ggtitle(paste(gene_id, annotation$gene_name[match(gene_id, annotation$gene_id)],
sep=": "))
 print(p)}

plot_gene ('ACA1_XXXXXX', dgList)
```

#Buidling a design matrix

```
design <- model.matrix(~ 0 + group, data = dgList$samples)
design
```

#Sample pairing

#Estimating dispersion

```
dgGlm <- estimateDisp(dgList, design, robust = TRUE)
plotBCV(dgGlm)

fit <- glmQLFit(dgGlm, design, robust = TRUE)
plotQLDisp(fit)
```

#Testing for DE genes

```
contrasts <- data.frame(variable='group', group1='Untreated', group2='Treated',
stringsAsFactors = FALSE)
contrasts

contrast_names <- apply(contrasts, 1, function(contrast)
paste(paste0(contrast[1], make.names(contrast[3])), paste0(contrast[1],
        make.names(contrast[2])), sep="-"))
contrast_names

contrast.matrix <- makeContrasts(contrasts = contrast_names, levels = design)
contrast.matrix

de <- glmQLFTest(fit, contrast = contrast.matrix[,1])

top_genes <- topTags(de, n=100)
top_genes
```

#Test different genes with plot_gene

```
plot_gene('ACA1_095540', dgList)
```

#Heatmap

```
plot_heatmap <- function(plot_genes, title= '', inputDgList){
  annotation_col <- inputDgList$samples[with(inputDgList$samples, order(group,
Name)), c('Name', 'group')]
  plot_genes <- plot_genes[plot_genes %in% rownames(inputDgList)]
  expression <- cpm(inputDgList)[plot_genes, rownames(annotation_col)]
  plotmatrix <- log2(expression + 0.1)
  rownames(plotmatrix) <- annotation[rownames(plotmatrix), 'gene_id']
  grid::grid.newpage()
  pheatmap( plotmatrix,
    show_rownames = T,
    annotation_col = annotation_col,
    border_color = NA,
    legend = FALSE,
    cluster_cols = FALSE,
    cluster_rows = TRUE,
    scale = 'row',
    color = colorRampPalette(rev(RColorBrewer::brewer.pal(n = 7, name =
"RdYlBu")))(100),
```

```
   main = title)}

plot_heatmap(rownames(top_genes), inputDgList =  dgList)
```

#Extracting results

```
results <- topTags(de , n=nrow(dgList), sort.by = 'none')$table
results <- results[rownames(dgList),]

write.csv(results, file = 'Differential_results_Apoptosis Xhour(s).csv')
```

#Filtering significant genes

```
fdr_treshold <- 0.001
fc_treshold <- 2

top_genes <- topTags(de, n=100)
top_genes

plot_gene ('ACA1_089990', dgList)

diffexp_genes <- rownames(results)[abs(results$logFC) >= log2(fc_treshold) &
results$FDR <= fdr_treshold ]

print(paste(length(diffexp_genes), 'genes are differentially expressed at fold change of
at least', fc_treshold, 'and a maximum FDR of', fdr_treshold))
```

#visualising results

#Smear Plot

```
plotMD(de, status = decideTestsDGE(de, p.value = 0.05))
abline(h=c(-1,1))
```

#Volcano plot

```
volcano_plot <- function(results_table, fc_treshold, fdr_treshold,
                         log=FALSE){
  results_table$significant <- 'no'
  results_table$significant[ abs(results_table$logFC) >=
                               log2(fc_treshold) & results_table$FDR <= fdr_treshold ] <- 'yes'
  if(! log){
```

```
    results_table$logFC <- sign(results_table$logFC)* 2^abs(results_table$logFC)}

  ggplot(results_table, aes(logFC, -log10(FDR), color=significant)) +
    geom_point(alpha = 0.5) +
    scale_colour_manual(name = 'significant', values = setNames(c('red',
'grey'),c('yes','no'))) +
    theme_bw()}

volcano_plot(results, fc_treshold, fdr_treshold)

volcano_plot(results, fc_treshold, fdr_treshold, log = TRUE)
```

APPENDIX 2

Acanthamoeba GS isolate, 18S gene sequence

>GCTTGTCCCAAAGACTAAGCCATGCATGTGTAAGTATAAACTTATTTATACGGCGA
ACCTGCGGAAGGCTCATTAAATCAGTTATAGTTTATTTGATGGTCTCTTTTGTCTTT
TTTTACCTACTTGGATAACCGTGGTAATTCTAGAGCTAATACATGCGCAAGGTCCC
GAGCGCGGGGGGCAGGGCTTCACGGCCCTGTCCTCGCATGCGCAGAGGGATGT
ATTTATTAGGTTAAAAACCAGCGGCAGGGGTCAGCAATGGCCCCTGCCAAACACT
CCTGGTGATTCATAGTAACTCTTTCGGATCGCATTCATGTCCTCCTTGTGGGGACG
GCGACGATTCATTCAAATTTCTGCCCTATCAACTTTCGATGGTAGGATAGAGGCCT
ACCATGGTCGTAACGGGTAACGGAGAATTAGGGTTCGATTCCGGAGAGGGAGCCT
GAGAAATGGCTACCACTTCTAAGGAAGGCAGCAGGCGCGCAAATTACCCAATCCC
GACACGGGGAGGTAGTGACAATAAATAACAATACAGGCGCTCGATAAGAGTCTTG
TAATTGCAATGAGTACAATTTAAACCCCTTAACGAGTAACAATTGGAGGGCAAGTC
TGGTGCCAGCAGCCGCGGTAATTCCACCTCCAATAGCGTATATTAAAGTTGTTGCA
GTTAAAAAGCTCGTAGTTGGATCTAGGGACGCGCATTTCAAGCGCCCGTGTCGTC
GGGTCAAACCGGCGACTGCGTTGGCGTTGCGGGCTCGGTCCGTCGGTGGACCCT
CGTGGTCTTAATCGGCGTGTCAACCGGCCCGCCCGTCCCCTCCTTCTGGATTCCC
GTTCCTGCTATTGAGTTAGTGGGGACGTCACAGGGGGCTCATCGTCGTCATGCAA
ATGGCGGCGGTGGGTCCCTGGGGCCCAGATCGTTTACCGTGAAAAAATTAGAGTG
TTCAAAGCAGGCAGATCCAATTTTCTGCCACCGAATACATTAGCATGGGATAATGG
AATAGGACCCTGTCCTCCTATTTTCAGTTGGTTTTGGCAGGCGCGAGGGACTAGG
GTAATGATTAATAGGGATAGTTGGGGGCATTAATATTTAATTGTCAGAGGTGAAATT
CTTGGATTTATGAAAGATTAACTTCTGCGAAAGCATCTGCCAAGGATGTTTTCATTA
ATCAAGAACGAAAGTTAGGGGATCGAAGACGATCGAATACCGTCCTTCACCGTCG
AGACTGGGGTCAAACCTCTTCAACGAGGAATTCCTAATAACCGCGAGT

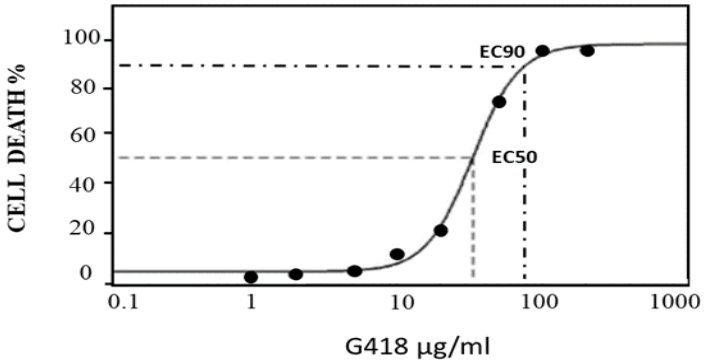

Figure 2.1: The killing of *Acanthamoeba* by a range of concentrations of G418 established that the EC50 value is 32 ± 3 µg/mL while the EC_{90} value is 75 ± 5 µg/mL. Cells were incubated with G418 in NSB for 24 hours at 37ºC prior to determining cell death by trypan blue exclusion.

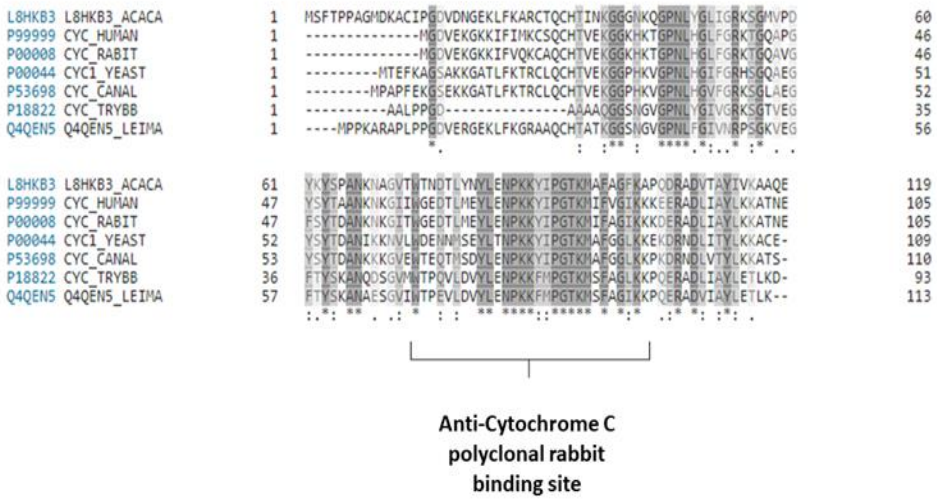

Figure 2.2: A line-up of cytochrome c proteins from various species with Acanthamoeba at the top. The peptide used to raise the antibody used is highlighted showing that this is highly conserved. Note also the cysteine residue at position 13 in the *Acanthamoeba* sequence which is unusual. The blots shows a band at around 25 kDa rather than the expected 14 kDa but cytochrome c is known to polymerize (Hirota et al. 2010) and so it is likely that the epitope recognised by the antibody is a cytochrome c dimer.

Figure 2.3: Phylogenetic tree of *Acanthamoeba* metacaspsase protein. Acmcp is mentioned in a red frame. Maximum likelihood method, 100 bootstrap replications, MEGA 7, (Kimura, 1980; Kumar 2016; Felsenstein, 1985).

Appendix 3 - Publications

Experimental Parasitology 183 (2017) 109–116

Contents lists available at ScienceDirect

Experimental Parasitology

journal homepage: www.elsevier.com/locate/yexpr

Vannella pentlandii n. sp., (Amoebozoa, Discosea, Vannellida) a small, cyst-forming soil amoeba

Sutherland K. Maciver*, Alvaro De Obeso Fernandez Del Valle, Zisis Koutsogiannis

Centre for Integrative Physiology, Biomedical Sciences, Edinburgh Medical School, University of Edinburgh, Hugh Robson Building, George Square, Edinburgh, EH8 9XD, Scotland, UK

HIGHLIGHTS

- A new species of *Vannella* is described.
- Forms aggregated cyst mass.
- Smallest cyst of any *Vannella* to date.
- Groups with *Vannella fimicola*, *V. placida*, and *V. epipetala*.

GRAPHICAL ABSTRACT

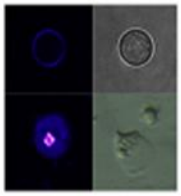

ARTICLE INFO

Article history:
Received 22 June 2017
Received in revised form
4 July 2017
Accepted 30 July 2017
Available online 1 August 2017

This paper is dedicated to the memory of Dr Conrad A. King, a friend and mentor.

Keywords:
Vannella
Cyst forming
Amoebozoa
Phylogenetics
Amoeba

ABSTRACT

We describe a new species of cyst-producing soil amoeba *Vannella pentlandii* from course pasture in the Pentland Hills, Scotland. Analysis of the 18S rDNA gene reveals that it belongs to the sub-group within the genus, presently composed of *V. placida*, *V. epipetala* and *V. fimicola* (the PEF group). This group share features such as longitudinal folds/ridges on the lamella (the anterior hyaline region of the trophozoite), stubby floating forms and cyst production. While each PEF species contain cyst producing strains, not all strains within these species do so. *V. fimicola* produces cysts on stalks leading to its former classification as a slime mould, however no such stalks were evident in the *V. pentlandii*, instead groups of cysts become piled on top of each other forming clumps. The encysting amoebae crawl toward each other, pushing some off the surface to form these mounds. The *V. pentlandii* trophozoites are of typical size for the genus but the cysts at 6.9 μm in diameter, are the smallest so far described in genus *Vannella*. Other cyst producing species are found in various branches within the *Vannella* phylogenetic tree, probably meaning that this ability was ancestral but lost in many branches (particularly in marine species), and perhaps re-gained in others.

1. Introduction

The genus *Vannella* was created by Bovee in 1965 to include flattened, often fan-shaped amoebae with a large hyaline leading edge while in active locomotion (Bovee, 1965). *Vannella* was differentiated from *Platyamoeba* as the later did not possess glycostyles visible under E.M. but instead had a "fuzzy" glycocalyx which may be arranged in a hexagonal pattern (Page, 1988). Electron microscopy of the early branching Vannellid, *Paravannella minima* (Kudryavtsev, 2014) indicates that the ancestral state appears to bear long pentagonal glycostyles and simple, longer filaments that have subsequently been lost in some groups. Until the year 2000, another recognised distinction between *Vannella* and *Platyamoeba* was that *Vannella* lacked the cyst stage that

* Corresponding author.
E-mail address: smaciver@ed.ac.uk (S.K. Maciver).

http://dx.doi.org/10.1016/j.exppara.2017.07.011
0014-4894/

References

Abrahão J. S., Dornas F. P., Silva L. C., Almeida G. M., Boratto P. V., Colson P., La Scola B. and Kroon, E. G., (2014), *Acanthamoeba polyphaga* mimivirus and other giant viruses: an open field to outstanding discoveries, *Virology journal*, 11 (120), pp:120

Adl S. M., Simpson A. G., Farmer M. A., Andersen R. A., Anderson O. R., Barta J. R., Bowser S. S, Brugerolle G., Fensome R. A., Fredericq S., James T.Y., Karpov S., Kugrens P., Krug J., Lane C. E., Lewis L. A., Lodge J., Lynn D. H., Mann D. G., McCourt R. M., Mendoza L., Moestrup O., Mozley-Standridge S. E., Nerad T. A., Shearer C. A., Smirnov A. V., Spiegel F. W. and Taylor M. F., (2005), The new higher level classification of eukaryotes with emphasis on the taxonomy of protists, *Journal of Eukaryotic Microbiology*, 52 (5), pp: 399–451

Adler V., Yin Z., Fuchs S., Benezra M., Rosario L., Tew K., Pincus M., Sardana M., Henderson C., Wolf C., Davis R. and Ronai Z., (1999), Regulation of JNK signaling by GSTp, *EMBO J.*, 18 (5), pp: 1321-1334

Aggarwal T., Suzuki T., Taylor W. L., Bhargava A. and Rao R. K., (2011), Contrasting effects of ERK on tight junction integrity in differentiated and under-differentiated Caco-2 cell monolayers, *Biochemical Journal*, 433 (1), pp: 51–63

Aherfi S., Boughalmi M., Pagnier I., Fournous G., La Scola B., Raoult D. and Colson P., (2014), Complete genome sequence of Tunisvirus, a new member of the proposed family Marseilleviridae, *Arch Virol*., 159 (9), pp: 49-58

Aherfi S., Philippe C., La Scola B. and Raoult D., (2016), Giant Viruses of Amoebae: An Update, *Front Microbiol*, 7, pp: 349

Akematsu T. and Endoh H., (2010), Role of apoptosis-inducing factor (AIF) in programmed nuclear death during conjugation in Tetrahymena thermophila. *BMC Cell Biol*., 11, pp: 13

Alvarez, V. E., Kosec G., Sant'Anna C., Turk V., Cazzulo J. J. and Turk B., (2008) Autophagy is involved in nutritional stress response and differentiation in *Trypanosoma cruzi. J. Biol. Chem*, (283), pp: 3454–3464

Al-Olayan E. M., Williams G. and Hurd H., (2002), Apoptosis in the malaria protozoan, Plasmodium berghei: a possible mechanism for limiting intensity of infection in the mosquito. *Int J Parasitol*, (32), pp: 1133-1143

Amann R., Springer N., Schönhuber W., Ludwig W., Schmid E. N, Müller K. D. and Michel R., (1997), 'Obligate intracellular bacterial parasites of *Acanthamoeba*e related to Chlamydia spp.', *Applied and Environmental Microbiology*, 63 (1), pp: 115–121

Ameisen J. C., Idziorek T., Billaut-Mulot O., Loyens M., Tissier J. P, Potentier A. and Ouaissi A., (1995), Apoptosis in a unicellular eukaryote (*Trypanosoma cruzi*): Implications for the evolutionary origin and role of programmed cell death in the control of cell proliferation, differentiation and survival, *Cell Death Differ,* 2, (4), pp: 285-300

Ambit A., Fasel N., Coombs G. H. and Mottram J. C., (2008), An essential role for the Leishmania major metacaspase in cell cycle progression, *Cell Death Differ*., (15), pp: 113–122

Anand, C. M., Skinner A. R., Malic A. and Kurtz J. B., (1983), Interaction of L. pneumophilia and a free living amoeba (Acanthamoeba palestinensis), *The Journal of Hygiene*, 91 (2), pp: 167–178

Anderson I. J., Watkins R. F., Samuelson J., Spencer D. F., Majoros W. H., Gray M. W. and Loftus B. J., (2005), Gene discovery in the *Acanthamoeba castellanii* genome. *Protist*, (156), pp: 203-14

Anderlini P., Przepiorka D. and Luna M., (1994), *Acanthamoeba* meningoencephalitis after bone marrow transplantation. *Bone Marrow Transplant*, (14) pp: 459–461

Andreani J., Aherfi S., Yaacoub Bou Khalil J., Di Pinto F., Bitam Idir, Raoult D., Colson P. and La Scola B., (2016), Cedratvirus, a Double-Cork Structured Giant Virus, is a Distant Relative of Pithoviruses, *Viruses*, 8 (11), pp: 300-311

Andreani J., Khalil JYB., Sevvana M., Benamar S., Di Pinto F., Bitam I., Colson P., Klose T., Rossmann M. G, Raoult D. and La Scola B., (2017), Pacmanvirus, a New Giant Icosahedral Virus at the Crossroads between Asfarviridae and Faustoviruses., *J Virol*., 91 (14), pp: 211-217

Andrieu C., Taieb D., Baylot V., Ettinger S. and Soubeyran P., (2010), Heat shock protein 27 confers resistance to androgen ablation and chemotherapy in prostate cancer cells through eIF4E, *Oncogene* (29), pp: 1883–1896

Antonsson A. and Person J. I., (2009), Induction of Apoptosis by Staurosporine Involves the Inhibition of Expression of the Major Cell Cycle Proteins at the G2/M Checkpoint accompanied by Alterations in Erk and Akt Kinase activities, *Anticancer Research.,* 29 (8), pp: 2893-2898

Antwerpen M. H., Georgi E., Zoeller L., Woelfel R., Stoecker K. and Scheid P., (2015), Whole-Genome Sequencing of a Pandoravirus Isolated from Keratitis-Inducing *Acanthamoeba,* G*enome Announc,* 3 (2)

Arambage S. C., Grant K. M., Pardo I., Ranford-Cartwright L. and Hurd H., (2009), Malaria ookinetes exhibit multiple markers for apoptosis-like programmed cell death in vitro *Paras Vectors*, 2 (1), pp: 32-40

Arbel N. and Shoshan-Barmatz V., (2010), Voltage-dependent Anion Channel 1-based Peptides Interact with Bcl-2 to Prevent Antiapoptotic Activity, *The Journal of Biological Chemistry*, 285 (9), pp: 6053–6062

Arnoult D., Tatischeff I., Estaquier J., Girard M., Sureau F., Grodet A. and Dellinger M., (2001), On the evolutionary conservation of the cell death pathway: mitochondrial release of an apoptosis-inducing factor during *Dictyostelium discoideum* cell death, *Mol Biol Cell*, 12 (10), pp: 16-30

Ashkenazi A. and Dixit V. M., (1998), Death receptors: signaling and modulation, *Science,* 28 (281), pp: 1305-1308

Aurrecoechea C., Barreto A., Brestelli J., Brunk B. P., Caler E. V., Fischer S., Gajria B., Gao X., Gingle A., Grant G., Harb O. S., Heiges M., Iodice J., Kissinger J. C., Kraemer E. T., Li W., Nayak V., Pennington C., Pinney D. F., Pitts B., Roos D. S., Srinivasamoorthy G., Stoeckert C. J. Jr, Treatman C. and Wang H., (2011), AmoebaDB and MicrosporidiaDB: functional genomic resources for Amoebozoa and Microsporidia species, *Nucleic Acids Research*, 39 (1), pp: 612–619

Azad M. A., Finnin B. A., Poudyal A., Davis K., Li J., Hill P. A., Nation R. L., Velkov T. and Li J., (2013), Polymyxin B Induces Apoptosis in Kidney Proximal Tubular Cells, *Antimicrob Agents Chemother*; 57 (9), pp: 4329-4335

Azad M. A., Akter J., Rogers K. L., Roger L. N., Velkov T. and Li J., (2015), Mechanisms of Action: Physiological Effects Major Pathways of Polymyxin-Induced Apoptosis in Rat Kidney Proximal Tubular Cells Mohammad, *Antimicrob. Agents Chemother*, 59 (4), pp: 2136-2143

Bacon J. A., Linseman D. A, Raczniak T. J., (1990), In vitro cytotoxicity of tetracyclines and aminoglycosides in LLC-PK1, MDCK and Chang continuous cell lines, *Toxicology in Vitro*, 4 (4-5), pp: 384-388

Bader M. and Steller H., (2009), Regulation of cell death by the ubiquitin-proteasome system, *Current Opinion in Cell Biology*, 21 (6), pp: 878-890

Baehrecke E.H., (2002), How death shapes life during development, *Nat Rev Mol Cell Biol*, 3 (10) pp: 779–787

Bai L., Smith D.C., Wang S., (2014), Small-molecule SMAC mimetics as new cancer therapeutics, *Pharmacology Therapeutics*, 144 (1), pp: 82–95

Baksh S., Tommasi S., Fenton S., Yu V. C., Martins L. M., Pfeifer G. P., Latif F., Neel D.G., Downward J., (2005), The tumor suppressor RASSF1A and MAP-1 link death receptor signaling to Bax conformational change and cell death, *Mol. Cell,* 18 (6), pp: 637–650

Bapteste E., (2002), The analysis of 100 genes supports the grouping of three highly divergent amoebae: *Dictyostelium, Entamoeba and Mastigamoeba*, Proceedings of the *National Academy of Sciences*, 99 (3), pp: 1414–1419

Bastianutto C., Clementi E., Codazzi F., Podini P., De Giorgi F., Rizzuto R., (1995), Overexpression of calreticulin increases the Ca^{+2} capacity of rapidly exchanging Ca^{+2} stores and reveals aspects of their lumenal microenvironment and function, *J Cell Biol*, 130 (4), pp: 847–855

Brindley N, Matin A., Khan N. Ahmed, (2009), *Acanthamoeba* castellanii: High antibody prevalence in racially and ethnically diverse populations, 121 (3), pp: 254-256

Bursch, W., (2001), The autophagosomal-lysosomal compartment in programmed cell death, *Cell Death Differ*., 8 (6), pp: 569 – 581

Byun J.Y., Yoon C.H., An S., Park I.C., Kang C.M., Kim M.J., Lee S.J., (2009), The Rac1/MKK7/JNK pathway signals upregulation of Atg5 and subsequent autophagic cell death in response to oncogenic Ras, *Carcinogenesis,* 30 (11), pp:1880–1888

Behera H.S., Satpathy G, (2016), Characterisation and expression analysis of trophozoite and cyst proteins of *Acanthamoeba* spp. isolated from *Acanthamoeba* keratitis (AK) patient, *Mol Biochem Parasitol*., 205 (1-2) pp: 29-34

Besteiro, S., Williams, R. A. M., Morrison, L. S., Coombs, G. H. and Mottram, J. C., (2006), Endosome sorting and autophagy are essential for differentiation and virulence of *Leishmania* Major, J. *Biol. Chem*, 281 (16), pp: 11384–11396

Boughalmi M., Pagnier I., Aherfi S., Colson P., Raoult D., La Scola B., (2013), First Isolation of a Marseillevirus in the Diptera Syrphidae Eristalis tenax, *Intervirology,* 56 *(*6), pp: 386–394

Bootmana D, Chehaba T., Bultynckb G., Parysb B., Rietdorfa K., (2018), The regulation of autophagy by calcium signals: Do we have a consensus?, *Cell Calcium*, 70, pp: 32–46

Bradley S.G. and Marciano-Cabral F., (1996), Diversity of free-living 'naked' amoeboid organisms, Journal of Industrial Microbiology, 17 (3-4), pp: 314-321

Brennanda A., Gualdrón-López M., Coppens I., Rigdend D. J., Ginger M. L., Michels A.M., (2011), Autophagy in parasitic protists: Unique features and drug targets, *Molecular and Biochemical Parasitology*, 177 (2), pp: 83–99

Brindley, N., Matin, A. and Khan, N. A., (2009), '*Acanthamoeba castellanii*: High antibody prevalence in racially and ethnically diverse populations', *Experimental Parasitology*, 121(3), pp: 254–256

Brown T. J., Cursons R. T. and Keys E. A., (1982), Amoebae from antarctic soil and water*, Applied Environmental Microbiology,* 44 (2), pp: 491-493

Brustovetsky, N., Brustovetsky, T., Jemmerson, R. and Dubinsky, J. M., (2002), Calcium-induced cytochrome c release from CNS mitochondria is associated with the permeability transition and rupture of the outer membrane, *Journal of Neurochemistry*, 80 (2), pp: 207–218

Booton, G. C., Kelly D. J., Chu Y. W., Seal D. V., Houang E., Lam D. S., Byers T. J. and Fuerst P., (2002), 18S ribosomal DNA typing and tracking of *Acanthamoeba* species isolates from corneal scrape specimens, contact lenses, lens cases and home water supplies of *Acanthamoeba* keratitis patients in Hong Kong, *Journal of Clinical Microbiology*, 40 (5), pp: 1621–1625

Bok, J., Wang, Q., Huang, J. and Green, S. H., (2007), CaMKII and CaMKIV mediate distinct prosurvival signaling pathways in response to depolarization in neurons. Molecular and Cellular Neurosciences, 36 (1), pp: 13–26

Callsen D. and Brune B., (1999), Role of mitogen-activated protein kinases in S-nitrosoglutathione-induced macrophage apoptosis, *Biochemistry,* 38 (8), pp: 2279–2286

Cammaroto G., Astorga F. J., Navarro A., Olive T. and Pumarola F., (2015), *Acanthamoeba* rhinosinusitis: A paediatric case report and a review of the literature, *International Journal of Pediatric Otorhinolaryngology,* 10 (3), pp: 70–73

Cangol and Chambar, (2010), ERK and cell death: Mechanisms of ERK-induced cell death apoptosis, autophagy and senescence, *FEBS Journal,* 277 (1), pp: 2–21

Carrijo-Carvalho L. C., Santana V. P., Foronda A. S., de Freitas D. and de Souza Carvalho F. R., (2017), Therapeutic agents and biocides for ocular infections by free-living amoebae of *Acanthamoeba* genus, *Survey of Ophthalmology*, 62 (2) , pp: 203-218

Casper T., Basset D. and Leclercq C., (1999), Disseminated *Acanthamoeba* infection in a patient with AIDS: response to 5-fluorocytosine therapy, *Clin Infect Dis*., 29 (4), pp: 944-945

Cavalier-Smith T., Chao E. and Oates B., (2004), Molecular phylogeny of Amoebozoa and the evolutionary significance of the *Phalansterium*, *Eur. J. Protistol.,* 40 (1), pp: 4821–4823

Chafké A. B., Hillion J. and Ségal-Bendirdjian E., (2001), *Oncogene*, Staurosporine induces apoptosis through both caspase-dependent and caspase-independent mechanisms, 7 (20), pp: 3354-3362

Chaitankar V., Karakülah G., Ratnapriya R., Giuste F., Brooks M. J. and Swaroop A., (2016), Next generation sequencing technology and genomewide data analysis: Perspectives for retinal research, *Prog Retin Eye Res*, 55, pp:1-31

Chappell C. L., Wright J. A., Coletta M. and Newsome A. L., (2001), Standardized method of measuring *Acanthamoeba* antibodies in sera from healthy human subjects, *Clinical and Diagnostic Laboratory Immunology*, 8 (4), pp: 724–730

Chipuk J. E. and Douglas R. G, (2005), Do inducers of apoptosis trigger caspase-independent cell death?, *Nature Reviews Molecular Cell Biology,* 6 (3), pp: 268–275

Christensen P., Owens T. G., Devol A. H. and Packard T. T., (1980), Respiration and physiological state in marine bacteria, *Mar. Biol*.,55 (4), pp: 267-276

Chiu V. K., Bivona T., Hach A., Bernard Sajous J., Silletti J., Wiener H., Johnson R. L., Cox A.D. and Philips M.R., (2002), Ras signalling on the endoplasmic reticulum and the Golgi, *Nature cell biology*, 4 (5), pp: 343-350

Choi D. W., (1992), Calcium: still center-stage in hypoxic-ischemic neuronal death, *Journal Neurobiol*., 18 (2), pp: 58-60

Circu M. L. and Aw, T. Y., (2012), Glutathione and modulation of cell apoptosis, *Biochimica et Biophysica Acta*, 1823 (10), pp: 1767–1777

Cirillo J. D., Falkow S. and Tompkins L. S., (1994), Growth of *Legionella pneumophila* in *Acanthamoeba* castellanii enhances invasion, *Infect Immun*., 62 (8), pp: 3254-3261

Cirillo J. D., Falkow S., Tompkins L. S. and Bermudez L. E., (1997), Interaction of *Mycobacterium avium* with environmental amoebae enhances virulence, *Infection and Immunity*, 65 (9), pp: 3759–3767

Clapham, (2007), Calcium Signalling, *Cell*, 131 (6), pp: 1047-1058

Clarholm M., (2002) Bacteria and protozoa as integral components of the forest ecosystem -Their role in creating a naturally varied soil fertility, *International Journal of General and Molecular Microbiology*, 81 (1-4), pp: 309–318

Clarke P. G. and Clarke S., (1995), Historic apoptosis, *Nature* 378 (6554), pp: 230

Clarke P. G. and Clarke S., (1996), Nineteenth century research on naturally occurring cell death and related phenomena, *Anat Embryol,* 193 (2), pp: 81–99

Clarke B., Sinha A.., Parmar D.N. and Sykakis E., (2012), Advances in the Diagnosis and Treatment of *Acanthamoeba* Keratitis, *Journal of Ophthalmology*, 2012; 484892

Clarke, M., Lohan J. A., Liu B., Lagkouvardos I., Roy S, Zafar N., Bertelli C, Schilde C., Kianianmomeni A., Bürglin T.R., Frech C., Turcotte B., Kopec K, Synnott M.J., Choo C., Paponov I., Finkler A., Soon Heng Tan C., Hutchins A.P., Weinmeier T., Rattei T, Chu J.S.C., Gimenez G., Irimia M, Rigden D.J., Fitzpatrick D.A., Lorenzo-Morales J., Bateman A., Cheng-Hsun Chiu, Tang P, Hegemann P., Fromm H., Raoult D., Gilbert Greub, Miranda-Saavedra D., Nansheng C., Nash P., Ginger M. L., Horn M, Schaap P., Caler L. and Loftus B.J., (2013), Genome of *Acanthamoeba castellanii* highlights extensive lateral gene transfer and early evolution of tyrosine kinase signaling, Genome Biology, 14 (2)

Creach V., Baudoux A. C., Bertru G., Rouzic B. L., (2003), Direct estimate of active bacteria: CTC use and limitations, *J. Microbiol. Methods,* 52 (1), pp: 19–28

Cohen G. M., (1997), Caspases: the executioners of apoptosis, *Biochem,* 326 (1), pp: 1–16

Colson P., Pagnier I., Ghislain N.Y., La Scola B. and Raoult D., (2013), Marseilleviridae, a new family of giant viruses infecting amoebae, *Archives of Virology*, 158 (4), pp: 915–920

Corney and Basturea, (2015), RNA-seq Using Next Generation Sequencing, *Labome*, *MATER METHODS* (3), pp: 203

Cory S. and Adams J. M., (2002), The Bcl2 family: regulators of the cellular life-or-death switch, *Nature Reviews Cancer*, 2 (9), pp: 647–656

Corsaro D., Walochnik M. J., Köhsler M. and Rott B., (2015), *Acanthamoeba* misidentification and multiple labels: redefining genotypes T16, T19 and T20 and proposal for *Acanthamoeba micheli spp*. nov., (Genotype T19), *Parasitology research*, 114 (7), pp: 2481–2490

Costas M. and Griffiths A. J., (1980), The suitability of starch-gel electrophoresis of esterases and acid-phosphatases for the study of Acanthamoeba taxonomy', *Archiv fur Protistenkunde*, 123 (3), pp: 272–279

Costas, M. and Griffiths A. J., (1985), Enzyme composition and the taxonomy of *Acanthamoeba*, *The Journal of Protozoology*, 32 (4), pp: 604–607

Cuadrado A. and Nebreda A. R., (2010), Mechanisms and functions of p38 MAPK signaling, *Biochem J*ournal, (429), pp: 403-17

Culbertson C. G., Smith J. W. and Minner J. R., (1958), *Acanthamoeba*: Observations on Animal Pathogenicity', *Science*, 127 (3313), pp: 1506

Cullen P. and Lockyer P. J., (2002), Integration of calcium and RAS signalling, *Nature Reviews Molecular Cell Biology*, 3 (5), pp: 339–348

Cursons R. T., Brown T. J., Keys E. A., Moriarty K. M. and Till, D., (1980), Immunity to pathogenic free-living amoebae: Role of cellmediated immunity, *Infection and Immunity*, 29 (2), pp: 408–410

Dallaporta B., Hirsch T., Santos A., Zamzami S. N., Larochette N., Brenner C., Marzo I. and Kroemer G., (1998), Potassium Leakage During the Apoptotic Degradation Phase, *Journal Immunology*, 160 (11), pp: 5605-5615

Dart J. K., Saw V. P. and Kilvington S., (2009), *Acanthamoeba* keratitis: diagnosis and treatment update, *American Journal of Ophthalmology*., 148 (4), pp: 487-499

Das M., Mukherjee S. B. and Shaha C., (2001), Hydrogen peroxide induces apoptosis-like death in Leishmania donovani promastigotes, *Journal Cell Sci*., (114), pp: 2461-69

Datan E., Shirazian A., Benjamin S., Matassov D., Malorni W., Lockshin R. A., Garcia-Sastre A. and Zakeri Z., (2014), mTOR/p70S6K signaling distinguishes routine, maintenance-level autophagy from autophagic cell death during influenza A infection, *Virology*, 452–453, pp: 175–190

Degterev A., Hitomi J., Germscheid M., Ch'en IL, Korkina O., Teng X., Abbott D., Cuny G. D., Yuan C., Wagner G., Hedrick S. M., Gerber S. A., Lugovskoy A. and Yuan J., (2008), Identification of RIP1 kinase as a specific cellular target of necrostatins, *Nat Chem Biol*., 4(5), pp: 313-21

Dehne N., Rauen U., de Groot H. and Lautermann J., (2002), Involvement of the mitochondrial permeability transition in gentamicin ototoxicity, *Hear Res*, 169 (1-2), pp:47-55

Delic, J., Morange, M. and Magdelenat, H., (1993), Ubiquitin pathway involvement in human lymphocyte gamma-irradiation-induced apoptosis, *Molecular and Cellular Biology*, 13 (8), pp: 4875–4883

Detke, S. and Paule, M. R., (1975), DNA-dependent RNA polymerases from *Acanthamoeba castellanii*: Properties and levels of activity during encystment, *Biochimica e Biophysica Acta*, 383, pp: 67–77

De Jonckheere J. F., (1983), Isoenzyme and total protein analysis by agarose isoelectric focusing and taxonomy of the genus *Acanthamoeba*, *The Journal of Protozoology*, 30 (4), pp: 701–706

Deluol A. M., Teilhac M. F. and Poirot J. L., (1996), Cutaneous lesions due to *Acanthamoeba spp*. in a patient with AIDS, *Journal Eukaryot Microbiol*., 43 (5), pp: 130-131

Deniaud A., O Sharaf El D., Maillier E., Poncet D., Kroemer G., Lemaire C. and Brenne C., (2007), Endoplasmic reticulum stress induces calcium-dependent permeability transition, mitochondrial outer membrane permeabilization and apoptosis, *Oncogene*, 27 (3), pp: 285–299

Dey R., Hoffman P. S. and Glomski I. J., (2012), Germination and amplification of anthrax spores by soil-dwelling amoebae, *Applied and Environmental Microbiology*, 78 (22), pp: 8075–8081

Dhanasekaran D. N. and Reddy E. P., (2008), JNK Signaling in Apoptosis, *Oncogene*, 27 (48), pp: 6245–6251

Dickson J. M., Zetler P. J., Walker B. and Javer A. R., (2009), *Acanthamoeba* Rhinosinusitis, *Journal of Otolaryngology-Head and Neck Surgery*, 38 (3), pp: 87-90

Doczi J., Turiák L., Vajda S., Mándi M., Töröcsik B., Gerencser A. A., Kiss G., Konràd C., Adam-Vizi V. and Chinopoulos C., (2010) ,Complex Contribution of Cyclophilin D to Ca^{2+}-induced Permeability Transition in Brain Mitochondria, with Relation to the Bioenergetic State, *Biological Chemistry,* 286 (8), pp: 6345–6353

Dong Z., Saikumar P., Patel Y., Weinberg J. M. and Venkatachalam M. A., (2000), Serine protease inhibitors suppress cytochrome c-mediated caspase-9 activation and apoptosis during hypoxia-reoxygenation, *Biochem. J.*, 347 (3), pp: 669–677

Dornas F., Jacques Y. B., Pagnier I. K., Raoult D, Abrahao A. and La Scola B., (2015), Isolation of new Brazilian giant viruses from environmental samples using a panel of protozoa, *Front Microbiol*., 6 (1086), pp: 1086-94

Douglas, M., (1930), Notes on the classification of the amoeba found by Castellani in cultures of a yeast-like fungus, *Journal of Tropical Medicine and Hygiene*, 33 (160), pp: 258–259

Doutre G., Nadège P., Abergel S. and Claveriea J. M., (2014), Genome Analysis of the First Marseilleviridae Representative from Australia Indicates that Most of Its Genes Contribute to Virus Fitness, *Journal Virol*ojy, 88 (24), pp: 40-49

Doutre G., Arfib B., Rochette P., laverie J. M., Bonin P. and Abergel S., (2015), Complete Genome Sequence of a New Member of the Marseilleviridae Recovered from the Brackish Submarine Spring in the Cassis Port-Miou Calanque, France *Genome Announc*., 3(6)

Dunand V. A., Hammer S. M., Rossi R., Poulin M., Albrecht M. A., Doweiko J. P., DeGirolami P. C., Coakley E., Piessens E. and Wanke C. A.., (1997), Parasitic sinusitisand otitis in patients infected with human immunodeficiency virus: report of five cases and review, *Clin Infect Dis*., 25 (2), pp: 267-272

Duszenko M., Figarella K., Macleod E.T. and Welburn S.C., (2006), Death of a trypanosome: a selfish altruism, *Trends Parasitol*ogy, 22 (11), pp: 536-542

Duszenko, M., Ginger, M. L., Brennand, A., Gualdrón-López, M., Colombo, M. I., Coombs, G. H. and Michels, P. A., (2011), Autophagy in protists, *Autophagy*, 7 (2), pp: 127–158,

Edgar R. C., (2004), MUSCLE: multiple sequence alignment with high accuracy and high throughput, *Nucleic Acids Research*, 32 (5) pp: 1792-1797

Egger L., Schneider J., Rhême C., Tapernoux M, Häcki J. and Borner C., (2002), Serine proteases mediate apoptosis-like cell death and phagocytosis under caspase-inhibiting conditions, *Cell Death and Differentiation,* 10 (10), pp: 1188–1203

Elmore S., (2007), Apoptosis: A Review of Programmed Cell Death, *Toxicol Pathol.,* 35 (4) pp: 495–516

El-Etr, S., Jeffrey H., Margolis J., Monack D, Robison R. A, Cohen M., Moore E. and Rasley A., (2009) Francisella tularensis type A strains cause the rapid encystment of *Acanthamoeba castellanii* and survive in amoebal cysts for three weeks postinfection', *Applied and Environmental Microbiology*, 75 (23), pp: 7488–7500

Essig A., Heinemann M., Simnacher U. and Marre R., (1997), Infection of *Acanthamoeba castellanii* by *Chlamydia pneumoniae*, *Applied and Environmental Microbiology*, 63 (4), pp: 1396–1399

Fabre E., Jeudy S., Santini S., Legendre M., Trauchessec M., Couté Y., Claverie J. M. and Abergel S., (2017), Noumeavirus replication relies on a transient remote control of the host nucleus, *Nature Communications,* 8 (15), pp:147-151

Fedurco M., Romieu A., Williams S., Lawrence I. and Turcatti G., (2006), BTA, a novel reagent for DNA attachment on glass and efficient generation of solid-phase amplified DNA colonies, *Nucleic Acids Res*., 34 (3), e: 22

Felsenstein J., (1985), Confidence limits on phylogenies: An approach using the bootstrap, *Evolution*, 39 (4) pp: 783-791

Fernald K. and Kurokawa M., (2013), Evading apoptosis in cancer, *Trends in Cell Biology*, 23 (12), pp: 620–633

Festjens N., Berghe V. T. and Vandenabeele P., (2006), Necrosis, a well-orchestrated form of cell demise: signaling cascades, important mediators and concomitant immune response, *Biochim Biophys Acta*, 1757, pp: 1371–1387

Fink S. L. and Cookson B. T., (2005), Apoptosis, pyroptosis and necrosis: mechanistic description of dead and dying eukaryotic cells, *Infect Immun*., 73(4), pp: 1907-16

Florey O., Kim S. E., Sandoval C. P., Haynes C.M. and Overholtzer M., (2011), Autophagy machinery mediates macroendocytic processing and entotic cell death by targeting single membranes, *Cell Biol.*, 13 (11), pp :1335–1343

Fukui Y. and Katsumaru H., (1980), Dynamics of nuclear actin bundle induction by dimethyl sulfoxide and factors affecting its development, *J. Cell Biology*, 84 (1), pp: 131-140

Fournier G., Ducet A. and Crevat, (1987), Action of cyclosporine on mitochondrial calcium fluxes, *Journal of Bioenergetics and Biomembranes*, 19 (3), pp: 297-301

Galburt E. A. and Stoddard B. L., (2002), Catalytic Mechanisms of Restriction and Homing Endonucleases, *Biochemistry*, 41 (47), pp: 13851-13860

Galluzzi, L., Vitale, I., Aaronson, S. A., Abrams, J. M., Adam, D., Agostinis, P., Alnemri, E. S., Altucci, L., Amelio, I., Andrews, D. W., Annicchiarico-Petruzzelli, M., Antonov, A. V., Arama, E., Baehrecke, E. H., Barlev, N. A., Bazan, N. G., Bernassola, F., Bertrand, M., Bianchi, K., Blagosklonny, M. V., Blomgren, K., Borner, C., Boya, P., Brenner, C., Campanella, M., Candi, E., Carmona-Gutierrez, D., Cecconi, F., Chan, F. K., Chandel, N. S., Cheng, E. H., Chipuk, J. E., Cidlowski, J. A., Ciechanover, A., Cohen, G. M., Conrad, M., Cubillos-Ruiz, J. R., Czabotar, P. E., D'Angiolella, V., Dawson, T. M., Dawson, V. L., De Laurenzi, V., De Maria, R., Debatin, K. M., DeBerardinis, R. J., Deshmukh, M., Di Daniele, N., Di Virgilio, F., Dixit, V. M., Dixon, S. J., Duckett, C. S., Dynlacht, B. D., El-Deiry, W. S., Elrod, J. W., Fimia, G. M., Fulda, S., García-Sáez, A. J., Garg, A. D., Garrido, C., Gavathiotis, E., Golstein, P., Gottlieb, E., Green, D. R., Greene, L. A., Gronemeyer, H., Gross, A., Hajnoczky, G., Hardwick, J. M., Harris, I. S., Hengartner, M. O., Hetz, C., Ichijo, H., Jäättelä, M., Joseph, B., Jost, P. J., Juin, P. P., Kaiser, W. J., Karin, M., Kaufmann, T., Kepp, O., Kimchi, A., Kitsis, R. N., Klionsky, D. J., Knight, R. A., Kumar, S., Lee, S. W., Lemasters, J. J., Levine, B., Linkermann, A., Lipton, S. A., Lockshin, R. A., López-Otín, C., Lowe, S. W., Luedde, T., Lugli, E., MacFarlane, M., Madeo, F., Malewicz, M., Malorni, W., Manic, G., Marine, J. C., Martin, S. J., Martinou, J. C., Medema, J. P., Mehlen, P., Meier, P., Melino, S., Miao, E. A., Molkentin, J. D., Moll, U. M., Muñoz-Pinedo, C., Nagata, S., Nuñez, G., Oberst, A., Oren, M., Overholtzer, M., Pagano, M., Panaretakis, T., Pasparakis, M., Penninger, J. M., Pereira, D. M., Pervaiz, S., Peter, M. E., Piacentini, M., Pinton, P., Prehn, J., Puthalakath, H., Rabinovich, G. A., Rehm, M., Rizzuto, R., Rodrigues, C., Rubinsztein, D. C., Rudel, T., Ryan, K. M., Sayan, E., Scorrano, L., Shao, F., Shi, Y., Silke, J., Simon, H. U., Sistigu, A., Stockwell, B. R., Strasser, A., Szabadkai, G., Tait, S., Tang, D., Tavernarakis, N., Thorburn, A., Tsujimoto, Y., Turk, B., Vanden Berghe, T., Vandenabeele, P., Vander Heiden, M. G., Villunger, A., Virgin, H. W., Vousden, K. H., Vucic, D., Wagner, E. F., Walczak, H., Wallach, D., Wang, Y., Wells, J. A., Wood, W., Yuan, J., Zakeri, Z., Zhivotovsky, B., Zitvogel, L., Melino, G. and Kroemer, G., (2018), Molecular mechanisms of cell death: recommendations of the Nomenclature Committee on Cell Death 2018, *Cell Death and Differentiation*, 25 (3), pp: 486–541

Gautam P. L., Sharma S., Puri S., Kumar R., Midha V. and Bansal, R., (2012), A rare case of survival from primary amebic meningoencephalitis, *Indian Journal of Critical Care Medicine,* 16 (1), pp: 34–36

Gimble F. and Wang J., (1996), Substrate Recognition and Induced DNA Distortion by the PI-SceI Endonuclease, an Enzyme Generated by Protein Splicing, *Journal of Molecular biology*, 263, (2), pp: 163-180

Gokhale N. S., (2008), Medical management approach to infectious keratitis, *Indian Journal of Ophthalmology*, 56 (3), pp: 215–220

Golstein P. and Kroemer G., (2007), Cell death by necrosis: towards a molecular definition, Trends *Biochem Sci,* (32) pp: 37–43

Gordon D. J., Eisenberg E. and Korn E. D., (1976), Characterization *Acanthamoeba* of cytoplasmic actin isolated from *Acanthamoeba castellanii* by a new method, *The Journal of Biological Chemistry*, 251 (15) pp: 4778–4786

Green D. R. and Kroemer G., (2004), The pathophysiology of mitochondrial cell death, *Science,* 305 (5684), pp: 626–629

Greub G. and Raoult D., (2004), Microorganisms resistant to free-living amoebae, *Clinical Microbiology Reviews*, 17 (2), pp: 413–433

Greub G. and Scola B. La., (2003), Parachlamydia *acanthamoeba* is endosymbiotic or lytic for *Acanthamoeba polyphaga* depending on the incubation temperature, *Annals of the New York Academy of Sciences*, 990, pp: 628–634

Gooday A. J., Aranda da Silva A. and Pawlowski J., (2011), Xenophyophores (Rhizaria, Foraminifera) from the Nazaré Canyon (Portuguese margin, NE Atlantic), *The Geology, Geochemistry and Biology of Submarine Canyons West of Portugal*, 58 (23–24), pp: 2401–2419

Gotoh T., Terada K., Oyadomari S. and Mori M., (2004), hsp70-DnaJ chaperone pair prevents nitric oxide- and CHOP-induced apoptosis by inhibiting translocation of bax to mitochondria., *Cell Death Differ*., (11), pp: 390–402

Guenette R. S., Mooibroek M., Wong K., Wong P. and Tenniswood M., (1994), Cathepsin B, a cysteine protease implicated in metastatic progression, is also expressed during regression of the rat prostate and mammary glands, *Eur J Biochem,* 226 (2), pp: 311–321

Gunter T. E., Buntinas L., Gunter K. K. and Sparagna G. C., (2004), The rapid mode of calcium uptake into heart mitochondria (RaM): comparison to RaM in liver mitochondria, *Biochimica et Biophysica Acta (BBA) – Bioenergetics,* 1504 (2-3), pp: 248-261

Guarner J., Bartlett J., Shieh W., Paddock C., Visvesvara G. and Zaki S., (2007), Histopathologic spectrum and immunohistochemical diagnosis of amebic meningoencephalitis, *Modern pathology*, 20, (12), pp: 1230–1237

Gump J. M. and Thorburn A., (2011), Autophagy and apoptosis- what's the connection? Trends in Cell Biology, 21 (7), pp: 387–392

Gutierrez-Carmona, Frohlich K. U., Kroemer G. and Madeo F., (2010), Metacaspases are caspases. Doubt no more*, Cell Death and Differentiation*, 17 (3), pp: 377–378

Haas B., Dobin A., Stransky N., Li B., Yang X., Tickle T., Bankapur A., Ganote C., Doak T., Pochet N., Jing Sun, Wu C., Gingeras T. and Regev A., (2017), STAR-Fusion: Fast and Accurate Fusion, Transcript Detection from RNA-Seq, Cold Spring Harbor, bioRxiv: 120295

Hara T., Nakamura K., Matsui M., Yamamoto A., Nakahara Y., Suzuki-Migishima R., Yokoyama M., Mishima K., Saito I., Okano H. and Mizushima N., (2006), Suppression of basal autophagy in neural cells causes neurodegenerative disease in mice, *Nature*, 441 (7095), pp: 885–889

Harvey R., Cornellisen C. N. and Fisher D. B., (2013), Protozoa', in Richard A. Harvey Lippincott's Illustrated Reviews: Microbiology, Third. Baltimore: Walters Kluwer, pp: 448

Harwood C. R., Rich G. E., McAleer R. and Cherian G., (1988), Isolation of *Acanthamoeba* from a cerebral abscess, *Med J*., 148 (1), pp: 47–49

Hassan M., Feyen A. O., Mirmohammadsadegh A., Essmann F., Tannapfel A., Gulbins E., Schulze-Osthoff K. and Hengge H., (2008), The BH3-only member Noxa causes apoptosis in melanoma cells by multiple pathways, *Oncogene,* 27 (33), pp: 4557–4568

Helms M., Ambit A., Appleton P., Tetley L., Coombs G. H. and Mottram J. C., (2006), Bloodstream form Trypanosoma brucei depend upon multiple metacaspases associated with RAB11-positive endosomes, *Journal of Cell Science,* 119 (6), pp: 1105-1117

Hibberd, D. J., (1971), Observations on the cytology and ultrastructure of *Chrysamoeba radians klebs* (Chrysophyceae), *British Phycological Journal*, 6 (2), pp: 207–223

Hill S. M., Hao X., Liu B. and Nyström T., (2014), Life-span extension by a metacaspase in the yeast *Saccharomyces cerevisiae*, *Science*, 344 (6190), pp: 1389–1392

Holley S. L., Fryer A. A., Haycock W. J., Grubb S.W., Strange C. R. and Hoban P.R, (2007), Differential effects of glutathione S -transferase pi (GSTP1) haplotypes on cell proliferation and apoptosis , *Carcinogenesis*, 28 (11), pp: 2268–2273

Hoon Jae Bae, Jong-Wook Park and Taeg Kyu Kwon, (2003), Ruthenium red, inhibitor of mitochondrial Ca2+ uniporter, inhibits curcumin-induced apoptosis via the prevention of intracellular Ca^{+2} depletion and cytochrome c release, *Biochemical and Biophysical Research Communications*, 4 (303), pp: 1073-1079

Hosoi T., Keisuke T., Kanako N. and Koichiro O., (2014), Caffeine attenuated ER stress-induced leptin resistance in neurons, *Neuroscience Letters*, 569, pp: 23-26

Howard P. L., Chia M. C., Del Rizzo S., Liu F. F., Pawson T., (2003), Redirecting tyrosine kinase signaling to an apoptotic caspase pathway through chimeric adaptor proteins, *Proceedings of the National Academy of Sciences*, 100 (20), pp: 11267–11272

Huang S., Jia K., Wang Y., Zhou Z. and Levine B., (2013), Autophagy genes function in apoptotic cell corpse clearance during C. elegans embryonic development, *Autophagy*, 9 (2), pp: 138–149

Hunt S. J., Reed S. L. and Mathews W. C., (1995), Cutaneous *Acanthamoeba* infection in the acquired immunodeficiency syndrome: response to multidrug therapy, *Cutis*, 56 (5), pp: 285-287

Hunter, D. R. and Haworth, R. A., (1979), The Ca2+-induced membrane transition in mitochondria. I. The protective mechanisms, *Archives of Biochemistry and Biophysics,* 195 (2), pp: 453–459

Hughes F. M., Evans-Storms R. B. and Cidlowski J. A., (1998), Evidence that non-caspase proteases are required for chromatin degradation during apoptosis, *Cell Death Differ*., 5 (12), pp: 1017–1027

Howe C. L., Valletta J. S., Rusnak A. S., Mobley W. C., (2001), NGF signaling from clathrincoated vesicles: evidence that signaling endosomes serve as a platform for the Ras-MAPK pathway, *Neuron* 32 (5), pp: 801–14

Ikeda Y., Miyazaki D., Yakura K., Kawaguchi A., Ishikura R., Inoue Y., Mito T., Shiraishi A., Ohashi Y., Higaki S., Itahashi M., Fukuda M., Shimomura Y. and Yagita K., (2012), Assessment of realtime polymerase chain

reaction detection of *Acanthamoeba* and prognosis determinants of *Acanthamoeba* keratitis, *Ophthalmology*, 119 (6), pp: 1111–1119

Inbal B., Bialik S., Sabanay I., Shani G. and Kimchi A., (2002), DAP kinase and DRP-1 mediate membrane blebbing and the formation of autophagic vesicles during programmed cell death, *Journal Cell Biol*., 157 (3), pp: 455–46

Inglis T. J., Rigby P., Robertson T. A., Dutton S. N., Henderson M. and Chang J. B., (2000), Interaction between Burkholderia pseudomallei and *Acanthamoeba* Species Results in Coiling Phagocytosis, Endamebic Bacterial Survival and Escape, *Infect Immun*., 68 (3), pp: 1681–1686

Iturriaga R., Zhang S., Sonek G. J. and Stibbs H., (2001), Detection of respiratory enzyme activity in Giardia cysts and Cryptosporidium oocysts using redox dyes and immunofluorescence techniques, *Journal Microbiol. Methods,* 46 (1), pp: 19–28

Jang E. R. and Galperin E., (2016), The function of Shoc2: A scaffold and beyond, *Communicative and Integrative Biology*, 9 (4), pp: 241-247

Jesenberger V. and Jentsch S., (2002), Deadly encounter: ubiquitin meets apoptosis, *Nat Rev Mol Cell Biol*., 3 (2), pp: 112-121

Jin Q.H., Zhao B. and Zhang X.J., (2004), Cytochrome c release and endoplasmic reticulum stress are involved in caspase-dependent apoptosis induced by G-418, *Cell. Mol. Life Sci*., 61 (14), pp: 1816-21

Johnson N. L., Gardner A. M., Diener K. M., Lange-Carter C. A., Gleavy J., Jarpe M. B., Minden A., Karin M., Zon L. I. and Johnson G. L., (1996), Signal Transduction Pathways Regulated by Mitogen-activated/Extracellular Response Kinase Kinase Kinase Induce Cell Death, *Journal Biol. Chem.*, 271 (6), pp: 3229–3237

Johnson D.E., (2000), Non-caspase proteases in apoptosis, *Leukemia*, 14 (9), pp: 1695 – 1703

John T., Lin J. and Sahm D. F., (1990), *Acanthamoeba* keratitis successfully treated with prolonged propamidine isethionate and neomycin-polymyxin-gramicidin, *Annual Ophthalmol*, 22 (1), pp: 20-3

Joza N., Susin S. A., Daugas E., Stanford W. L., Cho S. K., Li C.Y., Sasaki T., Elia A. J., Cheng H. Y., Ravagnan L., Ferri K. F., Zamzami N., Wakeham A., Hakem R., Yoshida H., Kong Y. Y., Mak T. W., Zúñiga-Pflücker J. C., Kroemer G., Penninger J. M., (2001), Essential role of the mitochondrial apoptosis-inducing factor in programmed cell death, *Nature*, 29 (410), pp: 549-54

Kalai M., Van Loo G., Vanden B. T, Meeus A., Burm W., Saelens X. and Vandenabeele P., (2002), Tipping the balance between necrosis and apoptosis in human and murine cells treated with interferon and dsRNA, *Cell Death Differ*., 9 (9), pp :981-94

Karasawa T. and Steyger P. S., (2011), Intracellular mechanisms of aminoglycoside-induced cytotoxicity, *Integrative Biology*, 3 (9), pp: 879–886

Kauffmann-Zeh A., Rodriguez-Viciana P., Ulrich E., Gilbert C., Coffer P., Downward J. and Evan G., (1997), Suppression of c-Myc-induced apoptosis by Ras signalling through PI(3)K and PKB, *Nature*, 385 (6616), pp: 544–548

Kennedy D., Jäger R., Mosser D. D. and Samali A., (2014), Regulation of apoptosis by heat shock proteins, *IUBMB Life*., 66 (5), pp :327-38

Kim S. H., Moon E. K. , Hong Y., Chung D. I. and Kong H. H., (2015), Autophagy protein 12 plays an essential role in *Acanthamoeba* encystation, *Exp Parasitol*, (159), pp:46-52

Kimura M., (1980), A simple method for estimating evolutionary rate of base substitutions through comparative studies of nucleotide sequences, *Journal of Molecular Evolution,* 16 (2), pp: 111-120

King C. H, Shotts Jr., Wooley R. E. and Porter K. G., (1988), Survival of coliforms and bacterial pathogens within protozoa during chlorination, *Applied and Environmental* Microbiology, 54 (12), pp: 3023–3033

Kliescikova J., Kulda J. and Nohynkova E., (2011a), Propylene glycol and contact-lens solutions containing this diol induce pseudocyst formation in *acanthamoeba*e, *Experimental Parasitology*, 127 (1), pp: 326–328

Kliescikova J., Kulda J. and Nohynkova E., (2011b), Stress-induced pseudocyst formation - A newly identified mechanism of protection against organic solvents in *Acanthamoeba*e of the T4 genotype, *Protist*, 162 (1), pp: 58–69

Köhsler M., Leitsch D., Fürnkranz U., Duchêne M., Aspöck H. and Walochnik J., (2008), *Acanthamoeba* strains lose their abilities to encyst synchronously upon prolonged axenic culture, *Parasitol. Res*., 102 (5), pp: 1069-1072

Komatsu M., Waguri S., Chiba T., Murata S., Iwata J., Tanida I., Ueno T., Koike M., Uchiyama Y., Kominami E. and Tanaka K.., (2006), Loss of autophagy in the central nervous system causes neurodegeneration in mice, *Nature*, 441 (7095), pp: 880–884

Kong H. and Chung D., (1996), PCR and RFLP variation of conserved region of small ribosomal DNA among *Acanthamoeba* isolates assigned to either *A*. *castellanii* or A. polyphaga, *The Korean Journal of Parasitology*, 34 (2), pp: 127–134

Kosec G., Alvarez V. E., Agüero F., Sánchez D., Dolinar M., Turk B., Turk V. and Cazzulo J. J., (2006), Metacaspases of *Trypanosoma cruzi*: possible candidates for programmed cell death mediators, *Mol. Biochem. Parasitol*ogy, 145 (1), pp: 18–28

Kroemer G., Galluzzi L., Vandenabeele P., Abrams J., Alnemri E., Baehrecke E., Melino G., (2009), Classification of cell death*, Cell Death Differ*., 16 (1), pp: 3–11

Kruman I., Guo Q. and Mattson M. P., (1998), Calcium and reactive oxygen species mediate staurosporine-induced mitochondrial dysfunction and apoptosis in PC12 cells, *Neurosci. Res*., 51 (3), pp: 293–308

Kumar S., Stecher G. and Tamura K., (2016), MEGA7: Molecular Evolutionary Genetics Analysis Version 7.0 for bigger datasets, *Molecular Biology and Evolution,* 33 (7), pp: 1870–1874

Kwon J., Keiji Mochida, Yu-Lai Wang, Satoshi Sekiguchi, Tadashi Sankai, Shunsuk Aoki , Atsuo Ogura, Yasuhiro Yoshikaw and Keiji Wada., (2005), Ubiquitin C-Terminal Hydrolase L-1 Is Essential for the Early Apoptotic Wave of Germinal Cells and for Sperm Quality Control During Spermatogenesis, *Biology of Reproduction*, (73), pp: 29–35

Kwon J., Wang, Y. L., Setsuie R., Sekiguchi S., Sato, Y., Sakurai M. and Wada K., (2004), Two Closely Related Ubiquitin C-Terminal Hydrolase Isozymes Function as Reciprocal Modulators of Germ Cell Apoptosis in Cryptorchid Testis, *The American Journal of Pathology*, 165 (4), pp: 1367–1374

LaFerla F. M., Tinkle B. T., Bieberich C. J., Haudenschild C. C. and Jay G., (1995), The Alzheimer's A beta peptide induces neurodegeneration and apoptotic cell death in transgenic mice, *Nat Genetics,* 9 (1), pp: 21–30

Lalitha M. K., Anandi V., Srivastava A., Thomas K., Cherian A. M. and Chandi S. M., (1985), Isolation of *Acanthamoeba* culbertsoni from a patient with meningitis, *Journal Clin. Microbiol*., 21 (4) pp: 666–667

Legendre M., Defne A., Chantal A. and Claverie J. M., (2012), Genomics of Megavirus and the elusive fourth domain of Life, *Communicative and Integrative Biology*, 5 (1), pp: 102-106

Lanneau D., de Thonel A., Maurel, S., Didelot C. and Garrido C., (2007), Apoptosis Versus Cell Differentiation: Role of Heat Shock Proteins HSP90, HSP70 and HSP27, *Prion*, 1 (1), pp: 53–60

Lanneau D., Brunet M., Frisan E., Solary E., Fontenay M. and Garrido C., (2008), Heat shock proteins: essential proteins for apoptosis regulation, *Journal of Cellular and Molecular Medicine*, 12 (3), pp: 743–761

Łanocha-Arendarczyk N., Kolasa-Wołosiuk A., Wojciechowska-Koszko I., Kot K., Roszkowska P., Krasnodębska-Szponder B., Paczkowska E., Machaliński B., Łuczkowska K., Wiszniewska B. and Kosik-Bogacka D, (2018), Changes in the immune system in experimental acanthamoebiasis in immunocompetent and immunosuppressed hosts, *Parasites and vectors*, 11 (1), pp: 517

La Scola B., Desnues C., Pagnier I., Robert C., Barrassi L., Fournous G., Merchat M., Monti M. S., Forterre P., Koonin E. and Raoult D., (2008), The virophage as a unique parasite of the giant mimivirus, *Nature*, 455, pp: 100–104

Lau S., Patnaik N., Sayen M. R. and Mestril R., (1997), Simultaneous overexpression of two stress proteins in rat cardiomyocytes and myogenic cells confers protection against ischemia-induced injury, 96 (7), pp: 2287–2294

Legendre M., Lartigue A., Bertaux L., Jeudy s., Bartoli J., Lescot M., Alempic J. M., Ramus C., Bruley C., Labadie K., Shmakova L., Rivkina E., Couté Y., Abergel C. and Claverie J. M., (2015), In-depth study of Mollivirus sibericum, a new 30,000-y-old giant virus infecting *Acanthamoeba*, *PNAS,* 112 (38), pp: 327-335

Legendre M., Fabre e., Poirot O., Jeudy S., Lartigue A., Alempic J. M., Beucher L., Nadege P., Bertaux L., Labadie K., Coute Y., Abergel C. and Claverie J.M., (2017), Diversity and evolution of the emerging Pandoraviridae family, *Nature Communications*, 9,

Lee N., Gannavaram S., Selvapandiyan A. and Debrabant A., (2007), Characterization of Metacaspases with Trypsin-Like Activity and Their Putative Role in Programmed Cell Death in the Protozoan Parasite Leishmania, *Eukaryotic Cell*, 6 (10), pp: 1745–1757

Lehninger A. L., (1970), Mitochondria and calcium ion transport, *Biochem. J*., 119 (2), pp: 129-138

Leist, M. and Jäättelä M., (2001b), Four death and a funeral: from caspases to alternative mechanisms, *Cell Biol.*, 2 (8), pp: 589 – 598

LeStourgeon W. M., Forer A., Yang Y., Bertram J. S. and Rusch H. P., (1975), *Biochim biophys acta*, 379

Levine B., Kroemer G., (2008), Autophagy in the Pathogenesis of Disease, *Cell* 132 (1), pp: 27–42

Li W., Yuan X. M., Olsson A. G. and Brunk U. T., (1998), Uptake of oxidized LDL by macrophages results in partial lysosomal enzyme inactivation and relocation, *Arterioscler Thromb Vasc Biol*, 18 (2), pp: 177–184

Li L. Y., Luo X. and Wang X., (2001), Endonuclease G is an apoptotic DNase when released from mitochondria, *Nature*, 412 (6842), pp: 95-99

Li F. J., Shen Q., Wang C., Sun Y., Yuan A. Y. and He C. Y., (2012), A role of autophagy in *Trypanosoma brucei* cell death, *Cell. Microbio*logy, 14 (8), pp: 1242–1256

Liao Y., Smyth G. K. and Shi W., (2014), FeatureCounts: An efficient general purpose program for assigning sequence reads to genomic features, *Bioinformatics*, 30 (7), pp: 923–930

Lin Kuo-Hua, Ming-Yii Huang, Wei-Chung Cheng, Shu-Chi Wang, Shih-Hua Fang, Hung-Pin Tu, Chia-Cheng Su, Yung-Li Hung, Po-Len Liu, Chi-Shuo Chen, Yu-Ting Wang and Chia-Yang L, (2018), RNA-seq transcriptome analysis of breast cancer cell lines under shikonin treatment, *Scientific reports*, (8), 2672

Lloyd, D., (2014), Encystment in *Acanthamoeba castellanii*: A review, *Experimental Parasitology*, 145, pp: 20–27

Lomonosova E. and Chinnadurai G., (2008), BH3-only proteins in apoptosis and beyond: an overview, *Oncogene*, (27), pp: 2–19

Lorenzo-Morales J., Khan N. A. and Walochnik J., (2015), An update on *Acanthamoeba* keratitis: diagnosis, pathogenesis and treatment, *Parasite,* 22, 10

Lowe S. and Lin A. W., (2000), Apoptosis in cancer, *Carcinogenesis*, (21) 3, pp: 485–495

Lu G. D., Shen H. M., Chung M. C. and Ong C. N., (2007), Critical role of oxidative stress and sustained JNK activation in aloe-emodin-mediated apoptotic cell death in human hepatoma cells, *Carcinogenesis*, 28 (9), pp: 1937–1945

Lum J., Bauer D. E., Kong M., Harris M. H., Li C., Lindsten T. and Thompson C. B., (2005), Growth factor regulation of autophagy and cell survival in the absence of apoptosis, *Cell,* 120 (2), pp: 237–248

Maciver S. K., Asif M., Simmen M. and Lorenzo-Morales J., (2013), A systematic analysis of *Acanthamoeba* genotype frequency correlated with source and pathogenicity: T4 is confirmed as a pathogen-rich genotype, *European journal of protistology*, 49 (2), pp: 217-221

Maciver S. K., (2016), Asexual amoebae escape Muller's ratchet through polyploidy, *Trends in Parasitology*, 32 (11), pp: 855–862

Madeo F., Herker E., Maldener C., Wissing S., Lächelt S., Herlan M., Fehr M., Lauber K., Sigrist S. J. and Wesselborg S., (2002), A caspase-related protease regulates apoptosis in yeast*, Mol Cell*, 9 (4), pp: 911-917

Majid M. A., Mahboob T., Mong B. G. J., Jaturas N. and Richard R. L., (2017) Pathogenic waterborne free-living amoebae: An update from selected Southeast Asian countries, *PLOS ONE,* 12 (5): e0177564

Marciano-Cabral F., Han K., Powell E., Ferguson T. and Cabral G., (2003), Interaction of an *Acanthamoeba*human isolate harboring bacteria with murine peritoneal macrophages, *Journal of Eukaryotic Microbiology*, 50, pp: 516–519

Martinez S., Gonzalez-Mediero M. G., Santiago P., Rodriguez de Lope A., Diz J., Conde C. and Visvesvara G. S., (2000), Granulomatous amebic encephalitis in a patient with AIDS: isolation of *Acanthamoeba spp*. group II from brain tissue and successful treatment with sulfadiazine and fluconazole, *Journal Clin. Microbiol*., 38 (10), pp:3892–3895

Martinez S. and Visvesvara G. S., (1997), Free-living, amphizoic and opportunistic amebas, *Brain Pathol*., 7 (1), pp: 583-598

Martikainen P., Kyprianou N., Tucker R. W. and Isaacs J. T., (1991), Programmed death of nonproliferating androgen-independent prostatic cancer cells, *Cancer Res*., 51 (17), pp: 4693–4700

Maumus F. and Blanc G., (2016), Study of Gene Trafficking between *Acanthamoeba* and Giant Viruses Suggests an Undiscovered Family of Amoeba-Infecting Viruses, *Genome Biology and Evolution*, 8 (11), pp: 51–63

McClellan K., Howard K., Mayhew E., Niederkorn J. and Alizadeh H., (2002), Adaptive immune responses to *Acanthamoeba* cysts, *Exp Eye Res*, 75 (3), pp: 285-93

Meersseman W., Lagrou K., Sciot R., de Jonckheere J., Haberler C., Walochnik J., Peetermans W. E. and van Wijngaerden E., (2007), Rapidly fatal *Acanthamoeba* encephalitis and treatment of cryoglobulinemia. *Emerging infectious diseases*, 13 (3), pp: 469-471

Melino G., Knight R. A. and Nicotera P., (2005), How many ways to die? How many different models of cell death?, *Cell Death and Differentiation,* (12), pp: 1457–1462

Meslin B., Barnadas C., Boni V., Latour C., De Monbrison F., Kaiser K. and Picot S., (2007), Features of apoptosis in *Plasmodium falciparum* erythrocytic stage through a putative role of PfMCA1 metacaspase-like protein*, J Infect Dis*., 195 (12), pp: 1852-1859

Michel R. and Hauröder B., (1997), Isolation of an *Acanthamoeba* strain with intracellular Burkholderia pickettii infection, *Zentralblatt für Bakteriologie*, 285 (4), pp: 541–557

Miller A. D. and Rosman G. J., (1989), Improved Retroviral Vectors for Gene Transfer and Expression, *BioTechniques*, 7 (9), pp: 980–990

Milliman C. L., Korsmeyer S. J., Wang K., Yin X. M. and Chao D. T., (1996), BID: a novel BH3 domain-only death agonist, *Genes Dev.,* 10 (22), pp: 2859–2869

Miltner E. C. and L. E. Bermudez, (2000), Mycobacterium avium grown in *Acanthamoeba* castellanii is protected from the effects of antimicrobials, *Antimicrobial Agents and Chemotherapy*, 44, (7), pp: 1990–1994

Mingeot-Leclercq M. P., Glupczynski Y. and Tulkens P. M., (1999), Aminoglycosides: Activity and Resistance, *Antimicrobial Agents and Chemotherapy*, 43 (4), pp: 727–737

Minden A., Lin A., McMahon M., (1994), Differential activation of ERK and JNK mitogen-activated protein kinases by Raf-1 and MEKK, *Science*, 266 (5191), pp: 1719-23

Mizushima N., Komatsu M., (2011), Autophagy: renovation of cells and tissues, *Cell*, 147 (4), pp: 728–34

Mochizuki H., Goto K., Mori H. and Mizuno Y., (1996), Histochemical detection of apoptosis in Parkinson's disease, *J Neurol Sci,* 137 (2), pp: 120–123

Moliner C., Raoult D. and Fournier P. E., (2009), Evidence of horizontal gene transfer between amoeba and bacteria, *Clinical Microbiology and Infection*, 15, pp: 178–180

Molmeret M., Horn M., Wagner M., Santic M. and Abu Kwaik Y., (2005), Amoebae as training grounds for intracellular bacterial pathogens, *Applied and Environmental Microbiology*, 71 (1), pp: 20–28

Moon E. K., Chung D. I., Hong Y. and Kong H. H., (2011), Atg3-Mediated Lipidation of Atg8 Is Involved in Encystation of *Acanthamoeba*, *The Korean Journal of Parasitology*, 49 (2), pp:103–108

Moon E. K., Hong Y., Chung D. I. and Kong H.-H., (2013), Identification of Atg8 Isoform in Encysting *Acanthamoeba*, *The Korean Journal of Parasitology,* 51 (5), pp: 497–502

Moreira D., von der Heyden S., Bass D., López-García P., Chao E. and Cavalier-Smith T., (2007), Global eukaryote phylogeny: Combined small- and large-subunit ribosomal DNA trees support monophyly of Rhizaria, Retaria and Excavata, *Mol. Phylogenet. Evol*., 44 (1), pp: 255–66

Murakawa G. J., McCalmont T., Altman J., Telang G. H., Hoffman M. D., Kantor G. R. and Berger T. G., (1995), Disseminated acanthamebiasis in patients with AIDS. A report of five cases and a review of the literature, *Arch Dermatol*., 131 (11), pp: 1291-1296

Mylnikov A. P., Weber F., Jürgens K., Wylezich C., (2015), Massisteria marina has a sister: Massisteria voersi sp. nov., a rare species isolated from coastal waters of the Baltic Sea". *European Journal of Protistology,* 51 (4), pp: 299–310

Nakamura K., Bossy-Wetzel E., Burns K., Fadel M. P., Lozyk M., Goping I. S., (2000), Changes in endoplasmic reticulum luminal environment affect cell sensitivity to apoptosis, *J Cell Biol*., 150 (4), pp: 731–740

Nedelcu A. M., (2009), Comparative genomics of phylogenetically diverse unicellular eukaryotes provide new insights into the genetic basis for the evolution of the programmed cell death machinery, *Journal Mol Evol*., 68 (3), pp: 256-268

Neff R. J., (1964), Chapter 4 Induction of synchronous encystment (differentiation) in *Acanthamoeba* sp., *in Methods in Cell Biology*, pp: 55–83

Neff R. J., Benton, W. F. and Neff, R. H., (1964), Composition of mature cyst wall of soil ameba *Acanthamoeba* sp', in *Journal of Cell Biology*, p. A66

Neiva, L. B. M., Cassiane F. D., Watanabe, Vattimo M., Fernandes F. M., (2013), Polymyxin B: dose and time dependent nephrotoxicity effect in vitro, *Acta Paulista de Enfermagem*, 26 (1), pp: 57-62

Nelson C. and Baehrecke E. H., (2014), Eaten to death, *FEBS* J, 281 (24), pp: 5411–5417

Neutzner A, Li S, Xu S. and Karbowski M, (2012), The ubiquitin/proteasome system-dependent control of mitochondrial steps in apoptosis, *Semin Cell Dev Biol*., 23, (5) pp: 499-508

Nicotera P. and Orrenius S., (1998), The role of calcium in apoptosis, *Cell Calcium*, 23 (2-3), pp: 173–180

Nicotera P., Hartzell P., Davis G. and Orrenius S., (1986), The formation of plasma membrane blebs in hepatocytes exposed to agents that increase cytosolic Ca^{+2} is mediated by the activation of a non lysosomal proteolytic system, *FEBS Lett*., 209 (1), pp:139-44

Niemi N. and MacKeigan J. P., (2013), Mitochondrial Phosphorylation in Apoptosis: Flipping the Death Switch, *Antioxidants and Redox Signaling*, 19 (6), pp: 572–582

Nikolaev Sergey I., Berney C., Fahrni C.F., Bolivar I., Polet S., Mylnikov P. A., Aleshin V., Petrov N. B. and Jan Pawlowski (2004), The twilight of Heliozoa and rise of Rhizaria, an emerging supergroup of amoeboid eukaryotes, *Proceedings of the National Academy of Sciences,* 101 (21), pp: 8066–8071

Nikolaev S. I., Berney C., Petrov N. B., Mylnikov A. P., Fahrni J. F. and Pawlowski J., (2006), Phylogenetic position of *Multicilia* marina and the evolution of Amoebozoa. *Int J Syst Evol Microbiol,* (56) pp: 1449–1458

Nikoletopoulou V., Markaki M., Palikaras K. and Tavernarakis N., (2013), Crosstalk between apoptosis, necrosis and autophagy, *Biochimica et Biophysica Acta (BBA) - Molecular Cell Research,* 1833 (12), pp: 3448-3459

Niyaz Y., Yutin N., Colson P., Shabalina S. A., Pagnier I., Robert C., Azza S, Klose T., Wong J., Rossmann G. M., La Scola B., Raoult D. and Koonin E. V., (2012), Related Giant Viruses in Distant Locations and Different Habitats: *Acanthamoeba* polyphaga moumouvirus Represents a Third Lineage of the Mimiviridae That Is Close to the Megavirus Lineage *Genome Biol Evol*., 4 (12), pp: 1324–1330

Nunes R. dos S., Souza F. C., Rammé A. N., Finoketti F., Côrrea R. A., Cano-Ortiz L., Assis f. L., Souza T. Arantes, Roehe P. M. and Franco A. C., (2016), A new marseillevirus isolated in Southern Brazil from Limnoperna fortune, *Scientific Reports,* (6), Article number: 35237

Nuprasert W., Putaporntip C., Pariyakanok L. and Jongwutiwes S., (2010), Identification of a novel T17 genotype of *Acanthamoeba* from environmental isolates and T10 genotype causing keratitis in Thailand, *Journal of Clinical Microbiology*, 48 (12), pp: 4636–4640

Nyoma and Luder, (2013), Apoptosis-like cell death pathways in the unicellular parasite *Toxoplasma gondii* following treatment with apoptosis inducers and chemotherapeutic agents: a proof-of-concept study, *Apoptosis*, 18 (6), pp: 664

Oka N., Lixing W., Wenyu M., Wei Z., Osami H. and Caldarone C. A., (2008), Cyclosporine A revents apoptosis-related mitochondrial dysfunction after neonatal cardioplegic arrest, *J Thorac Cardiovasc Surg*, 135 (1), pp: 123-130

Oldenburg C. E., Acharya N. R., Tu E. Y., Zegans M. E., Mannis M. J. and Gaynor B. D., (2011), Practice patterns and opinions in the treatment of *Acanthamoeba* keratitis, *Cornea*, 30 (12), pp: 1363

Ong T. Y. Y., Khan N. A. and Siddiqui R., (2017), Brain-Eating Amoebae: Predilection Sites in the Brain and Disease Outcome, *Journal of Clinical Microbiology*, 55 (7), pp: 1989–1997

Orlowski R. Z., (1999), The role of the ubiquitin-proteasome pathway in apoptosis, *Cell Death Differ*, (6), pp: 303–313

Orrenius S., Zhivotovsky B. and Nicotera P., (2003) Regulation of cell death: the calcium-apoptosis link. Nat *Rev Mol Cell Biol*, (4), pp: 552–565

Ozaki T. and Nakagawara A., (2011), Role of p53 in Cell Death and Human Cancers. *Cancers*, 3 (1), pp: 994–1013

Ozkan P. and Mutharasan R., (2002), A rapid method for measuring intracellular pH using BCECF-AM, *Biochimica et Biophysica Acta*, 1572 (1), pp: 143-148

Pagnier I., Yutin N., Croce O., Makarova K. S., Wolf Y. I., Benamar S., Raoult D., Koonin E. V. and La Scola B., (2015), Babela massiliensis, a representative of a widespread bacterial phylum with unusual adaptations to parasitism in amoebae, *Biol Direct*., 10 (13)

Paltiel M., Powell E., Lynch J., Baranowski B. and Martins C., (2004), Disseminated Cutaneous Acanthamebiasis: A Case Report and Review of the Literature, *Cutis*, 73 (4), pp: 241-248

Parija S. C., Dinoop K. and Venugopal H., (2015), Management of granulomatous amebic encephalitis: Laboratory diagnosis and treatment *Tropical parasitology*, 5 (1), pp: 23-28

Patil V., Bråte J, Shalchian-Tabrizi K., Jakobsen K. S., (2009), Revisiting the phylogenetic position of synchroma grande, *Journal of Eukaryotic Microbiology*, 56 (4), pp. 394–396

Pearson W. R., (2013), An Introduction to Sequence Similarity ("Homology") Searching, *Curr. Protoc. Bioinformatics,* 42 (1)

Petronilli V, Cola C., Massari S., Colonna R. and Bernardi P., (1993), Physiological effectors modify voltage sensing by the cyclosporine A-sensitive permeability transition pore of mitochondria, *J Biol Chem,* 268 (29), pp: 21939–21945

Pham, T. T., Angus S. P. and Johnson G. L, (2013), MAP3K1: Genomic Alterations in Cancer and Function in Promoting Cell Survival or Apoptosis, *Genes and Cancer*, 4, (11-12), pp: 419–426

Philips M., Bivona T. G., Quatela S. E., Bodemann B. O., Ahearn I. M., Soskis M. J. and Mor A., (2006), PKC regulates a farnesyl-electrostatic switch on K-Ras that promotes its association with Bcl-XL on mitochondria and induces apoptosis, *Mol Cell*, 21 (4), pp: 481–93

Pinton P., Ferrari D., Rapizzi E., Di Virgilio F., Pozzan T. and Rizzuto R., (2001), The Ca^{2+} concentration of the endoplasmic reticulum is a key determinant of ceramide-induced apoptosis: significance for the molecular mechanism of Bcl-2 action, *EMBO J*., 20 (11), pp: 2690–2701

Pinton P., Brini M., Bastianutto C., Tuft R. A., Pozzan T. and Rizzuto R., (1998), New light on mitochondrial calcium, *Biofactors*., 8 (3-4), pp: 243–253.

Pinton P., Ferrari D., Di Virgilio F., Pozzan T., Rizzuto R., (2001a), Molecular machinery and signalling events in apoptosis, *Drug Dev Res*., pp: 558–570,

Pinton P., Ferrari D., Magalhaes P., Schulze-Osthoff K., Di Virgilio F. and Pozzan T., (2000), Reduced loading of intracellular $Ca^{(2+)}$ stores and downregulation of capacitative Ca(2+) influx in Bcl-2-overexpressing cells, *Journal Cell Biol*., 148 (5), pp: 857–862

Pittella, (2013), Neuroparasitology and Tropical Neurology, *Handbook of Clinical Neurology*, 114 (3rd series)

Prior and Hancock, (2012), Ras trafficking, localization and compartmentalized signaling, Seminars in Cell and *Developmental Biology*, (23) 2, pp: 145-153

Pussard M. and Pons R., (1977), Morphology of cystic wall and taxonomy of genus *Acanthamoeba* (Protozoa, Amoebida), *Protistologica*, 13 (4), pp: 557–598

Rosen L. B., Ginty G. B., Weber J. M. and Greenberg M. E., (1994), Membrane depolarization and calcium influx stimulate MEK and MAP kinase via activation of Ras, *Neuron*, 12, (6), pp: 1207-1221

Qu X., Z. Zou, Q. Sun, K. Luby-Phelps, Cheng P., Hogan R. N., Gilpin C. and Levine B., (2007), Autophagy gene-dependent clearance of apoptotic cells during embryonic development, *Cell*, 128, (5), pp: 931-946

Radoshevich L., Murrow L., Chen N., Fernandez E., Roy S., Fung C. and Debnath J., (2010), ATG12 Conjugation to ATG3 Regulates Mitochondrial Homeostasis and Cell Death, *Cell*, 142, (4), pp: 590–600

Ramaker R. C., Lasseigne B. N., Hardigan A. A., Palacio L., Gunther D. S., Myers R. M. and Cooper, S. J., (2017), RNA sequencing-based cell proliferation analysis across 19 cancers identifies a subset of proliferation-informative cancers with a common survival signature, *Oncotarget*, 8 (24), pp: 38668–38681

Reape T. J. and Mc Cabe P. F., (2010), Apoptotic-like regulation of programmed cell death in plants, *Apoptosis*, 15 (3), pp: 249-256

Rico E., Alzate J. F., Arias A. A., Moreno D., Clos J., Gago F., Moreno I., Dominguez M. and Jimenez-Ruiz A., (2009), *Leishmania infantum* expresses a mitochondrial nuclease homologous to EndoG that migrates to the nucleus in response to an apoptotic stimulus, *Mol. Biochem. Parasitol*., 163 (1), pp: 28–38

Ritchie M. E., Phipson B., Wu, D., Hu, Y., Law C. W., Shi W. and Smyth, G. K., (2015), limma powers differential expression analyses for RNA-sequencing and microarray studies, *Nucleic Acids Research*, 43 (7),

Rivera M. and Padhya T., (2002), *Acanthamoeba*: a rare primary case of rhinosinusitis, *Laryngoscope* 112 pp: 1201–1203

Ruvolo R. R, Deng X., Ito T., Carr B. K. and May W. S., (1999), Ceramide induces Bcl2 dephosphorylation via a mechanism involving mitochondrial PP2A, *Journal of Biological* Chemistry, 274 (29), pp: 20296–20300,

Saheb Tryzna and Bush, (2016), Caspase-like proteins: Acanthamoeba castellanii metacaspases and Dictyostelium discoideum paracaspase, what are their functions?, *J. Biosci*., (39), pp: 909–916

Sajid M. and McKerrow J., (2002), Cysteine proteases of parasitic organisms, *Mol Biochem Parasitology*, 120 (1), pp: 1-21

Samali A., Cai J., Zhivotovsky B., Jones D. P. and Orrenius S., (1999), Presence of a pre-apoptotic complex of pro-caspase-3, Hsp60 and Hsp10 in the mitochondrial fraction of Jurkat cells, *EMBO Journal*, 18 (8), pp: 2040–2048

Sangruchi T., Martinez A. J. and Visvesvara G. S., (1994), Spontaneous granulomatous amebic encephalitis: report of four cases from Thailand, *Southeast Asian J. Trop. Med*., (25), pp: 309–313

Sanchez, A., ALvarez M., Benito M. and Fabregat I., (1997), Cycloheximide Prevents Apoptosis, Reactive Oxygen Species Production and Glutathione Depletion Induced by Transforming Growth Factor b in Fetal Rat Hepatocytes in Primary Culture, *Hepatology*, 26 (4), pp: 935-943

Scheid and Balczun, (2017), Failure of molecular diagnostics of a keratitis-inducing *Acanthamoeba* strain, *Exp Parasitol*., 183, pp: 236-239

Schlesinger T. K., Bonvin C. and Jarpe M. B., (2002), Apoptosis stimulated by the 91-kDa caspase cleavage MEKK1 fragment requires translocation to soluble cellular compartments, *J Biol Chem.,* 277 (12), pp: 10283-91

Schroeder J. M., Booton G. C., Hay J., Niszl I. A., Seal D. V., Markus M. B., Fuerst P. A. and Byers T. J., (2001), Use of subgenic 18S ribosomal DNA PCR and sequencing for genus and genotype identification of *Acanthamoeba* from humans with keratitis and from sewage sludge, *Journal of Clinical Microbiology*, 39 (5), pp: 1903–1911

Scorrano L., Oakes S. A., Opferman J. T., Cheng E. H., Sorcinelli M. D. and Pozzan T., (2003), BAX and BAK regulation of endoplasmic reticulum Ca^{2+}: a control point for apoptosis, *Science*, 300 (5616), pp: 135–139

Senderowicz A. M., (2005), Inhibitors of cyclin-dependent kinase modulators for cancer therapy, *Prog Drug Res.,* 63, pp: 183-206

Sensibar J. A., Liu X. X., Patai B., Alger B. and Lee C., (1990), Characterization of castration-induced cell death in the rat prostate by immuno-histochemical localization of cathepsin D, *Prostate*, 16 (3), pp: 263–276

Sharma S., Garg P. and Rao G. N., (2000), Patient characteristics, diagnosis and treatment of noncontact lens related Acanthamoeba keratitis, *The British journal of ophthalmology*, 84 (10), pp: 1103-1108

Siddiqui R., Aqeel Y. and Khan N. A., (2016), The development of drugs against *Acanthamoeba* infections, *Antimicrob Agents Chemother,* 60 (11), pp: 6441–6450

Smirnov A., Nassonova E., Berney C., Fahrni J., Bolivar I. and Pawlowski J., (2005), Molecular phylogeny and classification of the lobose amoebae, *Protist*, 156 (2), pp: 129–142

Smirnov A. V., Chao E., Nassonova E. S. and Cavalier-Smith T., (2011), A revised classification of naked lobose amoebae (Amoebozoa: lobosa), *Protist*, 162 (4), pp:545-70

Sridharan S., Jain K. and Basu A., (2011), Regulation of Autophagy by Kinases, *Cancer*, 3 (2), pp: 2630–2654

Stankiewicz A. R., Livingstone A. M., Mohseni N. and Mosser D. D., (2009), Regulation of heat-induced apoptosis by mcl-1 degradation and its inhibition, by Hsp70., *Cell Death Differ*., 16 (4), pp: 638–647

Steenbergen J. N., Shuman H. and Casadevall A., (2001), Cryptococcus neoformans interactions with amoebae suggest an explanation for its virulence and intracellular pathogenic strategy in macrophages, *Proceedings of the National Academy of Sciences of the United States of America,* 98 (26), pp: 15245–15250

Steinberg J. P., Galindo R., Kraus E. S. and Ghanem K. G., (2002), Disseminated acanthamoebiasis in a renal transplant recipient with osteomyelitis and cutaneous lesions: case report and literature review, *Clin. Infect. Dis*., 35 (5), pp: 43–49

Stevens A. R. and Pachler P. F., (1973), RNA synthesis and turnover during densityinhibited growth and encystment of *Acanthamoeba castellanii*, *Journal of Cell Biology*, 57 (2), pp: 525–537

Stewart J. R. and Weisman R. A., (1972), Exocytosis of latex beads during the encystment of *Acanthamoeba*, *J Cell Biol*., 52 (1), pp:117-130

Siddiqui R. and Khan N. A., (2012a), *Acanthamoeba* is an evolutionary ancestor of macrophages: a myth or reality?, *Experimental Parasitology*, 130 (2), pp: 95–97

Siddiqui R. and Khan N. A., (2012b), Biology and pathogenesis of *Acanthamoeba*, *Parasites and Vectors,* 5 (1), pp: 6

Siddiqui R. and Khan N. A., (2012c), War of the microbial worlds: who is the beneficiary in *Acanthamoeba*-bacterial interactions, *Experimental Parasitology*, 130 (4), pp: 311–3.

Silverblatt F. J. and Kuehn C., (1997), Autoradiography of gentamicin uptake by the rat proximal tubule cell, *Kidney Int*., 15 (4) pp: 335-45

Singh P., Ravanan P. and Talwar P., (2016), Death Associated Protein Kinase 1 (DAPK1): A Regulator of Apoptosis and Autophagy, *Frontiers in Molecular Neuroscience*, 9, (46)

Song S. M., Han B. I., Moon E. K., Lee Y. R., Yu H. S., Jha B. K., Danne D. B., Kong H. H., Chung D. I.and Hong Y., (2012), Autophagy protein 16-mediated autophagy is required for the encystation of *Acanthamoeba* castellanii*, Mol Biochem Parasitol.,*183 (2), pp:158-65

Storey N. M. and Lambert D. G., (2017), Mitochondrial pharmacology turns its sights on the Ca^{2+} uniporter, *Cell Death Discovery*, 3, 17064

Sundström J. F., Vaculova A., Smertenko A. P., Savenkov E. I., Golovko A., Minina E., Tiwari B. S. and Rodriguez-Nieto S., (2009), Tudor staphylococcal nuclease is an evolutionarily conserved component of the programmed cell death degradome, *Nat Cell Biol*., 11 (11), pp: 1347-1354

Sun L. and Carpenter G., (1998), Epidermal growth factor activation of NF-kappaB is mediated through IkappaBalpha degradation and intracellular free calcium, *Oncogene*, 16 (16), pp:2095-102

Suzanne M. and Steller H., Shaping organisms with apoptosis, *Cell Death Differ*, (2013), 20 (5), pp: 669–675

Suzuki Y., Imai Y., Nakayama H., Takahashi K., Takio K. and Takahashi R., (2001), A serine protease, HtrA2, is released from the mitochondria and interacts with XIAP, inducing cell death., *Mol. Cell*, 8 (3), pp: 613 – 621

Roach H. I. and Clarke N. M., (2000), Physiological cell death of chondrocytes in vivo is not confined to apoptosis. New observations on the mammalian growth plate*, Journal Bone Joint Surg,* 82 (4), pp: 601–613

Robinson M. D. and Oshlack A., (2010) A scaling normalization method for differential expression analysis of RNA-seq data, *Genome Biology*, 11 (3), pp: 25

Robinson J. T., (2013), Integrative Genomics Viewer, *Nature Biotechnology*, 29 (1), pp: 24–26

Rodriguez D., Phipps K., Ishiguro T. and Ridgway H. F., (1992), Use of a Fluorescent Redox Probe for Direct Visualization of Actively Respiring Bacteria, *Applied and Environmental Microbiology*, 58 (6), pp: 1801-1808

Rodríguez-Zaragoza S., (2008), Ecology of Free-Living Amoebae, *Critical Reviews in Microbiology*, 20 (3), pp: 225-241

Rubio-Moscardo F., Blesa D., Mestre C., Siebert R., Balasas T., Benito A., Rosenwald A., Climent J., Martinez J. I., Schilhabel M., Karran E. L., Gesk S., Esteller M., de Leeuw R., Staudt L. M., Fernandez-Luna J. L., Pinkel D., Dyer M. J. and Martinez-Climent J. A., (2005), Characterization of 8p21.3 chromosomal deletions in B-cell lymphoma: TRAIL-R1 and TRAIL-R2 as candidate dosage-dependent tumor suppressor genes, *Blood,* 106 (9) pp: 3214–3222

Ruscoe J. E., Rosario L. A., Wang T., Gaté L., Arifoglu P., Wolf C. R., Henderson C. J., Ronai Z. and Tew K. D., (2001), Pharmacologic or genetic manipulation of glutathione S-transferase P1-1 (GSTpi) influences cell proliferation pathways, J*. Pharmacol. Exp. Ther*., 298 (1), pp: 339-345

Takahashi A., Camacho P., Lechleiter J. D. and Herman B., (1999), Measurment of intracellular calcium, *physiologiacal rev.,* 79 (4), pp: 1089-1115

Takemura M., (2016), Morphological and Taxonomic Properties of Tokyovirus, the First Marseilleviridae Member Isolated from Japan, *Microbes Environ*, 31 (4), pp: 442–448

Tan K. S. and Nasirudeen A. M., (2005), Protozoan programmed cell death–insights from *Blastocystis deathstyles, Trends Parasitol,* 21 (12) pp: 547–550

Tavares M., Correia da Costa J. M., Carpenter S., Caldas S. A., Aguiar A., Pereira J., Cardoso I. A., Schuster F. L., Yagi S., Sriram R. and Visvesvara G. S., (2006), Diagnosis of first case of *Balamuthia* amoebic encephalitis in Portugal by immunofluorescence and PCR, *Journal Clin. Microbiol.,* (44) pp: 2660–2663

Teng R.-J., Jing X., Michalkiewicz T., Afolayan A. J., Wu T.-J. and Konduri G. G., (2017), Attenuation of endoplasmic reticulum stress by caffeine ameliorates hyperoxia-induced lung injury, *American Journal of Physiology - Lung Cellular and Molecular Physiology*, 312 (5), pp: 586–598

Teknos T. N., Poulin M. D., Laruentano A. M. and Li K. K., (2001), *Acanthamoeba* rhinosinusitis: characterization, diagnosis and treatment, *Am. J. Rhinol*. 14 (6), pp: 387–391

Thorburn A., (2008), Apoptosis and Autophagy: regulatory connections between two supposedly different processes. Apoptosis, *An International Journal on Programmed Cell Death*, 13 (1), pp: 1–9

Thuret G., Chiquet C., Herrag S., Dumollard J.-M., Boudard D., Bednarz J., Gain P., (2003), Mechanisms of staurosporine induced apoptosis in a human corneal endothelial cell line. *The British Journal of Ophthalmology*, 87(3), 346–352

Tice A. K., Shadwick L. L., Fiore-Donno A .M., Geisen S., Kang S., Schuler G. A., Spiegel F. W., Wilkinson K. A., Bonkowski M., Dumack K., Lahr D. J. G., Voelcker E., Clauß S., Zhang, J. and Brown M. W., (2016), Expansion of the molecular and morphological diversity of Acanthamoebidae (Centramoebida, Amoebozoa) and identification of a novel life cycle type within the group, *Biology Direct*, 11 (1), pp: 1–21
7
Torriglia A., Perani P., Brossas J. Y, Altairac S., Zeggai S., Martin E., Treton J., Courtois Y. and Counis M. F., (2000), A caspase-independent cell clearance program. The LEI/L-DNase II pathway, *Ann. N.Y. Acad. Sci.*, 926, pp: 192–203

Tsiatsiani L., Van Breusegem F., Gallois P., Zavialov A., Lam E. and Bozhkov P. V., (2011), Metacaspases, *Cell Death and Differentiation*, 18 (8), pp: 1279–1288

Turella P., Cerella C., Filomeni G., Bullo A., De Maria F., Ghibelli L., Ciriolo M.R., Cianfriglia M., Mattei M., Federici G., Ricci G. and Caccuri A. M, (2005), Proapoptotic activity of new glutathione S-transferase inhibitors, *Cancer research*, 65 (9), pp: 3751-61

Turk B., Bieth J. G., Björk I., Dolenc I., Turk D., Cimerman N., Kos J., Čolič A., Stoka V. and Turk V., (1995), Regulation of the activity of lysosomal cysteine proteinases by pH-induced inactivation and/or endogenous protein inhibitors, cystatins, *Biol. Chem*., 376 (4), pp: 225 – 230

Uren G. A., O'Rourke K., Aravind L. A., Pisabarro M. T., Seshagiri S., Koonin E. V. and Dixit V. M., (2000), Identification of paracaspases and metacaspases: two ancient families of caspase-like proteins, one of which plays a key role in MALT lymphoma, *Mol. Cell*, 6 (4), pp: 961–967

Van den Berghe T., Linkermann A., Jouan-Lanhouet S., Walczak H. and Vandenabeele P., (2014) Regulated necrosis: The expanding network of non-apoptotic cell death pathways. *Nature reviews molecular cell biology*, 15 (2), pp: 134-146

Van der Henst C., Scrignari T., Maclachlan C. and Blokesch M., (2016), An intracellular replication niche for Vibrio cholerae in the amoeba *Acanthamoeba castellanii, The ISME Journal,* 10 (4), pp: 897–910

Van Loo G., van Gurp M., Depuydt B., Srinivasula S. M., Rodriguez I., Alnemri E. S., Gevaert K., Vandekerckhove J., Declercq W. and Vandenabeele P., (2002), The serine protease Omi/HtrA2 is released from mitochondria during apoptosis, Omi interacts with caspase-inhibitor XIAP and induces enhanced caspase activity, *Cell Death Differ*., 9 (1), pp: 20 – 26

Van Zandbergen G., Lüder C. G., Heussler V. and Duszenko M., (2010), Programmed cell death in unicellular parasites: a prerequisite for sustained infection?, *Trends Parasitol*., 26 (10), pp: 477-83

Vattimo Mde. F., Watanabe M., da Fonseca C. D., Neiva L. B., Pessoa E. A and Borges F. T., (2016), Polymyxin B Nephrotoxicity: From Organ to Cell Damage. PLOS ONE 11 (8)

Vaux D. L. and Korsmeyer S. J., Cell death in development. *Cell*, (1999), 96 (2), pp: 245–254

Verani, J. R., Lorick, S. A., Yoder, J. S., Beach, M. J., Braden, C. R. and Roberts, J. M., … for the *Acanthamoeba* Keratitis Investigation Team, (2009), National Outbreak of *Acanthamoeba* Keratitis Associated with Use of a Contact Lens Solution, United States. *Emerging Infectious Diseases*, 15 (8), pp: 1236–1242

Villalba J. D., Gomez C., Medel O., Sanchez V., Carrero J. C., Shibayama M. and Perez Ishiwara D. G., (2007), Programmed cell death in Entamoeba histolytica induced by the aminoglycoside G-418, *Microbiology*, 153, pp: 3852–63

Vincent T., Bertelli C., Collyn F., Casson N., Telenti A., Goesmann A., Croxatto A. and Greub G., (2013), Lausannevirus, a giant amoebal virus encoding, Environmental Microbiology 13 (6), pp:1454–1466

Visvesvara G. S., Moura H. and Schuster F. L., Pathogenic and opportunistic free-living amoebae: Acanthamoeba spp., *Balamuthia mandrillaris, Naegleria fowleri and Sappinia diploidea*, *FEMS Immunol. Med. Microbiol*., 50 (1), pp: 1–26

Visvesvara G. S., Sriram R., Qvarnstrom Y., Bandyopadhyay K., Da Silva A. J., Pieniazek N. J. and Cabral G. A., (2009*), Paravahlkampfia francinae* n. sp. masquerading as an agent of primary amoebic meningoencephalitis. J Eukaryot Microbiol. 56 (4), pp: 357-66

Visvesvara G. S., (2013), Infections with free-living amebae. *Handb Clin Neurol*., 114, pp: 153–68

Volkonsky M., (1931), 'Hartmannella castellanii' Douglas et classification des Hartmannelles ('Hartmanellinae' nov. subfam.,' *Acanthamoeba'* nov. gen.,' Glaeseria' nov. gen.). H. LeSoudier.

Vos M. D., Ellis C. A., Bell A., Birrer M. J. and Clark G. J., (2000), Ras Uses the Novel Tumor Suppressor RASSF1 as an Effector to Mediate Apoptosis, The journal of biological chemistry, 275 (46), pp: 35669–35672

Vos M. D., Martinez A., Ellis C. A., Vallecorsa T. and Clark G. J., (2003), The proapoptotic Ras effector Nore1 may serve as a Ras-regulated tumor suppressor in the lung, J*. Biol. Chem*., 278 (24), pp: 21938–21943

Wajant H., (2002)., The Fas signaling pathway: more than a paradigm, Science 296 (5573), pp: 1635–36

Wang I. J., Hong J. P. and Hu F. R., (1997), Clinical features and outcomes of *Acanthamoeba* keratitis. *J Formos Med Assoc*, 96 (11), pp: 895–900

Wang K., (2000), Calpain and caspase: can you tell the difference?, *Trends Neurosci.,* 23 (1), pp: 20 – 26

Wang X., Yang C., Chai J., Shi Y. and Xue D., (2002), Mechanisms of AIF-mediated apoptotic DNA degradation in *Caenorhabditis elegans*. *Science*, 298 (5598): pp: 1587-1592

Wang W. J., Li Q. Q., Xu J. D., Cao X. X., Li H. X., Tang F., Chen Q., Yang J. M., Xu Z. D. and Liu X. P., (2008), Over-expression of ubiquitin carboxy terminal hydrolase-L1 induces apoptosis in breast cancer cells, *International Journal of Oncology*, 33 (5), pp: 1037–1045

Wang R., Wei B., Wei J., Li Z., Tian Y. and Du C., (2016), Caspase-related apoptosis genes in gliomas by RNA-seq and bioinformatics analysis, Journal of Clinical Neuroscience 33, pp: 259-263

Wang H., Park B. S., Lim W. A. and Ki J. S., (2018), CpMCA, a novel metacaspase gene from the harmful dinoflagellate Cochlodinium polykrikoides and its expression during cell death, 651, (20), pp: 70-78

Webster D., Umar I., Kolyvas G., Bilbao J., Guiot M. C., Duplisea K., Qvarnstrom Y. and Visvesvara G. S., (2012) 'Case report: Treatment of granulomatous amoebic encephalitis with voriconazole and miltefosine in an immunocompetent soldier', American Journal of *Tropical Medicine and Hygiene*, 87 (4), pp: 715–718

Wheat W. H., Casali A. L., Thomas V., Spencer J. S., Lahiri R., Williams D. L, McDonnell G. E., Gonzalez-Juarrero M.,. Brennan P. J. and Jackson M., (2014), 'Long-term survival and virulence of Mycobacterium leprae in amoebal cysts', PLoS Neglected Tropical Diseases, 8 (12)

Weekers P. H., Gast R. J., Fuerst P. A. and Byem T. J., (1994), 'Sequence variations in small-subunit ribosomal RNAs of Hartmannella vermiformis and their phylogenetic implications.' *Molecular Biology and Evolution*, 11 (4), pp: 684–690

Weekers P. H. H., Bodelier P. L. E., Wijen J. P. H. and Vogels G. D., (1993), Effects of grazing by the free-living soil amoebae *Acanthamoeba castellanii*, *Acanthamoeba polyphaga* and *Hartmanella vermiformis* on various bacteria, *Applied and Environmental Microbiology*, 59 (7), pp: 2317–2319

Weekers P. H. H. and Van Der D. C., (1993), Nitrogen metabolizing enzyme activities in the free-living soil amoebae *Acanthamoeba* castellanii, *Acanthamoeba* polyphaga and Hartmannella vermiformis*, Journal of Eukaryotic Microbiology*, 40 (3), pp. 251–254

Westwick J. K, Bielawska A. E, Dbaibo G., Hannun Y. A and Brenner D. A., (1995), *J. Biol. Chem*., 270, pp: 89 -92

Hu W. L., Dong H. Y., Li Y., Ojcius D. M., Li S. J. and Yan J., (2017), Bid-Induced Release of AIF/EndoG from Mitochondria Causes Apoptosis of Macrophages during Infection with Leptospira interrogans, *Frontiers in Cellular and Infection Microbiology,* 7, pp: 471-478

Weisman R. A. and Shaw G. B., (1976), 'Differentiation in *Acanthamoeba castelanii*', *Annual Review of Microbiology*, 30, pp: 189–219

Williams M. S. and Henkart P. A., (1994), Apoptotic Cell Death Induced by Intracellular Proteolysis, *The journal of Immunology*, (153) pp: 4247

Williams R. A. M., Tetley L., Mottram J. C. and Coombs G. H., (2006), Cysteine peptidases CPA and CPB are vital for autophagy and differentiation in Leishmania mexicana. Mol. *Microbiol*., 61 (3), pp: 655–674

Widmann C., Gibson S., Jarpe M. B. and Johnson G. L., (1999), Mitogen-activated protein kinase: conservation of a three-kinase module from yeast to human, *Physiol. Rev*., 79 (1), pp: 143–180

Winding A, Binnerup S. J. and Sorensen J., (1994), Viability of indigenous soil bacteria assayed by respiratory activity and growth*, Appl. Environ. Microbiol*., 60 (8), pp: 2869–2875

Wojcik C., (1999), Proteasomes in apoptosis: villains or guardians? *Cell Mol. Life Sci.*, 56 (11-12), pp: 908–917

Walochnik J., Picher O*.,* Aspöck C*.,* Ullmann M*.,* Sommer R. and Aspöck H*.,* (1999), Interactions of "Limax amoebae" and gram-negative bacteria: experimental studies and review of current problems, *The Tokai Journal of Experimental and Clinical Medicine,* 23 (6), pp: 273–278

Woods L. E., Cole C. V., Elliott E. T., Anderson R. V. and Coleman D. C., (1982), 'Nitrogen transformations in soil as affected by bacterialmicrofaunal interactions', *Soil Biology and Biochemistry*, 14 (2), pp: 93–98

Wright, S. J. L., Redhead K. and Maudsley H., (1981*), Acanthamoeba castellanii*, a Predator of Cyanobacteria, *Journal of General Microbiology*, 125, pp: 293-300

Xanthoudakis S., Roy S., Rasper D., Hennessey T. and Aubin Y., (1999), Hsp60 accelerates the maturation of pro-caspase-3 by upstream activator proteases during apoptosis, *EMBO J*., 18 (8), pp: 2049–2056

Xia Y., Makris C. and Su B., (2000), MEK kinase 1 is critically required for c-Jun N-terminal kinase activation by proinflammatory stimuli and growth factor-induced cell migration. *Proc Natl Acad Sci*, 97 (10), pp: 5243-8

Xu X. Z, Moebius F., Gill D. L. and Montell C., (2001), Regulation of melastatin, a TRP-related protein, through interaction with a cytoplasmic isoform. *Proc Natl Acad Sci*, 98 (19), pp: 10692–10697

Xu T., Nicolson S., Denton D. and Kumar S., (2015), Distinct requirements of Autophagy-related genes in programmed cell death. Cell Death and Differentiation, 22 (11), pp: 1792–1802

Yang C., Gao Y., Gao S., Gang Y., Xiong C., Chang J., Li H. and Ye Z., (2015), Transcriptome profile analysis of cell proliferation molecular processes during multicellular trichome formation induced by tomato Wov gene in tobacco, *Genomics Data*, 16, pp: 173-174

Yang S., Zhao X., Xu H., Chen F., Xu Y., Li Z., Sanchis D., Jin L., Zhang Y. and Ye J., (2017), AKT2 Blocks Nucleus Translocation of Apoptosis-Inducing Factor (AIF) and Endonuclease G (EndoG) While Promoting Caspase Activation during Cardiac Ischemia, *International Journal of Molecular Sciences*, 18 (3), pp: 565-75

Yoshiki S., Matsunaga-Udagawa R., Aoki K., Kamioka Y., Kiyokawa E. and Matsuda M., (2010), Ras and Calcium Signaling Pathways Converge at Raf1 via the Shoc2 Scaffold Protein, *Molecular Biology of the Cell,* 21 (6), pp: 1088–1096

Yuste V, Bayascas J. R, Llecha N., Sánchez-López I., Boix J. and Comella J. X., (2001), The Absence of Oligonucleosomal DNA Fragmentation during Apoptosis of IMR 5 Neuroblastoma Cells disappearance of the caspase-activated dnase*, the Journal of Biological Chemistry*, 276 (25), pp: 22323-22331

Zamora A., Henderson H. and Swiatlo E., (2014), *Acanthamoeba* encephalitis: A Case Report and Review of Therapy*, Surgical Neurology International,* 5 (68)

Zhu J., Woods D., McMahon M. and Bishop J. M., (1998), Senescence of human fibroblasts induced by oncogenic Raf, *Genes Dev*., 12 (19), pp: 2997–3007